Identification and Characterization of Novel Genes involved in Quinone Synthesis in the Odoriferous Defensive Stink Glands of the Red Flour Beetle, *Tribolium castaneum*

Dissertation

for the award of the degree
"Doctor rerum naturalium" (Dr.rer.nat.)
of the Georg-August-Universität Göttingen

within the doctoral program 'Biology'
of the Georg-August University School of Science (GAUSS)

Submitted by

Bibi Atika

From Abbottabad, Pakistan

Göttingen, 2020

Thesis Committee:

Prof. Dr. Ernst A. Wimmer (advisor)

(Department of Developmental Biology, Johann-Friedrich Blumenbach-Institute of Zoology and Anthropology, Georg-August-Universität Göttingen)

Prof. Dr. Ivo Feußner

(Department of Plant Biochemistry, Albrecht-von-Haller-Institute of Plant Sciences, Georg-August-Universität Göttingen)

Members of the Examination Board:

First referee: **Prof. Dr. Ernst A. Wimmer**

Second referee: **Prof. Dr. Ivo Feußner**

Prof. Dr. Gregor Bucher

(Department of Evolutionary Developmental Genetics, Johann-Friedrich Blumenbach-Institute of Zoology and Anthropology, Georg-August-Universität Göttingen)

Prof. Dr. Ralf Heinrich

(Department of Cellular Neurobiology, Johann-Friedrich- Blumenbach-Institute of Zoology and Anthropology, Georg-August-Universität Göttingen)

Prof. Dr. Michael Rostás

(Department of Crop Sciences Agricultural Entomology, Georg-August-Universität Göttingen)

Prof. Dr. Sven Bradler

(Department of Animal Evolution and Biodiversity, Johann-Friedrich-Blumenbach-Institut für Zoologie und Anthropologie, Georg-August-Universität Göttingen)

Oral examination Date: 22.01.2021

Declaration

I, Bibi Atika, hereby declare that the dissertation entitled **"Identification and Characterization of Novel Genes involved in Quinone Synthesis in the Odoriferous Defensive Stink Glands of the Red Flour Beetle, *Tribolium castaneum*"** is written by me on the basis of my doctoral project experimental work in the Department of Developmental Biology, Georg-August-University Göttingen. All sources utilized in this thesis research work are properly quoted. In addition, I confirmed that this thesis is written by me and not under consideration in any other university for award of doctoral degree or any other degree.

Göttingen, 2020.

Dedication

I dedicate the successful completion of this thesis to my loving parents, Rabia Tabassum and Muhammad Abid Khan, husband, Dr. Fazal Wahab and kids, Muhammad Sanan Khan and Alisha Wahab.

Acknowledgement

My sincere and deep gratitude to my mentor and doctoral supervisor Prof. Ernst Wimmer for his continues encouragement, guidance, support and freedom to work on my own research ideas and interests. He has been very kind and supportive during both my research and write-up. His contribution during my doctoral work has made the experiences productive. His logical way of thinking and wide knowledge have been of great value for me. His personal guidance has provided a sound base for the present thesis.

I am deeply obliged to Prof. Dr. Ivo Feußner, University of Goettingen, Goettingen, Germany, for being my doctoral thesis committee member and for his encouragement, valuable suggestions, detailed and constructive comments.

I wish to express my warm thanks to Prof. Gregor Bucher, Dr Kirstine Feussner, Dr. Nico Posnien, Prof. Dr. Sigrid Hoyer-Fender and Dr. Ufuk Günesdogan for all the suggestions during these years of Ph.D. work.

I am greatly thankful to Merle Eggers, Birgit Rossi and Bettina Hucke for providing the congenial environment and facilitation with paper work. Many thanks to Helma Griess, Angelika Löffers, Katrin Kanbach, Elke Küster and Claudia Hinner for technical support. I am greatly thankful to Daval Patel and Tarek Morsi for their great help with computer system related problems and to Beate Preitz for her assistance with teaching of microscopy and for her continuous help whenever I need it. My warmest thanks to Sabrina, Musa Dan'azumi Isah, Hassan Mohammed Mutasim Ahmed, Kolja N. Eckermann, Ingrid Curril, Amel Chtioui, Constanza Tapia Contreras, Vera, Elisa Buchberger, Marita Büscher and Jürgen Dönitz who were always very welcoming whenever I asked them for support. All the members of Lab-1, Lab-2 and Lab-3 are very much appreciated for their scientific discussion and support. I would like to thank Neelam, Sidra, Asia, Nuzat, Muzna, Ammara, Zobia, Sumra and the Pakistani friends in Goettingen for the lively and enjoyable company outside of the campus.

Many thanks to my parents, husband Fazal Wahab and kids, Sanan and Alisha, who were always encouraging, supportive and believed in me that kept me going during the whole period of this doctoral study.

At last but not the least, the financial support in form of Ph.D. stipendium (18 months) of the European Union's Eramus Mundus Program is geartly acknowledged. I am also grateful to Prof. Dr. Ernst Wimmer, University of Goettingen for providing me a Ph.D. stipendium for remaining period of my doctoral work.

Table of contents

Abbreviations

RNAi	RNA interference
CHST5	carbohydrate sulfotransferase 5
ARSB	arylsulfatase B
SUMF1	sulfate modifying factor-1
SLC26A11	sodium independent sulfate transporter
GC-MS	gas chromatography-mass spectrometry
LC-MS	Liquid chromatography–mass spectrometry
MBQ	2-methyl-1,4-benzoquinone
EBQ	2-ethyl-1,4-benzoquinone
BQ-less	benzoquinone-less
C-15	1-pentadecene
C-17	1-heptadecene
OGS	official gene set
PAPS	3-phosphoadenosine-S-phosphosulfate
SULT	sulfotransferase
qPCR	quantitative PCR
GAGs	glycosaminoglycans
MPS VI	mucopolysaccharidosis VI
ARS	arylsulfatase
ER	endoplasmic reticulum
MSD	multiple sulfatase deficiency
FGE	formylglycine generating enzyme
dsRNA	double-stranded RNA
SG	stink gland candidates internal numbering

NOF	non-overlapping fragments
iB	original iBeetle fragments
FC	fold change
OGS	official gene set
wt	wildtype
abd	abdominal gland
thx	prothoracic gland
fm	female individual
m	male individual
DsRed	*Discosoma* species red fluorescent protein
UV/Vis	ultraviolet–visible spectroscopy
HRMS	high Resolution Mass Spectrometry
MS	mass Spectrometry
BQ	benzoquinone

1 General Summary

Defense strategies are common in insects including Coleoptera, the largest animal taxon containing various types of beetles. Stink gland secretion of beetles is playing an important role in their defense against detrimental factors in the environment. These glands produce and release defensive secretions containing several specific varieties of substituted benzoquinone compounds. These defensive chemicals act toxic, repellent and as pesticides. Beetles respond to invaders, parasitic microbes and predators with the secretion of defensive substances. Particularly, these defensive substances of beetle performs several functions such as boiling bombardment or as surfactants against many life-threatening organisms. The defensive compounds of beetles are biosynthesized and stored in a specialized storage and secretory organ called odoriferous defensive stink glands. *Tribolium castaneum* (Coleoptera: Tenebrionidae) produces *p*-benzoquinones and 1-alkenes in stink glands. Morphology of tenebrionid beetles stink gland has been characterized in detail in the past, but not much is known about the genes that are important for the defensive substance production in the stink glands. Understanding molecular mechanisms of the stink gland development and unveiling the metabolic pathway, its regulation, and the enzymes participating in synthesis of defensive chemicals are essential to understand the self-protected mechanism in synthesis of toxic compounds. In the present study, identification and characterization of novel genes playing key roles in the protected biosynthesis of quinones in stink glands of the *T. castaneum* is done by following two genome-wide approaches: 1) tissue specific transcriptomics based on RNA-seq, and 2) genome-wide phenotypic screen based on RNAi-mediated gene silencing. Gland-specifically expressed genes and genes causing a gland-specific knockdown phenotype were analyzed by GC-MS to uncover functions in benzoquinone synthesis. Four such identified candidates genes being part of sulfate metabolism, carbohydrate sulfotransferase 5 (*CHST5*), arylsulfatase B (*ARSB*), sulfate modifying factor-1 (*SUMF1*) and sodium independent sulfate transporter (*SLC26A11*) were then characterized in detail.

In the first part of the study, the RNAi data of the 1st and 2nd phases of the iBeetle screen were analyzed and 130 genes were identified having a potential role in stink gland biology. However, in the rescreen only 69 genes were confirmed. In transcriptomic data, previously 77 genes were identified to be specifically highly expressed in the stink glands. Functional analysis showed that 29 genes are necessary for stink gland function. Importantly, in comparative analysis of the

different functional genomics approaches such as differential expression in transcriptomic data and phenotypic screen only revealed one common candidate gene, which suggests that one approach is not sufficient to uncover the majority of genes that play an essential role in stink gland biology. Our findings suggest that a combination of functional genomic approaches are necessary to uncover genes essential for stink gland development. Particularly, phenotypic screens and transcriptomics approaches complement each other in functional genomics of defensive stink gland physiology.

In the second part of the study, RNAi-mediated gene silencing screening of 4748 genes from the 3rd phase of iBeetle screen was employed to uncover genes essential for development, gland morphological changes and physiology of stink glands. The main purpose of the 3rd phase screen were to identify lethal genes but additional screens were added to identify genes with function in different biological processes. Particularly, I used this screen to uncover further genes essential for morphologyical changes and physiology of stink glands. In this screen, 178 genes were identified to be essential for morphology alterations and changes in gland volatile composition. Gene ontology analysis demonstrated that the majority of these genes encodes for enzymes, regulator/receptor binding, transcription factors, receptors, transporters and 40% with unknown function. From this screen one gene, *CHST5,* that has been analyzed in this study is involved in sulfate conjugation of toxic compounds in the self-protection mechanism. To get a more comprehensive insight into stink-gland function, we also re-analyzed a gland-specific transcriptomic dataset, which was generated in 2013 by Li *et al*. The very recently assembled gene set reference of *Tribolium* (OGS3) allowed us to increase the mapping rates by about 30% compared to the initial analysis. 33 transcripts from the new analysis were not detected previously, since they were only newly annotated in the current version of the *T. castaneum* genome. Since they are very highly expressed in the *Tribolium* gland tissue compared to the control sample, it is definitely worth to analyze these genes in more detail on a functional level.

In the third part of the study, a detailed characterization of a set of newly identified genes with a role in protected biosynthesis of benzoquinone in odoriferous stink glands of the red flour beetle were performed. Especially *CHST5*, *ARSB*, *SUMF1* and *SLC26A11* were selected and characterized in depth. *ARSB* was selected from the study of *Li et al.* (2013), *SUMF1* and *SLC26A11* from the 2nd phase and *CHST5* from the 3rd phase of iBeetle screen on the basis of

strongly altered gland phenotypes and differential expression. Sulfate conjugation is used by many insect for detoxification of phenolic compounds. However, sulfate role in stink gland was not identified before. Sulfonation is used by some insects to neutralize plant defensive substances. On the basis of stink gland transcriptome and iBeetle screen data, we studied the function of *CHST5, ARSB*, *SUMF1* and *SLC26A11* via RNAi-mediated gene knockdowns, qPCR, GC-MS, LC-MS and *in situ* hybridization. LC-MS analysis showed presence of sulfate precursors i.e., sulfated glycosylated phenolic precursors in the knockdown situation of the sulfatase. Put together, these studies suggest that these genes play an impotant role in the self-protected biosynthesis of benzoquinone in the red flour beetle stink glands.

2 General Introduction

2.1 *T. castaneum* as an insect model

Arthropods make the largest phylum of animals. Arthropods constitute more than 80 per cent of animals species on earth. Insecta is the largest class among phylum arthropoda. They are making up more than half of the living animals' species (Stork, 2009). Within insecta, Coleoptera with more than 380,000 known species of beetles is the most diverse and species rich order (Crowson, 1960; Hunt et al., 2007; Stork, 2009). Beetles make up ~25% of all reported species of animals on this planet (Crowson, 1960; Stork, 2009) and still many species need to be described (Grove and Stork, 2000).

Beetles have adopted to survive in almost all kinds of environments on earth (Crowson, 1981). To successfully adapt in various kinds of habitats globally, beetles have developed a variety of strategies for coping with adverse environmental conditions and avoiding attack by parasites, pathogens and predators. For example, externally the sclerotized exoskeleton of beetles not only protects them from desiccation but also from the infestation of microorganisms (Crowson, 1981; Noh et al., 2016; Schierling and Dettner, 2013; Stork, 2009). Internally, many beetle families have developed a specialized set of secretory organs called odoriferous or stink glands for chemical defenses (Tschinkel, 1975). In these glands, the synthesis of different types of chemicals for defense purposes occurs. These chemicals are released in emergency situations or condition to the environment. One of the families of beetles which produced defensive substances for their defense is Tenebrionidae. Tenebrionid beetles, which are commonly called darkling beetles, are producing large amounts of hydrocarbon-containing defensive secretions bearing several specific varieties of substituted benzoquinone compounds (Blum, 1981; Brown et al., 1992). These defensive chemicals act as toxic, repellent, bacteriostatic and fungistatic oils (Pedrini et al., 2015; Yezerski et al., 2007). One important group of darkling beetles is of flour beetles which belong to genera *Tribolium*.

T. castaneum (red flour beetle) is a member of the beetle genera *Tribolium* (Hunt et al., 2007). *T. castaneum* is a pest of cereal products. It attacks stored wheat, and many other grains in storage. In recent years, it has emerged as one of the key insect models second only to *Drosophila*. It is one of the

best model organisms for understanding metamorphosis, comparative evolutionary developmental biology, insect/beetle diversity, basic physiology and insect pest control (Brown et al., 2009). The red flour beetle is also widely used in basic insect physiology and insect pest management research. The development of red flour beetle linkage maps, on the basis of molecular markers that have about 1 cM (~300 kb) genome wide marker resolution, have made *T. castaneum* an important model organism for genetic studies (Beeman et al., 1996; Lorenzen et al., 2005). In particular, the availability of a number of genomic and genetic tools for *T. castaneum* made it one of the great genetic model organism (Brown et al., 2009). Important genetics tools for the red flour beetle are: development of molecular markers based linkage maps (Beeman et al., 1996; Lorenzen et al., 2005), transposon-based genetic transformation (Lorenzen et al., 2003), expression systems (Schinko et al., 2010), a misexpression system on basis of heat-shock (Schinko et al., 2012), systemic RNAi response based reversed genetics and the RNAi-based genome-wide iBeetle screen (Bucher et al., 2002; Schmitt-Engel et al., 2015), insertional mutagenesis based forward genetics (Lorenzen et al., 2005; Trauner et al., 2009) as well as detailed stink gland transcriptomic data (Li et al., 2013). Therefore, *T. castaneum* is a very useful model for physiology, genetics, comparative evolutionary developmental biology, adult insect diversity, metamorphosis, ethological and food safety research.

In *T. castaneum*, the process of synthesis of the defensive compounds in stink gland is molecularly still not fully understood. There are not much data available on which genes are involved in this process. A major constituent of defensive secretion of the red flour beetle are *p*-benzoquinones and their derivatives (Loconti and Roth, 1953; Markarian et al., 1978). There are just two publications (Happ, 1968; Görgen et al., 1990), which investigated the process of the quinone and alkene synthesis. The chemical secretions of *Tribolium* beetles have attracted special attention of the scientists when they observed change in color of flour medium due to the beetle secretion (Payne, 1925; Lis et al., 2011). Moreover, deciphering the mechanisms for self protection against the defensive compounds is also important factor for making the red flour beetle an ideal insect model.

2.2 Functional genomics approaches to identify tissue specific functions

2.2.1 The iBeetle screen

The German scientists working on *T. castaneum* have initiated a collaborative large scale genome-wide RNAi-mediated gene disruption screening known as the iBeetle screen (Schmitt-Engel et al., 2015). The

aim of iBeetle project is to unveil genes involved in different processes which are either peculiar to beetle and absent from *Drosophila* (embryonic leg development, stink gland, etc.) or are not easy to explore in the fly (somatic stem cells, involuted head, etc.) (Li et al., 2013; Posnien et al., 2010). This work will make *T. castaneum* as a model system for identification of genes important for different conserved processes (such as *Drosophila* muscle development) which are not present due to species specific gene loss in well-known model organisms or functional redundancy due to gene duplication, etc (Schmitt-Engel et al., 2015). Till date, in the iBeetle screen, many novel genes pivotal for stink glands, formation of gametes, embryonic development and metamorphosis have been uncovered.

In the iBeetle screening, along other genotype and phenotypic information, all gland phenotypic information is stored and provided online. The iBeetle online database information is freely available to everyone and the altered phenotypes documented in iBeetle can be repeated (Dönitz et al., 2015). The identification of these genes is not possible by the candidate gene selection approach because many of these genes are either not present in *Drosophila* or were not observed by difference in analysis of gene expression such as physiology of stink gland (Li et al., 2013; Schmitt-Engel et al., 2015; Schultheis et al., 2018; Siemanowski et al., 2015). The iBeetle screen has been done in three phases. In the first phase, the effects of dsRNA injections in larva and pupa were carried out and are already completed (Schmitt-Engel et al., 2015). This screen purpose was to unveil genes essential for metamorphosis and embryonic phenotypes of beetles. In first phase, 4480 genes were check in the larval screen and 5300 RNAi-mediated genes disruption effect were screened in the pupae. However, consistent data are obtained for 3400 genes for both larval and pupal screenings. In this screen, the phenotypes of late metamorphosis and embryological defects, especially effect of gene RNAi induced gene knockdown was checked on ovaries and stink glands along with other alterations. In the second phase, pupal screening of 3200 genes was performed with dsRNA injection of different randomly selected genes function in various biological processes such as stink gland biology, ovary development, muscle formation and embryogenesis (Schultheis et al., 2019).

In the 3rd phase of iBeetle screen, RNAi-mediated gene silencing screening of 4748 genes was done to identify lethal genes. In addition, I used this screen to uncover further genes essential for development, morphological changes and physiology of stink glands. I as a screener performed the screening of the stink gland biology in the 3rd phase of iBeetle screening.

2.2.2 Transcriptome analysis of stink gland

Li and colleagues (2013) have carried out for the first time transcriptome analysis of *T. castaneum* defensive stink glands. This provided a very useful data set for uncovering of new genes that have a role in production of defensive stink gland secretion. Approximately, 27.8–29.7 RNA-seq million reads were obtained for each sample. Of note, 55 to 61% of obtained mRNA reads were mapped to *T. castaneum* genome at the time (Kim et al., 2010; Wang et al., 2007). To complement the functional analysis of genes related to stink gland, we reanalyzed the transcriptomic dataset provided by Li *et al.* (2013). This dataset contained samples from various gland types, including prothoracic and abdominal glands from female and male beetles (see Li et al. 2013 and Material and Methods). We used a newly assembled genome (Herndon et al., 2020) to map the gland-specific transcripts in order to find potentially new genes that are important for the stink gland function in *Tribolium.*

Transcriptomic datasets generated using High Throughput Sequencing (HTS) techniques have the advantage that they – in theory – include all transcripts that are expressed in a specific tissue at a specific time point in contrast to e.g., Micro Array datasets. Final detection of expressed transcripts relies heavily on the reference genome that is used to map the reads against. Transcriptomic references and assemblies of genomes are improving constantly and therefore re-mapping 'older' RNAseq datasets against a new reference gene set provides the opportunity to gain new knowledge without necessarily generating and sequencing new samples. We chose this approach to find new gland-specific transcripts, which could not have been detected in the analysis of 2013, due to the fact, that the reference genes were missing in the old genomics reference. Using the very recently assembled gene set reference of *Tribolium* (OGS3), allowed us to increase the mapping rates by about 30% compared to the initial analysis.

2.3 Stink glands

2.3.1 Structure of stink glands in *T. castaneum*

In both sexes of *T. castaneum*, the chemical defensive function is performed by two pairs of specialized defensive stink glands (Markarian et al., 1978). These glands are highly specialized for synthesis and secretion of various chemicals for beetle defence. One pair of the stink glands is

present in the abdomen and the other in prothoracic region (Roth, 1943). The abdominal glands are connected to the last abdominal sternites in posterior region of the beetle abdomen and open to outside through the last abdominal pleurite (Roth, 1943; Sokoloff, Ackermann and Overton, 1967; Sokoloff, 1972). The prothoracic glands are elongated sacs and are lying in the anterolateral portion of the beetle thoracic cavity. The prothoracic glands are opening of a membrane between the prothorax and the head (Sokoloff, 1972) Figure 1.

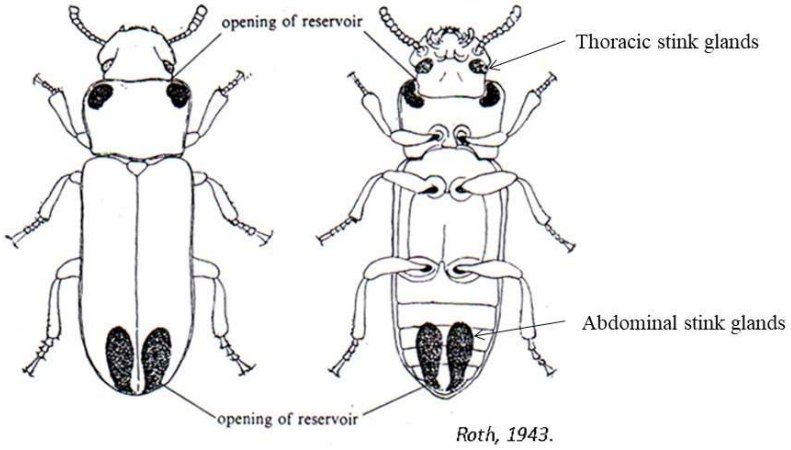

Figure 1. Defensive stink glands in *Tribolium.* Diagram shows the position of prothoracic and abdominal glands (dorsal; and ventral view) in *T. casteneum* (Roth, 1943).

In the *T. castaneum* stink glands, there are two main portions of each gland: manufacturing portion and storing portion. In the manufacturing portion, the defensive secretions are produced in the glandular cells (Eisner et al., 1964; Happ, 1968). The storing portion is consisting of a chitinous reservoir. There are two distinct types of defensive secretion manufacturing glandular cells in *T. castaneum* abdominal stink glands. These cells are called type I cells (cell-1) and type II cells (cell-2). The cell-1 covers all the surface of the storage reservoir and are present as single or paired cells. Each individual cell possesses a large vesicle, inside which a cuticle-lined organelle is present (Eisner et al., 1964; Happ, 1968). The organelle can be divided to a head and a cylindrical body. This organelle is connected via a cuticle-lined efferent tubule with the gland reservoir (Happ, 1968). The cell-1 is not present in thoracic glands (Eisner et al., 1964; Roth, 1943).

The cell-2 of stink glands of red flour beetles form lobules. Each individual cell-2 is formed by two cells, 2a and 2b. Both 2a and 2b cells contain a nucleus and a large vesicle in the middle (Happ, 1968). Just like cell-1, there is a cuticle lined organelle in the middle of cell-2 vesicle. However, the structure of cell-2 vesicle is very complex in comparison to vesicle of cell-1. The head of organelle is situated in vesicle 2a, constricts and subsequently expands into a bulb inside the vesicle 2b. The bulb narrows down to a tubule that passes through cell aggregates before entering the reservoir. Cell-type 1 is absent in thoracic glands, while the cells type 2 structure is similar in both prothoracic and abdominal glands (Eisner et al., 1964; Roth, 1943).

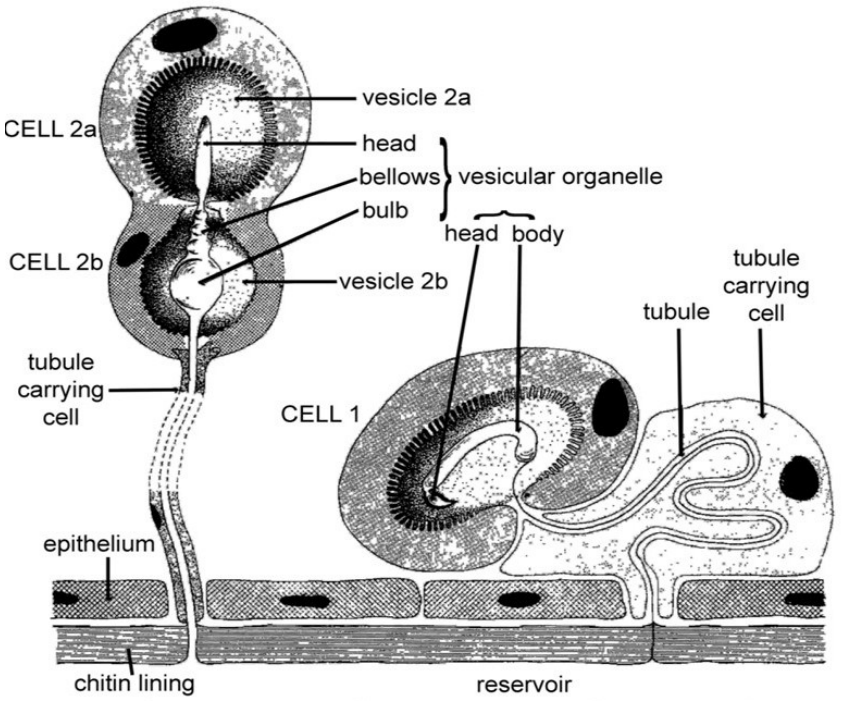

Figure 2. Reference diagram of secretion producing cells in defensive stink glands of *E. longicollis* and *T. castaneum (*Happ, 1968).

2.3.2 Composition of *T. castaneum* Stink Gland Secretion

Ultraviolet-visible spectrometry and chemical analyses identified that quinones and hydrocarbons are two major groups of chemical compounds present in stink glands of beetles. The main quinones

derivatives noted in stink glands are 2-ethyl-*p*-benzoquionone (EBQ), 2-methyl-*p*-benzoquinone (MBQ) and hydroquinone (Alexander and Barton, 1943; Ladisch et al.,1967; Markarian et al., 1978; Howard, 1987). In 1995, Pappas and Morrison described the methods for extraction of defensive secretion and identified EBQ and MBQ in defensive glands of *T. castaneum* and *T. confusum* (Pappas and Morrison, 1995). Besides quinone, a number of hydrocarbons are also present in glandular secretions of many *Tribolium* species. In particular, 1-pentadecene is a major non-quinone component of *T. castaneum* and other species of the *Tribolium* secretion (Endt and Wheeler, 1971; Suzuki et al., 1975; Keville and Kannowski, 1975; Markarian et al., 1978; Luciana Villaverde et al., 2007).

In 2013, Li and coworkers demonstrated that both prothoracic and abdominal glands of the red flour beetle showed the same set of volatile secretion by the GC-MS analysis. They noted that five main constituents of the stink gland secretion are *para*-benzoquinones MBQ, EBQ, hydrocarbons 1 pentadecene, 1-heptadecene and 1,8-heptadecadiene (Figure 3) (Li et al., 2013; Suzuki et al., 1975). As compared to MBQ, EBQ levels are higher (Markarian et al., 1978; Pappas and Wardrop, 1996a; Unruh et al., 1998) in both male and female *T. castaneum* glands. There was no sex specific differences in levels of MBQ and EBQ.

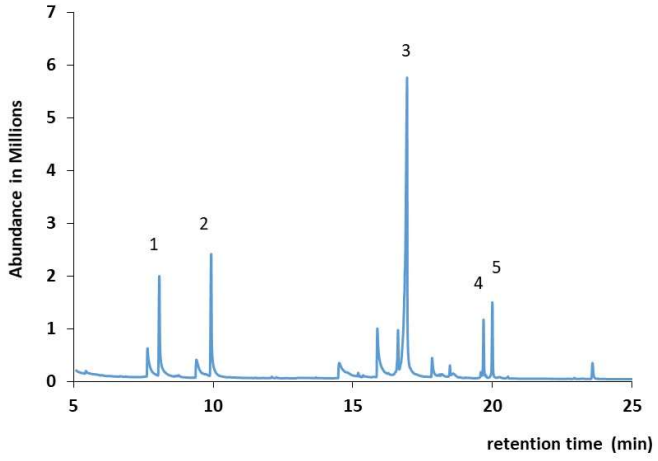

Figure 3. Chromatogram of the GC-MS analysis of stink glands. The main volatile substances noted in wild type beetle stink glands are: 1: MBQ, 2: EBQ, 3: 1-pentadecene, 4: 1,8-heptadecadiene, 5: 1-heptadecene.

2.3.3 Benzoquinones in the beetle defensive secretions

Benzoquinones are volatile, highly unstable reactive and toxic. It has been noted that cuticular linings of beetles are protected internally and externally from their own secretions (Roth, 1943; Happ, 1968). Roth and Howland (1941) reported that exposure of juvenile beetle to high concentrations of adult beetles stink gland benzoquinones caused a premature death. For prevention of autointoxification, the secretion biosynthesis in the stink gland of the adult beetle commences after completion (4 days post-hatching) of the cuticle tanning process (Wirtz et al., 1978; Unruh et al., 1998). In *Tribolium* beetles, the gland secretion is produced in cuticle-lined organelles that is isolated from somatic cells (Happ, 1968) and also stored in cuticle line storage sacs (Roth, 1943).

The defensive secretion of beetles performs several functions. The defensive secretion of adult beetles is rich in quinone, which has wide activity against bacteria and other microbes (Prendeville and Stevens, 2002). This has been denoted as immune defense that provides protection against pathogens (Joop et al., 2014; Rafaluk-Mohr et al., 2018). The benzoquinones such as MBQ and EBQ present in stink glands of beetle and other insects have toxic, repellents and irritant effect (Eisner et al., 1964; Tschinkel, 1975; Blum, 1981; Howard, 1987) while alkenes, in particular 1-pentadecene, also have some unpleasant and spreading activity (Schildknecht et al., 1964; Peschke and Eisner, 1987; Unruh et al., 1998).

The red flour beetle infested grains and flour become pinkish with unpleasant odour due to benzoquinones ((Payne, 1925; Roth, 1943; Smith et al., 1971). It has been reported that benzoquinones act as anti-aggregation pheromones, forcing *T. castaneum* to disperse from high-density population and look for fresh food resources (Duehl, Arbogast and Teal, 2011). The benzoquinone has been documented to have activity similar to quinones (Roth and Howland, 1941), cresols and phenols (Markarian et al., 1978).

2.3.4 Benzoquinone synthesis model in *T. castaneum*

In 1968, Happ carried out a detail histochemical analysis of the tenebrionoids *T. castaneum* and *Eleodes longicollis* quinone-producing glands. According to the model proposed by Happ, the defensive gland cytoplasm and quinone synthesis chambers are separately present. The *para*-

quinone is sequentially synthesized in a two-chambered secretory unit that consist of cuticular organelles, secretory cells and their associated vesicles, and afferent tubules.

The biosynthesis of benzoquinone occurs in cell type 2 secretory cells of stink glands. Phenolic ß -glucoside, the proposed precursors of quinone, located in the cytoplasm of cell type 2a secretory cells is secreted into the lumen of cell type 2a vesicle. Inside that vesicle, the phenolic ß -glucoside is supposedly hydrolysed to quinol and glucose by a ß-glucosidase and resulting glucose may enter back to the cytoplasm. Subsequently, the free and nontoxic quinol is transferred to the vesicular organelles where under the action of polyphenol oxidase a portion of quinol is oxidized to 1,4 quinones. The quinol and 1,4 quinone mixture is transported through the efferent duct to where a haemoprotein peroxidase induce oxidization of the remaining quinol. This results in formation of highly reactive toxic *para*-quinones in cuticle-lined reaction chamber. The *para*-quinones are produced and stored in the head of vesicular organelle which is separated from the cytoplasm of the secretory cells (Eisner et al., 1964; Happ, 1968).

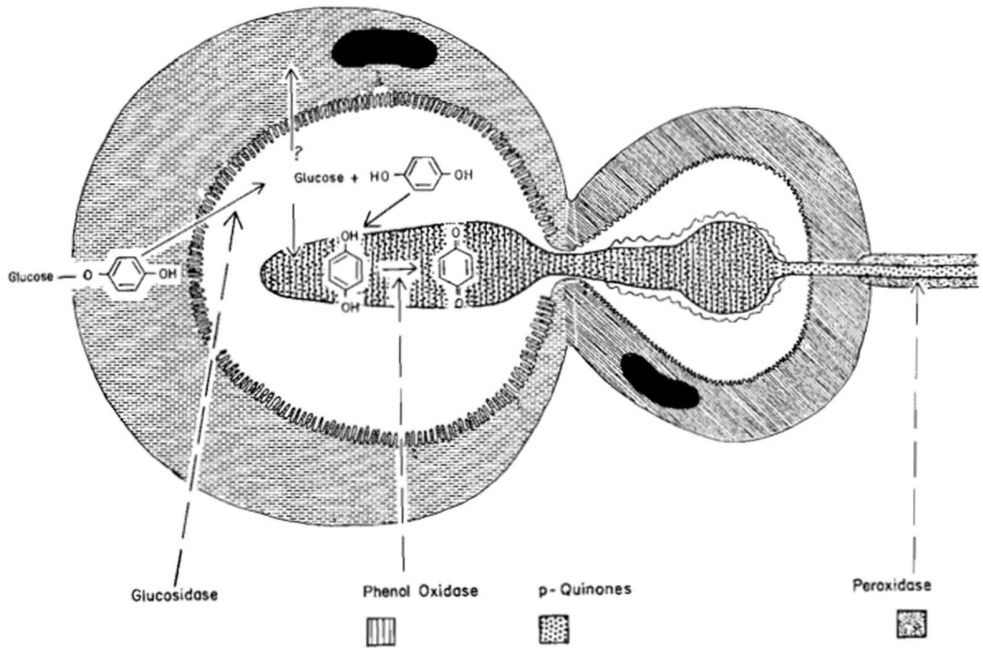

Figure 4. Hypothetical scheme of quinone production in secretory unit 2 of the defensive glands of *E. longicollis* and *T. casteneum (*Happ, 1968).

In the secretory cells of glands, phenolic ß-glucoside is present in the apical portion. This phenolic ß-glucoside precursor is transported to inside of the gland and then converted to active benzoquinones by action of a number of various enzyme actions (Happ, 1968). The benzoquinone is used by the red flour beetles and many other arthropods in chemical defense. As bezoquinone is very toxic and reactive, hence, it requires careful handling and self-protection detoxication systems.

2.3.5 Self-protection mechanism in stink glands

In order to decrease the autodetoxicative effects of defense compounds, the insects including beetles have evolved a number of mechanisms for detoxication (Blum, 1981). Benzoquinones are major defensive compounds of beetles. These compounds are very unstable, reactive and toxic. *Tribolium* beetles have developed a complex system to safely produce benzoquinones (Blum, 1981). The tenebrionids beetles are protected from toxic effect of their secretions through the formation of cuticular linings in structures associated with toxic defensive compounds production, storage and secretion (Roth, 1943; Happ, 1968). In *Tribolium* beetles, the self-protection is achieved by the partition of the defensive secretion from other adjacent body cells. The defensive secretions are produced in the organelles which are lined by cuticle (Happ, 1968) and are stored in reservoirs which arise from the cuticle invaginations. Of important note, the young *T. castaneum* adults do not possess the defensive secretions, indicating that defensive secretions are produced only after formation of a self-protective cuticle linning barrier (Unruh et al., 1998). Hence, if the development of adequate self-protective barrier is disturbed then the pests will harm themselves. This can lead to better control and management of beetle pests.

2.4 Sulfate metabolism in respect to detoxification and self-protection

2.4.1 Sulfate conjugation system

The sulfate conjugation system is a very important detoxification mechanism in many organisms. In several insect species, sulfate conjugation is a common mechanism for phenolic compound detoxification (Kerkut, 1985). *In vivo* sulfoester conjugation occurs in a number of insect species after phenolic compounds treatment. Of note, sulfate conjugation is considered as a primitive type of detoxification mechanism because *Peripatus*, a primitive arthropod, has been reported to

detoxify phenols by phosphate and sulfate conjugation with absence of glycoside conjugation (Jordan, McNaught and Smith, 1970). The insect and mammalian sulfotransferases (SULTs) have been documented to show similar properties especially with regard to subcellular localization, cofactor requirements and pH optima (Capinera, 2008).

The SULT presence has been noted in gut, fat body and malpighian tubules in different insects' species. The insect SULT system proper function depends on Mg^{2+}, ATP and inorganic sulfate for the sulfonation. In insects, sulfate conjugation occurs in a 3-step reaction as shown below (Abou-Donia, 2015).

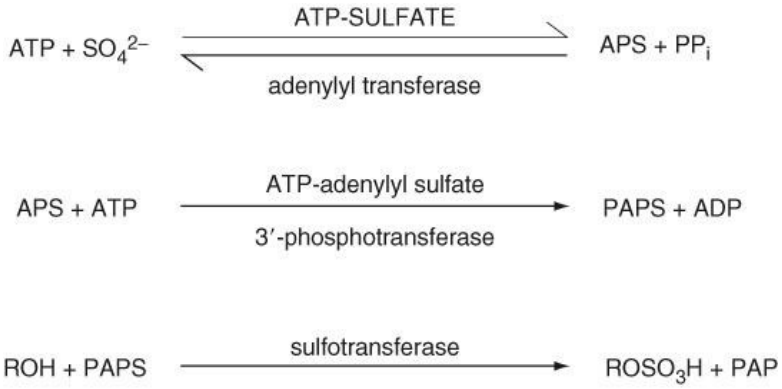

During sulfate conjugation of phenol, suphate is transferring to phenolic hydroxyl groups from the 3-phosphoadenosine-S-phosphosulfate (PAPS) by the action of SULT (Falany, 1997). SULTs catalyze sulfate transfer to the amino group or hydroxyl of a number of different acceptors molecules, such as carbohydrates, peptides, lipids, xenobiotics, hormone precursors, etc. In this reaction, a sulfate ester bond is formed by SULTs by catalyzing transfer of a sulfate ($-SO_3$) from the PAPS donor to a nitrogen or oxygen of the acceptor molecule (Falany, 1997). On the basis of cellular presence, SULTs are distinguished into either cytosolic or membrane bound enzymes (Chapman et al., 2004). Both membrane bound and cytosolic SULTs are present in *Caenorhabditis elegans* (Hattori et al., 2006). Cytosolic SULTs have been reported from different arthropods species of insects, such as *Spodoptera frugiperda* (Grün et al., 1996), *Bombyx mori* (Hattori et al., 2007) and *Drosophila melanogaster* (Hattori et al., 2008; Liu et al., 2008). Sulfonation of both synthetic and natural chemicals and biomolecules take place in all organisms from bacteria to humans (Chapman et al., 2004; Gibbs et al., 2006; Niehrs et al., 1990; Strott, 2002). Even though

the insects detoxification systems have not been given great attention, however, insects detoxification system is basically similar to well-reported mammalian detoxification systems.

2.5 Objective of the study

General Objective

The general overall objective of the present study was to identify and characterize novel genes with a role in benzoquinone synthesis in the stink glands of the red flour beetle.

Specific Objectives: We specifically aimed to:

I. carry out comparative functional genomic analysis of RNAi-mediated gene disruption and RNA-seq data in the identification of novel genes with a role in benzoquinone biosynthesis in *T. castaneum* stink glands.
   - The RNAi-mediated stink gland phenotype data were obtained from 1st and 2nd phases of iBeetle screen while transcriptomic data were taken from Li *et al.* 2013.
   - Rescreening was performed for confirmation of morphological phenotypes.
   - GC-MS analysis was done for alterations in gland contents.
   - Bioinformatics analysis was carried out for the selected genes with a confirmed role in stink gland function.

II. perform gland phenotype screening in the 3rd phase of iBeetle Screen
   - In the 3rd phase, the pupal screening was done with dsRNA injection of remaining genes models in different biological processes including stink gland biology.
   - I, as a screener, performed the screening of stink glands morphology and GC-MS analysis for alterations in gland contents.after RNAi-mediated gene disruption.
   - Bioinformatics analysis was carried out for the selected genes with a confirmed role in stink gland.
   - Re-analysis of the stink gland tanscriptome data with novel genomic gene set.

III. decipher molecular genetic function of selected genes reported for the quinone production.
   - Genes were selected based on the altered stink gland morphology from 2nd and 3rd of the iBeetle screen as well as from the transcriptome data.
   - Rescreening was performed for the confirmation of morphological phenotypes.

- GC-MS analysis of gland tissue was done for alterations in gland contents.
- *In situ* hybridization was performed.
- Semiquantitative RT-PCT was done.
- LC-MS analysis was done on gland tissues.
- Specifically, I worked on the unveiling the role of genes regulating sulphur metabolism in stink glands of *T. castaneum* such as *CHST5*, *ARSB*, *SUMF1* and *SLC26A11* to identify these genes involvement in the protective biosynthesis of benzoquinone.

3 Results

The results of this thesis are arranged in form of three manuscripts that comprise of the following sections, preceded by a page describing:

- The manuscript major aim in relation to the thesis as a whole
- Contribution of authors in the research work
- Status of the manuscript

References quoted in the manuscript are also listed at the end of each manuscript. Of important note, references cited in the general introduction and the general discussion are listed at the end of the thesis chapter **5.**

3.1 Phenotypic screen and transcriptomics approach complement each other in functional genomics of defensive stink gland physiology of the red flour beetle (*Tribolium castaneum*) stink glands.

Chapter 1 summary

In this chapter, comparative analysis of the effectiveness of different functional genomics techniques such as a genome-wide phenotypic screen based on RNAi interference (RNAi) and a transcriptomics approach based on RNA-Seq have been explored in uncovering functions of various genes in respect to biology and volatile content in the red flour beetle stink glands. In two completed phases of RNAi screening in the iBeetle project, 130 genes were noted to be important for stink gland functioning. In a rescreen, we could confirm 69 genes. Based on the stink gland transcriptomic data, 77 genes were identified to be specifically highly and differentially expressed in the stink gland. RNAi-mediated disruption and GC-MS analysis showed that 29 genes were necessary for the stink gland function. Only one gene was identified in both type of genome-wide screen. This indicates that one type of functional genomic data is not sufficient in uncovering most genes important for stink gland function. Our comparative functional analysis suggests that a phenotypic screen and a transcriptomics approach complement each other in functional genomics of the defensive stink gland physiology.

Sabrina Lehmann[1], **Bibi Atika[1]**, Bernhard Weißbecker[2], Gregor Bucher[3], Ernst A. Wimmer[1†]

Authors contribution to the practical work

Sabrina Lehmann: 1st phase genes reconfirmation , GC-MS analysis and microscopy

Bibi Atika: 2nd phase genes reconfirmation, GC-MS analysis and microscopy

Status: Work in progress

Phenotypic screen and transcriptomics approach complement each other in functional genomics of defensive stink gland physiology of the red flour beetle (*Tribolium castaneum*) stink glands.

Sabrina Lehmann[1*], **Bibi Atika[1*]**, Jianwei Li[1‡], Bernhard Weißbecker[2], Gregor Bucher[3], Ernst A. Wimmer[1†]

Sabrina.Lehmann@web.de

bibi.atika@biologie.uni-goettingen.de

Jianwei.Li@ars.usda.gov

bweissb@gwdg.de

gregor.bucher@bio.uni-goettingen.de

ewimmer@gwdg.de

[1] Georg-August-University Goettingen, Johann-Friedrich-Blumenbach-Institute for Zoology and Anthropology, Dept. of Developmental Biology, GZMB, Ernst-Caspari-Haus, Justus-von-Liebig-Weg 11, 37077 Goettingen, Germany

[2] Georg-August-University Goettingen, Buesgen-Institute, Dept. of Forest Zoology and Forest Conservation, Buesgenweg 3, 37077 Goettingen, Germany

[3] Georg-August-University Goettingen, Johann-Friedrich-Blumenbach-Institute for Zoology and Anthropology, Dept. of Evolutionary Developmental Genetics, GZMB, Ernst-Caspari-Haus, Justus-von-Liebig-Weg 11, 37077 Goettingen, Germany

[*] Equal contribution

[†] Corresponding author: ewimmer@gwdg.de, Tel.: +49 551 39 28666; Fax: +49 551 39 25416

[‡] Present address: The Pirbright Institute, Ash Road, Pirbright, Woking, GU24 0NF, UK

Abstract

Tribolium castaneum is a significant worldwide pest of stored grains. It produces and releases defensive secretions containing several specific varieties of substituted benzoquinone compounds. These defensive chemicals act as toxic, repellent, bacteriostatic and fungistatic oils. Unveiling the metabolic pathway, its regulation, and the enzymes participating in synthesis of these defensive chemicals is essential for developing potential targeted controlling strategies for not only this important beetle pest but possible also other devastating beetles. The present study aims to combine several functional genomic approaches such as a genome-wide phenotypic screen based on RNA interference (RNAi) and a tissue specific transcriptomics approach based on RNA-Seq to help uncover benzoquinone biosynthetic, potential self-protection and detoxification genes. In the RNAi data of the iBeetle screen, 130 genes were identified to have a potential role in the stink gland biology. However, in a rescreen we confirmed only 69 genes (about 53%), with a stink gland phenotype. Of those, 60 genes showed the exact iBeetle-annotated gland phenotype, whereas the knockdown of other nine genes resulted in gland phenotypes different from the iBeetle-noted ones, which may be due to a different amount of injected dsRNA and thus a doses-dependent effect. In previously analyzed transcriptomic data, 77 genes were identified to be specifically and highly expressed in stink glands. However, functional analysis showed that knockdown of the 29 genes caused a visible stink gland phenotype. Strikingly, our analysis indicates that one set of functional genomic data is not sufficient in elucidating the majority of the genes important for a stink glands biology. Our findings suggest that the combination of functional genomic approaches is required to uncover a majority of genes essential for stink gland development. Particularly, phenotypic screen and transcriptomics approach complement each other in functional genomics of defensive stink gland physiology.

Introduction

Recent advances in functional genomic technologies permit establishment of sequence and/or gene expression databases to explore economically important species (Aw et al., 2010; Mckenna, 2017; Kumar et al., 2018; Schoville et al., 2018; McKenna et al., 2019; Seppey et al., 2019). Functional genomics is a broad approach for uncovering functions and interactions of different genes and their protein products not only within different regions of body but also single type of a specific cell (Kaushik, Kaushik and Sharma, 2019). It aims to correlate the genotype and phenotype on genome-wide level. Functional genomics includes a wide range of cellular and molecular techniques with the overall aim of unveiling structure, function and regulation of a gene by utilizing high-throughput methods. Major platform technologies of functional genomics include large-scale mutagenesis, expression profiling (mRNA and protein levels), homology searching, structural comparisons and protein interaction analysis (Kaushik, Kaushik and Sharma, 2019). Most of the functional genomic techniques have been widely used in *T. castaneum* (Dittmer et al., 2012; Kumar et al., 2018; Li et al., 2013, p. 20102; Posnien et al., 2009; Schmitt-Engel et al., 2015b; Trauner et al., 2009; Ulrich et al., 2015).

Coleoptera with about 400,000 known species of beetles is the biggest order of not only phylum Insecta but also whole kingdom Animalia (Crowson, 1960; Stork, 2009; Bouchard et al., 2011). Beetles survive in almost all kinds of environments on earth (Crowson, 1981). To successfully adopt in various kinds of habitat globally, beetles have developed a variety of strategies for coping with adverse environmental conditions and avoiding attack by parasites, pathogens and predators. For example, externally the sclerotized exoskeleton of beetles not only protects them from desiccation but also from infestation of microorganisms (Schierling and Dettner, 2013; Noh et al., 2016). Internally, many beetle families have developed a specialized set of secretory organs called stink glands for chemical defenses (Tschinkel, 1975; Brown et al., 1992). In these glands, the synthesis of different types of chemicals for defense purposes occurred. These chemicals are released in emergency situations. One of the species of beetles which produces defensive substances for their defense is *T. castaneum* (Markarian et al., 1978).

T. castaneum secretes a variety of defensive chemicals (Loconti and Roth, 1953). The chemical secretions of *Tribolium* beetles have attracted special attention of scientists when they observed

change in color of flour medium due to beetle secretion (Payne, 1925; Lis et al., 2011). These defensive chemicals act as toxic, repellent, bacteriostatic and fungistatic oils (Yezerski et al., 2007; Pedrini et al., 2015). A major constituent of defensive secretion of the red flour beetle is *p*-benzoquinones and its derivatives (Loconti and Roth, 1953; Markarian, Florentine and Pratt, 1978). In both sexes of *T. castaneum*, the chemical defensive function is performed by two pairs of specialized defensive stink glands (Markarian et al., 1978). One pair of the stink glands is present in the abdomen and other in the prothorax (Roth, 1943). In *T. castaneum* stink glands, there are two distinct portions: one is producing the secretion while second region is responsible for the storage of defensive secretion (Eisner et al., 1964; Happ, 1968).

The examination of gland secretion via UV spectral and chemical analyses identified MBQ (2-methyl-1,4-benzoquinones) and EBQ (2-ethyl-1,4-benzoquinones) as major constituents (Yezerski et al., 2000; El-Desouky et al., 2018) in both abdominal and prothoracic glands of female and male of *T. castaneum*. Besides quinone, a number of hydrocarbons are also present in glandular secretion of many *Tribolium* species. In particular, 1-pentadecene is a major non-quinone component of *T. castaneum* and other species of the genus *Tribolium* (Tschinkel, 1975; Howard, 1987; Luciana Villaverde et al., 2007; Suzuki et al., 1975a). Moreover, Markarian and colleagues (1978) documented the presence of low amounts of 1,6-pentadecadiene in *T. castaneum* secretion (Markarian et al., 1978). In 2013, Li and coworkers demonstrated that both prothoracic and abdominal glands of the red flour beetle showed the same set of volatiles secretion by GC-MS (Li et al., 2013) analysis. Five main constituents of the stink gland secretion are *para*-benzoquinones MBQ, EBQ, hydrocarbons 1 pentadecane, 1,8-heptadecadiene and 1-heptadecene (Li et al., 2013; Suzuki et al., 1975). As compared to MBQ, EBQ levels are higher (Unruh et al., 1998) in both male and female *T. castaneum*. However, molecular mechanism of defensive chemical synthesis, storage and release is poorly understood.

The iBeetle project is an important part of the red flour beetle functional genomics (Dönitz et al., 2015). It aims to elucidate the role of all *Tribolium* genes and their encoding protein products in *Tribolium* development and physiology after RNAi-mediated gene disruption (Dönitz et al., 2015; Schmitt-Engel et al., 2015). RNAi is a mechanism of post-transcriptional regulation of gene function (Farrell, 2010). RNAi is working systematically in *Tribolium* (Bucher, Scholten and Klingler, 2002). The application of RNAi in *Tribolium* studies deducing functional genomics

provide novel opportunities for genetic studies and also in pest management (Ulrich et al., 2015). In the iBeetle project, RNAi screening is done at developmental stages such as larva and pupa of *Tribolium* (Schmitt-Engel et al., 2015). Many *Tribolium* genes can be promptly monitored for particular knockdown phenotypes after knockdown via administering the respective dsRNA at different development stages. Besides the RNAi approach of functional genomic, comprehensive data on role of specific genes and their functions in beetle can be obtained from bulk and single cell RNA-seq data (Dittmer et al., 2012; Li et al., 2013). A major aim of this study is to uncover and describe genes involved in the stink gland biology. Different techniques of functional genomic can be applied to the study of the stink gland biology. Particularly, in this study, we comparatively analyzed transcriptomics and genome-wide phenotypic screen findings to help unveil and describe genes with a role in the protective benzoquinone synthesis in *Tribolium* stink glands.

Materials and Methods

Beetle strain maintenance

T. castaneum (San Bernardino) wildtype strain which originated from Alexander Sokoloff, California were used in 1st and 2nd iBeetle screening phases. The beetles were maintained at 27°C temperature on whole grain flour. The relative humidity was kept between 30-50%. Injected pupae were kept at 32°C on whole grain flour for gene knockdown experiments. The phenotypic analysis were conducted on ten days adult beetles.

Origins of candidate genes

iBeetle rescreen

In 1st phase of the iBeetle rescreen, candidate genes with altered stink glands phenotypes were selected from the iBeetle database (Schmitt-Engel et al., 2015; Dönitz et al., 2015). For the confirmation of these phenotypes, the selected candidate genes were rescreened. In rescreening, dsRNA was designed for non-overlapping fragments (NOF) independent from the original iBeetle (iB) fragments. These NOF were used to rolled out the possibility that reported alteration in gland phenotypes might be caused by an off-target effects of the dsRNA injection. However, overlapping fragments were used in rescreen for the genes having short coding sequence.

In the 2nd phase of the iBeetle rescreen, 73 candidate genes were selected. dsRNA of the original iBeetle (iB) fragments of the selected candidate genes were injected for phenotype confirmation. 28 genes resulted in altered phenotype and were confirmed, 19 genes were selected for injection with non-overlapping fragments. Out of these 19 genes, 18 genes were confirmed and 1 gene was selected on the basis of their strong phenotype.

Gland transcriptome data

In 1st and 2nd iBeetle rescreening, transcriptome data of *Tribolium* stink gland were examined for genes with alteration in genes expression in the gland tissues for their fold change (FC) value and total number of reads. The stink gland transcriptome data has been previously documented in Li et al. (2013).

Identification of conserved domains

The nucleotide or amino acid conserved domains were identified using the National Center for Biotechnology Information online search tool (http://www.ncbi.nlm.nih.gov/Structure/cdd/wrpsb.cgi) in 1st and 2nd iBeetle rescreening phase.

Gene knockdown via RNA interference Technique

Double-stranded RNA Synthesis

To knockdown gene in beetle through RNAi, double-stranded RNAs (dsRNAs) were either self-designed or purchased from Eupheria Biotech GmbH (Dresden, Germany). In 1st phase of iBeetle screening, dsRNAs was self-designed. The selection of best fragments with no off-targets effect for synthesis of dsRNA was performed with the German cancer research center the E-RNAi web service (Horn and Boutros, 2010). After selection, these fragments were cloned and the PCR product were purified. The Ambion® MEGA script® T7 Kit (Life Technologies GmbH, Darmstadt, Germany). *In vitro* transcription, T7-RNA Polymerase was employed as enzyme.

In 2nd phase of iBeetle screening, original iB-fragments and non-overlapping fragments of 3 µg/µl concentrations were ordered from Eupheria Biotech GmbH (Dresden, Germany). The resuspension and dilution of the synthesized dsRNAs were made in same 10x buffer stock (0.3

mM KH2PO4, 0.7 mM Na2HPO4 2H2O, 14 mM NaCl, 40 mM KCl) used for injection and freeze at -20°C until utilized in experiments.

dsRNA injection to beetles

The dsRNA was injected to both female and male beetles at mid-pupal stage. Before injection, pupae were put for 5 min on ice and then placed in a line on a microscopic glass slide on an adhesive tape. Borosilicate glass capillaries (wall thickness: 0.21 mm, outside-diameter: 1 mm, length: 100 mm, Heinemann Labortechnik GmbH, Duderstadt, Germany) were pulled with micropipette puller (Sutter Instruments, Novato, USA) to form injection needles and Femtotips® (Eppendorf, Hamburg, Germany) were used for loading the dsRNA. The semiautomatic injections were carried out with a microinjector (Eppendorf, Hamburg, Germany) that is linked to a Helmut Saur Laborbedarf micromanipulator (Reutlingen, Germany).

In the 1st phase of iBeetle rescreen, 2 µg/µl dsRNAs (non-overlapping fragment Additional file.1. Table S1) concentration were administered to beetle. However, in some genes dsRNAs injections, the altered stink gland phenotypes were not observed. For further confirmation, a higher dose of dsRNA (3 µg/µl) was injected in rescreening. While in the 2nd iBeetle phase, 1 µg/µl of dsRNAs (original iB-fragment) were injected for rescreening. For confirmation of their phenotype 2 µg/µl NOF (non-overlapping fragment Additional file 2. Table S2) concentration were injected in the beetles.

Gland volatile analysis with semi-quantitative gas chromatography-mass spectrometry (GC-MS)

Both prothoracic and abdominal gland tissues of knockdown and control (wildtype) beetles were independently analyzed by GC-MS. In the beginning of the 1st phase of iBeetle screen for the confirmation of the iBeetle rescreen identified stink gland phenotypes, a mixture of the gland secretions of one female and one male beetle injected with dsRNA (NOF) was analyzed. While in 2nd phase of iBeetle screening, male and female beetles injected with original iB- fragment and nonoverlapping fragment were analyzed separately from the begining. The abdominal and prothoracic glands were collected separately from 10 days old male and female RNAi injected adult beetles. The glands were homogenized in methanol (Merck Millipore KGaA, Darmstadt,

Germany), 50 µl (1 beetle) or 100 µl (3 beetles). GC-MS analysis was done within 48 h. The homogenized gland tissue samples were put at -20°C before the GC-MS analysis.

An Agilent Technologies 5975C mass spectrometer system and 7890A gas chromatogram were used to carried out the GC-MS analysis. In the GC-MS system, a Multipurpose Sampler (MPS, Gerstel, Mülheim, Germany) is linked to a mass spectrometer and a gas chromatograph (Agilent Technologies, Santa Clara, USA). The MSD ChemStation (Agilent Technologies, Santa Clara, USA) software was used for analysis of the GC-MS obtained data. The Wiley 9th edition (Wiley, Hoboken, USA) and National Institute for Standards and Technology 2008 databases (Gaithersburg, USA) were used for identification of the volatile secretion compounds. In both wildtype and knockdown situations, Microsoft excel was used for the volatile substances semi-quantitative analysis in gland secretion and for showing comparative chromatograms

For these analyses, the volatile chemicals in wildtype (buffer injected) beetle gland mean values of abundances were calculated and considered as 100%. Subsequently, the relative alterations in secretion substances in gene knockdown beetle glands in relation to the respective wildtype mean were determined in percent, where values >100% show an augmentation of the particular chemical glands of the knockdown beetles in comparison to the wildtype control and <100% values indicate a reduction of a chemical substance in the gland. The main volatile compounds such as MBQ, EBQ, alkenes 1-pentadecene and 1-heptadecene were analyzed in gland secretion.

Databases

The following online databases sources were employed in this study: the Tcas 4.0 (http://bioinf.uni-greifswald.de/gb2/gbrowse/tcas4/) and 5.2 (http://bioinf.uni-greifswald.de/gb2/gbrowse/tcas5/) versions of iBeetle Genome Browser. For annotations of *Tribolium* gene, the iBeetle-Base (http://ibeetle-base.uni-goettingen.de/; Dönitz et al., 2015) was used for genes affecting stink glands.

Microscopy (Photo imaging)

Dissection of the abdominal glands of RNAi-induced knockdown and wildtype beetles were done using a stereomicroscope Leica MZ16FA connected with a Q-imaging camera (Leica Microsystems GmbH, Wetzlar, Germany). Adobe Photoshop CS5 was used for arranging photos.

Results

Search for stink gland phenotypes in the iBeetle-Base

In the phenotypic RNAi-mediated gene knockdown screen, iBeetle, 5300 genes in its first phase and 3200 genes in its second phase have been screened to identify novel genes which are important for insect development and regulation of various physiological processes. The beetle stink glands have been analyzed for morphological defects after gene knockdown. This analysis was part of the larval injections in the first screening phase and was done after pupal injections in the second phase due to a shortened screening schedule, in which the larval injection part has been skipped. All morphological stink gland abnormalities from both screening phases have been annotated in the publicly available online iBeetle database (http://ibeetle-base.uni-goettingen.de). To find genes that are potentially involved in stink gland function, we searched for annotated stink gland with altered phenotypes in the iBeetle-Base after the end of the first and second screening phases. In total, in the iBeetle-Base, 130 genes were annotated with diverse morphologically abnormal stink gland phenotypes, affecting various characteristics of the gland secretions (color, filling quantity, mixing of compounds) as well as the reservoir size of the glands (Additional file 3. Table S3).

Re-screen of iBeetle-identified gland genes

To confirm the iBeetle-identified gland genes, we performed a rescreen of the 130 candidates in a different beetle strain, partly with different dsRNA fragments and a different injection stage (Kitzmann et al., 2013). For 69 genes (about 53%), we also observed a stink gland phenotype. Of those, 60 genes showed the exact iBeetle-annotated gland phenotype, whereas the knockdown of the other nine genes resulted in gland phenotypes different from the iBeetle-noted ones, which may be due to a different amount of injected dsRNA and thus a doses-dependent effect (Table 1, Additional file 3. Table S3).

Gene ontology (GO) of confirmed iBeetle-identified gland genes

The iBeetle-screen together with the GC-MS analysis of gland volatiles identified 69 gland genes that are potentially involved in the regulation of stink gland function and, to be more specific, in volatile secretion production. Not unexpected for a biosynthesis process, gene ontologies revealed 20 enzymes, five transporters and three channels (Figure 2, Additional file 4. Table S4). In

addition, two transcription factors and 28 other proteins, mainly receptors and enzyme regulators, were found. Interestingly, twelve genes are not yet characterized in *Drosophila* or any other organism.

Morphological stink gland phenotypes after RNAi-mediated gene knockdown

The gland phenotypes that we detected in the rescreen were categorized into seven groups (Figure 1). The color of the secretion was either darker (Fig. 1C) or colorless (Fig. 1F), the reservoir size was either increased or decreased (Fig. 1E), glands were necrotic and/or empty (Fig. 1B), contained less secretion (Fig. 1H) or melanin-like material (Fig. 1D), or showed an asymmetrical partition of compounds in gland (Fig. 1G). An additional gland phenotype described as "condensed" has also been observed by Li et al. (2013), resulting from the knockdown of a gene identified in a gland transcriptomics-based approach for gland candidate gene selection. Here, this stink gland phenotype is referred to as "turbid secretion" (Figure 1I, Additional file 3. Table S3).

Alterations of stink gland volatile compounds in knockdown beetles

To test whether or not the knockdown of gland genes also influences the defensive secretion production, we used GC-MS analysis to analyze the volatile compounds of gland secretions of all 69 confirmed gland genes in respective knockdown beetles. In wildtype (buffer-injected) beetles, the main volatiles present are the EBQ and MBQ and the alkenes, 1-Heptadecene (C-17) and 1-Pentadecene (C-15). In male and female beetles, the volatile secretion composition is similar, whereas slight differences exist in the volatile abundances (Unruh, Xu and Kramer, 1998). In the secretions of the rescreen knockdown beetles, the abundances of the four main volatiles were altered to different degrees, reaching from no alteration to completely missing chemical(s) (Table 2). In total, from the 69 confirmed iBeetle gland genes, we found 51 that showed strong volatile changes (≥ 50% reduction) in at least one type of chemical (*para*-benzoquinones or alkenes) in at least one gender or one type of gland. The knockdown of nine genes led to very strong reductions of both benzoquinones and alkenes in thoracic and abdominal glands, independent of the beetle's gender, suggesting that those gene products may play a fundamental role in the production of secretion volatiles. Interestingly, 13 genes caused strong reduced levels of benzoquinones (BQ) alone, indicating a specific function in the beetle's BQ synthesis. On the contrary, none of the 69 genes led to alkene-specific reductions in both gland types. In ten cases, reductions of volatile

levels were observed to be gland-type specific (6 thx, 4 abd), and for seven genes the secretion phenotype was found to be gender-dependent (2 male, 5 female). However, it should be noted that measurements have been done only once with a small number of individuals. Therefore, a confirmation of the secretion volatile analysis is highly recommended. In general, no coincidence was found between the morphological phenotype detected in the rescreen and the secretion volatile phenotype, with one exception. The three genes (*Tc_010251*, *Tc_016314*, *Tc_033122*) that caused the morphological phenotype 'colorless' all showed a lack of benzoquinones for both genders and in both types of glands in the volatile secretion analysis, linking the yellowish color in wildtype stink glands to the presence of benzoquinones in the secretions (Table 2).

iBeetle transcriptome

Notably, we found that only 14 of the 69 gland genes are highly differentially expressed in stink gland tissue (FC ≥ 2), indicating that almost 80% of genes with potential functions in stink glands would have been missed by using differential expression data for candidate gene selection alone. Most importantly, we found that only nine of the 51 gland genes with a strong secretion phenotype possess an expression fold change of two or higher in stink gland tissue. Thus, the other 43 genes that showed a morphological phenotype as well as alterations in the secretion volatiles would have been easily missed in a transcriptomics-based approach, as they are not differentially and highly expressed in the glands (Additional file 5. Table S5).

Coverage of transcriptomics-identified gland genes in the iBeetle screen

Based on transcriptomic stink gland data, Li et al. (2013) identified 77 genes which are specifically expressed at high level in the stink glands (FC ≥ 64). 71 of them were analyzed in gene knockdown for morphological and secretion volatile stink gland phenotypes (Additional file 3. Table S3). 36 of them have also been analyzed in iBeetle phase 1 and 2.

29 of the 71 genes showed morphological and secretion volatile phenotypes in the stink glands, 13 of which were also covered by the iBeetle screen so far. However, from these 13, only one gene (*Tc_005389*), which caused a melanized phenotype, has been identified and confirmed in the iBeetle screen, and three gene knockdowns led to adult lethality before the glands were inspected 40 days/20 days after hatching (first phase/second phase). And two further genes were only part

of the pupal screen of the first phase, in which stink gland analysis was only intended for the larval part and thus not analyzed. The gland phenotypes of the residual seven genes were not observed during the iBeetle screen. For six of them the gland phenotypes are not easy to detect and therefore could have easily been missed, but one gene (*Tc_007254*), which caused a melanized phenotype, should have been identifiable in the iBeetle screen (Figure 3). In summary, the iBeetle screen missed seven gland genes that have been identified (among 22 others) in the transcriptomics-based approach by Li et al. (2013). Unchanged /unremarkable phenotypes are indicated with phenotype 'non detected' (n.d.). Genes that have not been analyzed for a stink gland phenotype as they were only part of the pupal screen are listed as not analyzed (n.a.). In italics, the 13 genes are marked that cause a gland phenotype upon knockdown and are also covered in the iBeetle screen. RNAi-knockdown of genes highlighted in bold resulted in easily detectable and strikingly changed stink glands, and therefore should have been detected in the iBeetle screen (Additional file 6. Table S6).

Discussion

This study aimd to combine RNAi and RNA-seq approaches to help identify and characterize novel genes role in stink gland function. The RNAi data was obtained from iBeetle database (Dönitz et al., 2015). iBeetle is a large online database for uncovering genes related to different phenotypes including stink glands in red flour beetle (Dönitz et al., 2015; Schmitt-Engel et al., 2015). Findings of a RNAi-mediated knockdown screen of the *T. casteneum* genome is summarized in this online database (Dönitz et al., 2015). About 5300 genes in the first phase while approximately 3200 genes in the second phase of iBeetle screening had been knocked down via dsRNA injection, checked for morphological and developmental defects, and reported in the online iBeetle-database (Dönitz et al., 2015; Schmitt-Engel et al., 2015). In total, 57 genes in the first phase and 73 genes in the second phase were identified by checking the iBeetle-database for entries describing alteration in morphology and secretion of the adult beetle stink glands. These 130 genes were annotated with diverse morphologically altered stink gland phenotypes, affecting various characteristics of the gland secretions.

In the rescreen of these 130 genes, the stink gland phenotype of RNAi mediated gene disruption with injection of non-overlapping fragments could not be reproduced for 61 genes, even with injections of larva and higher concentrations of dsRNA. For 69 genes (about 53%), we observed a

stink gland phenotype. Of those, 60 genes showed the exact iBeetle-annotated gland phenotype, whereas the knockdown of the other nine genes resulted in gland phenotypes different from the iBeetle-noted ones, which may be due to a different amount of injected dsRNA and thus a dose-dependent effect. Notably, in RNA-seq data we found that only 14 of the 69 confirmed gland genes are highly differentially expressed in stink gland tissue (FC ≥ 2), indicating that almost 80% of genes important for stink gland function would have been missed by using differential expression data for candidate gene selection alone.

The reasons for unreproducibility of 61 genes in stink gland phenotypes are not clear. Intriguingly, majority of these genes had been annotated in iBeetle database with stink gland phenotypes that are hard to identify, such as 'less secretion', 'irregular reservoir size' and 'secretion color darker'. As wild type beetles stink gland secretions also display natural variation in degree of filling, color and shape, it is possible that these genes were assigned as false-positives. This possibility can simply be checked by re-administration of the original iBeetle fragment dsRNA and dsRNA of a non-overlapping fragment. Additionally, quantity and quality of RNAi-induced phenotypes related to the particular injected strain. The rescreen was carried out in the San Bernardino wildtype *Tribolium* strain, while for the larval screen in the iBeetle project the larvae were taken from a cross between pearl and D17X red strains of *Tribolium* (Schmitt-Engel et al., 2015). Moreover, it has been reported by Kitzmann and colleagues (Kitzmann et al., 2013) that different animal strains may show variation in RNAi sensitivity. Nevertheless, higher concentrations (3 µg/µl) of dsRNA injection during rescreen also did not reproduce the phenotypes, showing that variation in effect of dsRNA doses between strains is not responsible for lack of effect on phenotype in this particular case.

Conclusions

Our study found out that one set of functional genomic data is not sufficient in uncovering genes important for stink gland function. Our comparative functional analysis suggests that a genome-wide phenotypic screen and a transcriptomics approach complement each other in functional genomics of defensive stink gland physiology. We identified a large variety of genes for involvement in the red flour beetle stink gland benzoquinone biosynthesis through RNAi-mediated gene silencing and differential gene expression analyses. However, attention should be paid when

using RNAi and comparative RNA-seq data for uncovering gene important for benzoquinone-biosynthesis. As revealed by the functional analysis through GC-MS analysis of confirmed unveiled candidate genes. RNAi analysis and RNA-seq data are not often indicating an exact role for a particular gene. In this regard, GC-MS analysis also helps in confirmation of a gene role. In future, further detailed functional genomic analysis of the candidate genes uncovered in our study will help in the identification of enzymes and molecular factors involved in benzoquinone biosynthesis and self-protection.

References

Aw, T. *et al.* (2010) 'Functional genomics of mountain pine beetle (Dendroctonus ponderosae) midguts and fat bodies', *BMC Genomics*, 11(1), p. 215. doi: 10.1186/1471-2164-11-215.

Bouchard, P. *et al.* (2011) 'Family-group names in Coleoptera (Insecta)', *ZooKeys*, (88), pp. 1–972. doi: 10.3897/zookeys.88.807.

Brown, W. V. *et al.* (1992) 'Chemical Composition and Taxonomic Significance of Defensive Secretions of Some Australian Tenebrionidae (coleoptera)', *Australian Journal of Entomology*, 31(1), pp. 79–89. doi: 10.1111/j.1440-6055.1992.tb00461.x.

Bucher, G., Scholten, J. and Klingler, M. (2002) 'Parental RNAi in Tribolium (Coleoptera)', *Current Biology*, 12(3), pp. R85–R86. doi: 10.1016/S0960-9822(02)00666-8.

Crowson, R. A. (1960) 'The Phylogeny of Coleoptera', *Annual Review of Entomology*, 5(1), pp. 111–134. doi: 10.1146/annurev.en.05.010160.000551.

Crowson, R. A. (1981) 'Chapter 1 - Introduction: The Study of Beetles', in Crowson, R. A. (ed.) *The Biology of the Coleoptera*. Academic Press, pp. 1–14. doi: 10.1016/B978-0-12-196050-6.50006-3.

Dittmer, N. T. *et al.* (2012) 'Proteomic and transcriptomic analyses of rigid and membranous cuticles and epidermis from the elytra and hindwings of the red flour beetle, Tribolium castaneum', *Journal of Proteome Research*, 11(1), pp. 269–278. doi: 10.1021/pr2009803.

Dönitz, J. *et al.* (2015) 'iBeetle-Base: a database for RNAi phenotypes in the red flour beetle Tribolium castaneum', *Nucleic Acids Research*, 43(Database issue), pp. D720–D725. doi: 10.1093/nar/gku1054.

Eisner, T., McHenry, F. and Salpeter, M. M. (1964) 'Defense mechanisms of arthropods. XV. Morphology of the quinone-producing glands of a tenebrionid beetle (ELEODES longicollis lec.)', *Journal of Morphology*, 115(3), pp. 355–399. doi: 10.1002/jmor.1051150304.

El-Desouky, T. A. *et al.* (2018) 'Impact of Insect Densities Tribolium Castaneum on the Benzoquinone Secretions and Aflatoxins Levels in Wheat Flour During Storage Periods', *The Open Biotechnology Journal*, 12(1). doi: 10.2174/1874070701812010104.

Farrell, R. E. (2010) 'Chapter 23 - RNAi: Take a RISC – Role the Dicer', in Farrell, R. E. (ed.) *RNA Methodologies (Fourth Edition)*. San Diego: Academic Press, pp. 539–560. doi: 10.1016/B978-0-12-374727-3.00023-1.

Happ, G. M. (1968) 'Quinone and hydrocarbon production in the defensive glands of Eleodes longicollis and Tribolium castaneum (Coleoptera, Tenebrionidae)', *Journal of Insect Physiology*, 14(12), pp. 1821–1837. doi: 10.1016/0022-1910(68)90214-X.

Horn, T. and Boutros, M. (2010) 'E-RNAi: a web application for the multi-species design of RNAi reagents—2010 update', *Nucleic Acids Research*, 38(suppl_2), pp. W332–W339. doi: 10.1093/nar/gkq317.

Howard, R. W. (1987) 'Chemosystematic Studies of the Triboliini (Coleoptera: Tenebrionidae): Phylogenetic Inferences from the Defensive Chemicals of Eight Tribolium spp., Palorus ratzeburgi (Wissmann), and Latheticus oryzae Waterhouse', *Annals of the Entomological Society of America*, 80(3), pp. 398–405. doi: 10.1093/aesa/80.3.398.

Kaushik, Shalini, Kaushik, Sandeep and Sharma, D. (2019) 'Functional Genomics', in Ranganathan, S. et al. (eds) *Encyclopedia of Bioinformatics and Computational Biology*. Oxford: Academic Press, pp. 118–133. doi: 10.1016/B978-0-12-809633-8.20222-7.

Kitzmann, P. *et al.* (2013) 'RNAi phenotypes are influenced by the genetic background of the injected strain', *BMC genomics*, 14, p. 5. doi: 10.1186/1471-2164-14-5.

Kumar, H. *et al.* (2018) 'Red flour beetle (Tribolium castaneum): From population genetics to functional genomics', *Veterinary World*, 11(8), pp. 1043–1046. doi: 10.14202/vetworld.2018.1043-1046.

Li, J. *et al.* (2013) 'Odoriferous Defensive Stink Gland Transcriptome to Identify Novel Genes Necessary for Quinone Synthesis in the Red Flour Beetle, Tribolium castaneum', *PLoS Genetics*, 9(7). doi: 10.1371/journal.pgen.1003596.

Lis, Ł. *et al.* (2011) 'The carcinogenic effects of benzoquinones produced by the flour beetle', *Polish Journal of Veterinary Sciences*, 14(1). doi: 10.2478/v10181-011-0025-8.

Loconti, J. D. and Roth, L. M. (1953) 'Composition of the Odorous Secretion of Tribolium Castaneum', *Annals of the Entomological Society of America*, 46(2), pp. 281–289. doi: 10.1093/aesa/46.2.281.

Luciana Villaverde, M., Juárez, M. P. and Mijailovsky, S. (2007) 'Detection of Tribolium castaneum (Herbst) volatile defensive secretions by solid phase microextraction–capillary gas chromatography (SPME-CGC)', *Journal of Stored Products Research - J STORED PROD RES*, 43, pp. 540–545. doi: 10.1016/j.jspr.2007.03.003.

Markarian, H., Florentine, G. J. and Pratt, J. J. (1978) 'Quinone production of some species of Tribolium', *Journal of Insect Physiology*, 24(12), pp. 785–790. doi: 10.1016/0022-1910(78)90096-3.

Mckenna, D. (2017) 'Beetle Genomes in the 21 st Century: Prospects, Progress and Priorities', *Current Opinion in Insect Science*, 25. doi: 10.1016/j.cois.2017.12.002.

McKenna, D. D. *et al.* (2019) 'The evolution and genomic basis of beetle diversity', *Proceedings of the National Academy of Sciences*, 116(49), pp. 24729–24737. doi: 10.1073/pnas.1909655116.

Noh, M. Y. *et al.* (2016) 'Cuticle formation and pigmentation in beetles', *Current Opinion in Insect Science*, 17, pp. 1–9. doi: 10.1016/j.cois.2016.05.004.

Pappas, P. W. and Wardrop, S. M. (1996) 'Quantification of benzoquinones in the flour beetles. Tribolium castaneum and Tribolium confusum', *Preparative Biochemistry & Biotechnology*, 26(1), pp. 53–66. doi: 10.1080/10826069608000050.

Payne, N. M. (1925) 'Some Effects of Triboliumon on Flour', *Journal of Economic Entomology*, 18(5), pp. 737–744. doi: 10.1093/jee/18.5.737.

Pedrini, N. *et al.* (2015) 'Tenebrionid secretions and a fungal benzoquinone oxidoreductase form competing components of an arms race between a host and pathogen', *Proceedings of the National Academy of Sciences of the United States of America*, 112(28), pp. E3651–E3660. doi: 10.1073/pnas.1504552112.

Posnien, N. *et al.* (2009) 'RNAi in the red flour beetle (Tribolium)', *Cold Spring Harbor Protocols*, 2009(8), p. pdb.prot5256. doi: 10.1101/pdb.prot5256.

Roth, L. M. (1943) 'Studies on the Gaseous Secretion of Tribolium Confusum Duval II. the Odoriferous Glands of Tribolium Confusum', *Annals of the Entomological Society of America*, 36(3), pp. 397–424. doi: 10.1093/aesa/36.3.397.

Schierling, A. and Dettner, K. (2013) 'The Pygidial Defense Gland System of the Steninae (Coleoptera, Staphylinidae): Morphology, Ultrastructure and Evolution.', *Arthropod structure & development*, 42, pp. 197–208. doi: 10.1016/j.asd.2013.03.001.

Schmitt-Engel, C. *et al.* (2015) 'The iBeetle large-scale RNAi screen reveals gene functions for insect development and physiology', *Nature Communications*, 6(1), p. 7822. doi: 10.1038/ncomms8822.

Schoville, S. D. *et al.* (2018) 'A model species for agricultural pest genomics: the genome of the Colorado potato beetle, Leptinotarsa decemlineata (Coleoptera: Chrysomelidae)', *Scientific Reports*, 8. doi: 10.1038/s41598-018-20154-1.

Seppey, M. *et al.* (2019) 'Genomic signatures accompanying the dietary shift to phytophagy in polyphagan beetles', *Genome Biology*, 20(1), p. 98. doi: 10.1186/s13059-019-1704-5.

Stork, N. E. (2009) ‘Chapter 21 - Biodiversity’, in Resh, V. H. and Cardé, R. T. (eds) *Encyclopedia of Insects (Second Edition)*. San Diego: Academic Press, pp. 75–80. doi: 10.1016/B978-0-12-374144-8.00021-7.

Suzuki, Takahisa *et al.* (1975) ‘Hydrocarbon Repellents Isolated from *Tribolium castaneum* and *T. confusum* (Coleoptera: Tenebrionidae)’, *Agricultural and Biological Chemistry*, 39(11), pp. 2207–2211. doi: 10.1271/bbb1961.39.2207.

Trauner, J. *et al.* (2009) ‘Large-scale insertional mutagenesis of a coleopteran stored grain pest, the red flour beetle Tribolium castaneum, identifies embryonic lethal mutations and enhancer traps’, *BMC Biology*, 7, p. 73. doi: 10.1186/1741-7007-7-73.

Tschinkel, W. R. (1975) ‘A comparative study of the chemical defensive system of tenebrionid beetles: Chemistry of the secretions’, *Journal of Insect Physiology*, 21(4), pp. 753–783. doi: 10.1016/0022-1910(75)90008-6.

Ulrich, J. *et al.* (2015) ‘Large scale RNAi screen in Tribolium reveals novel target genes for pest control and the proteasome as prime target’, *BMC Genomics*, 16(1), p. 674. doi: 10.1186/s12864-015-1880-y.

Unruh, L. M., Xu, R. and Kramer, K. J. (1998) ‘Benzoquinone levels as a function of age and gender of the red flour beetle, Tribolium castaneum’. Available at: https://pubag.nal.usda.gov/catalog/13250 (Accessed: 19 January 2020).

Yezerski, A. *et al.* (2007) ‘The Effects of a Naturally Produced Benzoquinone on Microbes Common to Flour’, *Journal of chemical ecology*, 33, pp. 1217–25. doi: 10.1007/s10886-007-9293-2.

Yezerski, A., Gilmor, T. P. and Stevens, L. (2000) ‘Variation in the Production and Distribution of Substituted Benzoquinone Compounds among Genetic Strains of the Confused Flour Beetle, Tribolium confusum’, *Physiological and Biochemical Zoology: Ecological and Evolutionary Approaches*, 73(2), pp. 192–199. doi: 10.1086/316733.

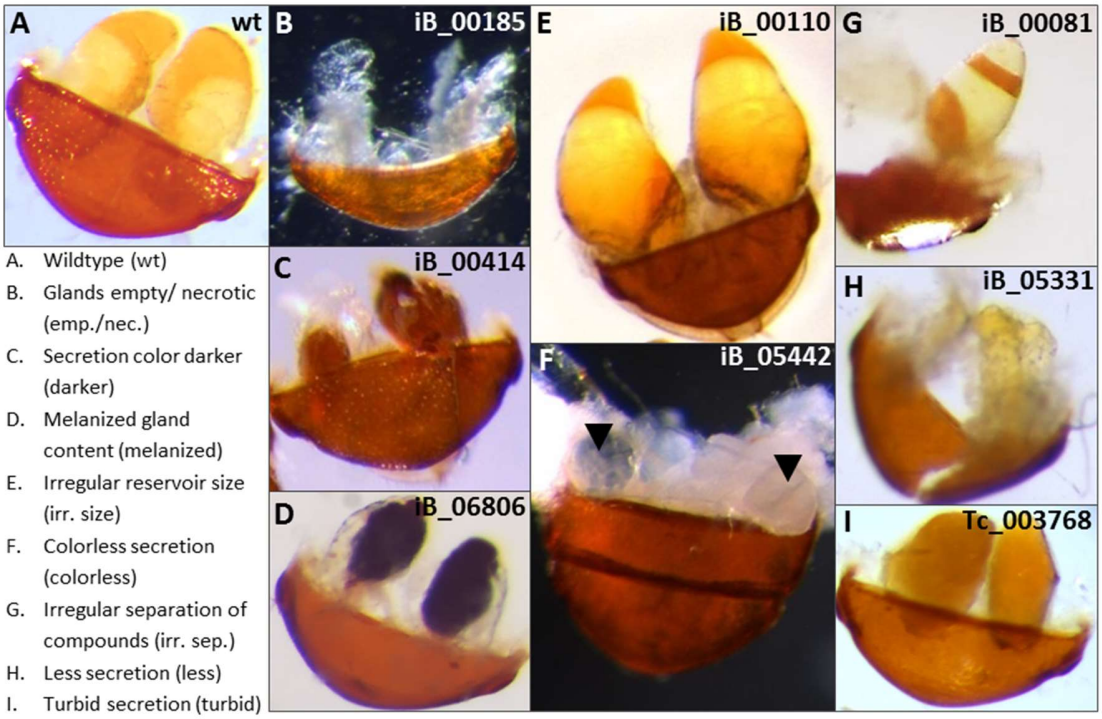

Figure 1. Phenotypic categories of abdominal glands.

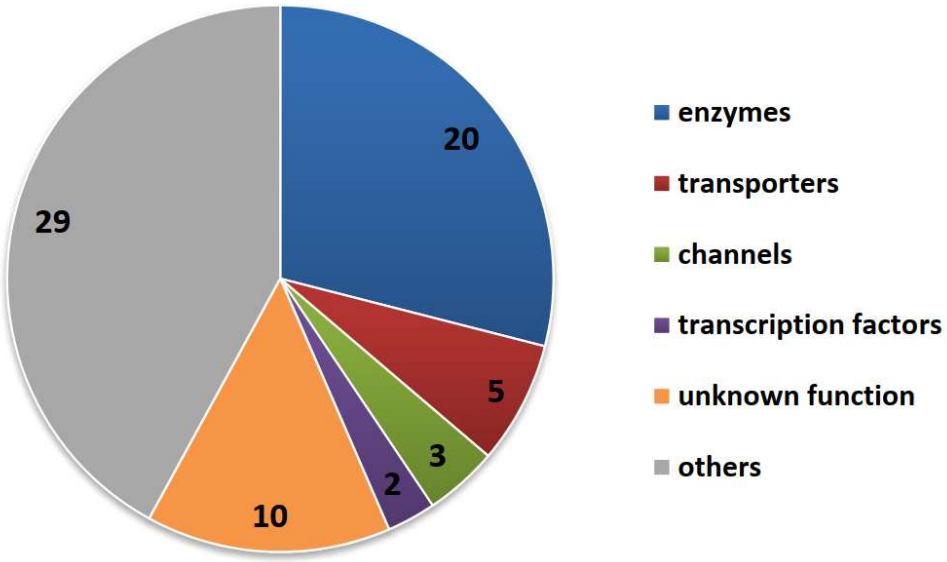

Figure 2. Stink gland ontology

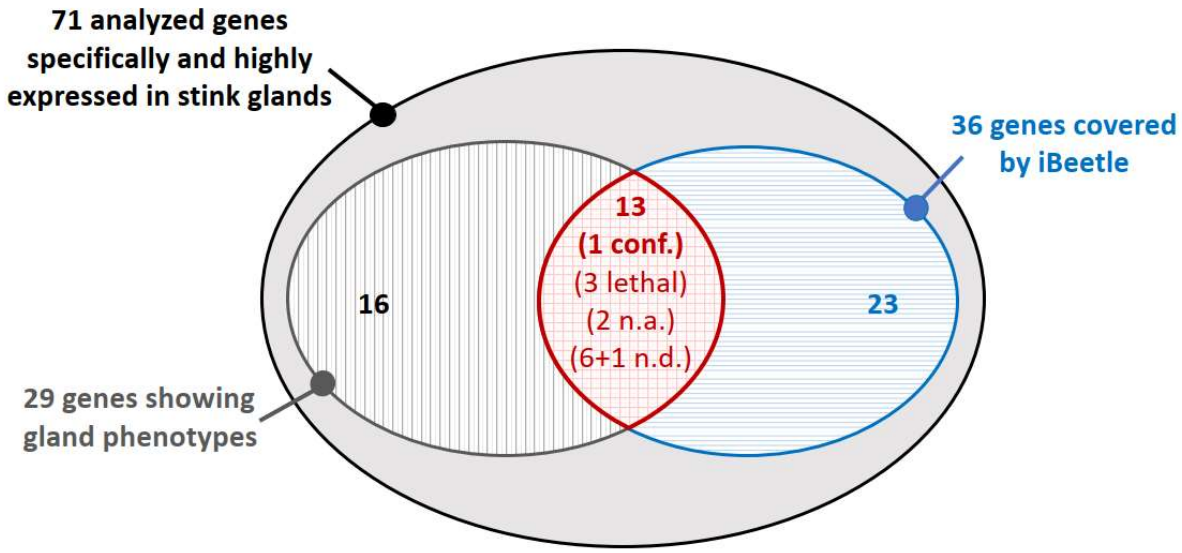

Figure 3. Representation of transcriptomics-identified genes in the iBeetle screen.

Table 1. Re-screen of iBeetle identified genes involved in the stink gland function.

	#	FC ≥ 2
iBeetle noted gland phenotypes	130	17
- re-screen confirmed iBeetle gland phenotypes	60	12
- re-screen observed different gland phenotypes	9	2
re-screen identified gland phenotypes	**69**	**14**

Table 2. Stink gland volatile compounds of confirmed iBeetle genes in knockdown beetles

iB_#	OGS_# (ass. 5.2)	morpholog. gland phenotype	thoracic								abdominal							
			MBQ		*EBQ*		*1-C15*		*1-C17*		*MBQ*		*EBQ*		*1-C15*		*1-C17*	
			♂	♀	♂	♀	♂	♀	♂	♀	♂	♀	♂	♀	♂	♀	♂	♀
iB_00081	*Tc_000379*	*irr. sep.*	54%		50%		147%		142%		197%		117%		97%		110%	
iB_00105	Tc_000476	emp./nec.	0%	0%	0%	0%	33%	23%	28%	18%	0%	0%	0%	0%	17%	15%	7%	10%
iB_00110	*Tc_000504*	*irr. size*	78%		83%		135%		162%		174%		148%		117%		158%	
iB_00185	Tc_000885	empt./nec.	0%		0%		11%		15%		0%		0%		4%		0%	
iB_00414	Tc_002616	darker	96%		74%		130%		148%		144%		98%		75%		67%	
iB_01044	Tc_006408	irr. sep.	30%		28%		169%		203%		118%		99%		103%		128%	
iB_01372	Tc_033883	irr. sep.	213%		200%		126%		105%		143%		108%		53%		44%	
iB_01798	Tc_011075	irr. sep.	99%		88%		111%		108%		361%		288%		146%		231%	
iB_01975	Tc_012387	darker	10%	0%	12%	1%	34%	9%	26%	6%	27%	26%	35%	30%	45%	10%	27%	4%
iB_02292	Tc_014494	less	288%	139%	176%	96%	132%	178%	135%	185%	280%	0%	187%	0%	142%	29%	220%	0%
iB_02297	Tc_014520	emp./nec.	78%		89%		133%		118%		189%		176%		116%		138%	
iB_02401	Tc_015095	darker	382%	376%	162%	180%	187%	138%	193%	137%	148%	55%	63%	28%	114%	89%	133%	87%
iB_02416	*Tc_015165*	*irr. sep.*	121%	133%	107%	138%	118%	115%	244%	130%	125%	119%	90%	93%	103%	95%	167%	125%
iB_02428	Tc_015203	irr. sep.	498%	103%	311%	51%	226%	192%	239%	167%	69%	177%	51%	116%	123%	175%	150%	215%
iB_02471	*Tc_015379*	*irr. size*	0%		0%		43%		48%		0%		0%		45%		36%	
iB_02516	*Tc_015811*	*melanized*	545%	170%	378%	113%	359%	132%	496%	128%	293%	52%	187%	33%	214%	55%	367%	53%
iB_02517	Tc_030914	melanized	0%	0%	0%	0%	68%	81%	83%	83%	0%	0%	0%	0%	27%	164%	43%	217%
iB_02563	Tc_030950	emp./nec.	87%		93%		115%		137%		108%		85%		98%		103%	
iB_02627	Tc_011288	less	0%	0%	0%	0%	22%	49%	32%	44%	40%	29%	30%	21%	71%	91%	103%	80%
iB_02673	Tc_032251	emp./nec.	0%	0%	0%	0%	8%	9%	0%	0%	21%	0%	16%	0%	66%	13%	57%	0%
iB_02716	Tc_002723	emp./nec.	139%	230%	100%	144%	187%	257%	178%	270%	81%	100%	69%	64%	133%	117%	200%	120%
iB_02774	Tc_008303	darker	0%	0%	0%	0%	14%	20%	12%	15%	3%	89%	5%	91%	33%	68%	26%	59%
iB_02931	*Tc_031247*	*irr. sep.*	0%	0%	0%	0%	99%	18%	107%	26%	0%	0%	0%	0%	118%	109%	127%	127%
iB_03294	Tc_002074	darker	0%	0%	0%	0%	0%	0%	0%	0%	3%	5%	1%	10%	18%	25%	10%	11%
iB_03552	*Tc_032367*	*darker*	76%		68%		64%		55%		41%		40%		46%		44%	
iB_03695	Tc_004129	irr. sep.	45%	0%	38%	0%	47%	8%	96%	19%	246%	0%	198%	0%	159%	14%	217%	21%
iB_03913	Tc_005167	emp./nec.	0%		0%		14%		18%		0%		0%		10%		16%	
iB_04420	Tc_008047	irr. sep.	57%	115%	86%	126%	95%	117%	93%	143%	81%	134%	88%	150%	111%	120%	103%	104%
iB_04702	Tc_031200	darker	0%	0%	0%	3%	27%	49%	24%	44%	14%	3%	13%	3%	62%	44%	47%	16%
iB_04717	Tc_009877	melanized	0%	0%	0%	3%	19%	28%	14%	21%	0%	0%	0%	0%	72%	67%	57%	36%
iB_04797	*Tc_010251*	*colorless*	0%	0%	0%	0%	84%	240%	75%	252%	0%	0%	0%	0%	142%	62%	237%	63%
iB_05119	*Tc_034419*	*less*	63%	61%	70%	68%	41%	61%	25%	59%	55%	164%	57%	160%	46%	129%	26%	151%
iB_05264	Tc_012539	emp./nec.	79%		78%		67%		66%		0%		0%		34%		32%	
iB_05278	Tc_034399	emp./nec.	185%		174%		131%		136%		28%		20%		37%		33%	
iB_05329	Tc_012828	irr. sep.	0%	109%	0%	76%	41%	81%	57%	100%	71%	126%	39%	75%	50%	58%	70%	68%
iB_05331	Tc_012834	less	97%		100%		94%		107%		157%		101%		102%		85%	
iB_05442	*Tc_033122*	*colorless*	0%		0%		23%		28%		0%		0%		7%		0%	
iB_05518	Tc_032992	melanized	30%	30%	22%	20%	73%	51%	78%	61%	29%	38%	18%	19%	63%	66%	107%	107%
iB_05712	Tc_033471	less	0%	30%	0%	22%	57%	91%	80%	141%	0%	0%	0%	0%	6%	31%	29%	50%
iB_05719	Tc_014887	irr. sep.	164%	0%	111%	0%	178%	158%	193%	170%	304%	67%	207%	41%	148%	99%	230%	132%
iB_06359	Tc_031191	darker	0%	4%	9%	11%	94%	73%	89%	58%	9%	29%	15%	42%	80%	76%	57%	31%
iB_06806	Tc_000393	melanized	148%	28%	165%	32%	106%	90%	114%	95%	68%	99%	83%	84%	84%	102%	70%	84%
iB_07043	Tc_003827	less	122%	98%	134%	113%	119%	121%	125%	142%	104%	0%	111%	0%	93%	7%	77%	2%
iB_07361	Tc_009459	melanized	0%	0%	0%	0%	20%	72%	18%	69%	0%	0%	0%	0%	10%	0%	6%	0%
iB_07900	Tc_001243	darker	81%	79%	99%	110%	72%	104%	66%	100%	123%	0%	127%	0%	124%	0%	142%	0%
iB_07902	Tc_001275	darker	37%	0%	58%	0%	42%	54%	36%	49%	51%	4%	62%	11%	45%	52%	28%	28%
iB_07918	*Tc_001376*	*less*	104%	45%	134%	51%	118%	93%	139%	91%	91%	114%	108%	108%	114%	119%	134%	105%
iB_08184	Tc_032964	less	128%	18%	127%	25%	108%	88%	111%	71%	98%	89%	109%	96%	89%	108%	76%	74%
iB_08398	Tc_033206	darker	0%	32%	0%	54%	76%	64%	72%	65%	5%	132%	13%	131%	84%	78%	66%	53%
iB_08468	Tc_015328	darker	58%	20%	54%	26%	95%	64%	102%	58%	78%	68%	67%	70%	75%	104%	56%	123%
iB_08506	Tc_015537	less	114%	67%	142%	83%	99%	109%	80%	129%	73%	147%	81%	147%	83%	123%	57%	114%
iB_08760	Tc_033755	melanized	0%	0%	0%	0%	47%	63%	49%	67%	3%	31%	5%	38%	48%	96%	29%	78%
iB_08861	Tc_006177	melanized	9%	6%	13%	9%	58%	52%	57%	52%	12%	16%	18%	20%	77%	58%	65%	24%
iB_09043	*Tc_016314*	*colorless*	0%	0%	0%	0%	36%	53%	22%	35%	0%	0%	0%	0%	97%	98%	75%	65%
iB_09050	Tc_033022	less	46%	24%	51%	31%	99%	87%	70%	74%	2%	55%	0%	52%	16%	93%	7%	70%
iB_09103	Tc_014482	melanized	0%	0%	0%	0%	4%	6%	6%	11%	0%	0%	0%	0%	26%	15%	18%	8%
iB_09239	Tc_008912	less	100%	85%	121%	94%	124%	133%	140%	185%	82%	133%	95%	132%	118%	135%	128%	143%
iB_09355	Tc_006363	darker	83%	36%	7%	52%	92%	93%	85%	92%	116%	168%	131%	155%	97%	129%	83%	130%
iB_09413	*Tc_005389*	*melanized*	0%	4%	6%	12%	41%	73%	28%	59%	9%	0%	21%	3%	85%	83%	63%	44%
iB_09430	Tc_005306	darker	11%	45%	20%	61%	80%	103%	71%	105%	79%	100%	87%	109%	88%	110%	65%	73%
iB_09736	Tc_003116	darker	27%	27%	33%	27%	125%	115%	129%	111%	91%	125%	98%	129%	131%	111%	111%	104%
iB_09988	Tc_014025	less	37%	54%	45%	68%	114%	112%	115%	126%	100%	89%	108%	98%	92%	99%	81%	64%

iB_09991	Tc_014033	darker	8%	26%	12%	41%	62%	79%	48%	66%	86%	78%	91%	92%	81%	107%	63%	103%
iB_10104	Tc_013627	darker	0%	0%	9%	3%	68%	74%	64%	79%	30%	11%	37%	17%	84%	65%	61%	30%
iB_10133	Tc_014774	less	38%	37%	42%	40%	87%	88%	72%	84%	125%	91%	124%	90%	108%	102%	7%	84%
iB_10156	Tc_033320	less	57%	68%	65%	69%	97%	104%	97%	123%	52%	41%	64%	42%	86%	74%	68%	40%
iB_10159	*Tc_015429*	*darker*	75%	24%	98%	31%	100%	89%	112%	84%	115%	114%	114%	101%	64%	80%	42%	52%
iB_10181	Tc_015547	darker	9%	0%	19%	5%	95%	77%	111%	81%	17%	10%	24%	14%	80%	84%	85%	79%
iB_10701	Tc_014985	melanized	15%	49%	21%	56%	92%	100%	97%	122%	34%	122%	42%	114%	84%	116%	100%	147%

FC ≥ 2
iBeetle noted gland
phenotype confirmed

0%	chemical not present
1-50%	chemical strongly reduced
51-85%	chemical reduced
≥ 86%	chemical not reduced; wt=100%

Additional file 1. Table S1. Non-overlapping fragments (NOF's) for re-screen in the first phase of iBeetle

iB_#	OGS_# (ass. 3.0)	dsRNA sequence (5' --> 3')	notes*
iB_00081	Tc_000379	CCACATTGGTGAGACGGAGCGAAAGTGTTTCATTGAGGAAATCCCCGACGAAACAAAC GTCATAGTCAATTACAAAGTGGAGCTTTATGACCCTCGAAGCGGTGGGTTCATGCCGTC GTCCCCCGGGATCGGCATGCATGTGGAGGTCCGCGACCCAGATGACAAGGTCCTCCTGT CTCGAGT GTACAGCTCTGAGGGAAAAATCTCGTTCACCTCGCAT	partial overlap with original iB-fragment
iB_00110	Tc_000504	ACCGTGGCCACTGCCCTACAGATTTACCAAAAACCAAGTGGCGACTCCGTCCCAAGCCG TCACACTCGAAACCAAGCTAAAATTACCGAAAAAACGTAAAGATAAACGCCGAGTGAAA AGTAACAGCGAGTCTCAAACGCAAGCGGTTTCATCGCAACAGCTTGCCCAAGATATTGA GGCTTTCATTGGCCAGCCTTTGCAAATGCAAAATAATTCCGGACAGAATTACAACCAAGC GCAAAGTCCCCCAGAAATATCCAGCTCGCAGTCGCAACATAATTTGCTAGTAACCCCTGA TATTCCATCGCCGATGCCCAAATTTTCCTGGGAGACTCCTTGGAGCACCGCTGCTGCGGC CTCGTGCGAGAAATTCGTTTGGTCGCAACCAGCGACTTCCCCGGGGATGAAGCCGATGG TGGCCTCAGCT C	
iB_00185	Tc_000885	ACCAAGCCAGACGGGTCGGTGGAATGCATCGTCGTCCAAAATGCCTACTACCCGAAAAA GTACGTCGATCCGGCAATGATTGGGATCTTGGTCGCTATGTTTCTCATGTTTATTACAATT TGTGTCGTTTTGCGATTGTTCAGCAGGGCACGTTGGAGGGAGAACCGAACCATATTTAA CACGCCCAACCCGCGCTTGATGAACGTCTCTCTGCTTCGTGAAAACAAGCTTTTACACAC GGACCGGCGAGGGTCTCGGAGCAGTGCCAGGGGCCCCAGCAGGCAGCCAAGTATGGC ATCTCTAAGAGCTCACTCCCCAAACTCTCAAGGGCGTTTGTTTCTAGGATCTCGTCGCGG ATCCCGAGGCAGCAGCAACGCGTCAGCGACTTCGAACCGATCGAACAAGAGTCCGCCCC AAGCGGCCAATTTGAGTTCGGCGACGACGCCCATGCTGGAGAGCGTCACCGTCGAGGT GCAA	partial overlap with original iB-fragment
iB_00414	Tc_002616	GATGGGTTTGCTGGGCTATATCGCCTATGGGTCTGATGTTGCAGACACCATCACCATTAA CTTATCCCCAGAGGATGTCCTAGCACAGGTGGCTAAAATAATGTTAGCCATAGCTATCTA CATCACGCATCCTCTGCAGATGTACGTGGCTATTGATATTATATGGAACGAATATTTAGC GTCAAGATTTGAAAAAAGCCGCTACCAGCTGTTTTTCGAATATGCTGTGCGAACTG	
iB_00754	Tc_004698	GAGACACCAAAGACAAGCCCAGCCCCCGCGACAGGGCTCCACGCCGCCTGCCTACAAC GGAAACAACTTCCAGGGAGATCCCCCGACTTTGAATCCCCCCAAAAACCTTTCGCCCCCC TCCAATGGAGACAAACTAGTCCAACCAACACCAAATGTGATCCCGAGCTGCGCGAGGGA CATAACCATGCCCGTTTCGGGGCAAAATTCAGCAGACATGGACGTGAGTGAGGAAGAA TTGAAGGAC TTCCTCTCGCAGAAGGATCTAGCAACGACGCTC	
iB_01044	Tc_006408	AGCAACAACACCAAGTTCGGAATAGGGGCTAAATACGACTTGGATCAAGACGCCGCGA TTCGCGCCAAGGTCAACAATTCCAGTCAGATCGGTTTGGGGTATCAGCAGCGTTTGCGT GAAGGTGTGACTCTAACTTTGTCGGCCCTCATTGACGGCAAGAACTTCAATAACG	
iB_01236	Tc_007650	TGCGGCATTTTGACCCTAATTGCGGCAACGTATCGCAAAGACGTTCGAGTCACTAGTATT GAAGAGAACAAAATCTTGTACGATTTAACCGATACTTTGGTCAAAAAACGTAATTTCAAT ATTCGCCTAGTTAACGGTAACTCTAACACGATTACAACGCGCCCAGCGCCCTGTAATTTG ATAGTAACGGAGATTTTTGACGCG	
iB_01372	Tc_008608	GCTTGGAGACGGCGTTACTTTTGACACAACAACGACCAAACAACTGGAAGAAGTGATCG AAAAGAATGATTTCATCGTTTATATCAATCACATCAAACCCAAACGACGAATTGTACATA ATGCAGAGACGCTTTTTGCGGTTGAATTTCCAGGAACCGATCAGAAATTTGAGCTTAAAC TTGATAGAAGCACGAAGCGAGTCATTGTTGAAACTGTGGAGGATGACCGTCGCCGAATC CAGCATTTCAAAGTTGACTCTCTTCATGAGAATAGCATCATCAAATCGCTGATTCTGGCC GTAAATCAGACACAACCAGGAGCACATG	
iB_01440	Tc_008936	CAAATCGGCGACTTCCTCCAAGAAATCGTCCAAAAAGTCTCCAAAAGTTCAAAAGAACG ATAACAATAACAACAGTAGTAATAACAGCAATGCAATCGTGAAAGAGAGATTGTACGCC AGACGCTCCGCTTTGCCCGAATCGACGAGTTCGAAGTTGAAAG	partial overlap with original iB-fragment

iB_01644	Tc_010033	GTGTCCTAGTCGGCGAAGGTGTCCTAGTTAAAATGTGCCGAAAGAAACCGAAAACCCGA CAGTTTTTTCTATTCAACGACATCTTAGTCTACGGCAACATCATAATAAACAAGAAGAAA TACAACAAGCAACATATCATTCCCTTAGAAGAAGTCAAATTGGAAAATCTCGAAGATGA CAATC GTAAGTGCCCAAACAAGTTT	
iB_01798	Tc_011075	TGATGATCTGCACCAGGTTGGCCGGAAGGGCCGTCATCAGAGTGGTCGGCCGGTGCAA CGAGGCCCAAGGAAATAACAATCTCGATCTCTCAAATTGCCAATTGATGCAAGTCCCCGA CGCCGTCTACCACCTCATGCGTCACACCGAACTGAAAACCTGTGATTTAAGTGATAATGT GATTACGAAAATACCTCCGAAATTCGCCGTTAAGTTCAGCTCGATAACGGACTTGAACTT GTCGCA CA	partial overlap with original iB-fragment
iB_01814	Tc_011159	AAAAATCGCATCTGCCAAACAAATGACAGTCAGAGACGCCCTAAATTCAGCCCTAGACG AGGAAATGACCCGCGATGAGCGGGTTTTCATCATCGGCGAAGAGGTGGCGCAGTACGA CGGCGCCTACAAGGTCACAAGGGGGCTGTGGAAGAAATACGGCGATAAGCGAGTCATC GACACGCCAATCACAGAAATGGGGTTCACAGGTTGTTGCTTAAAAGTGATTCGTTTAAA GGACTAATTTTTGGCCCCCCAGGAATCGCCGTGGGGGCTGCCATGGCCGGCCTGCGCCC CGTCTGCGAGTACATGACGTTCAACTTCGCCATGCAAGCCATCGACCAGATCATCAACTC GGCGGGAAAGACCTTCTACATGTCCGCGGGCCGCGTCAACGTCCCCATTGTCTT	
iB_01910	Tc_011969	AGACACGGTGGTTGAGCCCTACAATACTGTAATGTCGATTCACCATTTGGTCGAAAATAC CGACGAGACGTACATTATCGACAATGAGGCGTTGCATGACATTTGTTTCAGGACGCTGA AACTTTCAGCGCCGACTTTAGCCGATTTGAATCATTTAATCTCAGCTGCAATGTCTGGGA TAACGGCTTGTATTCGTTTTCCGGGGCAATTAAATGCCGATTTAAGAAAGATCCA	
iB_02292	Tc_014494	CCCATCCGATCATTGAACCGTCGGGTTTTTTGGTGCCGCAAATTTTAAACCAGTATGGAG AGGACTTCATGTTCCTCACTTGCATCCAGTACATAAACTCAGTAAAAAGCGGCCCTTTTG CCGAGCACTCGAACCAGCTTTGGAGCATAAGCGGAGTGTCCTCCTGGACGAAAATCAAC GGGGGCCTAATTAAAATGTACAAAGCGGAAGTTTTGAGCAAGTT	
iB_02297	Tc_014520	CGACGCACATGAGAAGGTTATACCAAGGGGGACCTCGACTCTTTTGCAGTTTTTCGAGA AATAACCTCCCGTCAGAAGTCACCACGAAATACGCCCAAAGCACCGATTTTCTCCTCAAC AATCTTAAAAATGCCAACAGTACCAAGAACGTCTTGGACATGGTCTCGCAACACAATGA CATCATGAACAACAAACACGTTATCCAAGCTTTACGTAGCTTATTCACTTTACAAAAAAAC GGAAATTCAGAAATGTCCACAAATGAAATTCTAGCCCACCAAGATTTTCGCAAATTG	
iB_02301	Tc_014544	TTTTCATCGCGTGCAAATACGAGGAGATGTATTTCCCCGAACTTTCAGACTTTGAATTTAT CTGTGATAATTCGTTCACAAAGAATCAGATTCTGCGGATGGAAATGAGCATTCTATCGTC GCTGAAATTCGAGTTGGGCAAACCTTTGTCAATTCACTTCTTGCG	partial overlap with original iB-fragment
iB_02367	Tc_014967	TAGTTTATCGGGGATCAGGGATTTCACTAACAGTGGTACCATCTACTTCCCCCATTTGCG GATTTCGGTTGAGAAACCTCGGGAGCAGTCGACGTTGGGCCAAAATCGGCGAAATATTA GTGGTAACTCGGAAGTGTTCACAAGTGACGAACTTGGAGTGGCCCGAGAGGAGGTTTA TCCCGCTGTAGTTGAAAAACAAGTTGATTTAATTAGGGAGAAAAAAAATAATCGGCCAA AATTCAGACCGGATTATTGGGACCACAACTATGCC	
iB_02401	Tc_015095	TGTGATCCAAGCAGGCATTAATATGTCGTTCAGCGCCATCTTACTACCGCAGCTGAACGA AAAGTCGAGTGATATACATATTTCCAAATCAGAGGCGTCTTGGATCGGTGGGTTTAGCC CGGTTATAGCCGATTTAACCGTTGTTTTTAGCAAGTATAGTCGCAATAGCCCTTCCAGCG GGTTCGTTGATCATCGGCCCGCTTATGGACCGCTTCGGGCGCAAAACTTTGTGTATTTGT ACGACTATACCCTTCGCCATCTCGTGGATAATC	
iB_02416	Tc_015165	AAACACGCGCGCTACTTAGAGAACGAAATCGACTTAAAACTCGTCGCGTTTAGTAAACT GGGGGCCGGTATCAAGTCGCCCCCAGCTCATTCGAGCTCCGATGCTGTGCCCCTTCTCTC AGGCGAGGACACTTTCGAGGCCATGTCTCTCGAAATTGAGGAATTGTTGAATAAAGTAA GCGGG CCCCCAAAAAATCACCCCAAATAACAATTCCTT	partial overlap with original iB-fragment
iB_02428	Tc_015203	GTTATAGGCAAATGGCCCAACACCTACACGTTCACCAAAGCTTTGGCCGAAGCTTTGATC AGAAACACCGCCACGAGTTTGCCTGTCGGGATTTTTCGACCAGCGATCGGTAGTAGAAA AAATTTGTATGTCATCCGTGAGATAACTGTCTATTTTAGTTATTTCAACGTACAAAGAACC AATGGAGAGTTGGATTGATAATTTGTATGGACCTACGGGGGCTGTAGCTGGGGCTGCTT CTGGACTTCTCCGTGTTTTTCCATGTAATGAGGATGTGGTGGCTGATATTGTACCAGTTG ACACGTGTGTGGCCGGAATTATCGCAGCGGCGTGGGATGTGACAAATAA	

iB_02471	Tc_015379	AATGGACCGTTGTTCGATTTATTGAAGAAACAACAAGGTGATGAAATTTTAAAGAAAGT TGAAGCAATTTCTGCAGACATGGAAGCACCTGATTTGGCCTTGGCCGCCTCTGATCGGA AGAAATTAGCCGAGGAAGTGGAAATGATTTATCATTGCGCTGCGACAATCAGATTTGAT GAATCTCTTCGTAAAGCCGTGTTTCTCAATACTAGGGGCACTAAACTAATGCTTGATTTG GCTAAAG AATGCAAAAAATTGATCGTTTTCGCCCATTTGAGCAC	
iB_02516	Tc_015811	CCAAAGCCGACCAAGTGTGGGACCCCGCCCTCCCCTGGCAGCCCATCCCAATTCACACG ACCCCCGAACTGGAGGACAACCTCCTCTCAATGAAAAAAAACTGCCCCAAATACAACTC GCTTCTAACCCAACTTTTCAAAACCGAGTTTTTCGCCAACATTAGTCGACAAAATCGGGA CTTGTACGCGTATTTGAGCAAAAATTCAGGGGCCAATATAACGTCCCTCGA	
iB_02517	Tc_015818	CCCCACAGGCGACTACACCTCCGACCAACCAACAATAATCACAGTGTCAGAAGATGACA CGATTAAAATCACCGTCTTGGGCATGACGTGCCAAAGCTGTGTCAAAAACATCGAAGAG ACCCTGAGTCGTAAACCCGGCATTTACAACATCAAAGTCAGCCTTCAGGAAAAAGCCGC TCTAGTCCATTATGACACACGCCAACTGACA	
iB_02542	Tc_015993	CCAAAACTGCCCGTCTATTCAAACCCCGTATTATTATCGCCGGTATCAGTTGCTACTCCCG TCCTCTGGACTACAAACGTTTCCGCGAGATTTGCAACGAAGTCGGTGCCTACCTCATGGC CGACATGGCCCACATTTCCGGTTTAGTTGCTGCCGGCGTCACCCCAAGTCCCTTCGAATA CGCCGACGTCGTCAGCACCACCACGCACAAGAGTTTGCGAGGACCTCGAGCCGGTGTCA TCTTCTTCCGAAAAGGCGTGCGGTCGCATAACGCTAAAGGCGAACCCATTATGTATGATC TTGAATCGAAGATCAACCAAGCTGTCTTTCCC	
iB_02563	Tc_016254	CCGGAACGACTTGATCGTAAACAGCAAAAATTTGAATATTGAAGCGGTGCATTTGATGC GAGATTGGAAAAGTGTTGAGATCGATAATGTGGAGGAAAATGTCGTTGATGAGGTTTT GATTG TTGAAAGTGAAGAGATTCTCTATCCGGGGATTT	
iB_02584	Tc_030051	GGAGTCCAGAAGGCGAATTGGTATGGGTCTGTTACCCAGGCTAGCACGGTTAGATTGG GTGGCGATGTCTACGTACCATTGGGCAAGTTGTTGCCAACGGTACATCCCGACGATTTG GTGAT TGATGGGTGGGATATCAGTTCGGCCAATTTGG	
iB_02625	Tc_011255	ATCGATGAGCTGTATGCTGAAATTTTGTACGAAATCTTACATAATGTTGGCTGTGATGTA AGTGTTGAGATAGGACAGACTGCCTTAATCTCGTACGCACAAGATGCATTTAAAATTCCT AACAATAAACATAATCAACTATTGTCTGAAGCTGAAAAGAAGGAGGCTCCTGAATTTTTG ATCAATGTCGAAGTTATCGAAGCCAAAGATTTGAAACCAAAGGATTCCAACGGGTTGAG	
iB_02633	Tc_011371	GCCGTTTACGACACCTGGGGCCGCAAAGTCCCCGGAAGAATCATCTTCTTCTCGTCGGA GGGCTCCACCAGCGCCCACGTGCCGCTCGTGGCGCTGCCCCACGTCGACGACGCCTACC CGCCCCAGAAGAAGTCCTTCCACATGCTCAAGTACCTGCACGACCACTTCGTCGACGAGT TCGAGTGGTTTGTGCGCGCCGACGACGACGTCTTCGTCAAAACCGAGCAG	
iB_02673	Tc_000240	AGGTGTGACAACAATGCTCAACTTTTTCACAACCTCAAACGGATTCCGTTCAACTTTGCC GGTGGTTTCGAATCTGACTGCCATGAATGTGTGGGACGGTGTGTGCATGTGTTTCATTTA CGCGTCCTTATTAGAATTCGTATGTGTGAATTACGTAGGAAGAAAACGACCGCTTCATAA CGT CGTCT	
iB_02692	Tc_003063	ACTGGTGTGCTACAGGCCAACCAAACGTGGACAAAGCCACCTCAATTTCCCAACTAATCA ACAAGCACCAGGAACAAAAGGAAGCCTTCCTCAAAGCTTGCACTTTGGCTCGAAGAACA GCCGAGACTTTTCTAAAATACACAACTCGAAGTCTCCAATTCTACAACTACTCCAACACCA CGAGCAATCACGAGACCAGAGTTAAGGGCATTTTGGAGAAGCT	
iB_03401	Tc_002550	CCAACTCCACCACCACCTCGCCCCACTCGCTCAGCCCCAAGGCGTTCCAGTTCGACACGG TGGTGCAAGGGGGCAGCGCGCCGCCCTCCAGTAAAGTGTCGCCGCTTATCAGGGACTTT GTGCAAGCCATCGACGATCGCGAGTGGCAAAACTCTTTGTATACTTTACTCCAGAACCAA ACGTATAATCAGTGTGAAGTGGACTTATTTGAACTTATGTGTAAAGTTTTGGACCAAAAT CTGTT CTCTCAAGTCGATTGGGC	
iB_03552	Tc_003409	TGAACCAGCTGTGCAAGGTCTGCGGAGAGCCAGCGGCCGGATTCCACTTTGGAGCTTTT ACCTGCGAGGGATGCAAGTCCTTCTTCGGTCGAACGTACAACAATATCAGCTCAATATCG GAATGCAAAAACAACGGCGAATGTGTGATCAACAAAAAAAAATCGGACAGCTTGCAAAG	partial overlap with original iB-fragment
iB_03637	Tc_003857	CATAAGGCCCCTAATGAGCAACGTGTTAATGGTAGGTGGGGGAACACATTTTGAGGGA GATACTCCCCTACCTGAAGATATACAAAAATTTTTGGACGGGGCTGAAAACGGAGCGAT	

		TTATTTCAGTCTTGGGACAAATGTTAAAAGCAAGGATTTGGACCAAGACACGAAAACAA CATTTTT GCAAGTATTTTCCGAACTGCCGTATAAAGTGTT	
iB_03693	Tc_004126	TTCGAAAGCGAATTTGAAACGAGACAAGAACAGCTTGAGTAAAAGCAAAACTATCGGA AATTCAATTTTAGACCACAGTGATTTTATTAGTCACTTGGACGACGACGAAATTAGTAAT AATTCATACGGGAGTCACACTTATCGCTTTAAGGACGAGAGTCACAAAGGCAGTGCCGA CGTTCT TGAAGATAACGAAGAGCAGGAAGAGAAGCGC	
iB_03695	Tc_004129	ATGGACCACATAGGCGACATGATCGAGCAGCAGGCACTGGGTGATCCGGTCGATTCTCC TGATGGCAGCGCGCATGCGGCTGGTGGCGGCGGCATGGAGACGCAGACCGTCCGCATG AGGTTGGTGTCGCGTGCTGTGGTGGAGAGGCGTCTTGTAAAACAGGAAG	
iB_03780	Tc_004533	TGCCTTTGGACGAAAGTAAAGACACACTAGGGGGTAAAAAAATCCGATTCAAGACCCCT GCGCGTGTTTTGTTCACTTCCGAGAGTAAAATCGACGACTTATTGCGAAATGACAAGGA GGCGCAAGAAGGGGAGGCAAAGAAAGGTAAACATTATAGTTTCAGGGGGCTCTCCAGT GTTGTCATTGCTTTTAGAGAGAAGTCCATCCCTGGCATCGTTCTTACAAGTGGAGTTGAC CCGTGACT	partial overlap with original iB-fragment
iB_03913	Tc_005167	AGCTTTCCACCGAAAATGGAAAGGTCCCAGATAGTGAATTCGATGGGTTCATCCGACCA GTTTCAAGAACAGACTTACATCCAGGCTCCCAGTTTTGTCCAAGCTCAAAACTACAGTAC TCC AACCCCCAGTCCTATCTATTCCCGTGCCTCC	
iB_04066	Tc_006098	CTCCAGAACCCGAAACTCCCAAACCAACTCCCTCAGAAACTCCAGAGCCCGAAACTCCAA AACCAACTCCACCCGAAGACAGAGATCCAGAATGTCCTTGGCCAGATCCTTTGGATCATA CT GTTCATCTACCACACGAAACGGATTGTACGAAGTTT	
iB_04137	Tc_006423	GTGCGTTTGTCAACGTCTCATGTCGTGCTGGTCTGGAGATGAAGACATAAACGCCCTTTA TGCCACAGTTGACAGGAGTAAAAAATGTCAACGCAATCAACCCACAGCTGCCAACTACG CCAACATAGCTCCCATGTCGGCCCCCACTGTTCCTACTTCTTCCAATTACGAAAACATGGA ATTTGCTCAAACTCTCAAACTGTACGAAAACAGCAAAGAAATCGTGGAAAA	
iB_04205	Tc_006735	GTTAGAGGCGAACACGGAGACAATTTCCCCTTTGACGGCAAAGGAGTGATTTTGGCGCA CGCTTTTTTCCCAAACGGTGGCCACAGCATCGACGTCCACTTCGACGCAGATGAGGCCTG GACAACTGTGCCCAACAGCGATGAAGGGACTAATTTATTCAATGTGGCGGC	
iB_04797	Tc_010251	CCTTCGAAAATATCCCCCAGGTCAAACTTTGAATCGCCGCTGTGTTAAAGACTACACCCTT CCAGGAACTAGCACAATCATTGAAAAAGGGACTCCCATCCTTATTTCTGCAATAGGAGTT CACAGGGATCCTGAGTATTATCCAGATCCTGAGAAATTTGATCCTGAGAGGTTTAGTGA AGAAAATAAAAAATTGAGACATCCGTTCGTTTATTTGCCATTTGGGGATGGACCAAGAA ATTGTATTGGAATGCGATTTGGAACTATGCAGTCTAAGTTAGGGATTGCATCAGTTGTGA AAAATT TTAAAGTGTCTGTTAGTCCCATAACAAAGCGGG	
iB_04839	Tc_010449	GTGTCCACTGTTACTCAACCCAGGACGGCAAAAAATTAAAAAGGAAAGTCAAAGCCGAA GGATACGTCGAATGCTCTGCCAAAACCAGGGAAGGACTGAAGGAAGTCTTCGAAGAGG CGATACGAGCGTACAAGAAGACCAAAATCAAAGCGAGACAAGTCAACTGTGC	partial overlap with original iB-fragment
iB_04850	Tc_010484	ATAAGGGCACGCAAATCAAGGGACAGGATTCTTGATTTGGAGGACGAAATGGCCGCAA TGACCGAAAAACAAGCAGCAAGGGAGCGCAGAGCGGCTAGGTTTAAGGCATTGGTTGC TGAAAGCACGGAACAAACTGAAGCGGCACAATCGGCCCTTCAAGCGATTAGCTTTAAGT CCAGGAGGGAACAAAGGACCTTGGAGGAGTA	
iB_05264	Tc_012539	GTCCAATTGTCATGGGTTGCACCATTCGATGGCAACTCCCCGATCACTCGTTACATGATC GAGTACAAGCAAAGCAAAGTCAGTTGGGAGGGAAACACCGAACGGGTACTAGTCCCAG GTGACCAAACTGAAGCTGGGGTTTTCACTCTGCGACCTGCCACCACGTATCA	
iB_05278	Tc_012610	CACTGCAGGGACTGGCACGGCTGCATCATGGCCCAGGCTATCATCGGACAGCACAACAT CCAGCCGTACAAGTTCTCCGAATGCAGTCGCTCGGATTACATCGACAGGCTGAGGACCG GGAACGGGATTTGCCTGCTGAACAAGCCCAACGAACTAGAGG	
iB_05284	Tc_012642	GGTTCTCCCGATTTTCGCTATAGGGATTATTACAGTTTACCGGAGAGTTGCTGTCCAGTT AATACGACTCACTGTTACCACACAAATGCCCACAAAAAACTCTGCAGTGTTAAACGTTTA ACCATTTGCGACGCAACCAAAGAGGCCTATTTGAGGAGTTACGTTATGTTACTGTTCATT CCTCTTATTGTAGCATCTGTAAGATTAAAAAAACTGGAGAACAAGTCCTACGCTTTTTTACAGG TTGTGCAAATAGCTCTGA	

iB_05329	Tc_012828	CCAATACCACCACCCCCTGTACTACCCCCAGCATATCCCCGTGCTCGACCACAACGGCGT CCCTGTCGAACCCGCCGCCAACCAACTCGCCCGCGCCGCCCATTACGCCGCCCATGCCGA AGCCAATGCTCGCACTGGTCATTATCCAATTTACGCCGCC	
iB_05331	Tc_012834	TACGTTGCACAGTTTCGGAGCAAAGTGTTACAGTTCGGAGTTTTTGGCTTATGACGTTAC GTGTGATACTTGGCAGGTGTTACAAGTGCCAAAGGATATTCACGCTGATTTGGCTCGTTT TGGTCATTCTGCCGTTACTTTTGAGGGTTCGTTGTACATTTATGGAGGGTTTGACGGACA AAT GTTGT	
iB_05342	Tc_012857	GTACTTAACGGAATTGGCCCCAGGTTTATTAAGGGGGTCCATGGGGGTGTTGTGCCCCCC TTGGCGTGACTTGTGGTGTCCTATTGGGGCAAGTTTTGTCCTTAGAAGGGATTTTAGGG AATGAGGATTATTGGCCCCATTTGTTGGCCTTCTATTTGCTACCTCTTGCTTCATGTAGTG TGATATTAGTATTTTTGCCTGAAAGTCCAAAGTATCTTTTTATAATCAAAAAGCAACCACA TCTA GCG	
iB_05442	Tc_013513	TTGACAACAAACGCTATCGGTACGCTTACCACCGGTCCTCGTGGCTGGTGGCGGGCAAG GCCGATCCTCCGGCTCCCTGCAGGATATACGCGCATCCGGACTCGCCCTTCTCCGGGGA GCAGCTACGAAAGCAAGTCGTCTCCTTCGAGAAGGTCAAACTCACCAACAACGAAA	complete overlap with original iB-fragment
iB_05518	Tc_013892	GCCGTTTCAGCCTGTTTCTACATTCTTGCAATTCAAAAATCCGAATCAAAATTATTTAACC CATCTCTAGTTGTCAGTTTTATCAAGCCAACAATTGTAGATTTGATTGATAAAAGTGTTGA AGAATCACGATGTGCCTCAGACCTAAAACAATTCATCACCGACTTGTTCAAACTCAAATG GTGGGCGATTCGAACTGAATACATCATCCCTTGCTACAAAGCAGACCCCGAAATCAACA AAT GCCTCCAACG	
iB_05584	Tc_014205	AGGACGAACTGACGCTCTTCCCCTCGCAATACAGCATAGACGTTCACGGCTATGTGCTCG TCTACAGCATCACCGATATCCGGTCGTTTGAAGTCGTTGGGACAATCTTTCACAAACTCC AGGACCTCAACGGGAAAATTCAGTGAGTTTGGCCCCTTTTGTGAGGCTGAGGCTAGAGC TTTT G	complete overlap with original iB-fragment
iB_05712	Tc_014870	CGCTCCGTGACAACCAATCGGCGCACGTCACGTGACGCCGCGTGTACCATGATAATTGG TCGAGACACCCACCAATTGGGCCCCAGCGCAGTCCGAGCCTCTAACATAACCTCAACATC GGC TGTCATCAGTTGGCTACCAGCCAACTCGAACCA	
iB_05719	Tc_014887	GCCAGTGCTGGATGTGGTGCCGCCATCGCCGAAGCCCTCGTCCGCGAAGGCCTCCAGGT GGTGGGTCTCGCCCGTCGCAAAGCCCGCGTCCAAACCCTCGCCGAAAAACTCGCACCAC ATCCCGGCAAACTCTACGCCGTAAAGTGCGACATGACGGTAGAATCTGACATTTTGGAG GCCTTCAAGTGGATCAAAACCACGCTAGGGC	partial overlap with original iB-fragment
iB_02627	Tc_011288	CAGACCTTGAACTGGAAGGTCTCTTCAAGAGACATTTCACAACTGTAGAGTTCTTCCAGG GTACCATCATGAACCCTATTGACCTTCAAAGGGTAAAGGTACACGAAGCTGATGCGTGT CTAGTCCTCGCCAACAAATACTGCCAAGATCCAGATGCTGAAGACGCAGCCAACATCAT GCGCGTCATTTCGATTAAGAACTACAGTGATGATATTAGAGTTATCATCCAGTTGATGCA GTACCACAACAAGGCTTACCTCCTGAACATTCCATCATGGGACTGGAAGCAAGGCGACG ACGTAATTTGTTTGGCTGAACTGAAGCTAGGTTTTATAGCTCAATCCTGTTTAGCGCCCG GTTTTTCGACAATGATGGCGAACTTGTTCGCTATGCGTTCGTTCAAAACGTCTCCAGACA TGCAGGTGTGGACCAATGACTATTTGCGAGGCACGGGAATGGAGATGTATACCGAGAC GCTCAGTCCGTCG TTTATAGGCATGC	partial overlap with original iB-fragment
iB_02716	Tc_002723	GCCTCGTCTCCTTCACCCCCGAGCAAGCCAAACCCCACTTAATCGACATCAAATTC AACGGAGAGACGGTGCGAGGATGCCCCTTCGTGTGCTCAGTCGCTGACACAAGCCG AGTGACTTTGAGTTTGAGTCACTTGGAGTTAATCCCCGTCAACCAAC	
iB_02931	Tc_011812	CCGTAACCAGGACCAGATGAAGGAGATCATCCACGAGATTGCCGTTTTAATGCAGTGCT CGTCGACGAATCGCGTGATTCGTCTGCACGAGGTCTACGAATCGGCCACGGAGATGGTG TTGGTGCTGGAATTGGCCGCCGGCGGCGAGCTCCAGCACATCCTCGACGGCGGCCAGT GTCTGGGCGAGGCGGAGGCGCGCAAAGCCATGAAGCAGATCCTGGACGGAGTGTCGTT TCTCCACGAA AGGAACATCGT	

* partial or complete overlap with original iB-fragment: e-rnai web service resulted in no alternative sequence to use and/or iB-fragment already spanned almost 100% of gene length

Additional file 2. Table S2. Non-overlapping fragments (NOF's) for re-screen in second phase of iBeetle

iB_#	OGS_# (ass. 3.0)	dsRNA sequence (5' --> 3')
iB_00105	TC000476	TCGCTGGAAAAGTATCCACACTCAGCAAATTTATGGATAAACATGGAGCTCTTGGCGAATTCTTGTTTGATAAG AAACTCCTCAGTGGAGAATTG
iB_01975	TC012387	ACTGCGAGATGGAGGTGTTCATGTCCGCAGTCAGGTGGCTCAAGTACGACTGGGCCAACAGGGATAAGTACA AGTATGAAGTGCTCAAGTGCGTCAGATTCGGAAACATAGCCGCTTGGCAACTTGTTGATATCAAGCGCAATCC CGAAAATCCCGAATTTATGGAGTTAGCCAAAGACCCAGCCATTTGCAAGCTCATCGATGACGGGCTGGCGTTT GTGATCATCAAGCACTGGTACGACCAC
iB_02774	TC008303	GCAACCATGTGAGGAAGGATCCGATGCCGATTAGTGACGATAGTGTTATTTATATAGACAGTGATGGGTTTAA TCCGATGAAGAAAAGTGATGATAATTACTGCCAAGTTATAGACTTATCTGATAAAGCCGAGTTCAAGAAAGAA GCGAAGAGTGTTCCAAAGAAGGAGACTAGTATCAGTCCGTTGATTCCCGAGCACGTGTCGAAACATCACGAAC TGAGTATTACCCCGACTTACCCCAAAATCGACCC
iB_03294	TC002074	GGAGAAGGATCGGGAGAGTCGCTGTGGTCACATGGAGACTTTTCTTCAAACCTTGATGGGGTTCGAGGGTGA CGATGACGATAATCTACCAATGATCGCAAAGACTTTGGCCAACATAATCCAAGACGATCACAAGTGCGGTGAG CTCAAGCCGGAACAAATGACTGACGATGAGCTGCTTGAAAGCATCAAGTTGCCACTGTTTGTCCTCTTCCAAAC GCT
iB_04702	TC031200	ACGTATCGAAGCGGAAAAGAAGCTCCTACTTCCCGAGAACGAACACGGCGCATTTTTGATCCGCGATTCGGAA AGCCGGCACAACGATTACTCGTTATCAGTCCGTGATGGAGATACCGTCAAACATTACAGAATCAGGCAACTGG ATGAAGGTGGTTTCTTCATCGCGCGGCGAACGACGTTTAGAACGCTTCAAGAACTAGTGGAACATTACAGTAA AGACCCAGACGGTCTGTGTGTCAATCTGTGCAAACCATGC
iB_04717	TC009877	AACTGCCCAACCACTTCTTGTCCGAAATTTACAAATGGGCCTTGGAATCTGTGGCTAGAGTCTCTTTGGACACT AGACTTGGCTGTCTAGAACCGAACCTGTCCCAAAATTCCGAATCACAGCGAATTATCAATTCCATAAACACCTT CTTCTGGAACGTGGCAGAAGTAGAACTGAAAATGCCCGTTTGGAGGGTTTACAAAAACAGAAGTTTCAAAAAA TACATCGGTGCTTTGGAAGAC
iB_06359	TC031191	TAGTCTGGAGCGAAGCTACAAGAGCCCCTTGTTACCAGAGCGGGCCCTCACTGGCCGTTATGACCCAGTTAGC GACATCA
iB_06806	TC000393	ACGCGCAGTATTCGTAGCTTAAGGATCCGAAAGCCGAAAGAACTTAAACTGCTTTTGAGAGAAATCTGGGAGC AGACCAAGGCCTTGTGCAAGCCGCCGCATCTCAGATATACCATAATTACGTGTCTGATCCAATTCGGCCTAACT ACAAGTTACTACACTTTGATGATTTGGTTCCCGGAGCTTTTCTACCGGTTTGAAGAGTTCGAAAATCTTCATCCG AACGAAAAAGCCACAGTGTGTG
iB_07361	TC009459	TGTAAACCGCGATGAAACAAATTTATTGTTTAATAACCGTCGTCGTTCTAATCCCGACACTCACTGCTCTTGAAA ATGAAGGGCAAAATCCTGATACAGCAAATTGTGTTGCGCTAGGTGGACAAAGAATCAAAGATTCTGAAATAGC AAAAATGGCTCATTGCATTCTCACCAA
iB_07902	TC001275	GGACAGAAAGGTGAGGACGAAGTGATGAATCAGATTCTAATAGAATGCATGAAACATTACAACCTGATTAAA AAATACACCAGTTTAGTAGCAGACTGTTTCAAAGAAATTATAACTTTGCAGTTCGTTCCAACGATTGTAATGATT TGCATTGCAATGTATAAAATATCCACGCTCGAGCCGTCGAACACGCAGTTTTGGTTTTTTGCGTTTACGGAACT CGGTGCTATAACCCAAATTTTCATTTACTGTTTCGTTGGCAATCTGGTCACTA
iB_08398	TC033206	CCCCAAAACGTTGATATTGCACGTGATAAGTTTCTAAGCGAGTTGCGGAGCGCTGAAGCGAAAAAAAACGAA AGTTCGCTCCACAACTCGTCTCCCTTGTTCTCGCACGTTTCCAAACCCCAAACCACCAAAGAGTTCACCAGGTCC GAGCCGGACTTGAACCTACCGGATAATCTAACCTTTGCTAACGCACTAACAGAAGACAAAGCTAAAAATGCTA CCCCGGTTTGTTGTCAGT
iB_08760	TC033755	GACGGTTCTCGGTTGAGAGAGACCCTCAAGCTCGATTTGAAGAATTCCGGGCTTTGTTAGAGCGCTTGCACAG ACTGCAGGACATAGCATTTTTGGTTTCGTATATTGACCCGAGCGATCAGGATTTGCTGCCAATCAACAATGATG ATAACCTTCGAAGGGCCTTAGCAAATGCAAAACCCCTCCTGAGGGTCATAATCCAAAGAAAAGGTGATAGTCT TGAACTGAATGGATACGGGA
iB_09043	TC016314	GTCTGGGAATGGACTCAGGATAATTGGTTGAATGACCCTGACGCCAAAGTGAAGAAAGGGGGCTCCTACCTC TGTCATGAGTCTTACTGTTGGAGGTATCGCTGCGCTGCAAGATCTTTCAATACCAAAGACAGTTCGGCCGGAA ATTTAGGCTTTCGATGTGCCGGTGATGTCAAATAATTTGGCAGTGAATAACAAACAAACCCAAGTACTTAAATC ATCCTGCCATCAAGTCTTCC
iB_09050	TC033022	ACGGGGTTTAGTGTGGAGTGTCAAGTGGACAGGTCTCAAGTGAAAAATCGTCAAATTGCTTTGGCTAAGTTGA GGGCTTTGATTTATCAACGTGATCTTGAAGAGCAGATAGCGAGGAACGAGAATATGAGGAAGAACCAAGTTA GGTCGAATTTTAGAAACGAGAAAATTAGGACTTATAATTTTCCGCAAGACAGGATCACTGATCATAGGTTACA GGGGTGCAATGT

iB_09103	TC014482	AATGGGGGCGGGTATTATCACTATTCCTATTCCGTGGTCAGGGGCTGTAACCGGATTATTCCGGTCGATATTTA CGTCCCGGGGTGTCCCCCAACCGCTGAGGCGCTCATGTATGGGATTTTGCAGCTTCA
iB_09413	TC005389	TGCTTGATTTTTCCCTCAGCTGATTATGTCCGAAATTTGGTGATTAAGCAATCGATGAGGCAAAAAATTCCGGT TGTTATCGACTGTTCACACATTTATGGTGCTGATTATACGGCAGCTACAGTCATTGAGAGTTTAACCAAAGATTT CAAAACGCGACAACAACCGCTGTTTTTTTACAATCTCAAGTCAAGTGTGAGCTCGGTTTTTGTCGGCCTAAACC TGGACTATTTTCTAGTCTATTACAACGAAGATGAGTTGGATGATATGCTCAAGAAGTGGACCGAAA
iB_10104	TC013627	TGCTGAAGAAGAGGCTCAAAATTTACGCAAGAAAGTGTCACGGATAGAAGATGATAATGAATCTTTGGTTTTG CAGCTGAAGAAAATGGCTACTCGAGCCAGAAGTCGTAAACTAAGTCCCACCAATAATTCAAGATTGACCCCAG AACCACCTTCTGAGAAAGGTGACGTATCAGACGACGAAGACCCCGCAGAAATCAAATTACAGTTAGAGTTGAG CGAACAAGAAGCTTCTGTTCTTCGACGCAAA
iB_10181	TC015547	GATGTACAGAGGGGGCAAGATCTGTCTCAGCGATCACTTCAAGCCTTTGTGGGCGCGAAACGTCCCCAAGTTT GGGATCGCGCACGCCATGGCGCTCGGGTTGGGGCCGTGGCTAGCCGTGGAAATCCCCGACTTGATCGCCAAA GGCGTGGTCACGCACAAGGAGAAA
iB_10701	TC014985	TCTCGTGTGTGCGTATCTCGCCAGAAATATATATTTTTATATTTTATTTATGTTTTTGAAACAATAATTCTTCTATT TATCTAGTTAGGTTCGTTAGTGTAAAAATTGCTCAGTCATTATTTGTGTTTGTGACCACACACGTCCATAAACAG GCGAGTCTGC

Additional file 3. Table S3. iBeetle identified genes involved in defensive stink gland function

iBeetle			re-screen categorized phenotype	OGS_# (ass. 5.2)	FC ≥ 2
iB_#	phase	phenotype			
iB_00081	**1st**	**abd gland partially color darker**	**irregular separation**	**Tc_000379**	**x**
iB_00105	**2nd**	**both glands darker, abd content decreased**	**empty/necrotic**	**Tc_000476**	
iB_00110	**1st**	**abd gland size increased**	**irregular reservoir size**	**Tc_000504**	**x**
iB_00185	**1st**	**abd color not present and shape irregular**	**empty/necrotic**	**Tc_000885**	
iB_00414	**1st**	**prothoracic glands partially color darker**	**secretion color darker**	**Tc_002616**	
iB_00754	1st	abd partially color darker	n.d.	Tc_031464 (Tc_004698)	
iB_01044	**1st**	**abd color darker**	**irregular separation**	**Tc_006408**	
iB_01236	1st	abd gland size decreased and irregular shape	n.d.	Tc_007650	
iB_01372	**1st**	**abd color darker**	**irregular separation**	**Tc_033883 (Tc_008608)**	
iB_01440	1st	abd gland color not present	n.d.	Tc_008936	
iB_01644	1st	abd color darker	n.d.	Tc_010033	
iB_01798	**1st**	**abd glands sometimes darker**	**irregular separation**	**Tc_011075**	
iB_01814	1st	abd glands mostly color darker	n.d.	Tc_011159	
iB_01910	1st	abd glands slightly color darker	n.d.	Tc_011969	
iB_01975	**2nd**	**both glands darker, abd content decreased**	**secretion color darker**	**Tc_012387**	
iB_02292	**1st**	**abd size decreased and partially color not present**	**less secretion**	**Tc_014494**	
iB_02297	**1st**	**unspecified alteration**	**empty/necrotic**	**Tc_014520**	
iB_02301	1st	abd color darker	n.d.	Tc_014544	
iB_02367	1st	abd gland color darker	n.d.	Tc_014967	
iB_02401	**1st**	**abd gland color darker**	**secretion color darker**	**Tc_015095**	
iB_02416	**1st**	**abd gland partially slightly color darker**	**irregular separation**	**Tc_015165**	**x**
iB_02428	**1st**	**abd gland shape and content irregular**	**irregular separation**	**Tc_015203**	
iB_02471	**1st**	**prothoracic glands partially darker color, abd glands size decreased**	**irregular reservoir size**	**Tc_015379**	**x**
iB_02516	**1st**	**glands content darker**	**Melanized**	**Tc_015811**	**x**
iB_02517	**1st**	**partially content darker**	**Melanized**	**Tc_030914 (Tc_015817, Tc_015818)**	
iB_02542	1st	gland content partially darker	n.d.	Tc_015993	
iB_02563	**1st**	**partially content not present**	**empty/necrotic**	**Tc_030950 (Tc_016253, Tc_016254)**	
iB_02584	1st	gland content not present	n.d.	Tc_030051	
iB_02625	1st	gland shape irregular	n.d.	Tc_011255	

iB_02627	**1st**	**abd glands partially content not present**	**less secretion**	**Tc_011288**	
iB_02633	1st	gland shape irregular, content partially not present	n.d.	Tc_031391 (Tc_011371)	
iB_02673	**1st**	**irregular shape, content partially not present**	**empty/necrotic**	**Tc_032251 (Tc_000239, Tc_000240)**	
iB_02692	1st	abd glands partially content not present	n.d.	Tc_003063	
iB_02716	**1st**	**abd glands mostly content not present, gland shape irregular**	**empty/necrotic**	**Tc_031046 and Tc_032493 (Tc_002723)**	
iB_02743	2nd	abd gland content partially not present	n.d.	Tc_003968	
iB_02774	**2nd**	**abd gland content darker**	**secretion color darker**	**Tc_008303**	
iB_02931	**1st**	**abd glands content darker**	**irregular separation**	**Tc_031247 (Tc_011810, Tc_011812)**	**x**
iB_03294	**2nd**	**abd gland content darker**	**secretion color darker**	**Tc_002074**	
iB_03401	1st	glands partially color darker	n.d.	Tc_002550	
iB_03552	**1st**	**gland color darker and partially decreased size**	**secretion color darker**	**Tc_032367 (Tc_003409)**	**x**
iB_03637	1st	sometimes gland size increased	n.d.	Tc_003857	
iB_03693	1st	gland size increased	n.d.	Tc_031485 (Tc_004126)	
iB_03695	**1st**	**gland color darker**	**irregular separation**	**Tc_004129**	
iB_03780	1st	glands darker	n.d.	Tc_031955 (Tc_004533, Tc_004534)	x
iB_03913	**1st**	**abd gland structure necrotic**	**empty/necrotic**	**Tc_005167**	
iB_04066	1st	abd gland color not present	n.d.	Tc_033952 (Tc_006098)	
iB_04137	1st	abd gland size increased	n.d.	Tc_034081 (Tc_006423)	
iB_04205	1st	abd glands not present	n.d.	Tc_006735	
iB_04420	2nd	abd mostly content decreased	irregular separation	Tc_008047	
iB_04702	**2nd**	**prothoracic glands darker**	**secretion color darker**	**Tc_031200 (Tc_009790, Tc_009792)**	
iB_04717	**2nd**	**both glands darker and content fragmented**	**Melanized**	**Tc_009877**	
iB_04797	**1st**	**abd gland size decreased and lighter color**	**Colorless**	**Tc_010251**	**x**
iB_04839	1st	both glands darker	n.d.	Tc_010449	
iB_04850	1st	abd glands partially color darker	n.d.	Tc_010484	
iB_05119	2nd	both glands darker, abd gland size decreased	less secretion	Tc_034419 (Tc_011865)	x
iB_05264	**1st**	**gland content mostly not present**	**empty/necrotic**	**Tc_012539**	
iB_05278	**1st**	**abd glands mostly content not present**	**empty/necrotic**	**Tc_034399 (Tc_012607,**	

				Tc_012609, Tc_012610)	
iB_05284	1st	abd glands content slightly darker	n.d.	Tc_034421 (Tc_012641, Tc_012642, Tc_012643, Tc_012644)	
iB_05329	**1st**	**abd glands content darker**	**irregular separation**	**Tc_012828**	
iB_05331	**1st**	**abd glands partially content not present**	**less secretion**	**Tc_012834**	
iB_05342	1st	abd glands content darker	n.d.	Tc_012857	
iB_05442	**1st**	**unspecified alteration**	**Colorless**	**Tc_033122 (Tc_013511, Tc_013513)**	**x**
iB_05518	**1st**	**abd gland color darker**	**Melanized**	**Tc_032992 (Tc_013892)**	
iB_05584	1st	abd glands partially color darker	n.d.	Tc_014205	
iB_05712	**1st**	**abd glands mostly content not present**	**less secretion**	**Tc_033471 (Tc_014869, Tc_014870)**	
iB_05719	**1st**	**abd glands partially content darker**	**irregular separation**	**Tc_014887**	
iB_05874	2nd	prothoracic glands darker	n.d.	Tc_015692	
iB_05942	2nd	abd gland size decreased, content darker	n.d.	Tc_031853 (Tc_016013, Tc_016016, Tc_016017, Tc_016018)	
iB_06333	2nd	abd gland content not present	n.d.	Tc_014550	
iB_06359	**2nd**	**abd content decreased and partially darker**	**secretion color darker**	**Tc_031191 (Tc_015926, Tc_015905)**	
iB_06684	2nd	abd content and size decreased, and abd content darker	n.d.	Tc_034492 (Tc_001853, Tc_001855)	
iB_06779	2nd	prothoracic glands darker	n.d.	Tc_004179	
iB_06806	**2nd**	**glands color darker and content fragmented**	**melanized**	**Tc_000393**	
iB_06868	2nd	abd gland color darker	n.d.	Tc_003208	
iB_07043	2nd	"stink glands"	less secretion	Tc_003827	
iB_07188	2nd	abd gland size increased, content opaque	n.d.	Tc_032832 (Tc_008176)	
iB_07361	**2nd**	**prothoracic glands darker**	**melanized**	**Tc_009459**	
iB_07747	2nd	abd content lighter and fragmented	n.d.	Tc_031768 (Tc_010623, Tc_010625)	
iB_07759	2nd	abd gland size and content decreased	n.d.	Tc_030320	
iB_07760	2nd	abd content decreased	n.d.	Tc_031822 (Tc_016034)	
iB_07764	2nd	abd content lighter & fragmented	n.d.	Tc_005075	
iB_07772	2nd	abd content decreased	n.d.	Tc_011144	

iB_07782	2nd	abd gland content spotted and partially darker	n.d.	Tc_006837	
iB_07783	2nd	abd gland content fragmented	n.d.	Tc_031904 (Tc_002154, Tc_002155)	
iB_07900	2nd	abd content lighter	secretion color darker	Tc_001243	
iB_07902	2nd	abd content decreased, fragmented	secretion color darker	Tc_001275	
iB_07917	2nd	abd content decreased, fragmented	n.d.	Tc_000183	
iB_07918	**2nd**	**abd content fragmented or potentially not present**	**less secretion**	**Tc_001376**	**x**
iB_07926	2nd	abd content split, lighter color, and size decreased	n.d.	Tc_003231	
iB_08184	2nd	abd gland color darker	less secretion	Tc_032964	
iB_08303	2nd	abd content potentially not present or darker	n.d.	Tc_030655	
iB_08398	**2nd**	**gland color darker, abd content partially not present**	**secretion color darker**	**Tc_033206**	
iB_08468	2nd	abd gland content not present	secretion color darker	Tc_015328	
iB_08506	**2nd**	**abd gland size and content decreased**	**less secretion**	**Tc_015537**	
iB_08561	2nd	abd gland size and content decreased	n.d.	Tc_004632	x
iB_08587	2nd	abd gland content not present, size decreased	n.d.	Tc_009420	
iB_08666	2nd	abd size decreased, and content split	n.d.	Tc_009201	
iB_08760	**2nd**	**abd gland content darker**	**melanized**	**Tc_033755 (Tc_009924)**	
iB_08861	**2nd**	**abd gland color decreased**	**melanized**	**Tc_006177**	
iB_09043	**2nd**	**both glands color darker, abd gland color not present**	**Colorless**	**Tc_016314**	**x**
iB_09050	**2nd**	**both glands color darker, abd gland content decreased**	**less secretion**	**Tc_033022 (Tc_013879, Tc_013880)**	
iB_09103	**2nd**	**abd content darker**	**melanized**	**Tc_014482**	
iB_09239	**2nd**	**abd gland content and size decreased**	**less secretion**	**Tc_008912**	
iB_09272	2nd	both gland content color darker, abd gland content not present	n.d.	Tc_006097	
iB_09308	2nd	abd content decreased, not present, or partially darker	n.d.	Tc_005489	
iB_09311	2nd	both glands color darker	n.d.	Tc_006635	
iB_09326	2nd	abd gland content decreased, irregular shape	n.d.	Tc_030081	
iB_09329	2nd	abd gland content not present, glands partially not present	n.d.	Tc_030130	
iB_09337	2nd	both glands color darker	n.d.	Tc_030243	

iB_09340	2nd	abd gland content not present, or darker	n.d.	Tc_032272 (Tc_000166, Tc_030316)	
iB_09355	**2nd**	**both glands color darker**	**secretion color darker**	**Tc_006363**	
iB_09403	2nd	abd gland content fragmented, abd gland color darker	n.d.	Tc_034170	
iB_09413	**2nd**	**both glands color darker**	**Melanized**	**Tc_005389**	**x**
iB_09430	**2nd**	**both glands darker and fragmented**	**secretion color darker**	**Tc_005306**	
iB_09661	2nd	abd glands potentially content decreased	n.d.	Tc_001099	x
iB_09736	2nd	abd gland color decreased	secretion color darker	Tc_003116	
iB_09896	2nd	abd gland content darker	n.d.	Tc_007557	
iB_09910	2nd	abd gland content decreased	n.d.	Tc_007292	
iB_09924	2nd	abd gland content potentially darker	n.d.	Tc_008270	
iB_09988	**2nd**	**abd gland content darker and decreased**	**less secretion**	**Tc_014025**	
iB_09991	**2nd**	**abd gland color darker**	**secretion color darker**	**Tc_014033**	
iB_10007	2nd	abd gland content split	n.d.	Tc_033075	
iB_10104	**2nd**	**both glands color darker**	**secretion color darker**	**Tc_013627**	
iB_10133	**2nd**	**abd gland content potentially not present or decreased**	**less secretion**	**Tc_014774**	
iB_10156	**2nd**	**abd gland content darker, or content not present**	**less secretion**	**Tc_033320 (Tc_015307)**	
iB_10159	2nd	abd gland content decreased or not present	secretion color darker	Tc_015429	x
iB_10181	**2nd**	**both glands color darker**	**secretion color darker**	**Tc_015547**	
iB_10206	2nd	abd gland content decreased or not present	n.d.	Tc_015049	
iB_10701	**2nd**	**abd gland content darker and decreased**	**Melanized**	**Tc_014985**	
iB_10748	2nd	abd gland content not present	n.d.	Tc_007828	

n.d. non detected (= wildtype)
bold confirmed specific gland phenotype
() former gene annotation (ass. 3.0)

Additional file 4. Table S4. Gene ontology of iBeetle identified genes affecting stink gland . function

iB_#	OGS_# (ass. 4.0)	*Tribolium castaneum* predictions (BLASTp on NCBI)	best *Drosophila melanogaster* hit [best characterized non-*Dm* hit]	gene ontology (GO)	
				inferred from FlyBase	category
iB_00081	Tc_000379	transmembrane emp24 domain-containing protein eca	eclair (CG33104)	Golgi vesicle transport	transporter
iB_00105	Tc_000476	ferritin subunit	ferritin 1 heavy chain homologue (CG2216)	iron import/ homeostasis/detoxification	others
iB_00110	Tc_000504	putative bifunctional UDP-N acetylglucosamine transferase and deubiquitinase ALG13 isoform X1	uncharacterized protein (CG3251) [*Zootermopsis nevadensis*: Protein ovarian tumor locus]	ovarian tumour protease activity, protein deubiquitination	enzyme
iB_00185	Tc_000885	uncharacterized protein LOC664170 isoform X1	uncharacterized protein encoded by *julius seizure* (CG14509, *slamdance*)	behavior, response to mechanosensory stimulus	unknown
iB_00414	Tc_002616	proton-coupled amino acid transporter 4	uncharacterized protein (CG7888) [*Oryctes borbonicus*: amino acid transporter]	amino acid transmembrane transport	transporter
iB_01044	Tc_006408	voltage-dependent anion-selective channel-like	porin (CG6647)	voltage-gated anion channel	channel
iB_01372	Tc_033883	cartilage oligomeric matrix protein	thrombospondin (CG11326)	cell adhesion, muscle attachment	others
iB_01798	Tc_011075	leucine-rich repeat-containing protein 40 isoform X2	sclp (CG2471)	muscle system process	others
iB_01975	Tc_012387	kelch repeat and BTB domain-containing protein 12	uncharacterized protein (CG30357) [*Harpegnathos saltator*: Kelch-like protein 26]		unknown
iB_02292	Tc_014494	serine/threonine-protein phosphatase 2A activator	phosphotyrosyl phosphatase activator (CG3289)	protein tyrosine phosphatase activator	others
iB_02297	Tc_014520	uncharacterized protein LOC660773, FAST kinase domain-containing protein 2	none found [*Zootermopsis nevadensis*: FAST kinase domain-containing protein 2]		enzyme
iB_02401	Tc_015095	facilitated trehalose transporter Tret1	trehalose transporter 1-2 (CG8234)	trehalose transmembrane transport	transporter
iB_02416	Tc_015165	Golgi SNAP receptor complex member 1	Golgi SNARE 28kDa (CG7700)	SNAP receptor activity, Golgi vesicle transport	others
iB_02428	Tc_015203	putative fatty acyl-CoA reductase isoform X1	waterproof (CG1443)	fatty acyl-CoA reductase activity	enzyme
iB_02471	Tc_015379	putative fatty acyl-CoA reductase	uncharacterized protein (CG1441) [*Camponutus floridanus*: fatty acyl-CoA reductase 1]	fatty acyl-CoA reductase activity	enzyme
iB_02516	Tc_015811	prostatic acid phosphatase	Acid-phosphatase 1 (CG7899)	acid phosphatase activity, dephosphorylation	enzyme

iB_02517	Tc_030914	copper-transporting ATPase 1 isoform X1	ATP7 (CG1886)	copper ion transmembrane transporter, copper ion homeostasis	enzyme
iB_02563	Tc_030950	glutamyl aminopeptidase	uncharacterized protein (CG8773) [*Acromyrmex echinatior*: glutamyl aminopeptidase]	aminopeptidase activity, dsRNA transport	enzyme
iB_02627	Tc_011288	calcium-activated potassium channel slowpoke isoform X2	slowpoke (CG10693)	calcium-activated potassium channel activity	channel
iB_02673	Tc_032251	pH-sensitive chloride channel isoform X5	glutamate-gated chloride channel GluClα (CG7535)	extracellular-glutamate-gated chloride channel activity	channel
iB_02716	Tc_002723	filamin-A	jitterbug (CG30092)	actin binding, establishment of body hair or bristle planar orientation	others
iB_02774	Tc_008303	yemanuclein-alpha isoform X1	yemanuclein (CG14513)	DNA binding, fertilization	others
iB_02931	Tc_031247	death-associated protein kinase related	death-associated protein kinase related (CG32666)	protein serine/threonine kinase activity	enzyme
iB_03294	Tc_002074	integrator complex subunit 3 homolog	integrator 3 (CG17665)	snRNA processing	others
iB_03552	Tc_032367	hypothetical protein	none found [none found]		unknown
iB_03695	Tc_004129	hepatocyte nuclear factor 6 isoform X3	onecut (CG1922)	transcriptional activator activity	transcription factor
iB_03913	Tc_005167	IQ motif and SEC7 domain-containing protein 1 isoform X2	schizo (CG32434)	guanyl-nucleotide exchange factor activity	others
iB_04420	Tc_008047	mucin-22-like	none [none]		unknown
iB_04702	Tc_031200	tyrosine-protein kinase Src42A isoform X2	src oncogene at 42A, isoform A (CG44128)	protein tyrosine kinase activity	enzyme
iB_04717	Tc_009877	probable cytochrome P450 49a1	cytochrome p450 49a1 (CG18377)	oxidoreductase activity	enzyme
iB_04797	Tc_010251	cytochrome P450 6a2	cytochrome P450 6a2 (CG9438)	oxidoreductase activity	enzyme
iB_05119	Tc_034419	uncharacterized protein LOC655706	tetraspanin 39D (CG8666)		unknown
iB_05264	Tc_012539	down syndrome cell adhesion molecule precursor	down syndrome cell adhesion molecule-1 (CG17800)	axon guidance receptor activity	others
iB_05278	Tc_034399	disintegrin and metalloproteinase domain-containing protein 11	mind-meld (CG42252)	metalloendopeptidase activity	enzyme
iB_05329	Tc_012828	cuticle protein 18.7	cuticular protein 92F (CG5494)	structural constituent of chitin-based cuticle	others
iB_05331	Tc_012834	attractin-like protein 1	distracted (CG5634)	synaptic target recognition	others
iB_05442	Tc_033122	T-box transcription factor TBX20	midline (CG6634)	transcriptional repressor activity	transcription factor
iB_05518	Tc_032992	protein takeout-like	uncharacterized protein (CG2016) [*Zootermopsis nevadensis*: protein takeout]		unknown
iB_05712	Tc_033471	RIMS-binding protein 2	RIM binding protein (CG43073)	cytoskeletal matrix organization at active	others

				zone, neuromuscular synaptic transmission	
iB_05719	Tc_014887	dehydrogenase/reductase SDR family member 11-like	antdh (CG1386)	carbonyl reductase (NADPH) activity, sensory perception of smell	enzyme
iB_06359	Tc_031191	adenylosuccinate synthetase	adenylosuccinate synthetase (CG17273)	adenylosuccinate synthase activity, neurogenesis	enzyme
iB_06806	Tc_000393	synaptic vesicle glycoprotein 2B-like isoform X3	uncharacterized protein (CG3168, isoform A) [*Papilio machaon*: Synaptic vesicle glycoprotein 2B]	transmembrane transporter activity	unknown
iB_07043	Tc_003827	zinc-finger autosomal protein-like	uncharacterized protein (CG31612, isoform A) [none found]	metal ion binding, nucleic acid binding	unknown
iB_07361	Tc_009459	TcOBP7A, Odorant binding protein -C21	C- odorant binding protein	chemosensation	others
iB_07900	Tc_001243	vacuolar protein sorting-associated protein 33B	vacuolar protein sorting 33B (CG5127)	vesicle-mediated transport, regulation of SNARE complex assembly	others
iB_07902	Tc_001275	odorant receptor 2a-like	odorant receptor 2a (CG3206)	olfactory receptor activity, sensory perception of smell	others
iB_07918	Tc_001376	hypothetical protein	uncharacterized protein (CG11318) [*Zootermopsis nevadensis*: putative G-protein coupled receptor 112]	G-protein coupled receptor activity, cell surface receptor signaling pathway	others
iB_08184	Tc_032964	hypothetical protein	none found [none found]		unknown
iB_08398	Tc_033206	PDZ and LIM domain protein Zasp	Z band alternatively spliced PDZ-motif protein 52 (CG30084)	muscle alpha-actinin binding, muscle structure development	others
iB_08468	Tc_015328	ubiquitin-conjugating enzyme E2 L3	ubiquitin conjugating enzyme 10 (CG5788)	ubiquitin protein ligase binding, protein ubiquitination, neurogenesis	enzyme
iB_08506	Tc_015537	protein GUCD1 isoform X1	uncharacterized protein (CG13760) [none found]		unknown
iB_08760	Tc_033755	partitioning defective 6 homolog beta	par-6, isoform A (CG5884)	protein binding, epithelium development, establishment of neuroblast polarity, regulation of cell shape	others
iB_08861	Tc_006177	uncharacterized protein LOC103313800	beat-Vc (CG14390)	heterophilic cell-cell adhesion via plasma membrane cell	others
iB_09043	Tc_016314	sulfatase-modifying factor 1	uncharacterized protein (CG7049) [*Papilio xuthus*: sulfatase-modifying factor 1]		enzyme
iB_09050	Tc_033022	peptide chain release factor 1-like, mitochondrial	uncharacterized protein (CG5705) [*Anopheles darlingi*: peptide chain release factor 1]	translation release factor activity, translational termination	others
iB_09103	Tc_014482	guanine nucleotide-binding protein subunit beta-1	G-protein beta-subunit 13F (CG10545)	GTPase activity, actin filament organization, asymmetric neuroblast division	others

iB_09239	Tc_008912	AP-3 complex subunit sigma-2 isoform X1	orange (CG3029)	protein transporter activity, compound eye pigmentation, intracellular transport, synaptic vesicle coating	others
iB_09355	Tc_006363	melanoma-associated antigen D2-like	MAGE (CG10059)	contributes to SUMO transferase activity, cellular response to DNA damage stimulus, neuron projection morphogenesis	others
iB_09413	Tc_005389	sodium-independent sulfate anion transporter	epidermal stripes and patches (CG7005)	secondary active sulfate transmembrane transporter activity, sulfate transmembrane transport	transporter
iB_09430	Tc_005306	serine/threonine-protein kinase RIO3	uncharacterized protein (CG3008) [*Oryctes borbonicus*: phosphotransferase]	protein serine/threonine kinase activity	enzyme
iB_09736	Tc_003116	FIT family protein CG10671	uncharacterized protein (CG10671) [P*apilio xuthus:* FIT family protein CG10671]	lipid storage	others
iB_09988	Tc_014025	slit homolog 3 protein-like	leucine-rich repeat-containing G protein-coupled receptor 2 (rickets; CG8930)	neuropeptide receptor activity, regulation of chitin-based cuticle tanning, neuropeptide signaling pathway	others
iB_09991	Tc_014033	sodium/potassium-transporting ATPase subunit beta-2-like	nervana 2, isoform C (CG9261)	sodium:potassium-exchanging ATPase activity, open tracheal system development, establishment of glial blood-brain barrier	enzyme
iB_10104	Tc_013627	putative leucine-rich repeat-containing protein DDB_G0290503 isoform X1	uncharacterized protein (CG18304) [*Habropoda laboriosa*: protein SOGA3]	Protein SOGA, regulation of autophagy	others
iB_10133	Tc_014774	histone acetyltransferase KAT2A	Gcn5 ortholog (CG4107)	histone acetyltransferase activity	enzyme
iB_10156	Tc_033320	probable anion transporter 2, chloroplastic	major facilitator superfamily transporter 9, isoform B (CG4288)	high-affinity inorganic phosphate:sodium symporter activity, transmembrane transport	transporter
iB_10159	Tc_015429	adiponectin receptor protein isoform X1	adiponectin receptor (CG5315)	adipokinetic hormone receptor activity, triglyceride homeostasis, glucose homeostasis	others
iB_10181	Tc_015547	ubiquitin-fold modifier-conjugating enzyme 1	uncharacterized protein (CG8386) [*Zootermopsis nevadensis*: Ufm1-conjugating enzyme 1]	Ubiquitin-fold modifier-conjugating enzyme 1	enzyme
iB_10701	Tc_014985	formin-binding protein 1-like	Cdc42-interacting protein 4, isoform B (CG15015)	phospholipid binding, Rho GTPase binding, cellular protein localization	others

Additional file 5. Table S5. Expression data of iBeetle detected gland genes function

iB_#	OGS_# (ass.3.0)	male - thx		female - thx		male - abd		female – abd		reference tissue (mid abdomen)		log2 FC (sample reads/reference reads)			
		reads	depth	reads	depth	reads	depth	reads	depth	reads	depth	male - thx	female - thx	male - abd	female - abd
iB_00081	Tc_000379	2466	143.28	2331	135.44	2332	135.50	3090	179.54	1031	59.91	1.258	1.177	1.178	1.584
iB_00105	Tc_000476	29304	1718.44	30781	1805.06	27672	1622.74	17243	1011.16	17513	1027.00	0.743	0.814	0.660	-0.022
iB_00110	Tc_000504	45	0.92	99	2.02	85	1.73	122	2.49	13	0.27	1.791	2.929	2.709	3.230
iB_00185	Tc_000885	144	5.85	113	4.59	54	2.19	10	0.41	157	6.37	-0.125	-0.474	-1.540	-3.973
iB_00414	Tc_002616	2227	58.77	2140	56.47	2323	61.30	3540	93.42	1747	46.10	0.350	0.293	0.411	1.019
iB_00754	Tc_004698	779	7.93	591	6.02	820	8.35	1094	11.14	2216	22.56	-1.508	-1.907	-1.434	-1.018
iB_01044	Tc_006408	7507	270.91	7545	272.28	8356	301.55	7917	285.70	14097	508.72	-0.909	-0.902	-0.755	-0.832
iB_01236	Tc_007650	361	6.30	356	6.21	423	7.38	450	7.85	336	5.86	0.104	0.083	0.332	0.421
iB_01372	Tc_008608	144	1.72	69	0.83	179	2.14	176	2.11	2111	25.25	-3.874	-4.935	-3.560	-3.584
iB_01440	Tc_008936	162	6.68	170	7.01	174	7.18	140	5.78	1216	50.17	-2.908	-2.839	-2.805	-3.119
iB_01644	Tc_010033	926	39.76	978	41.99	1311	56.29	871	37.40	603	25.89	0.619	0.698	1.120	0.531
iB_01798	Tc_011075	153	10.77	105	7.39	150	10.56	625	43.98	3516	247.42	-4.522	-5.065	-4.551	-2.492
iB_01814	Tc_011159	1588	55.72	1479	51.89	956	33.54	847	29.72	1829	64.18	-0.204	-0.306	-0.936	-1.111
iB_01910	Tc_011969	3	0.09	0	0	587	16.82	2	0.06	3	0.09	0	-	7.612	-0.585
iB_01975	Tc_012387	2	0.03	0	0	2716	34.13	0	0	4	0.05	-1.000	-	9.407	-
iB_02292	Tc_014494	456	13.25	492	14.29	546	15.86	463	13.45	372	10.81	0.294	0.403	0.554	0.316
iB_02297	Tc_014520	556	11.40	499	10.23	576	11.81	521	10.68	1025	21.01	-0.882	-1.039	-0.831	-0.976
iB_02301	Tc_014544	7	0.22	20	0.64	231	7.35	33	1.05	65	2.07	-3.215	-1.700	1.829	-0.978
iB_02367	Tc_014967	115	3.71	106	3.42	140	4.51	116	3.74	78	2.51	0.560	0.443	0.844	0.573
iB_02401	Tc_015095	1527	39.15	1831	46.95	1367	35.05	1031	26.44	881	22.59	0.793	1.055	0.634	0.227
iB_02416	Tc_015165	550	30.42	515	28.49	557	30.81	425	23.51	241	13.33	1.190	1.096	1.209	0.818
iB_02428	Tc_015203	427	10.36	344	8.35	515	12.50	73	1.77	251	6.09	0.767	0.455	1.037	-1.782
iB_02471	Tc_015379	616	16.57	487	13.10	2226	59.86	3212	86.38	132	3.55	2.222	1.883	4.076	4.605
iB_02516	Tc_015811	682	21.23	757	23.56	881	27.42	814	25.33	367	11.42	0.894	1.045	1.263	1.149
iB_02517	Tc_015817	4	0.44	3	0.33	11	1.20	5	0.55	31	3.39	-2.954	-3.369	-1.495	-2.632
	Tc_015818	1563	16.68	1182	12.61	2019	21.55	1442	15.39	1537	16.40	0.024	-0.379	0.394	-0.092
iB_02542	Tc_015993	6654	170.62	5142	131.85	1761	45.15	1126	28.87	4431	113.62	0.587	0.215	-1.331	-1.976
iB_02563	Tc_016253	50	2.48	65	3.23	52	2.58	41	2.04	234	11.62	-2.227	-1.848	-2.170	-2.513
	Tc_016254	767	10.69	710	9.89	3365	46.89	10312	143.69	2551	35.55	-1.734	-1.845	0.400	2.015
iB_02584	Tc_030051	1210	29.08	1089	26.17	1279	30.74	1205	28.96	621	14.93	0.962	0.810	1.042	0.956

iB_02625	Tc_011255	466	5.26	421	4.75	836	9.43	757	8.54	1731	19.52	-1.893	-2.040	-1.050	-1.193
iB_02627	Tc_011288	156	1.66	115	1.23	95	1.01	60	0.64	1637	17.44	-3.391	-3.831	-4.107	-4.770
iB_02633	Tc_011371	275	4.58	222	3.70	265	4.41	285	4.74	774	12.88	-1.493	-1.802	-1.546	-1.441
iB_02673	Tc_000239	1	0.19	1	0.19	1	0.19	1	0.19	10	1.86	-3.322	-3.322	-3.322	-3.322
	Tc_000240	16	0.40	22	0.55	16	0.40	36	0.90	279	6.97	-4.124	-3.665	-4.124	-2.954
iB_02692	Tc_003063	489	2.50	363	1.86	913	4.67	1518	7.77	3242	16.59	-2.729	-3.159	-1.828	-1.095
iB_02716	Tc_002723	2823	12.35	2279	9.97	3947	17.27	6931	30.33	4815	21.07	-0.770	-1.079	-0.287	0.526
iB_02743	Tc_003968	29	1.48	19	0.97	99	5.04	58	2.95	56	2.85	-0.949	-1.559	0.822	0.051
iB_02774	Tc_008303	419	6.28	343	5.14	448	6.72	449	6.73	620	9.29	-0.565	-0.854	-0.469	-0.466
iB_02931	Tc_011810	660	76.70	547	63.57	698	81.11	148	17.20	136	15.80	2.279	2.008	2.360	0.122
	Tc_011812	7031	261.94	7559	281.61	8061	300.31	2731	101.74	951	35.43	2.886	2.991	3.083	1.522
iB_03294	Tc_002074	347	4.33	314	3.92	384	4.79	340	4.24	806	10.06	-1.216	-1.360	-1.070	-1.245
iB_03401	Tc_002550	607	13.05	503	10.82	699	15.03	637	13.70	668	14.37	-0.138	-0.409	0.065	-0.069
iB_03552	Tc_003409	44	1.86	49	2.07	40	1.69	53	2.24	19	0.80	1.212	1.367	1.074	1.480
iB_03637	Tc_003857	0	0	0	0	2	0.07	0	0	45	1.50	-	-	-4.492	-
iB_03693	Tc_004126	91	0.56	41	0.25	25	0.15	17	0.10	821	5.02	-3.173	-4.324	-5.037	-5.594
iB_03695	Tc_004129	8	0.18	6	0.13	8	0.18	0	0	41	0.92	-2.358	-2.773	-2.358	-
iB_03780	Tc_004533	370	19.21	357	18.53	364	18.90	470	24.40	249	12.93	0.571	0.520	0.548	0.917
	Tc_004534	847	34.28	783	31.69	903	36.54	876	35.45	384	15.54	1.141	1.028	1.234	1.190
iB_03913	Tc_005167	670	9.19	672	9.22	1101	15.11	1069	14.67	1211	16.62	-0.854	-0.850	-0.137	-0.180
iB_04066	Tc_006098	12	0.07	16	0.09	40	0.23	36	0.21	2391	13.94	-7.638	-7.223	-5.901	-6.053
iB_04137	Tc_006423	2328	35.79	2109	32.42	1977	30.39	1778	27.33	1746	26.84	0.415	0.273	0.179	0.026
iB_04205	Tc_006735	248	4.47	232	4.19	3447	62.20	351	6.33	874	15.77	-1.817	-1.914	1.980	-1.316
iB_04420	Tc_008047	0	0	0	0	0	0	0	0	0	0	-	-	-	-
iB_04702	Tc_009790	404	33.89	360	30.20	368	30.87	183	15.35	450	37.75	-0.156	-0.322	-0.290	-1.298
	Tc_009792	2016	60.37	1991	59.62	1705	51.06	1261	37.76	1457	43.63	0.468	0.450	0.227	-0.208
iB_04717	Tc_009877	3	0.07	4	0.09	82	1.92	20	0.47	26	0.61	-3.115	-2.700	1.657	-0.379
iB_04797	Tc_010251	29710	760.26	33432	855.50	39562	1012.36	14185	362.98	1510	38.64	4.298	4.469	4.711	3.232
iB_04839	Tc_010449	963	62.23	754	48.73	406	26.24	866	55.97	555	35.87	0.795	0.442	-0.451	0.642
iB_04850	Tc_010484	341	11.16	172	5.63	312	10.21	1354	44.32	3204	104.87	-3.232	-4.219	-3.360	-1.243
iB_05119	Tc_011865	8620	328.88	7351	280.46	11479	437.95	11409	435.28	3498	133.46	1.301	1.071	1.714	1.706
iB_05264	Tc_012539	245	1.60	190	1.24	280	1.82	403	2.63	984	6.41	-2.006	-2.373	-1.813	-1.288
iB_05278	Tc_012607	0	0	0	0	1	0.10	0	0	3	0.31	-	-	-1.585	-
	Tc_012609	8	0.21	5	0.13	8	0.21	105	2.78	7	0.19	0.193	-0.485	0.193	3.907
	Tc_012610	85	1.02	43	0.51	109	1.30	69	0.82	147	1.76	-0.790	-1.773	-0.431	-1.091
iB_05284	Tc_012641	10	0.56	6	0.34	41	2.31	16	0.90	1993	112.20	-7.639	-8.376	-5.603	-6.961
	Tc_012642	0	0	0	0	43	2.04	0	0	1	0.05	-	-	5.426	-
	Tc_012643	0	0	0	0	33	1.9	0	0	0	0	-	-	-	-
	Tc_012644	0	0	0	0	467	13.5	0	0	0	0	-	-	-	-
iB_05329	Tc_012828	89	4.32	44	2.14	1020	49.50	433	21.01	927	44.99	-3.381	-4.397	0.138	-1.098
iB_05331	Tc_012834	449	4.54	401	4.05	672	6.79	486	4.91	931	9.40	-1.052	-1.215	-0.470	-0.938
iB_05342	Tc_012857	629	15.59	466	11.55	860	21.32	746	18.49	713	17.67	-0.181	-0.614	0.270	0.065
iB_05442	Tc_013511	238	11.46	238	11.46	418	20.13	127	6.12	10	0.48	4.573	4.573	5.385	3.667
	Tc_013513	444	15.12	484	16.48	826	28.13	204	6.95	21	0.72	4.402	4.527	5.298	3.280
iB_05518	Tc_013892	601	25.55	502	21.34	683	29.03	1110	47.18	1139	48.41	-0.922	-1.182	-0.738	-0.037

iB_05584	Tc_014205	302	20.90	268	18.55	340	23.53	401	27.76	350	24.23	-0.213	-0.385	-0.042	0.196
iB_05712	Tc_014869	0	0	1	0.02	1	0.02	0	0	44	0.87	-	-5.459	-5.459	-
	Tc_014870	1	0.01	2	0.03	9	0.13	0	0	77	1.14	-6.267	-5.267	-3.097	-
iB_05719	Tc_014887	210	10.43	168	8.35	504	25.04	2334	115.94	437	21.71	-1.057	-1.379	0.206	2.417
iB_05874	Tc_015692	137	3.59	108	2.83	73	1.91	101	2.65	141	3.70	-0.042	-0.385	-0.950	-0.481
iB_05942	Tc_016013	0	0	2	0.31	0	0	1	0.15	7	1.07	-	-1.807	-	-2.807
	Tc_016016	3	0.09	3	0.09	5	0.15	3	0.09	19	0.59	-2.663	-2.663	-1.926	-2.663
	Tc_016017	2	0.15	6	0.46	2	0.15	9	0.69	20	1.53	-3.322	-1.737	-3.322	-1.152
	Tc_016018	51	1.61	53	1.67	38	1.20	107	3.37	124	3.91	-1.282	-1.226	-1.706	-0.213
iB_06333	Tc_014550	7	0.34	4	0.19	137	6.60	17	0.82	24	1.16	-1.778	-2.585	2.513	-0.498
iB_06359	Tc_015905	0	0	0	0	180	12	0	0	6	0.40	-	-	4.907	-
	Tc_015926	31	2.97	47	4.51	57	5.47	66	6.33	46	4.41	-0.569	0.031	0.309	0.521
iB_06684	Tc_001853	1	0.04	3	0.11	0	0	1	0.04	2	0.07	-1.000	0.585	-	-1.000
	Tc_001855	2	0.06	0	0	0	0	1	0.03	3	0.09	-0.585	-	-	-1.585
iB_06779	Tc_004179	19	2.97	20	3.13	20	3.13	24	3.75	18	2.81	0.078	0.152	0.152	0.415
iB_06806	Tc_000393	163	3.96	284	6.89	210	5.10	7112	172.58	1192	28.92	-2.870	-2.069	-2.505	2.577
iB_06868	Tc_003208	535	23.21	501	21.73	761	33.01	500	21.69	406	17.61	0.398	0.303	0.906	0.300
iB_07043	Tc_003827	234	5.59	238	5.69	248	5.93	324	7.74	185	4.42	0.339	0.363	0.423	0.808
iB_07188	Tc_008176	1	0.02	6	0.11	15	0.27	0	0	9	0.16	-3.170	-0.585	0.737	-
iB_07361	Tc_009459	1	0.11	0	0	38	4.01	1	0.11	4	0.42	-2.000	-	3.248	-2.000
iB_07747	Tc_010623	1	0.06	1	0.06	1	0.06	2	0.11	1	0.06	0	0	0	1
	Tc_010625	11	0.11	2	0.02	7	0.07	14	0.14	26	0.25	-1.241	-3.700	-1.893	-0.893
iB_07759	Tc_030320	0	0	0	0	0	0	0	0	0	0	-	-	-	-
iB_07760	Tc_016034	79	1.59	26	0.52	53	1.07	32	0.65	371	7.48	-2.231	-3.835	-2.807	-3.535
iB_07764	Tc_005075	0	0.00	0	0.00	8	0.15	6	0.11	6	0.11	-	-	0.415	0.000
iB_07772	Tc_011144	583	16.30	514	14.37	639	17.87	600	16.78	430	12.02	0.439	0.257	0.571	0.481
iB_07782	Tc_006837	84	4.84	75	4.32	64	3.68	51	2.94	114	6.56	-0.441	-0.604	-0.833	-1.160
iB_07783	Tc_002154	7	0.24	4	0.14	4	0.14	0	0	0	0	-	-	-	-
	Tc_002155	1	0.02	0	0	0	0	0	0	0	0	-	-	-	-
iB_07900	Tc_001243	161	3.47	150	3.23	197	4.24	126	2.71	134	2.89	0.265	0.163	0.556	-0.089
iB_07902	Tc_001275	0	0	0	0	0	0	0	0	0	0	-	-	-	-
iB_07917	Tc_000183	319	25.25	336	26.60	277	21.93	238	18.84	226	17.89	0.497	0.572	0.294	0.075
iB_07918	Tc_013776	703	21.20	724	21.83	521	15.71	444	13.39	179	5.40	1.974	2.016	1.541	1.311
iB_07926	Tc_003231	8	0.50	17	1.06	10	0.62	6	0.37	104	6.46	-3.700	-2.613	-3.379	-4.115
iB_08184	Tc_032964	newly annotated gene													
iB_08303	Tc_030655	407	27.57	345	23.37	484	32.78	282	19.10	361	24.45	0.173	-0.065	0.423	-0.356
iB_08398	Tc_033206	newly annotated gene													
iB_08468	Tc_015328	1526	124.71	1615	131.98	2087	170.55	1157	94.55	1006	82.21	0.601	0.683	1.053	0.202
iB_08506	Tc_015537	740	40.93	570	31.53	816	45.14	528	29.21	461	25.50	0.683	0.306	0.824	0.196
iB_08561	Tc_004632	367	33.44	255	23.24	141	12.85	781	71.17	6	0.55	5.935	5.409	4.555	7.024
iB_08587	Tc_009420	462	4.19	455	4.13	667	6.05	1071	9.71	764	6.93	-0.726	-0.748	-0.196	0.487
iB_08666	Tc_009201	302	2.49	180	1.49	303	2.50	314	2.59	438	3.61	-0.536	-1.283	-0.532	-0.480
iB_08760	Tc_009422	781	48.97	714	44.77	819	51.36	518	32.48	415	26.02	0.912	0.783	0.981	0.320
iB_08861	Tc_006177	0	0	0	0	0	0	1	0.08	2	0.16	-	-	-	-1.000
iB_09043	Tc_016314	665	28.75	623	26.93	1315	56.85	1283	55.47	322	13.92	1.046	0.952	2.030	1.994

iB_09050	Tc_013879	159	5.19	119	3.88	145	4.73	120	3.92	210	6.86	-0.401	-0.819	-0.534	-0.807
	Tc_013880	0	0	0	0	0	0	0	0	1	0.20	-	-	-	-
iB_09103	Tc_014482	4	0.25	2	0.12	90	5.56	0	0	5	0.31	-0.322	-1.322	4.170	-
iB_09239	Tc_008912	257	16.95	207	13.66	170	11.22	203	13.39	294	19.40	-0.194	-0.506	-0.790	-0.534
iB_09272	Tc_006097	57	2.28	63	2.53	36	1.44	43	1.72	34	1.36	0.745	0.890	0.082	0.339
iB_09308	Tc_005489	12	0.44	12	0.44	4	0.15	1	0.04	11	0.41	0.126	0.126	-1.459	-3.459
iB_09311	Tc_006635	0	0	0	0	1	0.05	0	0	8	0.37	-	-	-3.000	-
iB_09326	Tc_030081	1	0.07	0	0	0	0	3	0.20	1	0.07	0.000	-	-	1.585
iB_09329	Tc_030130	0	0	0	0	0	0	0	0	0	0	-	-	-	-
iB_09337	Tc_030243	1	0.03	0	0	1	0.03	8	0.25	4	0.13	-2.000	-	-2.000	1.000
iB_09340	Tc_000166	4	0.13	18	0.6	7	0.23	0	0	1	0.03	2.000	4.170	2.807	-
	Tc_030316	2	0.07	2	0.07	3	0.10	0	0	0	0	-	-	-	-
iB_09355	Tc_006363	161	8.22	126	6.44	119	6.08	159	8.12	97	4.95	0.731	0.377	0.295	0.713
iB_09403	Tc_034170	newly annotated gene													
iB_09413	**Tc_005389**	4693	97.77	4731	98.56	5706	118.88	1632	34.00	25	0.52	7.552	7.564	7.834	6.029
iB_09430	Tc_005306	1414	34.51	1313	32.04	1591	38.83	1202	29.34	1226	29.92	0.206	0.099	0.376	-0.029
iB_09661	Tc_001099	860	35.03	874	35.60	1025	41.75	849	34.58	301	12.26	1.515	1.538	1.768	1.496
iB_09736	Tc_003166	0	0	0	0	0	0	0	0	0	0	-	-	-	-
iB_09896	Tc_007557	36	0.32	17	0.15	25	0.22	45	0.40	245	2.18	-2.767	-3.849	-3.293	-2.445
iB_09910	Tc_007292	214	7.93	149	5.52	282	10.44	298	11.04	598	22.15	-1.483	-2.005	-1.084	-1.005
iB_09924	Tc_008270	65	2.23	65	2.23	75	2.57	37	1.27	168	5.77	-1.370	-1.370	-1.163	-2.183
iB_09988	Tc_014025	1515	43.32	1535	43.89	1041	29.77	588	16.81	841	24.05	0.849	0.868	0.308	-0.516
iB_09991	Tc_014033	325	22.87	336	23.64	133	9.36	97	6.83	179	12.60	0.860	0.909	-0.429	-0.884
iB_10007	Tc_033075	newly annotated gene													
iB_10104	Tc_013627	295	1.87	205	1.30	130	0.82	651	4.13	10437	66.23	-5.145	-5.670	-6.327	-4.003
iB_10133	Tc_014774	584	9.48	538	8.74	596	9.68	610	9.91	535	8.69	0.126	0.008	0.156	0.189
iB_10156	Tc_015307	3197	52.94	2938	48.65	3400	56.30	4317	71.48	1868	30.93	0.775	0.653	0.864	1.209
iB_10159	Tc_015429	12496	401.73	14782	475.23	19055	612.60	8154	262.14	2891	92.94	2.112	2.354	2.721	1.496
iB_10181	Tc_015547	638	48.39	589	44.67	613	46.50	619	46.95	344	26.09	0.891	0.776	0.833	0.848
iB_10206	Tc_015049	215	2.51	181	2.11	211	2.46	180	2.10	196	2.29	0.133	-0.115	0.106	-0.123
iB_10701	Tc_014985	276	26.09	334	31.57	265	25.05	303	28.64	252	23.82	0.131	0.406	0.073	0.266
iB_10748	Tc_007828	1	0.12	0	0.00	2036	243.30	0	0	0	0	-	-	-	-

bold identified both by the phenoytpic iBeetle screen as well as transcriptomics

Additional file 6. Table S6. Representation of transcriptomics-identified genes in the iBeetle screen.

OGS_# (ass. 3.0)	GT#	categorized phenotype	iBeetle			annotation notes (ass. 5.2)
			iB_#	phase	phenotype	
Tc_000889	*GT01*	*turbid*	*iB_03099*	*2nd*	*n.d.*	
Tc_000917	*GT02*	*melanized*	*iB_00186*	*1st*	*lethal*	
Tc_001937	GT04	wildtype	iB_06143	1st	n.d.	
Tc_002483	GT06	less secretion				
Tc_002669	GT07	wildtype	iB_00423	1st	lethal	
Tc_002938	GT08	wildtype	iB_03472	2nd	n.d.	
Tc_003110	*GT09*	*less secretion*	*iB_03500*	*2nd*	*n.d.*	
Tc_003112	GT10	wildtype	iB_00517	2nd	n.d.	splitted in Tc_032318 and Tc_032319; iB_# refers to Tc_032318
Tc_003284	GT11	wildtype	iB_03534	1st	n.d.	
Tc_003768	GT12	turbid				splitted in Tc_032538 and Tc_032539
Tc_003771	GT13	empty/necrotic				
Tc_003835	GT14	less secretion				
Tc_004085	GT15	wildtype	iB_09573	2nd	n.d.	splitted in Tc_031224 and Tc_031871
Tc_004655	GT17	less secretion				
Tc_005106	GT18	melanized				unmapped
Tc_005384	GT19	wildtype	iB_00841	1st	n.d.	
Tc_005389	***GT20***	***melanized***	***iB_09413***	***2nd***	***conf.***	
Tc_005529	GT21	wildtype	iB_03974	1st	n.d.	
Tc_005635	GT22	melanized				not annotated as gene in iBeetle-Base
Tc_006131	GT23	wildtype				
Tc_006800	GT24	wildtype	iB_06393	1st	lethal	
Tc_007254	***GT25***	***melanized***	***iB_07205***	***2nd***	***n.d.***	
Tc_007317	GT26	wildtype	iB_04313	2nd	n.d.	
Tc_008412	GT27	wildtype	iB_04481	1st	n.d.	
Tc_008413	GT28	melanized				
Tc_008414	*GT29*	*less secretion*	*iB_04482*	*1st*	*lethal*	
Tc_008674	GT77	wildtype				
Tc_008677	GT30	wildtype				
Tc_008780	GT31	colorless				
Tc_008804	GT32	irregular size				splitted in Tc_033804 and Tc_033805
Tc_010236	*GT33*	*less secretion*	*iB_04792*	*2nd*	*n.d.*	*merged with Tc_006847 and Tc_006848 to Tc_031669; iB_# refers to Tc_031669*

Tc_010551	GT35	wildtype				
Tc_010909	*GT36*	*less secretion*	*iB_01760*	*1st*	*lethal*	
Tc_011094	GT37	wildtype				
Tc_011149	GT38	wildtype				
Tc_011211	*GT39*	*colorless*	*iB_01827*	*1st*	*n.d.*	
Tc_011236	GT40	wildtype	iB_04999	1st	n.d.	
Tc_011337	GT41	wildtype	iB_05015	1st	n.d.	
Tc_012298	GT42	wildtype	iB_01963	2nd	n.d.	
Tc_012613	GT43	wildtype				replaced by Tc_034402
Tc_012640	*GT44*	*less secretion*	*iB_05283*	*1st*	*n.d.*	
Tc_012841	GT45	wildtype	iB_05335	1st	n.d.	
Tc_012946	GT46	wildtype				
Tc_013059	GT47	turbid				
Tc_013065	GT48	wildtype				merged with Tc_013066 to Tc_033253
Tc_013108	GT49	wildtype	iB_05385	1st	n.d.	
Tc_013136	GT50	wildtype				
Tc_013434	GT51	wildtype				
Tc_013474	GT52	wildtype	iB_05439	2nd	n.d.	
Tc_013630	GT53	wildtype	iB_08367	2nd	n.d.	
Tc_013755	GT54	wildtype				
Tc_013827	GT55	wildtype	iB_05508	1st	n.d.	
Tc_014185	GT56	less secretion				
Tc_014359	GT57	wildtype				merged with Tc_014360 to Tc_033142
Tc_014388	GT58	melanized				
Tc_014479	GT59	wildtype				
Tc_014748	GT60	wildtype	iB_10470	2nd	n.d.	
Tc_015044	GT61	wildtype				
Tc_015151	*GT62*	*empty/necrotic*	*iB_05763*	*1st*	*n.a.*	
Tc_015346	GT63	colorless				
Tc_015382	GT64	wildtype				merged with Tc_015383 to Tc_033302
Tc_015448	GT65	wildtype	iB_05819	1st	n.a.	merged with Tc_015449 to Tc_033338
Tc_015546	*GT66*	*empty/necrotic*	*iB_05838*	*2nd*	*n.d.*	
Tc_015603	*GT67*	*less secretion*	*iB_05847*	*1st*	*n.a.*	*merged with Tc_015604 to Tc_033405; iB_# refers to Tc_033405*
Tc_015620	GT68	wildtype				
Tc_015886	GT70	less secretion				unmapped; replaced by Tc_031323

Tc_015918	GT71	wildtype	iB_05924	1st	n.a.	merged with Tc_015917 to Tc_033612
Tc_015932	GT72	wildtype	iB_09217	2nd	n.d.	replaced by Tc_033613
Tc_015950	GT73	wildtype				
Tc_016081	GT74	wildtype				partly merged with Tc_016082 and Tc_016083 to Tc_031339; partly replaced by Tc_031340
Tc_016280	GT75	empty/necrotic				

n.d.	non detected (= wildtype)
n.a.	not analyzed
lethal	no survivors at day of gland inspection
italics	gene knockdowns causing gland phenotypes also covered in iBeetle screen
bold	should have been detectable
bold-underlined	confirmed (conf.)

3.2 Genome-wide identification of genes involved in defensive stink gland function of the red flour beetle, *Tribolium casteneum*.

Summary

iBeetle screen, is a huge unbiased RNAi screen in the *Tribolium* beetles to uncover gene functions in cell biology, embryonic and postembryonic development. In the first two phases of the screen, we identified 69 genes to be involved in stink gland function. This chapter discusses findings of the 3rd phase of the iBeetle screen. In the 3rd phase of iBeetle screen, RNAi-mediated gene silencing screening of 4748 genes was done to identify lethal genes. In addition, I used this screen to uncover further genes essential for development, morphological changes and physiology of stink glands. In total, 178 genes were identified for morphological alterations and changes in gland volatile composition. Gene ontology analysis demonstrated that a large number of these genes encode for enzymes, regulator/receptor binding, transcription factors, receptor and transporters. However 40% are with unknown function. This might be explainable by the fact in the 3rd phase of the iBeetle screen, genes were targetted after a reannotation of the *Triboilum* genome, which was substantially improved by transcriptomics data, which allows for the annotation of species specific genes. First annotations are often homology based and thus cover more conserved genes. This might be particularly important for the identification of gene functions in a tissue so far not studied on a molecular biology level in other model organsims. Based on the new genome annotation, we re-analyzed an existing transcriptomic dataset (Li et al., 2013).

Bibi Atika[1*], Elisa Buchberger[1*], Musa Dan'azumi Isah[1], Bernhard Weißbecker[2], Gregor Bucher[3], Ernst A. Wimmer[1†]

Authors contribution to the practical work

Bibi Atika: Performed screening, GC-MS analysis, Microscopy, writing the first draft of the manuscript, and composition of figures and tables.

Elisa Buchberger: Performed the bioinformatics analysis and provided the respective tables and figures.

Musa Dan'azumi Isah: Performed the microscopy for altered gland phenotype of some genes.

Status: Work in progress

Genome-wide identification of genes involved in defensive stink gland function of the red flour beetle, *Tribolium casteneum*.

Bibi Atika[1*], Elisa Buchberger[1*], Musa Dan'azumi Isah[1], Bernhard Weißbecker[2], Gregor Bucher[3], Ernst A. Wimmer[1†]

Department of Developmental Biology, Johann-Friedrich-Blumenbach-Institute of Zoology and Anthropology, Göttingen Center for Molecular Biosciences, Georg-August-University Göttingen, 37077 Göttingen, Germany.

bibi.atika@biologie.uni-goettingen.de

Elisa-bucherger@biologie.uni-goettingen

musa-danazumi.isah@biologie.uni-goettingen.de

bweissb@gwdg.de,

gregor.bucher@bio.uni-goettingen.de

ewimmer@gwdg.de

[1] Georg-August-University Goettingen, Johann-Friedrich-Blumenbach-Institute for Zoology and Anthropology, Dept. of Developmental Biology, GZMB, Ernst-Caspari-Haus, Justus-von-Liebig-Weg 11, 37077 Goettingen, Germany

[2] Georg-August-University Goettingen, Buesgen-Institute, Dept. of Forest Zoology and Forest Conservation, Buesgenweg 3, 37077 Goettingen, Germany

[3] Georg-August-University Goettingen, Johann-Friedrich-Blumenbach-Institute for Zoology and Anthropology, Dept. of Evolutionary Developmental Genetics, GZMB, Ernst-Caspari-Haus, Justus-von-Liebig-Weg 11, 37077 Goettingen, Germany

[*] equal contribution

[†] corresponding author: ewimmer@gwdg.de, Tel.: +49 551 39 28666; Fax: +49 551 39 25416

Abstract

Stink gland secretion of beetles is playing an important role in their defense against detrimental factors in the environment. As the red flour beetle, *Tribolium casteneum,* is an insect pest and uses its stink gland secretion in defense, understanding mechanism of stink gland development, synthesis and storage of stink gland secretion will be pivotal for control of this insect pest. iBeetle screen, is a huge unbiased RNAi screen in the *Tribolium* beetles to uncover gene functions in cell biology, embryonic and postembryonic development. In the first two phases of the screen, we identified 69 genes to be involved in stink gland function. In the present study, the third phase of this large genome-wide RNAi-mediated gene silencing screening of 4748 genes was employed to uncover genes essential for development, morphological changes and physiology of stink glands. In sum, in all three phases of the genome-wide iBeetle screen altogether 13248 genes were screened. In the 3rd phase, 178 genes were identified to play role in regulation of gland morphology and 129 genes showed changes in gland volatile composition. Together with 69 previously identified genes in the iBeetle screen , thus 247 genes involved in stink gland function could be identified by this genome-wide phenotypic screen. In GC-MS analysis of the newly identified 129 RNAi-mediated knockdown genes, 28 genes showed strong reduction in both benzoquinone (MBQ and EBQ) and alkene (C-15 and C-17) levels in abdominal and prothoracic glands. Strongly reduced level of benzoquinone (MBQ and EBQ) in both abdominal and thoracic glands was observed in 55 genes. Gene ontology analysis demonstrated that the majority of these genes encodes for enzymes, regulator/receptor binding, transcription factors, other molecular function, receptor and transporters. However, 40% genes are with unknown function. This might be explainable by the fact in the 3rd phase of the iBeetle screen, genes were targeted after a reannotation of the *Triboilum* genome, which was substantially improved by transcriptomics data, which allows for the annotation of species specific genes. First annotations are often homology based and thus cover more conserved genes. This might be particularly important for the identification of gene functions in a tissue so far not studied on a molecular biology level in other model organsims. We re-analyzed an existing transcriptomic dataset (Li et al., 2013). This allowed us to identified 56 genes of which 33 are newly assembled transcripts and only one was identifies before that are potentially involved in *Tribolium* stink gland biology. This indicates that with improved genome annotation worthwhile to reanalyze former tissue specific transcriptomics datasets. Only two genes out of 178 genes of the 3rd phase iBeetle screen also identified by transcriptomics. Comparatively only two

genes found confirm previous finding that the different approaches of functional genomic-phenotypic screen and transcriptomics approaches complement each other in identifying genes functionally important for the physiology of a certain tissue.

3.1 Introduction

Insecta, containing 27 living and 12 extinct orders of insects, is a highly species rich class of not only phylum Arthropoda but also whole animal kingdom (Chapman, 2009). Indeed, species of insects are more than all other animal species together (Bouchard et al., 2011). However, most of the knowledge on insect molecular biology and development is derived from one insect species the vinegar fly *Drosophila melanogaster* (St Johnston, 2002; Jennings, 2011; Hales et al., 2015; Markow, 2015; Yamaguchi and Yoshida, 2018). Nevertheless, due to its derived situation, *Drosophila* does not show in various aspects the insect biology. For example, many insects species possess odoriferous stink glands which perform various function such as defense and communication (Packard, 1895). However, odoriferous stink glands are not present in *Drosophila*. Hence, developmental and molecular biology of stink glands cannot be understanding in *Drosophila*. Therefore, to better understand insect biology detailed molecular analysis of some other insect species has to be explored. In this regards, large scale genome wide genetic screens have been carried out for the beetle, *Tribolium castaneum* (Denell, 2008; Sulston and Anderson, 1996; Trauner et al., 2009; Wang et al., 2007).

RNA interference (RNAi)-mediated gene disruption has recently been widely employed to decipher function of various genes in many animal species and cell lines (Dietzl et al., 2007; Fraser et al., 2000; Sönnichsen et al., 2005). In this approach, genes are silenced with systemic RNAi injection and subsequently alterations in animal phenotypes are checked. In other insect models, mostly a candidate gene selection approach is used for selecting genes to study their function. These candidate genes are picked on their findings in other model systems, e.g., *Drosophila, C. elegans.,* etc (Cerny et al., 2008; Chen et al., 2000; Choe et al., 2006; Kittelmann et al., 2013; Schaeper et al., 2010). This candidate selection approach has many drawbacks. It is not possible with this approach to unveil function of genes in various processes of other insects that are not present in *Drosophila*. Moreover, lineage specific duplications or loss of genes and technical limitations restrict uncovering the full set of genes require for regulation of a specific process in a particular species. Therefore, it was long being felt to overcome these limitations by a large scale

unbiased genome wide systemic RNAi-mediated gene knockdown screen in a non-dipteran insect species (Schmitt-Engel et al., 2015). In this regards, reverse genetics based RNAi screen together with next generation sequencing open up new window of opportunity of unbiased large scale genome-wide screening in the *T. castaneum.*

Tribolium belongs to the coleoptera (beetles), animal taxon with most abundant species on earth, including a number of devastating pests. Hence, *Tribolium* can be a representative beetle model for the investigation of many other economical noteworthy beetles pest species of coleoptera pest species like the bark beetles, the boll weevil and a number of other beetles (Posnien et al., 2010; Schröder et al., 2008; Sokoloff, 1972). *T. castaneum* is a very good insect model for this purpose because (I) RNAi mediated gene silencing induces a strong phenotype that is mostly phenocopies of null phenotype (Bucher, Scholten and Klingler, 2002), (II) the genome of *Tribolium* is very well characterized, and (III) an up to date list of gene with splice site variants record on the basis of RNA sequencing (RNA-Seq) data (Herndon et al., 2020). Moreover, very efficient protocols for CRISPR/Cas system genome editing, transposon mediated insertion, and *in vivo* imaging for *Tribolium* have been established. Finally, an expanding toolkit for generation of transgenic *Tribolium* is available (Berghammer et al., 1999, 2009; Denell, 2008; Posnien et al., 2010; Schinko et al., 2010; Rylee et al., 2018).

The German scientists working on *Tribolium* have initiated a collaborative genome-wide screen known as the iBeetle screen. The aims of this project are to check the effect of every *Tribolium* gene loss of function and unveil genes involved in different processes which are either peculiar to beetle and/ or absent from *Drosophila* (embryonic leg development, stink gland, etc) (Li et al., 2013). This work will make *Tribolium* as a model system for identification of the genes involved in different processes, such as development of muscle in *Drosophila*, that are not present due to species specific gene loss in well-known model organisms or functional redundancy due to gene duplication, etc (Schmitt-Engel et al., 2015). Till date, in the iBeetle screen, many novel genes pivotal for formation of gametes, embryonic development, metamorphosis and stink gland biology have been uncovered. This unbiased study of *Tribolium* gene function is opening new research fields. The red flour beetle is a perfect model for understanding stink gland biology (Li et al., 2013). Many genes were uncovered in the iBeetle screen, which are important for the production

of defensive chemicals in beetle stink glands. The identification of these genes is not possible by the candidate gene approach because many of these are either not present in *Drosophila* or were not observed by difference in analysis of gene expression for example physiology of stink glands (Li et al., 2013; Schultheis et al., 2019, 2018; Siemanowski et al., 2015).

In the 3rd phase of the iBeetle screen, genes were targetted after a reannotation of the *Triboilum* genome, which was substantially improved by transcriptomics data, which allows for the annotation of species specific genes. First annotations are often homology based and thus cover more conserved genes. This might be particularly important for the identification of gene functions in a tissue so far not studied on a molecular biology level in other model organsims. To complement the functional analysis of genes related to stink gland, we reanalyzed a transcriptomic dataset provided by Li et al. 2013 based on the new genome annotation. This dataset contained samples from various gland types, including prothoracic and abdominal glands from female and male beetles (see (Li et al., 2013 and Material and Methods). We used a newly assembled transcriptome (Herndon et al., 2020) to map the gland-specific transcripts in order to find potentially new genes that are important for the stink gland function in *Tribolium*.

Transcriptomic datasets generated using HTS techniques have the advantage that they include all transcripts that are expressed in a specific tissue at a specific time point in contrast to e.g., Micro Array datasets. Assemblies of genomic and transcriptomic references are improving constantly and therefore re-mapping 'older' RNAseq datasets against a new reference gene set provides the opportunity to gain new knowledge without necessarily generating and sequencing new samples. Final detection of expressed transcripts relies heavily on the reference transcriptome that is used to map the reads against. We chose this approach to find new gland-specific transcripts which could not have been detected in the analysis of 2013, due to the fact, that the reference genes were missing in the old genome annotation.

The iBeetle screen has been done in three phases. In first phase, screening of 5300 genes, covering around 30% of *Tribolium* genome, was done in parallel in larval and pupal stages (Schmitt-Engel et al., 2015). This screen purpose was to unveil stink gland phenotypes, metamorphosis and embryonic phenotypes of beetles. In this screening, dsRNAs were injected in female larvae and pupae. In the second phase, screening of 3200 genes was done. In this phase, pupal screening was performed with dsRNA injection of different randomly selected genes to identify their function in

various biological processes such as stink gland biology, ovary development, muscle formation and embryogenesis. In the 3rd phase, the pupal screening was done with dsRNA injection of 4748. Main purpose of this phase to identify lethal genes but in addition screen were added on to identify genes with function in different biological processes. Particularly, I used this screen to uncover further genes essential for development, morphological changes and physiology of stink glands.

Materials and Methods

Beetle as a model organism

This study was done in the *Tribolium castaneum*. These beetles were maintained in the laboratory under standard temperature and light conditions (Brown et al., 2009). In the third phase of the iBeetle screen, the Double-stranded RNAs (dsRNA) injection for gene disruption was carried out in the transgenic line pBA19 (also called pig 19).

The iBeetle screening procedure

In third phase of iBeetle screening, pupal screening was carried out. The procedure of pupal screening is reported elsewhere in details (Schmitt-Engel et al., 2015). The pupal screening is briefly summarized here.

There are some differences in 1st, 2nd and 3rd phases of iBeetle screenings. In 1st and 2nd phases of iBeetle screening, screeners checked for everything including stink glands but without dissection of beetles. In contrast, in this 3rd phase of iBeetle screening, we did screening for gland morphology via dissection of beetles. This screening phase was a direct screen, no rescreen of iBeetle/base annotations was necessary.

Pupa sorting

Female pupae were separated on the basis of the genital papilla on the last abdominal segment. For each gene, 10 *pBA19* female pupae were injected along with controls. After injection, pupae were placed on petri-dishes with wheat flour and reared at 32°C in incubator with control humidity (40-60%). Then lethality, cuticle phenotypes (L1 larva) and alterations in the adult odoriferous stink glands development were checked for injected pupae. Pupa collection and other help were provided by technicians partially funded by Department of Developmental Biology, University of Göttingen and Bayer organization.

Double-stranded RNA Synthesis

For RNAi-mediated gene disruption experiments, dsRNAs were purchased commercially (Eupheria Biotech GmbH, Dresden, Germany). For resuspension, injection buffer was used to dilute the synthesized dsRNAs (10x stock: 40 mM KCl, 0.3 mM KH_2PO_4, 0.7 mM $Na_2HPO_4 \cdot 2H_2O$, 14 mM NaCl) and kept at -20°C until injected to beetles.

dsRNA injection to beetles

The procedure of dsRNA injection to beetles is described in detail in Chapter 3.1 (Material and method).

Stink gland analysis

The stink glands from these beetles were dissected at 21 days. The stink gland morphology of both abdominal and thoracic stink glands was checked under a microscope. If any alteration in color or morphology of stink gland in comparison to wildtype glands was observed, then I documented all the observations. All observations and alteration stink gland phenotype from first day to 21 days were documented in the online iBeetle database.

Gas chromatography-mass spectrometry analysis

GC-MS analysis was performed on the beetles provided by the iBeetle screener. Analysis of glands volatiles was carried out independently for prothoracic and abdominal glands of knockdown and wildtype beetles through semi quantitative GC-MS analysis. iBeetle screen identified altered stink gland phenotypes were confirmed through GC-MS analysis. For GC-MS analysis, three glands from adult ten days old beetles were isolated and mashed in 100 µl methanol (Merck Millipore, Darmstadt, Germany). GC-MS analysis was done within 48 h. The prepared samples were kept in -20°C freezer. This analysis is described in detail in Chapter 3.1 (Material and method).

Transcriptomic analysis

To reanalyze the transcriptomic data, we downloaded the latest version of the *Tribolium castaneum* transcriptome "OGS3_mRNA.fasta", (Herndon et al., 2020) from iBeetle base and selected for each transcript the longest isoform, which left us with 16,593 unique transcripts. We further downloaded a stink-gland specific transcriptome generated in Li et al. 2013 and included the following samples for our analysis:

female abdominal glands, female prothoracic glands, male abdominal glands male prothoracic glands and one control sample coming from anterior abdomen from wild type *T. castaneum* beetles. We mapped each sample to the current *T. castaneum* transcriptome, using Bowtie2 (Langmead and Salzberg, 2012) with default parameters in -local mode.

To make the analysis as comparable as possible, we then calculated the reads depth as described in Li et al. 2013, namely as: (# of reads mapped to the transcript * 38) / length of transcript (in base pairs). In cases, where 0 reads mapped to a transcript, we added 1 previously to this step, to not lose the information about the transcripts in the next step of calculating logFC. We then followed Li et al. 2013 and calculated the log2FC between each gland sample and the control sample (anterior abdomen) using the formula: log2(reads mapped to transcript in sample/ reads mapped to transcript in control). We then screened for all transcripts that showed FC >= 16 (== log2FC >= 4) and defined these as 'gland specific'. To compare our analysis to the datasets of Li et al. 2013, we filtered their dataset according to our more stringent parameters, including adding +1 to cases where no reads mapped to the sample. All described calculation steps, figures and calculation of overlap were analyzed with R, version 3.6.1 ("R: The R Project for Statistical Computing,").

Identification of conserved domains

Nucleotide sequence conserved domains and molecular function of the genes were checked through the National Center for Biotechnology Information (NCBI) database (http://www.ncbi.nlm.nih.gov/Structure/cdd/wrpsb.cgi).

Image processing

Images of the stink glands were acquired through Leica, Zeiss Axioplan 2 microscope. Adobe Photoshop (CS5) software were used for figures composition.

Results

iBeetle screen

In the 3rd phase of iBeetle screen, I identified 178 new genes with an altered stink gland phenotype. The altered phenotypes of 178 genes are divided in seven distinct categories (I-VII): (I) secretion color darker, (II) secretion color lighter, (III) irregular reservoir size, (IV) less secretion, (V) colorless secretion, (VI) melanized gland content and (VII) size decreased. Exemplary pictures of

seven categories out of 178 genes altered abdominal stink glands morphology after RNAi knockdown are compiled in Figure 1A. A list of all 178 genes given in (Additional file 1. Table S1) and in this list the gland phenotype is indicated by the same color code as used in Figure 1B. The seven altered phenotypic categories are represented by different color and their percentage (Figure 1B).

Gene ontology

Gene ontology analysis of the 178 genes are shown in the Figure 2. For the detail gene ontological analysis, the sequences of *Tribolium* were obtained from online Greifswald (Tcas 5.2) Genome Browser and checked for fly orthologues and conserved domains to infer the possible molecular function. On the basis of their possible molecular function, following groups of the 178 genes were identified: enzymes, regulator/receptor binding, transcription factors, other molecular function, receptor, transporters and 40 % with unknown function (Figure 2). 'Unknown function' gene group includes genes in which no conserved domains and nor any insect orthologue could be identified was noted. Details of the gene ontological analysis are shown in (Additional file 1. Table S1)

Gland secretion volatiles analysis by GC-MS

To check whether the morphologically identified altered glands also have a different composition of volatiles. 178 candidate genes were analyzed by GC-MS analysis but due to some technical problem 49 genes showed some error while the remaining 129 candidate genes showed a potential role in the production of beetle stink gland volatiles. GC-MS analysis was carried out with 10 days-old beetle gland content after knockdown of genes with injection of ds-RNA. In parallel, control 10 days old beetles (wt) received buffer injection. Prothoracic and abdominal gland contents were analyzed separately for each knockdown gene through GC-MS analysis.

Gland contents of two female beetles were analyzed together in one sample for the 178 iBeetle genes. For calculation of each substance abundance the respective value of wildtype was considered 100%. Subsequently, its abundance in knockdown situation was calculated in comparison to wildtype. A reduction is shown by <100% while >100% represents an increase of a compound in comparison to its level in wildtype beetle. 127 genes which resulted in altered gland phenotype also showed changes in abundance of volatile in glandular secretion in GC-MS analysis.

Importantly, 28 genes showed strongly reduced benzoquinones (MBQ and EBQ) and alkenes (C-15 and C-17) level of both the abdominal and thoracic glands (highlighted in red). Strongly reduced level of benzoquinone (MBQ and EBQ) in both abdominal and thoracic glands was observed in 55 genes. Slightly reduced levels of either MBQ or EBQ was observed in abdominal or in thoracic gland in ten genes. Six genes upon knockdown showed no benzoquinones level in thoracic gland and strongly reduced level in abdomen. Three genes showed benzoquinone-less level in abdominal gland and strongly reduced level in thoracic gland.Two showed totally wild type level of benzoquinone and alkenes in both abdominal and thoracic glands. A summary of 129 genes GC-MS analysis is provided in form of percentage value in (Additional file 2. Table S2).

Transcriptomic analysis

We remapped gland specific reads generated by Li et al. 2013 using bowtie2 as alignment tool and the current version of *T. castaneum* transcriptome (Herndon et al., 2020) as reference. This included a sample of female abdominal glands, female prothoracic glands, male abdominal glands and male prothoracic glands and one control sample coming from anterior abdomen from wild type *T. castaneum* beetles. Using a newly assembled transcriptome increased the mapping rate by ~30%, since mapping ratios in Li et al. (2013) ranged from 48.88% to 61.01% and in our analysis from 79.26% to 85.80%, which is most probably due to the increased quality of the newly assembled gene set version (Additional file 6. S6).

After mapping the 2013 dataset to the current version of the *T. castaneum* transcriptome, we found that from the 3rd phase 26 out of the 178 gland genes are highly differentially expressed in stink gland tissue (FC $\geq$ 2) (Additional file 3. Table 3) and 3 genes are higly expressed only in one of the gland type.75 transcripts found, which are specifically expressed in the odiferous stink glands of *T. castaneum* (FC >= 16). We applied the same filter to the dataset of 2013 (Li et al., 2013 after adding +1 to cases where no reads mapped to the sample) and found 61 gland-specific transcripts. 39 of these overlapped, whereas 33 of the remaining 36 transcripts from the new analysis, could not have been detected previously, since they were only newly annotated in the current version of the *T. castaneum* transcriptome. The remaining 3 “new transcripts” were also analyzed in the old analysis, but showed a slightly lower gland specific expression. 22 transcripts were not found in the new analysis (Figure 3). 5 out of the 61 transcripts that were found in the analysis of 2013 as “gland specific” were lower expressed according the new analysis and therefore did not pass the

filtering threshold of Log2FC >= 4. The remaining 17 out of 22 transcripts are not annotated in the new version of the transcriptome and could therefore not be found (they are "former" TC numbers) (Figure 5, Additional file 4. Table S4).

Overlap of Gland specific genes (new analysis), Gland-specific from Li et al. 2013 (includes the data from Li et al. 2013, but using a new filtering threshold) and Group1 (genes defined a s gland specific by Li et al. 2013 is explained in Figure 3. 13 genes are also found as gland specific, when we use the data processing from 2013, but with a different thresholding and the seven genes are not found in the new analysis (Figure 3). This allowed us to identified 56 additional genes of which 33 are newly assembled transcripts potentially involved in *Tribolium* stink gland biology.
Gene ontology of 56 Genes (36+13+7) which are gland specific were classified according to their predicted molecular function. On the basis of their possible molecular functionof 56 genes were identified as receptor, transporters, other molecular function, enzymes, and 33 % with unknown function (Figure 4). **Tc_008780** has been identified as gland specific Group 2013 analysis and in the completely new analysis 2020. **Tc_033013** is only found in the Gland specific set from the new analysis. Both of them were also covered in the 3rd phase of the iBeetle screen. Distribution of two genes (**Tc_008780** and **Tc_033013**) from 178 gland set genes (iBeetle 3rd phase) is explained in Figure 5.

Since our filtering steps to define 'gland specific' transcripts are slightly different than in Li et al. 2013 (see Dataset 2 for definition in Li et al., 2013), we compared how many genes overlap between two analyses. Li et al. defined 62 transcripts as being 'gland specific' (Group 1), and 41 overlap with the ones that were defined as gland-specific from the same dataset with Log2FC >= 4 (Gland Specific 2013). The remaining 21 transcripts that were found as "gland specific" with the filtering from Li et al. 2013, did not pass the threshold of Log2FC >= 4 in all samples, as used in our analysis (Figure 5).

Overlap of the three gland specific gene sets and the complete transcriptome 2020 is explaind in (Additional file 4. Table S4, Figure S1). Some discrepancies in which transcripts are called "gland specific", might not only come from differences in mapping and filtering, but also due to the fact, that a different transcriptome reference was used. Therefore we overlapped the gene sets with the complete transcriptome (OGS3) to understand which of the old transcripts are not included anymore in the OGS3 version. 3 genes from Group 1 were not found in the new transcriptome.

Additionally, 12 transcripts that passed the threshold for the filtering in Li et al. 2013, and also using log2FC>4 are not annotated in the new transcriptome version, as well as 5 transcripts that were only found as gland specific in the old dataset using the new threshold.

Discussion

Stink gland secretion of beetle is playing important role in their defense against dangerous factors in environment. As *Tribolium* is a insect pest and also use its stink gland secretion in defense, therefore, understanding mechanism of stink gland development, synthesis and storage of stink gland secretion will be pivotal for control of this beetle pest (Li et al., 2013; Ulrich et al., 2015). In this study, a large genome-wide RNAi-mediated gene silencing screening of 4748 genes was employed to uncover genes essential for development, gland morphological changes and physiology of stink gland. This screen was complemented with a re-analysis of a gland-specific transcriptomics dataset.

This screening is a part of iBeetle screen. Data obtained in the iBeetle screen are shared in iBeetle database (http://ibeetle-base.uni-goettingen.de/). This online database also includes gene essential for gland morphology, gland secretion production and storage. In three completed phases of RNAi-mediated gene disruption approach 13248 genes were screened and checked for their involvement in development and morphology of stink glands and all findings are documented in iBeetle database (Dönitz et al., 2015; Schmitt-Engel et al., 2015).

In 1st and 2nd phase 69 genes were confirmed. While in the 3rd phase of a large-scale RNAi mediated beetle genome screen, around 4748 genes had been knocked down from the *T. castaneum* genome. Subsequently, these beetles were analyzed for stink gland morphology, defects in morphology, developmental and documented in the iBeetle-Base. Out of these 4748 genes, 178 genes were found to cause alteration in stink gland morphology and volatile compound composition in the adult beetle (Figure 1A, Additional file 2. Table S2).

3rd phase of iBeetle was more efficient as compare to 1st and 2nd phase. In the 3rd phase, we identified a large number of candidate genes, because it was a direct screening of all the genes and we did the dissection of all the beetles. Stink gland was not analyzed specially through dissection before in 1st and 2nd phase in the screening. So some of phase 2 and all of phase 3 are not tested by

NOF. In the 3rd phase of the iBeetle screen, genes were targeted after a reannotation of the *Triboilum* genome, which was substantially improved by transcriptomics data, which allows for the annotation of species specific genes and we identified novel genes in this tissue specific screen. Fisrt annotations are often homology based and thus cover more conserved genes. This might be particularly important for the identification of gene functions in a tissue so far not studied on a molecular biology level in other model organsims. In 3rd phase we identified a large number of candidate genes, also possible novel tissue which are taxon specific genes not as well covered in first genome annotation.

The altered stink gland phenotypes of 247 genes induced by RNAi mediated disruption from 1st 2nd and 3rd phase were categorized into different types of altered stink gland phenotype. Gland secretion in majority of altered gland phenotypes showed less secretion, decrease in glands size, darker secretion color, secretion color lighter, irregular reservoir size, melanized gland content, irregular separation, empty glands and colorless secretion. These alterations in stink gland phenotypes suggest a key role of these genes in development and physiology of stink glands.

To get inside into molecular biology and physiology of these 247 genes, the gene ontology analysis of genes was carried out. On the basis of their possible molecular, following groups of the 247 genes were identified as enzymes, regulator/receptor binding, transcription factors, other molecular function, receptor, transporters and unknown function. ‘Unknown function’ gene group (33%) includes genes in which no conserved domains and nor any insect orthologs was noted channels.

From all the three phases around 198 genes showed changes in stink gland content. In GC-MS analysis of 198 confirmed gland genes from all the 3 phases of iBeetle screen in respective knockdown beetles were unveiled, which effect the composition of volatile chemical secretion of beetle stink glands. Importantly, 37 genes out of 198 genes showed strongly reduced benzoquinones (MBQ and EBQ) and alkenes (C-15 and C-17) levels in both abdominal and thoracic glands. Strongly reduced level of benzoquinone (MBQ and EBQ) in both abdominal and thoracic glands was observed in 71 genes.

To get a more comprehensive insight into stink-gland function, we re-analyzed a gland-specific transcriptomic dataset, which was generated 2013 by Li and colleagues. In contrast to e.g. Micro

Array datasets, transcriptomic datasets generated using HTS techniques have the advantage that they – in theory – include all transcripts that are expressed in a specific tissue at a specific time point. Nevertheless, the final detection of expressed transcripts relies heavily on the reference gene set that is used to map the reads against. Assemblies of genomic and transcriptomic references are improving constantly and therefore re-mapping 'older' RNAseq datasets against a new reference gene set provides the opportunity to gain new knowledge without necessarily generating and sequencing new samples. We chose this approach to find new gland-specific transcripts which could not have been detected in the analysis of 2013, due to the fact, that the reference transcripts were missing in the old gene set. Using the very recently assembled gene set reference of *Tribolium* (OGS3), allowed us to increase the mapping rates by about 30% compared to the initial analysis. The lack of replicates in the dataset did not allow us to use typical tools like DESeq2 (Love, Huber and Anders, 2014) to find differentially expressed genes between gland samples and the control sample (anterior abdomen). Even though there exist tools to analyze RNAseq datasets without replicates, like e.g. NOISeq (Tarazona et al., 2011, 2015), we decided to stick as close as possible to the initial analysis performed in Li et al. 2013, in order to compare the analysis better. We decided to define a gene a s 'gland-specific', when it was at least 16 times higher expressed over all stink gland samples compared to the control sample. Overall, we found differences in the number and identity of gland-specific genes compared to the initial analysis of the dataset, that could be assigned to a) different thresholding we applied a somewhat simpler, but not necessarily less stringent thresholding to define gland-specific genes compared to Li et al. 2013 and b) a more comprehensive reference dataset. We found 33 newly annotated genes, that were expressed at least 16 times higher compared to the control sample, which could not have been found in the initial analysis, since the transcripts had not yet been part of the reference gene set. Since they are so highly expressed in the *Tribolium* gland tissue compared to the control sample, it is definitely worth to analyze these genes in more detail on a functional level.

Conclusions

In summary, the third phase of the iBeetle screen uncovers 40% genes with unknown functions. This might be explainable by the fact in the 3rd phase of the iBeetle screen, genes were targeted after a reannotation of the *Triboilum* genome, which was substantially improved by transcriptomics data, which allows for the annotation of species specific genes. Fisrt annotations

are often homology based and thus cover more conserved genes. This might be particularly important for the identification of gene functions in a tissue so far not studied on a molecular biology level in other model organsims. In re-analysis of a gland-specific transcriptomic dataset, 3 completely new genes found, that were expressed at least 16 times higher compared to the control sample, which could not have been found in the initial analysis, potentially involved in *Tribolium* stink gland biology. This indicates that the improved new genome annotation to reanalyze the former tissue-specific transcriptomics datasets are worthwhile. Only two out of 178 genes of 3rd phase iBeetle screen identified by transcriptomics. This confirmes previous finding that the different approaches of functional genomic-phenotypic screen and transcriptomics approaches complement each otherin identifying genes functionally important for the physiology of a certain tissue.

References

Berghammer, A. *et al.* (1999) 'A system to efficiently maintain embryonic lethal mutations in the flour beetle Tribolium castaneum', *Development Genes and Evolution*, 209(6), pp. 382–389. doi: 10.1007/s004270050268.

Berghammer, A. J. *et al.* (2009) 'Red Flour Beetle (Tribolium) Germline Transformation and Insertional Mutagenesis', *Cold Spring Harbor Protocols*, 2009(8), p. pdb.prot5259. doi: 10.1101/pdb.prot5259.

Bouchard, P. *et al.* (2011) 'Family-group names in Coleoptera (Insecta)', *ZooKeys*, (88), pp. 1–972. doi: 10.3897/zookeys.88.807.

Boutros, M. *et al.* (2004) 'Genome-wide RNAi analysis of growth and viability in Drosophila cells', *Science (New York, N.Y.)*, 303(5659), pp. 832–835. doi: 10.1126/science.1091266.

Bucher, G. and Klingler, M. (2004) 'Divergent segmentation mechanism in the short germ insect Tribolium revealed by giant expression and function', *Development*, 131(8), pp. 1729–1740. doi: 10.1242/dev.01073.

Bucher, G., Scholten, J. and Klingler, M. (2002) 'Parental RNAi in Tribolium (Coleoptera)', *Current Biology*, 12(3), pp. R85–R86. doi: 10.1016/S0960-9822(02)00666-8.

Cerny, A. C. *et al.* (2008) 'The Tribolium ortholog of knirps and knirps-related is crucial for head segmentation but plays a minor role during abdominal patterning', *Developmental Biology*, 321(1), pp. 284–294. doi: 10.1016/j.ydbio.2008.05.527.

Chapman, A. (2009) *Numbers of Living Species in Australia and the World 2nd edn.*

Chen, G., Handel, K. and Roth, S. (2000) 'The maternal NF-kappaB/dorsal gradient of Tribolium castaneum: dynamics of early dorsoventral patterning in a short-germ beetle', *Development*, 127(23), pp. 5145–5156.

Choe, C. P., Miller, S. C. and Brown, S. J. (2006) 'A pair-rule gene circuit defines segments sequentially in the short-germ insect Tribolium castaneum', *Proceedings of the National Academy of Sciences*, 103(17), pp. 6560–6564. doi: 10.1073/pnas.0510440103.

Denell, R. (2008) 'Establishment of Tribolium as a Genetic Model System and Its Early Contributions to Evo-Devo', *Genetics*, 180(4), pp. 1779–1786. doi: 10.1534/genetics.104.98673.

Dietzl, G. *et al.* (2007) 'A genome-wide transgenic RNAi library for conditional gene inactivation in Drosophila', *Nature*, 448(7150), pp. 151–156. doi: 10.1038/nature05954.

Dönitz, J. *et al.* (2015) 'iBeetle-Base: a database for RNAi phenotypes in the red flour beetle Tribolium castaneum', *Nucleic Acids Research*, 43(Database issue), pp. D720–D725. doi: 10.1093/nar/gku1054.

Fraser, A. G. *et al.* (2000) 'Functional genomic analysis of C. elegans chromosome I by systematic RNA interference', *Nature*, 408(6810), pp. 325–330. doi: 10.1038/35042517.

Hales, K. G. *et al.* (2015) 'Genetics on the Fly: A Primer on the Drosophila Model System', *Genetics*, 201(3), pp. 815–842. doi: 10.1534/genetics.115.183392.

Herndon, N. *et al.* (2020) 'Enhanced genome assembly and a new official gene set for Tribolium castaneum', *BMC Genomics*, 21(1), p. 47. doi: 10.1186/s12864-019-6394-6.

Jennings, B. H. (2011) 'Drosophila – a versatile model in biology & medicine', *Materials Today*, 14(5), pp. 190–195. doi: 10.1016/S1369-7021(11)70113-4.

Kittelmann, S. *et al.* (2013) 'Changes in anterior head patterning underlie the evolution of long germ embryogenesis', *Developmental Biology*, 374(1), pp. 174–184. doi: 10.1016/j.ydbio.2012.11.026.

Langmead, B. and Salzberg, S. L. (2012) 'Fast gapped-read alignment with Bowtie 2', *Nature methods*, 9(4), pp. 357–359. doi: 10.1038/nmeth.1923.

Li, J. *et al.* (2013a) 'Odoriferous Defensive Stink Gland Transcriptome to Identify Novel Genes Necessary for Quinone Synthesis in the Red Flour Beetle, Tribolium castaneum', *PLoS Genetics*, 9(7). doi: 10.1371/journal.pgen.1003596.

Li, J. *et al.* (2013b) 'Odoriferous Defensive Stink Gland Transcriptome to Identify Novel Genes Necessary for Quinone Synthesis in the Red Flour Beetle, Tribolium castaneum', *PLoS Genetics*, 9(7). doi: 10.1371/journal.pgen.1003596.

Love, M. I., Huber, W. and Anders, S. (2014) 'Moderated estimation of fold change and dispersion for RNA-seq data with DESeq2', *Genome Biology*, 15(12), p. 550. doi: 10.1186/s13059-014-0550-8.

Markow, T. A. (2015) 'The secret lives of Drosophila flies', *eLife*, 4, p. e06793. doi: 10.7554/eLife.06793.

Packard, A. S. (1895) 'The Eversible Repugnatorial Scent Glands of Insects', *Journal of the New York Entomological Society*, 3(3), pp. 110–127.

Posnien, N. *et al.* (2010) 'Genetics, development and composition of the insect head - A beetle's view', *Arthropod structure & development*, 39, pp. 399–410. doi: 10.1016/j.asd.2010.08.002.

R: The R Project for Statistical Computing (no date). Available at: https://www.r-project.org/ (Accessed: 9 September 2020).

Richards, S. *et al.* (2008) 'The genome of the model beetle and pest Tribolium castaneum', *Nature*, 452(7190), pp. 949–955. doi: 10.1038/nature06784.

Rylee, J. C. *et al.* (2018) 'Expanding the genetic toolkit of Tribolium castaneum', *PLOS ONE*, 13(4), p. e0195977. doi: 10.1371/journal.pone.0195977.

Schaeper, N. D. *et al.* (2010) 'Evolutionary plasticity of collier function in head development of diverse arthropods', *Developmental Biology*, 344(1), pp. 363–376. doi: 10.1016/j.ydbio.2010.05.001.

Schinko, J. B. *et al.* (2010) 'Functionality of the GAL4/UAS system in Tribolium requires the use of endogenous core promoters', *BMC Developmental Biology*, 10(1), p. 53. doi: 10.1186/1471-213X-10-53.

Schmitt-Engel, C. *et al.* (2015) 'The iBeetle large-scale RNAi screen reveals gene functions for insect development and physiology', *Nature Communications*, 6(1), p. 7822. doi: 10.1038/ncomms8822.

Schröder, R. *et al.* (2008) 'From development to biodiversity--Tribolium castaneum, an insect model organism for short germband development', *Development Genes and Evolution*, 218(3–4), pp. 119–126. doi: 10.1007/s00427-008-0214-3.

Schultheis, D. *et al.* (2019) 'A Large Scale Systemic RNAi Screen in the Red Flour Beetle Tribolium castaneum Identifies Novel Genes Involved in Insect Muscle Development', *G3: Genes|Genomes|Genetics*, 9(4), pp. 1009–1026. doi: 10.1534/g3.118.200995.

Schultheis, D., Schwirz, J. and Frasch, M. (2018) 'RNAi screen in Tribolium reveals involvement of F-BAR proteins in myoblast fusion and visceral muscle morphogenesis in arthropods', *bioRxiv*, p. 397232. doi: 10.1101/397232.

Siemanowski, J. *et al.* (2015) 'Notch signaling induces cell proliferation in the labrum in a regulatory network different from the thoracic legs', *Developmental Biology*, 408(1), pp. 164–177. doi: 10.1016/j.ydbio.2015.09.018.

Sokoloff, A. (1972) *The biology of Tribolium: with special emphasis on genetic aspects*. Oxford: Clarendon Press.

Sönnichsen, B. *et al.* (2005) 'Full-genome RNAi profiling of early embryogenesis in Caenorhabditis elegans', *Nature*, 434(7032), pp. 462–469. doi: 10.1038/nature03353.

St Johnston, D. (2002) 'The art and design of genetic screens: Drosophila melanogaster', *Nature Reviews. Genetics*, 3(3), pp. 176–188. doi: 10.1038/nrg751.

Sulston, I. A. and Anderson, K. V. (1996) 'Embryonic patterning mutants of Tribolium castaneum', *Development*, 122(3), pp. 805–814.

Tarazona, S. *et al.* (2011) 'Differential expression in RNA-seq: a matter of depth', *Genome Research*, 21(12), pp. 2213–2223. doi: 10.1101/gr.124321.111.

Tarazona, S. *et al.* (2015) 'Data quality aware analysis of differential expression in RNA-seq with NOISeq R/Bioc package', *Nucleic Acids Research*, 43(21), pp. e140–e140. doi: 10.1093/nar/gkv711.

Trauner, J. *et al.* (2009) 'Large-scale insertional mutagenesis of a coleopteran stored grain pest, the red flour beetle Tribolium castaneum, identifies embryonic lethal mutations and enhancer traps', *BMC Biology*, 7, p. 73. doi: 10.1186/1741-7007-7-73.

Ulrich, J. *et al.* (2015) 'Large scale RNAi screen in Tribolium reveals novel target genes for pest control and the proteasome as prime target', *BMC Genomics*, 16(1), p. 674. doi: 10.1186/s12864-015-1880-y.

Wang, L. *et al.* (2007) 'BeetleBase: the model organism database for Tribolium castaneum', *Nucleic Acids Research*, 35(Database issue), pp. D476–D479. doi: 10.1093/nar/gkl776.

Yamaguchi, M. and Yoshida, H. (2018) 'Drosophila as a Model Organism', in Yamaguchi, M. (ed.) *Drosophila Models for Human Diseases*. Singapore: Springer (Advances in Experimental Medicine and Biology), pp. 1–10. doi: 10.1007/978-981-13-0529-0_1.

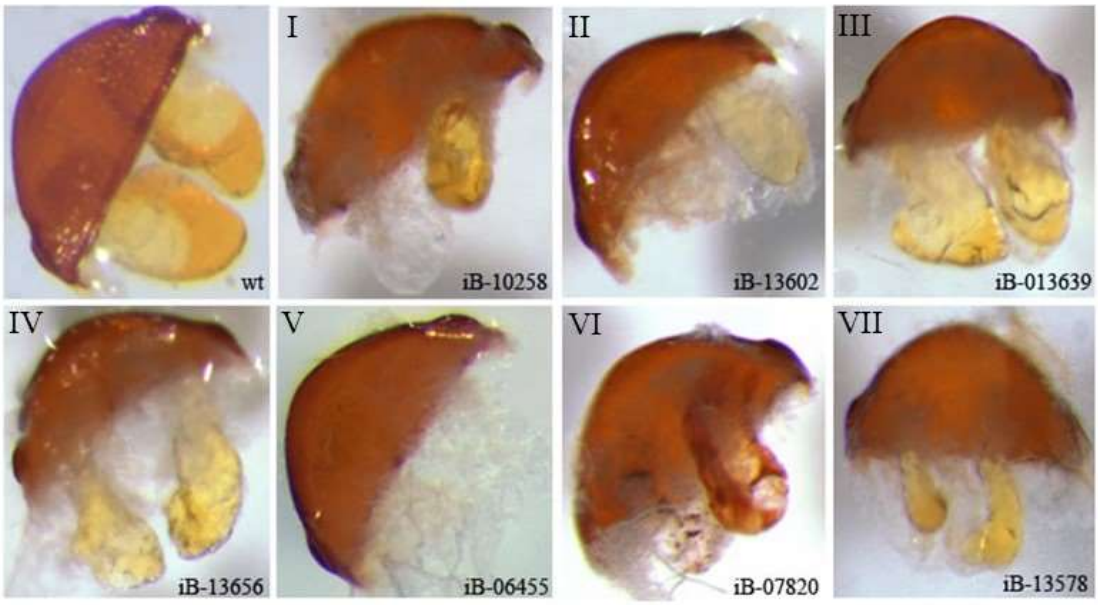

Figure 1A. Different categories of abdominal stink gland phenotypes. Alterations in morphology of abdominal gland after RNAi-mediated gene disruption are shown. Exemplary pictures of 7 categories out of 178 genes altered abdominal stink glands after RNAi knockdown are compiled in Figure 1B.

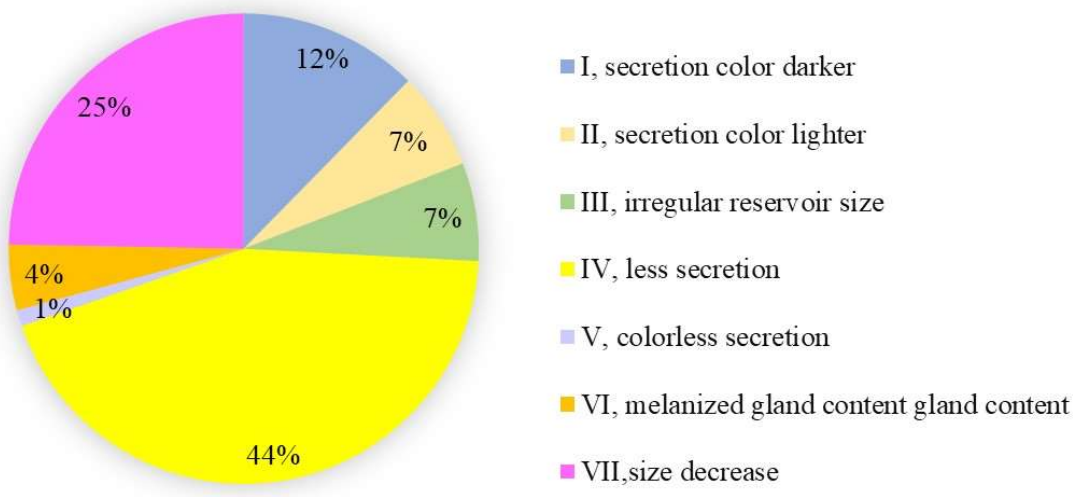

Figure 1B. Phenotype categories of the 178 genes. Seven different type of phenotype were observed and categorized into seven group (I-VII) shown by a color code. I. secretion color darker, II. secretion color lighter, III. irregular reservoir size, IV. less secretion, V. colorless secretion, VI. melanized gland content, VII. size decrease.

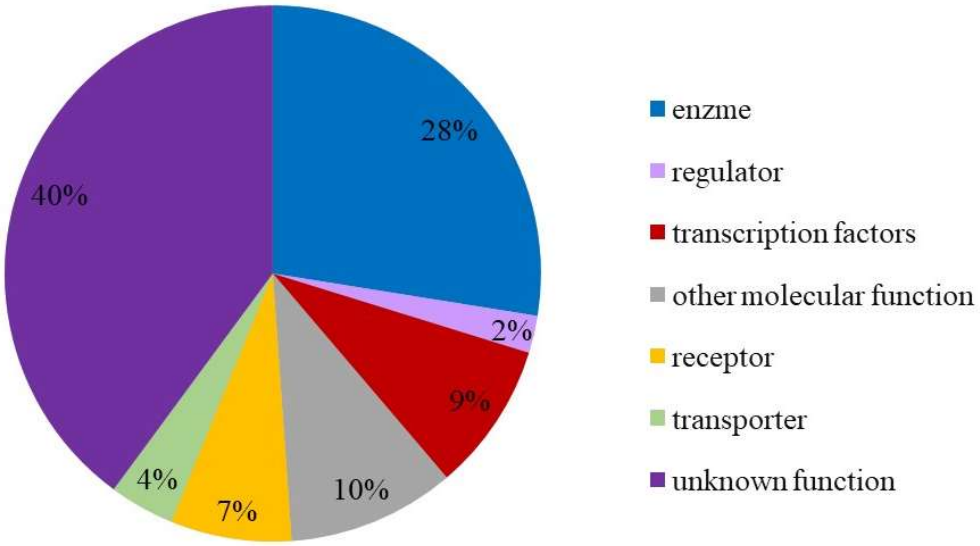

Figure 2. Gene ontology analysis of 178. Genes with altered gland phenotype were classified according to their predicted molecular function (Additional file 1. Table S1).

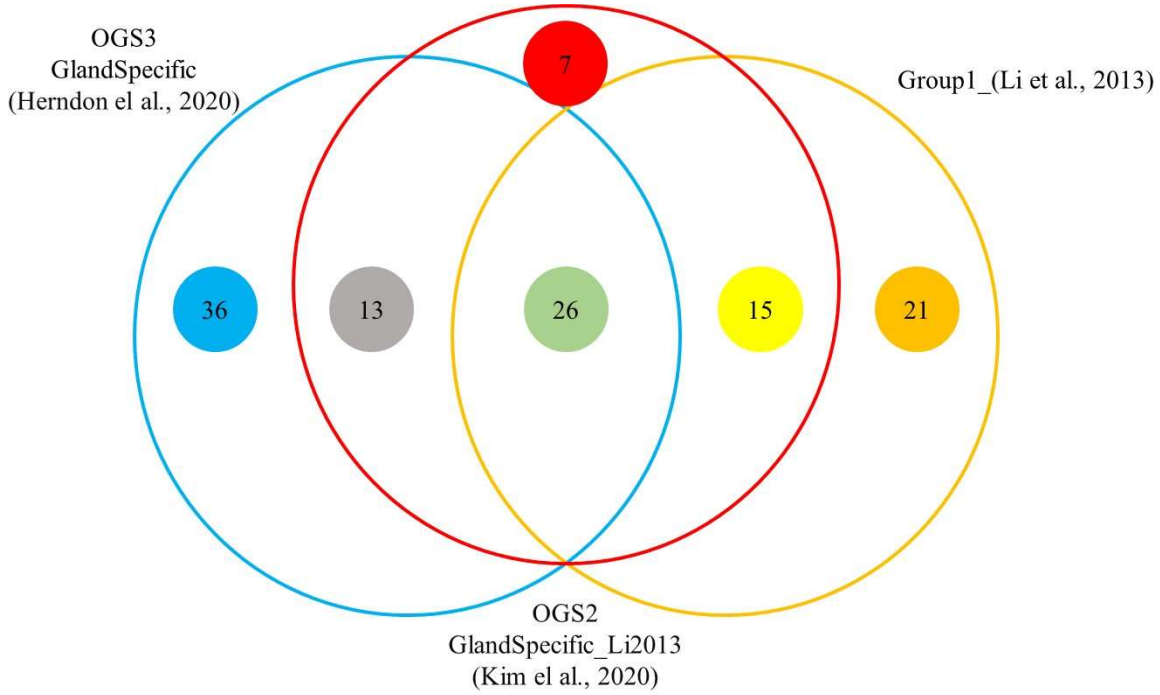

Figure 3. This figure shows the overlap of Gland specific genes (new analysis), Gland-specific from Li et al. 2013 (includes the data from Li et al. 2013, but using a new filtering threshold) and Group1 (genes defined a s gland specific by Li et al. 2013. Differences in what is considered as gland specific transcripts come mainly from different thresholding or because they were newly annotated and could not have been found by mapping the reads against the older version of the transcriptome. 36 transcripts from the new analysis, could not have been detected previously, since they were only newly annotated in the current version of the *T. castaneum* transcriptome 13 genes are also found as gland specific, when we use the data processing from 2013, but with a different thresholding and the seven genes are not found in the new analysis.

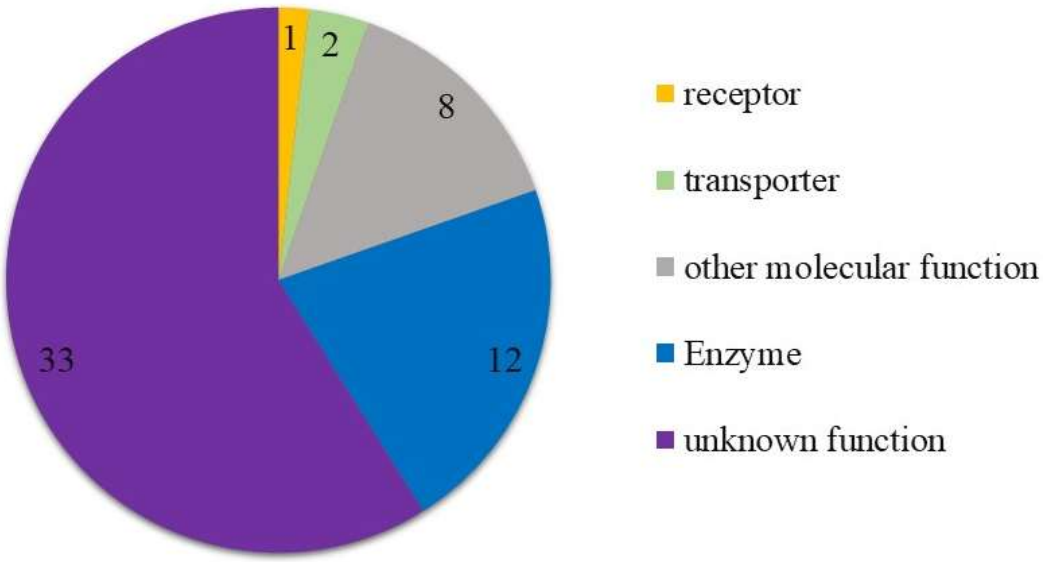

Figure 4. Gene ontology analysis of 56 genes. Genes (36+13+7) which are gland specific were classified according to their predicted molecular function. 36 transcripts from the new analysis, could not have been detected previously, 13 genes are also found as gland specific, when we use the data processing from 2013, but with a different thresholding and the seven genes are not found in the new analysis.

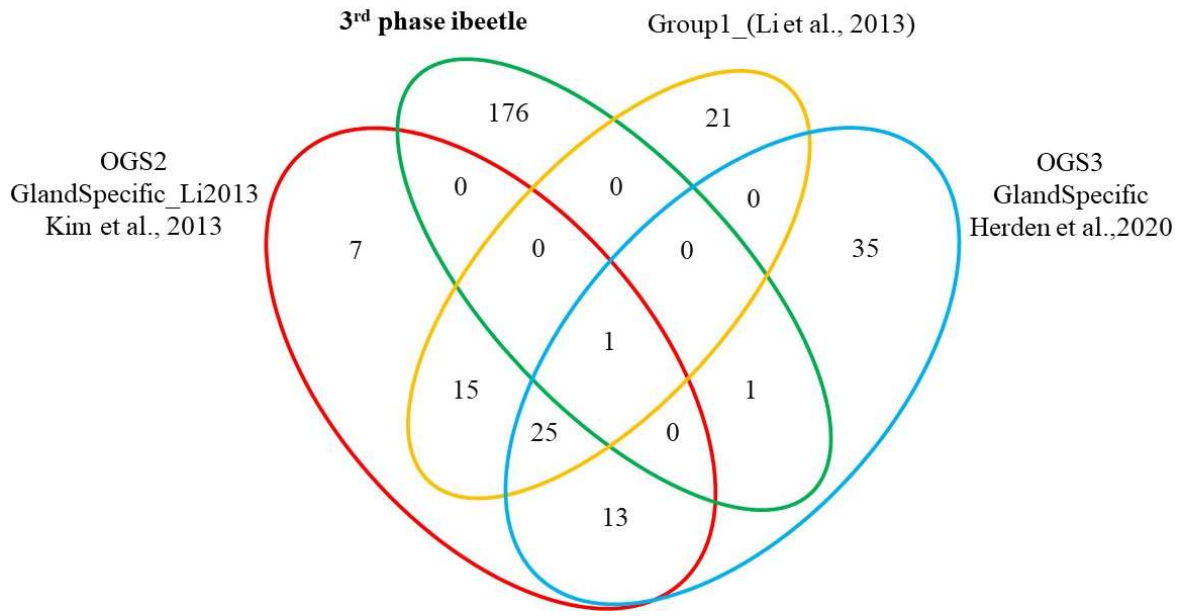

Figure 5. Overlap of two genes in the transcriptomics analysis. Distribution of two genes from 178 gland set genes of the 3rd phase iBeetle sceen with transcriptomics analysis. **Tc_008780** has been identified in GlandSpecific 2013 analysis and in the completely new analysis 2020. **Tc_033013** is found in the Gland specific set from the new analysis. Only these two were also covered by 3rd phase of iBeetle screen.

Additional file 1. Table S1. Gene ontological analysis of 178 genes with altered phenotype of stink glands. Conserved domains presence was checked via the conserved domain search of NCBI. iBeetle-Base was searched for closest *D. melanogaster* fly homologs. The stink gland phenotype after RNAi mediated knock down is abbreviated with SG color code and is shown in Figure 1B.

SG	# iB	OGS	conserved domains	fly ortholog/best hit
	iB_06455	Tc_012436	Ras super family	RabX5 - RabX5 (CG7980)
	iB_06635	Tc_001001	none	futsch - futsch (CG34387)
	iB_07379	Tc_001313	7 transmembrane receptors family (7tm)	Or42b - Odorant receptor 42b (CG12754)
	iB_07536	Tc_006542	Runt domain family	run - runt (CG1849)
	iB_07738	Tc_031704	Reverse transcriptase (RT) superfamily	none
	iB_07787	Tc_004104	PIN_SF (PilT N terminus) domain Superfamily	CG17652 - (CG17652)
	iB_07820	Tc_004888	F-box, Superfamily	CG33969 - (CG33969)
	iB_07886	Tc_000385	Protein kinase superfamily (PKc) Superfamily	hep - hemipterous (CG4353)
	iB_07950	Tc_001561	60KD_IMP (inner membrane protein), Superfamily	CG4942 - (CG4942)
	iB_07976	Tc_003545	none	SA - Stromalin (CG3423)
	iB_08057	Tc_002414	Tmemb_9 (transmembrane proteins), family	CG1161 - (CG1161)
	iB_08160	Tc_008320	Regulated-SNARE-like domain, Longin	Vamp7 - Vesicle-associated membrane protein 7 (CG1599)
	iB_08263	Tc_010415	SFP1 domain family	CG14655 - (CG14655)
	iB_08565	Tc_014905	Pex2_Pex12, domain family	Pex12 - Peroxin 12 (CG3639)
	iB_08572	Tc_015824	Transcription factor S-II (TFIIS_M), Superfamily	MED26 - Mediator complex subunit 26 (CG1793)
	iB_08877	Tc_031556	Lig_chan Superfamily (Ligand-gated ion channel)	Ir21a - Ionotropic receptor 21a (CG2657)
	iB_09271	Tc_006096	NADB_Rossmann superfamily	wat - waterproof (CG1443)
	iB_10094	Tc_014560	Eukaryotic Mediator 12 (Med12) subunit domain	kto - kohtalo (CG8491)
	iB_10258	Tc_009294	methyl-transferase (MT-A70) superfamily	Ime4 - Inducer of meiosis 4 (CG5933)
	iB_10282	Tc_009200	Vacuolar protein sorting-associated protein 62 (Vps62)	Desi - Desiccate (CG14686)
	iB_10307	Tc_033640	Laminin G-like domain (LamG) family	SP2353 - SP2353 (CG8403)
	iB_10350	Tc_009870	Syntaxin N-terminus (SynN) superfamily	Syx16 - Syntaxin 16 (CG1467)
	iB_10379	Tc_008830	CG8461 - (CG8461)	RRP36 Superfamily (rRNA biogenesis protein RRP36)
	iB_10398	Tc_033833	none	l(1)G0196 - lethal (1) G0196 (CG14616)
	iB_10399	Tc_010875	The Ligand-gated Ion Channel (LIC) Family	GluClalpha - GluClalpha (CG7535)
	iB_10410	Tc_008670	Replication Fork Protection Component Swi3 domain	CG10336 - (CG10336)
	iB_10416	Tc_008693	Retinoblastoma-binding protein 1(RBB1NT) family.	htk - hat-trick (CG34422)

	iB_10636	Tc_006130	Sodium Bile acid symporter family	none
	iB_10818	Tc_012600	7 transmembrane receptor (rhodopsin family)	Octbeta1R - Octopamine beta1 receptor (CG6919)
	iB_10843	Tc_001560	Zinc-finger associated domain (zf-AD) Superfamily	Opbp - Optix-binding protein (CG30443)
	iB_12106	Tc_002985	Ribosomal_L36e, Superfamily	RpL36 - Ribosomal protein L36 (CG7622)
	iB_12119	Tc_003441	Condensin (Cnd2), Superfamily	barr - barren (CG10726)
	iB_12122	Tc_003525	VHS_ENTH_ANTH, Superfamily	CG3529 - (CG3529)
	iB_12143	Tc_004593	Ferredoxin reductase (FNR), Superfamily	Nox - NADPH oxidase (CG34399)
	iB_12151	Tc_004701	Cobalamin (CobT), Superfamily	Cht5 - Chitinase 5 (CG9307)
	iB_12159	Tc_004875	7 transmembrane receptors family (7tm_6)	Or59c - Odorant receptor 59c (CG17226)
	iB_12160	Tc_004877	Aldo-keto reductases (AKRs) Superfamily	ARY - Aldehyde reductase Y (CG40064)
	iB_12164	Tc_004940	glutathione S-transferase superfamily (GstA)	GstE7 - Glutathione S transferase E7 (CG17531)
	iB_12171	Tc_005040	chromo-like superfamily.	none
	iB_12179	Tc_005125	hAT element superfamily)	none
	iB_12227	Tc_006117	YRB1(Ran-binding protein) Superfamily	Nup358 - Nucleoporin 358kD (CG11856)
	iB_12410	Tc_008647	Src homology 2 (SH2) superfamily	hop - hopscotch (CG1594)
	iB_12420	Tc_008757	PBP_GOBP, Superfamily	Obp44a - Odorant-binding protein 44a (CG2297)
	iB_12424	**Tc_008780**	Glycosyl hydrolase Superfamily	Gba1b - Glucocerebrosidase 1b (CG31414)
	iB_12502	Tc_009891	ABC transporter superfamily	CG4562 - (CG4562)
	iB_12548	Tc_010490	Cupredoxin superfamily	laccase2 - laccase 2 (CG42345)
	iB_12567	Tc_010739	none	none
	iB_12594	Tc_011162	none	CG30197 - (CG30197)
	iB_12808	Tc_013415	Tryp_SPc, with user query added Superfamily	snk - snake (CG7996)
	iB_12904	Tc_014568	protein kinase like Superfamily	msn - misshapen (CG16973)
	iB_12930	Tc_014956	Epimerase Superfamily	Gmer - GDP-4-keto-6-deoxy-D-mannose 3,5-epimerase/4-reductase (CG3495)
	iB_12934	Tc_014988	Anoctamin Superfamily	Axs - Abnormal X segregation (CG9703)
	iB_12946	Tc_015183	Synaptobrevin Superfamily	nSyb - neuronal Synaptobrevin (CG17248)
	iB_12953	Tc_015294	7 transmembrane receptors family (7tm_6)	Or49b - Odorant receptor 49b (CG17584)
	iB_12957	Tc_015339	Ketoacyl-synthetase_C_assoc Superfamily	FASN3 - Fatty acid synthase 3 (CG17374)
	iB_12988	Tc_015711	RNA recognition motif (RRM) Superfamily	Rbp2 - RNA-binding protein 2 (CG4429)
	iB_12995	Tc_015806	TGFb_propeptide Superfamily	Actbeta - Activin-beta (CG11062)
	iB_12998	Tc_015831	PRP40 (RNA processing)Superfamily	CG3542 - (CG3542)
	iB_13213	Tc_031234	DNA_breaking-rejoining enzyme, Superfamily	none
	iB_13267	Tc_031901	zf-AD, Superfamily	crol - crooked legs (CG14938)
	iB_13286	Tc_032059	Major Facilitator (MF)Superfamily	CG3690 - (CG3690)
	iB_13287	Tc_032061	Really Interesting New Gene (RING) Ubox, Superfamily	gol - goliath (CG2679)
	iB_13384	Tc_033142	p450 Superfamily	Cyp6a23 - Cyp6a23 (CG10242)

	iB_13393	Tc_033231	Chitin_bind_4 Superfamily	Cpr47Ef - Cuticular protein 47Ef (CG13214)
	iB_13397	Tc_033244	7 transmembrane receptor (rhodopsin family)	mthl15 - methuselah-like 15 (CG31720)
	iB_13400	Tc_033252	Immunoglobulin (Ig) Superfamily	unc-5 - unc-5 (CG8166)
	iB_13404	Tc_033289	Pkinase_C Superfamily	aPKC - atypical protein kinase C (CG42783)
	iB_13418	Tc_033437	Dynein_light Superfamily	ctp - cut up (CG6998)
	iB_13420	Tc_033443	7 transmembrane receptor (rhodopsin family)	Lgr4 - Leucine-rich repeat-containing G protein-coupled receptor 4 (CG34411)
	iB_13427	Tc_033511	rve, Superfamily	none
	iB_13436	Tc_033565	CBM_14, Superfamily	Mur2B - Mucin related 2B (CG14796)
	iB_13442	Tc_033617	NADB_Rossmann Superfamily	wat - waterproof (CG1443)
	iB_13443	Tc_033629	p31comet Superfamily	CG13599 - (CG13599)
	iB_13444	Tc_033633	Tryptophan synthase beta_II superfamily	Cbs - Cystathionine beta-synthase (CG1753)
	iB_13446	Tc_033680	SPEC Superfamily	shot - short stop (CG18076)
	iB_13447	Tc_033682	Ras superfamily	kappaB-Ras - kappaB-Ras (CG1669)
	iB_13455	Tc_033734	KU superfamily	CG13748 - (CG13748)
	iB_13462	Tc_033825	TAFH Superfamily	nvy - nervy (CG3385)
	iB_13470	Tc_033891	rve superfamily	none
	iB_13474	Tc_033927	Periplasmic_Binding_Protein_Type_1 superfamily	Gyc32E - Guanyl cyclase at 32E (CG33114)
	iB_13476	Tc_033970	Rhomboid superfamily	rho - rhomboid (CG1004)
	iB_13479	Tc_034016	WW (tryptophans domain) Superfamily	Wwox - WW domain containing oxidoreductase (CG7221)
	iB_13480	Tc_034021	Chitin_bind_4 Superfamily	resilin - resilin (CG15920)
	iB_13481	Tc_034049	cyclophilin Superfamily	Fbxl4 - F box and leucine-rich-repeat gene 4 (CG1839)
	iB_13490	Tc_034143	Sulfate_transp, Superfamily	Esp - Epidermal stripes and patches (CG7005)
	iB_13492	Tc_034186	Ion_trans Superfamily	Ca-alpha1T - Ca[2+]-channel protein alpha[[1]] subunit T (CG15899)
	iB_13507	Tc_034300	Aspartate aminotransferase (AAT_I) Superfamily	CG7433 - (CG7433)
	iB_13520	Tc_034418	tetraspanin_LEL, Superfamily	Tsp42Ea - Tetraspanin 42Ea (CG18817)
	iB_13523	Tc_034433	RTTN_N (Rotatin) superfamily	ana3 - anastral spindle 3 (CG13162)
	iB_13525	Tc_034455	Nucleoside_tran, Superfamily	Ent1 - Equilibrative nucleoside transporter 1 (CG11907)
	iB_13527	Tc_034461	ALP_like (alkaline phosphatases) superfamily	CG15695 - (CG15695)
	iB_13531	Tc_034478	ANK (Ankyrin repeats) Superfamily	CG30274 - (CG30274)
	iB_13538	Tc_034552	7tm Odorant receptor superfamily	Or49b - Odorant receptor 49b (CG17584)
	iB_13539	Tc_034560	MhpD Superfamily	CG5793 - (CG5793)
	iB_13541	Tc_034598	SAM (Sterile Alpha Motif) superfamily	-
	iB_13546	Tc_034629	bZIP (Basic leucine zipper) superfamily	Pdp1 - PAR-domain protein 1 (CG17888)
	iB_13550	Tc_034643	RimI Superfamily	san - separation anxiety (CG12352)
	iB_13552	Tc_034655	Immunoglobulin (Ig), superfamily	rtv - retroactive (CG1397)
	iB_13556	Tc_034670	Abhydrolase superfamily	Lip4 - Lipase 4 (CG6113)
	iB_13558	Tc_034684	Neuralized superfamily	neur - neuralized (CG11988)

	iB_13560	Tc_034694	none	none
	iB_13565	Tc_034733	homeodomain Superfamily	Dbx - Dbx (CG42234)
	iB_13568	Tc_034761	CBM_14, with user query added Superfamily	CG4835 - (CG4835)
	iB_13576	Tc_034847	Major Facilitator Superfamily (MFS) Superfamily	CG9254 - (CG9254)
	iB_13578	Tc_034897	THAP, with user query added Superfamily	none
	iB_13585	Tc_035033	none	none
	iB_13602	Tc_001666	SNARE superfamily	Bet1 - BET1 ortholog (S. cerevisiae) (CG14084)
	iB_13614	Tc_004281	Peptidase_M10 Superfamily	CG16863 - (CG16863)
	iB_13619	Tc_005085	LRR_8, with user query added Superfamily	conv - convoluted (CG8561)
	iB_13626	Tc_005432	Peptidase_C1, Superfamily	Swim - Secreted Wg-interacting molecule (CG3074)
	iB_13628	Tc_005475	none	CG10431 - (CG10431)
	iB_13639	Tc_006626	Hormone_5, Superfamily	none
	iB_13656	Tc_011350	Sulfotransfer_3 Superfamily	CG31637 - (CG31637)
	iB_13660	Tc_012397	RING_Ubox, with user query added Superfamily	CG31053 - (CG31053)
	iB_13667	Tc_012635	7tm_6 (7tm Odorant receptor) superfamily	Or67c - Odorant receptor 67c (CG14156)
	iB_13673	Tc_013464	SEC14 Superfamily (S. cerevisiae phosphatidylinositol transfer protein)	CG5958 - (CG5958)
	iB_13677	Tc_013821	Chitin_bind_4 Superfamily	Cpr76Bb - Cuticular protein 76Bb (CG9290)
	iB_13680	Tc_014087	protein kinase (PKc) superfamily	ninaC - neither inactivation nor afterpotential C (CG5125)
	iB_13692	Tc_030268	7tm_7 (Chemosensory receptor) Superfamily	Gr28a - Gustatory receptor 28a (CG13787)
	iB_13694	Tc_030367	7tm_6 (7tm Odorant receptor) superfamily	Or43a - Odorant receptor 43a (CG1854)
	iB_13698	Tc_030961	none	none
	iB_13701	Tc_031342	Acyl_transf_3, Superfamily	CG14205 - (CG14205)
	iB_13704	Tc_032134	ELO, Superfamily	CG33110 - (CG33110)
	iB_13707	Tc_032365	PI3K_C2 Phosphoinositide 3-kinase, C2 domain	Pkc53E - Protein C kinase 53E (CG6622)
	iB_13712	Tc_032843	CD36 Superfamily	Snmp1 - Sensory neuron membrane protein 1 (CG7000)
	iB_13723	Tc_033974	Toll/interleukin-1 receptor (TIR) Superfamily	Toll-9 - Toll-9 (CG5528)
	iB_13730	Tc_034797	ASC (Amiloride-sensitive sodium channel) Superfamily.	ppk16 - pickpocket 16 (CG34059)
	iB_13736	Tc_004248	7tm_7, (7tm Chemosensory receptor) Superfamily	none
	iB_13739	Tc_034703	pepsin_retropepsin_like Superfamily	CG3800 - (CG3800)
	iB_13754	Tc_000145	none	none
	iB_13761	Tc_000233	BLOC1S3 Superfamily (Biogenesis of lysosome-related organelles complex 1 subunit 3)	Blos3 - Biogenesis of lysosome-related organelles complex 1, subunit 3 (CG34255)
	iB_13815	Tc_001141	none	CG13606 - (CG13606)
	iB_13821	Tc_001282	none	CG10433 - (CG10433)
	iB_14407	Tc_010819	none	none

	iB_14666	Tc_014799	SMC_prok_A (structural maintenance of chromosomes) Superfamily	cmet - CENP-meta (CG6392)
	iB_14689	Tc_015027	none	none
	iB_14948	Tc_031796	none	none
	iB_14954	Tc_031816	none	none
	iB_14977	Tc_032119	none	none
	iB_15009	Tc_032351	none	none
	iB_15044	Tc_032638	CKAP2_C Superfamily, Cytoskeleton-associated protein 2 C-terminus:	none
	iB_15047	Tc_032680	none	none
	iB_15051	Tc_032701	none	CG12974 - (CG12974)
	iB_15097	**Tc_033013**	none	none
	iB_15098	Tc_033033	E1_UFD (Ubiquitin fold domain) Superfamily	none
	iB_15099	Tc_033038	Swi5 Superfamily	CG14104 - (CG14104)
	iB_15103	Tc_033054	PTZ00399 Superfamily, (cysteinyl-tRNA-synthetase)	none
	iB_15108	Tc_033099	none	none
	iB_15160	Tc_033548	none	none
	iB_15169	Tc_033618	PLA2_like Superfamily (Phospholipase A2)	sPLA2 - secretory Phospholipase A2 (CG11124)
	iB_15175	Tc_033669	none	none
	iB_15179	Tc_033697	none	none
	iB_15181	Tc_033706	Glutathione S-transferase (GST) Superfamily	AIMP3 - aaRS-interacting multifunctional protein 3 (CG30185)
	iB_15193	Tc_033767	none	none
	iB_15264	Tc_034059	SERPIN superfamily	Spn28B - Serpin 28B (CG6717)
	iB_15303	Tc_034372	none	none
	iB_15413	Tc_035015	EEP Superfamily (Exonuclease-Endonuclease-Phosphatase domain)	none
	iB_15423	Tc_002355	rve superfamily	CG14478 - (CG14478)
	iB_15460	Tc_004035	none	none
	iB_15474	Tc_033089	none	none
	iB_15476	Tc_007783	none	none
	iB_15482	Tc_030990	none	none
	iB_15490	Tc_032467	none	none
	iB_15493	Tc_032672	none	none
	iB_15516	Tc_003982	none	none
	iB_15531	Tc_000135	none	none
	iB_15626	Tc_013964	none	none
	iB_15646	Tc_034192	none	none
	iB.15676	Tc_014148	none	none
	iB_15744	Tc_034027	none	none
	iB_15758	Tc_031031	none	none
	iB.15780	Tc_003508	none	none
	iB_15798	Tc_016343	none	none

	iB_15842	Tc_035027	none	none
	iB_15862	Tc_033874	none	none
	iB_15886	Tc_033024	none	none
	iB_15894	Tc_007245	none	none
	iB_15895	Tc_012617	none	none

Bold: Tc_008780 identified as gland specific in GlandSpecific 2013 and in the completely new analysis and **Tc_033013** is only found in the Gland specific set from the new analysis 2020 transcriptomic analyis.

Additional file 2. Table S2. Analysis of 129 iBeetle identified genes via GC-MS. In GC-MS analysis of each knockdown gene, two prothoracic and abdominal gland contents value were analyzed separately. Levels of each chemical in gland contents were determined as percentage with respect to wildtype levels. For calculation of each substance abundance, the respective wildtype value was considered 100% and subsequently its abundance in knockdown situation was calculated. Benzoquinone-less genes (BQ-less) are marked by red color (0%) while milder (1-50%) GC-MS phenotypes are denoted by yellow color. Values between 51 to 75 % are shown in light green color while greater 76% values are shown in dark green color. 2-methyl-1,4-benzoquinone (MBQ), 2ethyl-1,4-benzoquinone (EBQ), 1-pentadecene (C15), 1-heptadecene (C17).

SG	# iB	OGS	abdominal glands				prothoracic glands			
			MBQ%	EBQ%	1-C15%	1-C17%	MBQ%	EBQ%	1-C15%	1-C17%
	iB_06455	Tc_012436	8	15	36	26	4	7	45	35
	iB_06635	Tc_001001	45	43	50	56	31	33	62	66
	iB_07536	Tc_006542	23	28	29	33	80	70	112	57
	iB_07787	Tc_004104	30	27	52	73	82	81	97	68
	iB_07820	Tc_004888	28	30	38	53	113	101	125	88
	iB_07950	Tc_001561	1	14	54	21	11	15	51	31
	iB_07976	Tc_003545	56	59	60	47	9	11	70	73
	iB_08057	Tc_002414	0	2	13	20	49	51	74	26
	iB_08263	Tc_010415	33	37	55	115	64	64	102	56
	iB_08565	Tc_014905	30	33	41	47	30	46	6	39
	iB_09271	Tc_006096	35	35	67	67	7	6	43	41
	iB_10094	Tc_014560	19	21	43	38	15	19	35	32
	iB_10258	Tc_009294	14	15	19	22	107	97	28	6
	iB_10282	Tc_009200	33	30	36	29	34	26	60	73
	iB_10307	Tc_033640	45	48	61	65	69	69	75	101
	iB_10350	Tc_009870	50	49	63	69	49	38	88	110
	iB_10379	Tc_008830	12	20	83	68	71	82	111	147
	iB_10399	Tc_010875	43	45	46	41	80	66	80	93
	iB_10410	Tc_008670	54	51	58	64	38	29	52	60
	iB_10416	Tc_008693	12	9	21	9	17	12	30	26
	iB_10636	Tc_006130	18	30	88	66	6	12	54	58
	iB_10843	Tc_001560	17	21	44	43	39	28	51	52
	iB_12106	Tc_002985	6	8	28	23	38	34	52	68
	iB_12119	Tc_003441	19	21	42	30	63	63	68	92
	iB_12122	Tc_003525	18	24	32	29	9	9	37	42
	iB_12143	Tc_004593	28	44	59	47	45	75	63	69
	iB_12151	Tc_004701	22	30	38	24	4	7	47	56
	iB_12159	Tc_004875	25	30	62	53	14	16	53	69
	iB_12160	Tc_004877	4	6	36	28	44	39	46	56
	iB_12164	Tc_004940	20	27	34	25	52	54	41	46
	iB_12171	Tc_005040	34	43	47	37	18	17	40	43
	iB_12179	Tc_005125	19	30	45	37	25	40	60	71
	iB_12410	Tc_008647	0	4	33	40	0	0	41	18

	iB_12420	Tc_008757	5	9	41	14	8	11	39	31
	iB_12424	**Tc_008780**	22	43	83	52	0	0	52	66
	iB_12502	Tc_009891	27	41	45	26	23	64	86	65
	iB_12548	Tc_010490	101	111	83	52	60	80	137	183
	iB_12567	Tc_010739	29	42	47	19	66	80	110	138
	iB_12808	Tc_013415	6	15	48	31	0	0	76	83
	iB_12904	Tc_014568	20	30	34	8	0	5	44	24
	iB_12930	Tc_014956	8	12	33	9	0	6	22	11
	iB_12934	Tc_014988	6	10	38	12	5	8	34	19
	iB_12946	Tc_015183	12	24	106	54	15	18	60	44
	iB_12953	Tc_015294	7	13	73	32	7	12	53	25
	iB_12957	Tc_015339	9	14	74	34	16	22	87	62
	iB_12988	Tc_015711	14	20	93	55	4	19	86	62
	iB_12995	Tc_015806	9	14	64	26	0	4	52	36
	iB_12998	Tc_015831	10	15	52	22	12	15	50	38
	iB_13213	Tc_031234	6	10	65	30	6	7	37	16
	iB_13267	Tc_031901	17	32	120	70	0	5	47	27
	iB_13286	Tc_032059	9	16	64	23	0	6	29	15
	iB_13287	Tc_032061	9	14	63	31	0	6	55	33
	iB_13384	Tc_033142	37	58	47	13	82	100	91	67
	iB_13393	Tc_033231	49	72	127	78	29	43	64	38
	iB_13397	Tc_033244	34	50	110	44	33	51	71	37
	iB_13400	Tc_033252	42	63	95	41	43	53	66	41
	iB_13404	Tc_033289	17	23	40	18	43	41	33	23
	iB_13418	Tc_033437	30	52	128	66	12	21	58	34
	iB_13420	Tc_033443	17	29	33	10	50	66	75	42
	iB_13427	Tc_033511	14	21	38	18	20	23	17	4
	iB_13436	Tc_033565	33	46	42	12	19	26	42	24
	iB_13442	Tc_033617	34	65	90	35	38	53	80	42
	iB_13443	Tc_033629	8	14	47	13	13	18	38	19
	iB_13444	Tc_033633	36	62	5	24	48	59	78	53
	iB_13446	Tc_033680	48	48	99	48	0	0	38	28
	iB_13447	Tc_033682	16	35	71	24	22	35	74	51
	iB_13455	Tc_033734	24	43	99	51	27	30	89	62
	iB_13462	Tc_033825	54	100	123	50	9	15	75	53
	iB_13474	Tc_033927	13	23	60	24	35	44	99	77
	iB_13476	Tc_033970	26	42	95	55	15	24	86	65
	iB_13479	Tc_034016	2	4	20	7	8	10	45	23
	iB_13480	Tc_034021	9	11	66	28	6	7	90	45
	iB_13481	Tc_034049	16	28	96	41	12	15	41	21
	iB_13490	Tc_034143	39	53	116	60	33	39	96	65
	iB_13492	Tc_034186	18	32	86	45	0	4	39	24
	iB_13520	Tc_034418	11	15	50	23	12	13	53	37
	iB_13523	Tc_034433	18	29	47	19	5	8	39	24
	iB_13525	Tc_034455	0	0	19	6	5	7	29	20
	iB_13527	Tc_034461	19	38	82	29	41	45	96	72
	iB_13531	Tc_034478	4	9	45	12	0	0	48	30
	iB_13538	Tc_034552	5	13	100	3	11	17	70	51
	iB_13539	Tc_034560	5	11	42	12	11	17	70	51
	iB_13546	Tc_034629	6	1	37	11	21	33	120	90
	iB_13550	Tc_034643	43	60	127	68	11	14	43	22
	iB_13552	Tc_034655	0	2	19	6	7	9	22	13
	iB_13558	Tc_034684	33	49	115	82	71	95	227	116

	iB_13560	Tc_034694	9	10	22	5	5	5	23	17
	iB_13565	Tc_034733	2	4	32	8	17	17	60	38
	iB_13576	Tc_034847	26	42	95	55	15	24	86	65
	iB_13602	Tc_001666	12	34	47	73	67	56	78	31
	iB_13656	Tc_011350	50	52	93	107	29	30	50	42
	iB_13701	Tc_031342	30	31	40	54	12	13	65	29
	iB_13761	Tc_000233	11	13	39	61	39	42	102	57
	iB_13821	Tc_001282	5	9	27	35	60	61	101	54
	iB_14407	Tc_010819	6	9	18	10	0	0	24	21
	iB_14666	Tc_014799	3	6	46	28	0	4	25	23
	iB_14689	Tc_015027	9	9	49	40	6	5	42	38
	iB_14948	Tc_031796	7	12	36	19	34	53	61	53
	iB_14954	Tc_031816	15	30	58	32	33	35	44	41
	iB_14977	Tc_032119	7	13	35	24	18	25	44	40
	iB_15009	Tc_032351	24	29	51	33	29	33	58	58
	iB_15044	Tc_032638	0	0	19	7	15	31	121	92
	iB_15051	Tc_032701	3	6	37	19	22	26	35	31
	iB_15097	**Tc_033013**	13	25	63	47	20	30	62	80
	iB_15098	Tc_033033	25	44	55	48	43	76	99	38
	iB_15108	Tc_033099	17	23	100	75	32	61	106	111
	iB_15160	Tc_033548	44	82	89	50	0	6	43	41
	iB_15169	Tc_033618	20	31	116	111	10	16	83	76
	iB_15179	Tc_033697	52	64	108	80	94	110	124	126
	iB_15181	Tc_033706	19	28	79	53	24	31	98	100
	iB_15193	Tc_033767	16	29	65	34	1	23	96	101
	iB_15303	Tc_034372	44	65	88	57	83	96	94	104
	iB_15423	Tc_002355	11	14	42	29	59	63	67	65
	iB_15460	Tc_004035	15	30	58	34	55	72	77	72
	iB_15474	Tc_033089	12	20	41	22	97	112	116	128
	iB_15476	Tc_007783	22	38	49	28	35	64	112	133
	iB_15482	Tc_030990	18	26	76	49	110	118	78	69
	iB_15490	Tc_032467	10	21	81	56	41	60	72	69
	iB_15493	Tc_032672	14	30	72	48	10	22	35	33
	iB_15531	Tc_000135	8	14	6	32	45	25	45	38
	iB.15676	Tc_014148	8	22	119	71	5	9	56	52
	iB_15744	Tc_034027	3	6	59	28	0	4	98	89
	iB_15758	Tc_031031	15	21	91	55	46	52	98	106
	iB_15798	Tc_016343	5	7	108	75	27	32	105	102
	iB_15842	Tc_035027	15	25	37	18	81	83	86	95
	iB_15862	Tc_033874	11	16	59	35	37	46	68	58
	iB_15886	Tc_033024	31	43	79	44	0	5	153	175
	iB_15894	Tc_007245	18	19	39	17	4	5	41	32
	iB_15895	Tc_012617	14	22	107	73	34	31	120	117

0%	substance not present
1-50%	strongly reduced
51-75%	Reduced
>76%	not reduced, wt=100%

Additional file 3. Table S3. Expression data of 178 detected gland genes.

SG	# iB	OGS	Gene Length	reference tissue reads (mid abd)	female-abd	female-thx	male-abd	male-thx	log2 FC (sample reads/ref. reads)				FC≥2
					reads	reads	reads	reads	female – abd	female - thx	male - abd	male - thx	
	iB_06455	Tc_012436	1382	159	324	213	211	182	1.03	0.42	0.41	0.19	
	iB_06635	Tc_001001	10374	2169	224	106	171	140	-3.28	-4.35	-3.67	-3.95	
	iB_07379	Tc_001313	1196	1	2	1	1	1	1	0	0	0	
	iB_07536	Tc_006542	1509	3	6	2	2	1	1.00	-0.59	-0.59	-1.59	
	iB_07738	Tc_031704	5755	8	1	7	4	6	-3.00	-0.19	-1.00	-0.42	
	iB_07787	Tc_004104	1168	355	168	255	254	284	-1.08	-0.48	-0.48	-0.32	
	iB_07820	Tc_004888	1638	480	262	504	422	624	-0.87	0.07	-0.19	0.38	
	iB_07886	Tc_000385	4007	519	213	210	254	242	-1.28	-1.31	-1.03	-1.10	
	iB_07950	Tc_001561	1277	286	161	149	126	167	-0.83	-0.94	-1.18	-0.78	
	iB_07976	Tc_003545	3099	17	11	33	44	37	-0.63	0.96	1.37	1.12	
	iB_08057	Tc_002414	995	662	1902	1323	1579	1393	1.52	1.00	1.25	1.07	x
	iB_08160	Tc_008320	1028	463	897	927	938	923	0.95	1.00	1.02	1.00	x
	iB_08263	Tc_010415	1381	169	111	6	34	19	-0.61	-4.82	-2.31	-3.15	
	iB_08565	Tc_014905	1399	620	997	894	961	962	0.69	0.53	0.63	0.63	
	iB_08572	Tc_015824	2308	1044	820	782	1123	926	-0.35	-0.42	0.11	-0.17	
	iB_08877	Tc_031556	2938	1	2	1	1	1	1.00	0.00	0.00	0.00	
	iB_09271	Tc_006096	1806	321	668	105	1600	128	1.06	-1.61	2.32	-1.33	
	iB_10094	Tc_014560	6627	2396	1582	907	4155	1177	-0.60	-1.40	0.79	-1.03	
	iB_10258	Tc_009294	2192	236	249	269	293	302	0.08	0.19	0.31	0.36	
	iB_10282	Tc_009200	1078	1	1	1	9	1	0.00	0.00	3.17	0.00	
	iB_10307	Tc_033640	3375	118	172	57	579	85	0.54	-1.05	2.29	-0.47	
	iB_10350	Tc_009870	1063	181	259	180	206	202	0.52	-0.01	0.19	0.16	
	iB_10379	Tc_008830	1052	343	169	259	297	289	-1.02	-0.41	-0.21	-0.25	
	iB_10398	Tc_033833	2981	1202	743	459	751	533	-0.69	-1.39	-0.68	-1.17	
	iB_10399	Tc_010875	3900	938	155	258	149	268	-2.60	-1.86	-2.65	-1.81	
	iB_10410	Tc_008670	1112	33	13	31	16	18	-1.34	-0.09	-1.04	-0.87	
	iB_10416	Tc_008693	5911	1736	522	396	498	509	-1.73	-2.13	-1.80	-1.77	
	iB_10636	Tc_006130	1217	99	268	215	219	253	1.44	1.12	1.15	1.35	x
	iB_10818	Tc_012600	3465	35	3	5	9	9	-3.54	-2.81	-1.96	-1.96	
	iB_10843	Tc_001560	3092	298	222	202	284	217	-0.42	-0.56	-0.07	-0.46	
	iB_12106	Tc_002985	1640	4140	4781	5568	5973	7542	0.21	0.43	0.53	0.87	
	iB_12119	Tc_003441	2275	220	234	185	473	209	0.09	-0.25	1.10	-0.07	
	iB_12122	Tc_003525	2229	1309	2880	3021	3891	2820	1.14	1.21	1.57	1.11	x
	iB_12143	Tc_004593	1707	734	94	233	245	142	-2.97	-1.66	-1.58	-2.37	
	iB_12151	Tc_004701	3192	9943	1179	631	611	1111	-3.08	-3.98	-4.02	-3.16	
	iB_12159	Tc_004875	1161	3	2	1	2	4	-0.59	-1.59	-0.59	0.42	
	iB_12160	Tc_004877	1038	746	886	526	233	906	0.25	-0.50	-1.68	0.28	
	iB_12164	Tc_004940	724	4929	3279	6168	6263	5377	-0.59	0.32	0.35	0.13	
	iB_12171	Tc_005040	693	3	4	40	22	9	0.42	3.74	2.87	1.59	x
	iB_12179	Tc_005125	660	3	3	3	7	6	0.00	0.00	1.22	1.00	
	iB_12227	Tc_006117	561	261	334	432	553	502	0.36	0.73	1.08	0.94	
	iB_12410	Tc_008647	6146	342	142	103	100	90	-1.27	-1.73	-1.77	-1.93	
	iB_12420	Tc_008757	399	3457	55085	13334	4352	16863	3.99	1.95	0.33	2.29	x
	iB_12424	**Tc_008780**	1613	11	151830	507049	561986	495721	13.75	15.49	15.64	15.46	x
	iB_12502	Tc_009891	3982	455	89	237	100	265	-2.35	-0.94	-2.19	-0.78	
	iB_12548	Tc_010490	1273	23	81	264	237	247	1.82	3.52	3.37	3.42	x
	iB_12567	Tc_010739	1173	9	2	11	19	8	-2.17	0.29	1.08	-0.17	
	iB_12594	Tc_011162	612	704	635	902	1179	1146	-0.15	0.36	0.74	0.70	
	iB_12808	Tc_013415	1152	105	481	63	38	74	2.20	-0.74	-1.47	-0.50	
	iB_12904	Tc_014568	4467	4780	2827	2821	3210	3042	-0.76	-0.76	-0.57	-0.65	
	iB_12930	Tc_014956	2065	472	752	700	971	783	0.67	0.57	1.04	0.73	
	iB_12934	Tc_014988	2692	5	4	1	116	3	-0.32	-2.32	4.54	-0.74	
	iB_12946	Tc_015183	504	1559	1750	1958	2525	2136	0.17	0.33	0.70	0.45	
	iB_12953	Tc_015294	1981	1	1	1	1	1	0.00	0.00	0.00	0.00	
	iB_12957	Tc_015339	6496	1241	1481	4	2115	1	0.26	-8.28	0.77	-10.28	
	iB_12988	Tc_015711	845	12	1	1	1	1	-3.59	-3.59	-3.59	-3.59	
	iB_12995	Tc_015806	1554	1082	537	753	1213	652	-1.01	-0.52	0.16	-0.73	
	iB_12998	Tc_015831	2748	803	669	631	635	618	-0.26	-0.35	-0.34	-0.38	

	iB_13213	Tc_031234	1414	333	365	354	501	332	0.13	0.09	0.59	0.00	
	iB_13267	Tc_031901	3470	138	109	75	128	102	-0.34	-0.88	-0.11	-0.44	
	iB_13286	Tc_032059	2356	433	63	173	114	115	-2.78	-1.32	-1.93	-1.91	
	iB_13287	Tc_032061	888	531	704	736	732	801	0.41	0.47	0.46	0.59	
	iB_13384	Tc_033142	2841	550	37	819	52	1484	-3.89	0.57	-3.40	1.43	
	iB_13393	Tc_033231	1438	410	25	162	64	114	-4.04	-1.34	-2.68	-1.85	
	iB_13397	Tc_033244	2182	153	124	171	118	173	-0.30	0.16	-0.37	0.18	
	iB_13400	Tc_033252	1552	115	18	11	16	17	-2.68	-3.39	-2.85	-2.76	
	iB_13404	Tc_033289	180	105	66	44	92	62	-0.67	-1.25	-0.19	-0.76	
	iB_13418	Tc_033437	1793	3172	4819	4325	6582	4672	0.60	0.45	1.05	0.56	
	iB_13420	Tc_033443	1479	30	9	11	28	19	-1.74	-1.45	-0.10	-0.66	
	iB_13427	Tc_033511	2118	3	5	22	18	15	0.74	2.87	2.59	2.32	x
	iB_13436	Tc_033565	1156	1	77	13	35	17	6.27	3.70	5.13	4.09	x
	iB_13442	Tc_033617	1800	54	24	36	20	24	-1.17	-0.59	-1.43	-1.17	
	iB_13443	Tc_033629	741	87	114	92	108	95	0.39	0.08	0.31	0.13	
	iB_13444	Tc_033633	3269	5040	3322	8781	6633	13153	-0.60	0.80	0.40	1.38	
	iB_13446	Tc_033680	25848	25987	5541	2284	4476	3096	-2.23	-3.51	-2.54	-3.07	
	iB_13447	Tc_033682	767	61	167	187	134	162	1.45	1.62	1.14	1.41	x
	iB_13455	Tc_033734	2266	187	905	414	2233	1121	2.27	1.15	3.58	2.58	x
	iB_13462	Tc_033825	2207	32	22	2	9	3	-0.54	-4.00	-1.83	-3.42	
	iB_13470	Tc_033891	2241	8	2	4	4	2	-2.00	-1.00	-1.00	-2.00	
	iB_13474	Tc_033927	3767	57	28	73	127	120	-1.03	0.36	1.16	1.07	
	iB_13476	Tc_033970	703	148	1	3	2	1	-7.21	-5.62	-6.21	-7.21	
	iB_13479	Tc_034016	1063	126	181	176	252	218	0.52	0.48	1.00	0.79	
	iB_13480	Tc_034021	1728	96	492	114	242	91	2.36	0.25	1.33	-0.08	x
	iB_13481	Tc_034049	3018	215	245	187	440	225	0.19	-0.20	1.03	0.07	
	iB_13490	Tc_034143	2046	259	244	299	204	282	-0.09	0.21	-0.34	0.12	
	iB_13492	Tc_034186	7240	438	43	305	157	488	-3.35	-0.52	-1.48	0.16	
	iB_13507	Tc_034300	1653	44	5	5	64	14	-3.14	-3.14	0.54	-1.65	
	iB_13520	Tc_034418	486	663	1869	1254	1763	1536	1.50	0.92	1.41	1.21	x
	iB_13523	Tc_034433	5139	230	215	206	248	336	-0.10	-0.16	0.11	0.55	
	iB_13525	Tc_034455	1473	169	11	24	59	35	-3.94	-2.82	-1.52	-2.27	
	iB_13527	Tc_034461	1766	15	12	28	42	16	-0.32	0.90	1.49	0.09	
	iB_13531	Tc_034478	4187	2	1	1	1	3	-1.00	-1.00	-1.00	0.59	
	iB_13538	Tc_034552	894	1	1	2	1	1	0.00	1.00	0.00	0.00	
	iB_13539	Tc_034560	413	87	7	8	5	5	-3.64	-3.44	-4.12	-4.12	
	iB_13541	Tc_034598	601	25	17	26	27	33	-0.56	0.06	0.11	0.40	
	iB_13546	Tc_034629	1028	1128	623	277	238	314	-0.86	-2.03	-2.24	-1.84	
	iB_13550	Tc_034643	513	305	609	326	327	459	1.00	0.10	0.10	0.59	
	iB_13552	Tc_034655	1208	7	20	23	37	31	1.51	1.72	2.40	2.15	x
	iB_13556	Tc_034670	1206	865	10	10	1	12	-6.43	-6.43	-9.76	-6.17	
	iB_13558	Tc_034684	1252	141	22	2	9	10	-2.68	-6.14	-3.97	-3.82	
	iB_13560	Tc_034694	1762	473	105	104	102	150	-2.17	-2.19	-2.21	-1.66	
	iB_13565	Tc_034733	1182	1	1	1	1	1	0.00	0.00	0.00	0.00	
	iB_13568	Tc_034761	492	70	15	9	11	11	-2.22	-2.96	-2.67	-2.67	
	iB_13576	Tc_034847	2160	1	3	4	2	2	1.58	2.00	1.00	1.00	x
	iB_13578	Tc_034897	1497	5	1	3	80	1	-2.32	-0.74	4.00	-2.32	
	iB_13585	Tc_035033	331	1	1	1	11	1	0.00	0.00	3.46	0.00	
	iB_13602	Tc_001666	1468	154	136	268	238	330	-0.18	0.80	0.63	1.10	
	iB_13614	Tc_004281	1356	12	6	5	1	1	-1.00	-1.26	-3.59	-3.59	
	iB_13619	Tc_005085	993	1	1	1	1	1	0.00	0.00	0.00	0.00	
	iB_13626	Tc_005432	1552	145	40	26	22	28	-1.86	-2.48	-2.72	-2.37	
	iB_13628	Tc_005475	354	5	1	1	1	2	-2.32	-2.32	-2.32	-1.32	
	iB_13639	Tc_006626	563	14	16	85	24	83	0.19	2.60	0.78	2.57	x
	iB_13656	Tc_011350	1705	599	629	602	404	518	0.07	0.01	-0.57	-0.21	
	iB_13660	Tc_012397	925	203	423	984	1309	1185	1.06	2.28	2.69	2.55	x
	iB_13667	Tc_012635	1353	1	1	1	1	1	0.00	0.00	0.00	0.00	
	iB_13673	Tc_013464	1183	16301	886	2316	1425	3235	-4.20	-2.82	-3.52	-2.33	
	iB_13677	Tc_013821	625	1	1	1	1	1	0.00	0.00	0.00	0.00	
	iB_13680	Tc_014087	4717	47	1	6	3	9	-5.55	-2.97	-3.97	-2.38	
	iB_13692	Tc_030268	1134	1	1	1	1	1	0.00	0.00	0.00	0.00	
	iB_13694	Tc_030367	1140	1	1	1	1	1	0.00	0.00	0.00	0.00	
	iB_13698	Tc_030961	303	20	11	11	1	16	-0.86	-0.86	-4.32	-0.32	
	iB_13701	Tc_031342	7728	5964	1	7	12	23	-12.54	-9.73	-8.96	-8.02	
	iB_13704	Tc_032134	930	19	3	25	1	39	-2.66	0.40	-4.25	1.04	
	iB_13707	Tc_032365	1221	249	159	60	138	75	-0.65	-2.05	-0.85	-1.73	

	iB_13712	Tc_032843	1542	3	1	3	4	5	-1.59	0.00	0.42	0.74	
	iB_13723	Tc_033974	2800	340	202	14	10	23	-0.75	-4.60	-5.09	-3.89	
	iB_13730	Tc_034797	1451	4	5	82	24	82	0.32	4.36	2.59	4.36	x
	iB_13736	Tc_004248	705	1	1	1	1	1	0.00	0.00	0.00	0.00	
	iB_13739	Tc_034703	4492	114	39	52	18	37	-1.55	-1.13	-2.66	-1.62	
	iB_13754	Tc_000145	411	1	1	1	1	1	0	0	0	0	
	iB_13761	Tc_000233	550	490	448	435	519	572	-0.13	-0.17	0.08	0.22	
	iB_13815	Tc_001141	4230	723	87	23	23	28	-3.05	-4.97	-4.97	-4.69	
	iB_13821	Tc_001282	324	197	267	432	209	672	0.44	1.13	0.09	1.77	
	iB_14407	Tc_010819	363	1	1	1	1	1	0.00	0.00	0.00	0.00	
	iB_14666	Tc_014799	2808	13	17	14	132	10	0.39	0.11	3.34	-0.38	
	iB_14689	Tc_015027	516	220	1	2	12	2	-7.78	-6.78	-4.20	-6.78	
	iB_14948	Tc_031796	704	132	1	1	1	1	-7.04	-7.04	-7.04	-7.04	
	iB_14954	Tc_031816	743	154	177	202	174	175	0.20	0.39	0.18	0.18	
	iB_14977	Tc_032119	615	127	529	41	57	20	2.06	-1.63	-1.16	-2.67	
	iB_15009	Tc_032351	401	1	1	1	1	1	0.00	0.00	0.00	0.00	
	iB_15044	Tc_032638	1209	30	14	8	63	11	-1.10	-1.91	1.07	-1.45	
	iB_15047	Tc_032680	1439	7089	2666	2906	2129	5892	-1.41	-1.29	-1.74	-0.27	
	iB_15051	Tc_032701	1843	332	57	48	70	44	-2.54	-2.79	-2.25	-2.92	
	iB_15097	**Tc_033013**	1300	186	3948	24456	10764	32168	4.41	7.04	5.85	7.43	x
	iB_15098	Tc_033033	668	48	1	3	1	1	-5.59	-4.00	-5.59	-5.59	
	iB_15099	Tc_033038	384	112	50	55	53	52	-1.16	-1.03	-1.08	-1.11	
	iB_15103	Tc_033054	1328	36	4	10	21	19	-3.17	-1.85	-0.78	-0.92	
	iB_15108	Tc_033099	994	406	182	109	108	132	-1.16	-1.90	-1.91	-1.62	
	iB_15160	Tc_033548	2127	8	7	3	76	2	-0.19	-1.42	3.25	-2.00	
	iB_15169	Tc_033618	884	1	1	1	119	1	0.00	0.00	6.89	0.00	x*
	iB_15175	Tc_033669	457	1	1	1	1	1	0.00	0.00	0.00	0.00	
	iB_15179	Tc_033697	913	26	1	1	3	2	-4.70	-4.70	-3.12	-3.70	
	iB_15181	Tc_033706	598	322	396	352	341	392	0.30	0.13	0.08	0.28	
	iB_15193	Tc_033767	1004	477	21	48	41	112	-4.51	-3.31	-3.54	-2.09	
	iB_15264	Tc_034059	3900	1	35	1	17	1	5.13	0.00	4.09	0.00	x*
	iB_15303	Tc_034372	2106	1895	35	290	57	319	-5.76	-2.71	-5.06	-2.57	
	iB_15413	Tc_035015	974	117	52	39	55	65	-1.17	-1.59	-1.09	-0.85	
	iB_15423	Tc_002355	282	2	1	1	1	1	-1	-1	-1	-1	
	iB_15460	Tc_004035	804	6328	18654	14825	10867	19387	1.56	1.23	0.78	1.62	x
	iB_15474	Tc_033089	3940	4301	2349	517	912	621	-0.87	-3.06	-2.24	-2.79	
	iB_15476	Tc_007783	2858	181	185	91	90	157	0.03	-0.99	-1.01	-0.21	
	iB_15482	Tc_030990	654	15	2	1	1	1	-2.91	-3.91	-3.91	-3.91	
	iB_15490	Tc_032467	2503	2211	2173	1694	2112	1979	-0.03	-0.38	-0.07	-0.16	
	iB_15493	Tc_032672	326	1	8	5	173	13	3.00	2.32	7.43	3.70	x
	iB_15516	Tc_003982	750	714	1608	7977	8104	7459	1.17	3.48	3.50	3.39	x
	iB_15531	Tc_000135	396	605	448	717	648	770	-0.43	0.245	0.099	0.348	
	iB_15626	Tc_013964	618	171	193	117	146	130	0.17	-0.55	-0.23	-0.40	
	iB_15646	Tc_034192	1276	355	235	83	134	138	-0.60	-2.10	-1.41	-1.36	
	iB.15676	Tc_014148	336	234	93	48	48	29	-1.33	-2.29	-2.29	-3.01	
	iB_15744	Tc_034027	400	324	1	1	1	20	-8.34	-8.34	-8.34	-4.02	
	iB_15758	Tc_031031	315	206	120	264	256	407	-0.78	0.36	0.31	0.98	
	iB.15780	Tc_003508	189	44	1	1	1	1	-5.46	-5.46	-5.46	-5.46	
	iB_15798	Tc_016343	989	1	1	1	112	1	0.00	0.00	6.81	0.00	x*
	iB_15842	Tc_035027	181	159	120	147	122	193	-0.41	-0.11	-0.38	0.28	
	iB_15862	Tc_033874	3113	22	19	3	10	12	-0.21	-2.87	-1.14	-0.87	
	iB_15886	Tc_033024	961	66	4	4	4	8	-4.04	-4.04	-4.04	-3.04	
	iB_15894	Tc_007245	444	42	4	6	4	16	-3.39	-2.81	-3.39	-1.39	
	iB_15895	Tc_012617	670	27	41	6	23	14	0.60	-2.17	-0.23	-0.95	

x* Genes FC values are highly expressed only in one of the gland type.

Additional file 4. Table S4. Overlap of the three gland specific gene sets 2013 (OGS2) and the complete transcriptome 2020 (OGS3)

OGS3 2020											OGS2 2013								
Gene	Gene Length	ref tissue (mid abd)	Reads				log FC (sample reads/reference reads)				ref tissue (mid abd)	reads				log FC (sample reads/reference reads)			
			Fm_ abd	Fm_ thx	Mal_ abd	Male_thx	Fm_ abd	Fm_ thx	Mal_ abd	Mal_ thx		Fm_ abd	Fm_ thx	Mal_ abd	Male_thx	Fm_ abd	Fm_ thx	Mal_ abd	Mal_ thx
TC002187	954	1	18	31	83	17	4.17	4.95	6.38	4.09	2	15	17	49	9	2.91	3.09	4.61	2.17
TC010790	285	1	21	19	78	215	4.39	4.25	6.29	7.75	1	17	14	66	163	4.09	3.81	6.04	7.35
TC012136	1725	3	77	186	209	109	4.68	5.95	6.12	5.18	3	45	113	112	69	3.91	5.24	5.22	4.52
TC031164	482	1	11959	49864	39982	47703	13.55	15.61	15.29	15.54									
TC031266	363	2	78	118	202	172	5.29	5.88	6.66	6.43									
TC031268	318	11	7317	34192	26767	38402	9.38	11.60	11.25	11.77									
TC031598	814	2	40	45	169	33	4.32	4.49	6.40	4.04									
TC031810	463	1	721	13344	3051	11729	9.49	13.70	11.58	13.52									
TC031871	442	6	29911	101627	88030	150163	12.28	14.05	13.84	14.61									
TC032266	1352	51	2223	3062	7550	2988	5.45	5.91	7.21	5.87									
TC032405	693	1	799	7016	4452	10244	9.64	12.78	12.12	13.32									
TC032449	835	15	253	448	455	397	4.08	4.90	4.92	4.73									
TC032450	876	1	67	284	276	464	6.07	8.15	8.11	8.86									
TC032523	448	1	51158	174820	170581	221816	15.64	17.42	17.38	17.76									
TC032539	1544	27	128680	636332	457694	537875	12.22	14.52	14.05	14.28									
TC032842	1066	6	219	287	533	346	5.19	5.58	6.47	5.85									
TC032979	1855	5	220	1407	937	1212	5.46	8.14	7.55	7.92									
TC032993	2361	97	1693	5235	4371	5603	4.13	5.75	5.49	5.85									
TC033013	1300	186	3948	24456	10764	32168	4.41	7.04	5.85	7.43									
TC033050	2356	73	2146	2478	5827	2252	4.88	5.09	6.32	4.95									
TC033121	1016	1	59	532	286	611	5.88	9.06	8.16	9.26									
TC033302	2065	19	789	1012	1942	1093	5.38	5.74	6.68	5.85									
TC033405	1552	115	10076	63301	37636	69916	6.45	9.10	8.35	9.25									
TC033612	5487	64	1967	6807	8261	6698	4.94	6.73	7.01	6.71									
TC033641	1226	40	673	1870	2679	2475	4.07	5.55	6.07	5.95									
TC033678	1705	21	364	547	662	557	4.12	4.70	4.98	4.73									
TC033804	994	1	283	775	954	648	8.14	9.60	9.90	9.34									
TC033805	1810	28	21182	47117	63763	45807	9.56	10.72	11.15	10.68									
TC034102	3783	75	13759	34886	39606	31078	7.52	8.86	9.04	8.69									
TC034113	276	1	9447	51	45775	184	13.21	5.67	15.48	7.52									
TC034210	447	4	4390	10259	14122	11429	10.10	11.32	11.79	11.48									
TC034245	995	1	23	6726	126	6228	4.52	12.72	6.98	12.60									
TC034402	927	1	16	57	371	47	4.00	5.83	8.54	5.55									
TC034776	1886	15	2926	9597	9149	7551	7.61	9.32	9.25	8.98									
TC034789	293	1	5111	28352	26401	33036	12.32	14.79	14.69	15.01									
TC035052	482	1	19956	56570	64195	57565	14.28	15.79	15.97	15.81									
TC000675	2242	331	9172	10651	35338	9667	4.79	5.01	6.74	4.87	319	8804	10266	33838	9163	4.79	5.01	6.73	4.84

TC002805	1572	164	7154	5306	5611	5086	5.45	5.02	5.10	4.95		111	5647	4080	4404	3857	5.67	5.20	5.31	5.12
TC003110	686	1	1507064	302	48	234	20.52	8.24	5.58	7.87		1	1521358	308	46	240	20.54	8.27	5.52	7.91
TC003157	1683	7	150	185	356	175	4.42	4.72	5.67	4.64		6	146	181	350	173	4.60	4.91	5.87	4.85
TC003835	674	1	39	491	203	435	5.29	8.94	7.67	8.76		1	39	432	183	387	5.29	8.75	7.52	8.60
TC006497	2872	19	508	719	2978	989	4.74	5.24	7.29	5.70		17	466	666	2777	919	4.78	5.29	7.35	5.76
TC007254	1508	4	128	13729	143	15772	5.00	11.74	5.16	11.95		4	88	9895	84	11308	4.46	11.27	4.39	11.47
TC011737	1016	8	225	322	626	448	4.81	5.33	6.29	5.81		8	227	325	631	437	4.83	5.34	6.30	5.77
TC011749	1214	7	145	408	243	479	4.37	5.87	5.12	6.10		4	108	287	183	357	4.75	6.16	5.52	6.48
TC012838	1561	279	5074	10843	17341	11469	4.18	5.28	5.96	5.36		273	4900	10357	16679	11107	4.17	5.25	5.93	5.35
TC013137	612	1	236	44	189	41	7.88	5.46	7.56	5.36		1	206	40	174	35	7.69	5.32	7.44	5.13
TC015349	1052	13	532	672	1137	869	5.35	5.69	6.45	6.06		12	518	639	1102	851	5.43	5.73	6.52	6.15
TC015841	820	23	436	933	921	1966	4.24	5.34	5.32	6.42		23	428	915	868	1939	4.22	5.31	5.24	6.40
TC001937	6778	5	137	480	776	445	4.78	6.58	7.28	6.48		5	134	473	710	451	4.74	6.56	7.15	6.50
TC003284	1708	1	3862	11185	10691	10247	11.92	13.45	13.38	13.32		1	4238	12067	11569	11359	12.05	13.56	13.50	13.47
TC003437	1470	1	110	66	51	59	6.78	6.04	5.67	5.88		1	107	68	52	63	6.74	6.09	5.70	5.98
TC005384	1683	13	2402	8701	4579	6585	7.53	9.39	8.46	8.98		13	2354	8605	4456	6443	7.50	9.37	8.42	8.95
TC005389	1980	27	1696	4928	5900	4846	5.97	7.51	7.77	7.49		25	1632	4731	5706	4693	6.03	7.56	7.83	7.55
TC007317	1821	40	15407	78596	56334	72661	8.59	10.94	10.46	10.83		34	15012	75686	54352	70016	8.79	11.12	10.64	11.01
TC008412	3709	36	8655	19079	18610	17626	7.91	9.05	9.01	8.94		37	8885	19505	19076	18239	7.91	9.04	9.01	8.95
TC008413	1583	1	19048	32122	79838	40462	14.22	14.97	16.28	15.30		1	16793	27712	69675	34891	14.04	14.76	16.09	15.09
TC008414	1580	81	3108	19582	12785	19992	5.26	7.92	7.30	7.95		77	2915	18210	11937	18683	5.24	7.89	7.28	7.92
TC008780	1613	11	151830	507049	561986	495721	13.75	15.49	15.64	15.46		8	134925	452545	505794	436210	14.04	15.79	15.95	15.73
TC010551	516	71	44729	117207	103013	113217	9.30	10.69	10.50	10.64		36	18487	46485	43824	50744	9.00	10.33	10.25	10.46
TC011149	497	1	706	126	2479	213	9.46	6.98	11.28	7.73		1	592	127	2409	196	9.21	6.99	11.23	7.61
TC011211	1750	98	17084	53238	57339	48435	7.45	9.09	9.19	8.95		87	16140	47146	52445	46017	7.54	9.08	9.24	9.05
TC011337	761	1	717	787	2533	1445	9.49	9.62	11.31	10.50		1	690	763	2427	1386	9.43	9.58	11.24	10.44
TC012841	1359	4	145	4150	431	6291	5.18	10.02	6.75	10.62		3	106	3034	295	4536	5.14	9.98	6.62	10.56
TC013059	588	3292	79529	227960	254584	242103	4.59	6.11	6.27	6.20		2803	69128	192836	218320	206572	4.62	6.10	6.28	6.20
TC013108	3798	331	6684	35878	27043	34483	4.34	6.76	6.35	6.70		296	6186	33098	24886	31633	4.39	6.81	6.39	6.74
TC013474	1455	20	766	2746	2924	2927	5.26	7.10	7.19	7.19		12	306	1136	1442	1236	4.67	6.56	6.91	6.69
TC013630	1292	1	203	690	485	740	7.67	9.43	8.92	9.53		1	145	517	383	548	7.18	9.01	8.58	9.10
TC014185	1083	3	467	1865	782	1346	7.28	9.28	8.03	8.81		2	271	1032	446	789	7.08	9.01	7.80	8.62
TC014388	1450	10	980	2591	3531	2112	6.61	8.02	8.46	7.72		6	887	2344	3221	1889	7.21	8.61	9.07	8.30
TC014479	771	6	141	378	1117	375	4.55	5.98	7.54	5.97		3	114	301	919	296	5.25	6.65	8.26	6.62
TC015151	1777	78	45394	125016	177136	114755	9.18	10.65	11.15	10.52		76	45114	124457	176434	114281	9.21	10.68	11.18	10.55
TC015346	3768	405	23492	50801	75322	50743	5.86	6.97	7.54	6.97		408	23427	50191	74674	50369	5.84	6.94	7.52	6.95
TC015546	1513	24	431	9460	1511	9467	4.17	8.62	5.98	8.62		24	459	10088	1593	10047	4.26	8.72	6.05	8.71
TC016280	1246	5	1502	4461	5751	4806	8.23	9.80	10.17	9.91		3	1165	3227	4182	3670	8.60	10.07	10.45	10.26
TC000189												18	783	1128	2520	978	5.44	5.97	7.13	5.76
TC000190												21	931	1302	3411	1285	5.47	5.95	7.34	5.94
TC000959	870	2	26	45	100	18	3.70	4.49	5.64	3.17		1	25	39	93	17	4.64	5.29	6.54	4.09
TC004632	905	54	1394	631	321	848	4.69	3.55	2.57	3.97		6	781	255	141	367	7.02	5.41	4.55	5.93
TC005078												2	43	58	201	44	4.43	4.86	6.65	4.46
TC008158												1	19	22	35	24	4.25	4.46	5.13	4.58
TC013772												67	2084	2373	5563	2158	4.96	5.15	6.38	5.01

TC002798	342	1	10	56	45	81	3.32	5.81	5.49	6.34		1	29	107	107	155	4.86	6.74	6.74	7.28
TC003768												74	129261	641884	463311	539533	10.77	13.08	12.61	12.83
TC004085												56	2376	6997	7839	16176	5.41	6.97	7.13	8.17
TC005635												7	9110	23168	26305	19437	10.35	11.69	11.88	11.44
TC008804												1	16609	34223	47022	33437	14.02	15.06	15.52	15.03
TC010236												6	2983	15530	10497	16544	8.96	11.34	10.77	11.43
TC010286												1	50	262	218	262	5.64	8.03	7.77	8.03
TC012613												1	26	83	455	66	4.70	6.38	8.83	6.04
TC014784	1207	2	26	28	748	36	3.70	3.81	8.55	4.17		1	25	26	651	29	4.64	4.70	9.35	4.86
TC015382												11	742	975	1880	1045	6.08	6.47	7.42	6.57
TC015467	1566	1	11	47	134	28	3.46	5.55	7.07	4.81		1	17	52	136	31	4.09	5.70	7.09	4.95
TC015603												97	8509	52245	31728	59376	6.45	9.07	8.35	9.26
TC015918												6	2063	7656	9110	7454	8.43	10.32	10.57	10.28
TC015932												8	598	2023	1764	1675	6.22	7.98	7.78	7.71
TC016081												26	3087	9379	8429	8807	6.89	8.49	8.34	8.40
TC000602	737	1	881	1	37	12	9.78	0.00	5.21	3.58		1	751	1	30	9	9.55	0.00	4.91	3.17
TC000765	327	1	1	18	14	6	0.00	4.17	3.81	2.58		1	1	18	14	4	0.00	4.17	3.81	2.00
TC002041	531	1	3	11	5	14	1.58	3.46	2.32	3.81		1	3	10	1	15	1.58	3.32	0.00	3.91
TC002279	159	1	1	1	1	1	0.00	0.00	0.00	0.00		1	20	1	1	2	4.32	0.00	0.00	1.00
TC002439												1	2	3	75	8	1.00	1.58	6.23	3.00
TC006376	342	1	12	1	1	1	3.58	0.00	0.00	0.00		1	9	2	1	1	3.17	1.00	0.00	0.00
TC006800	1874	410	423	501	515	574	0.05	0.29	0.33	0.49		1	12	50	72	46	3.58	5.64	6.17	5.52
TC008655												1	36	15	3	10	5.17	3.91	1.58	3.32
TC009338												1	1	1	6	4	0.00	0.00	2.58	2.00
TC011356	1600	1	6	4	335	10	2.58	2.00	8.39	3.32		1	6	4	343	10	2.58	2.00	8.42	3.32
TC011646	433	1	51	1	2	1	5.67	0.00	1.00	0.00		1	67	7	4	1	6.07	2.81	2.00	0.00
TC011780	1601	53	38	26	151	25	-0.48	-1.03	1.51	-1.08		1	5	1	108	1	2.32	0.00	6.75	0.00
TC012263	255	7	16	113	69	64	1.19	4.01	3.30	3.19		1	2	5	11	3	1.00	2.32	3.46	1.58
TC012640	751	5	37	488	343	425	2.89	6.61	6.10	6.41		3	27	361	258	326	3.17	6.91	6.43	6.76
TC013136	443	1	37	9	1	19	5.21	3.17	0.00	4.25		1	36	9	1	18	5.17	3.17	0.00	4.17
TC013910	312	1	2	23	14	20	1.00	4.52	3.81	4.32		1	7	17	12	18	2.81	4.09	3.58	4.17
TC014977	468	1	25	7	1	7	4.64	2.81	0.00	2.81		1	39	12	1	6	5.29	3.58	0.00	2.58
TC015190	857	1	10	7	49	8	3.32	2.81	5.61	3.00		1	10	7	46	6	3.32	2.81	5.52	2.58
TC015230	1805	1	2	2	91	2	1.00	1.00	6.51	1.00		1	2	2	90	2	1.00	1.00	6.49	1.00
TC016264	210	1	1	8	4	13	0.00	3.00	2.00	3.70		1	1	6	3	12	0.00	2.58	1.58	3.58
TC030085	981	1	9	33	15	19	3.17	5.04	3.91	4.25		1	2	14	9	8	1.00	3.81	3.17	3.00

	33 absent in OGS2 (2013), 3 not in OGS2 (2013)
	13 gland specific both in OGS3 (2020) and OGS2 (2013)
	26 also in both gland specific both in OGS3 (2020) and OGS2 (2013)
	5 not annotated any longer in OGS3 (2020), 2 not gland specific in OGS3 (2020 due to filtering threshold)
	12 not annotated any longer in OGS3 (2020), 3 not gland specific in OGS3 (2020 due to filtering threshold)
	3 in both OGS3 (2020) and 18 in OGS2 (2013) only identify by Li *et.at*. 2013

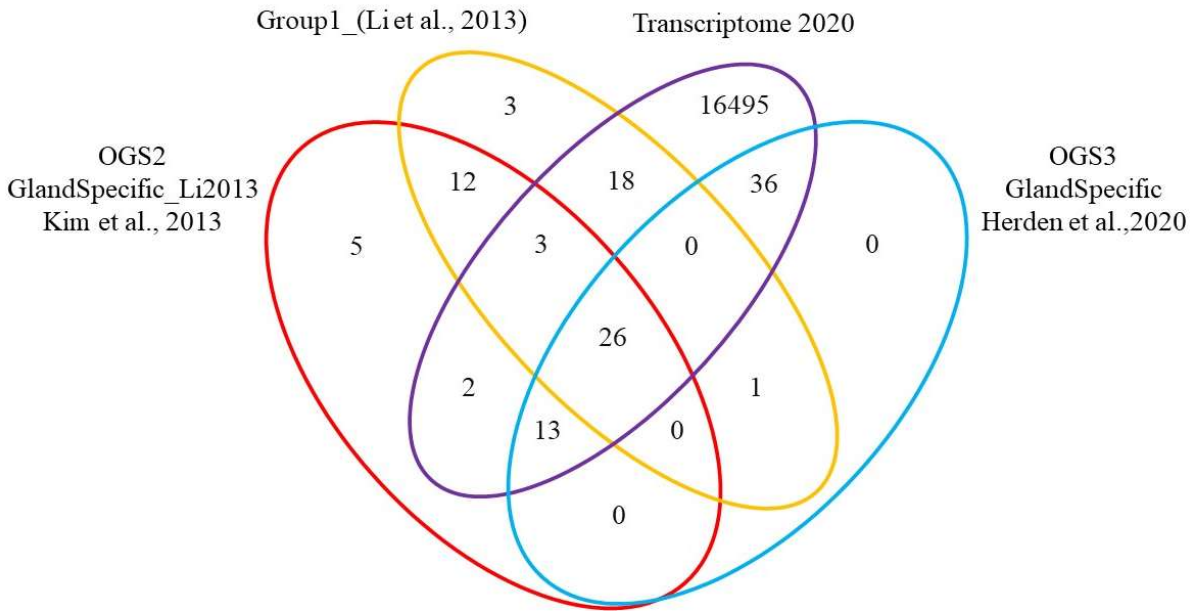

Additional file 5. Figure S1. 20 transcripts that were detected with the mapping from 2013 could not have been detected, since the TC numbers are not included in the new version of the transcriptome (5 + 12 + 3). 36 transcripts were detected completely newly. Of these 36, 33 are new TC numbers, and therefore could not have been detected in the old analysis.

Additional file 6. S6

Mapping rates from Bowtie2 – local, default parameters:

==========

JobID = 3016806

User = ebuchbe, Account = all

Partition = medium-fmz, Nodelist = gwdd095

==========

Anterior_abdomen.fastq:

29527715 reads; of these:

  29527715 (100.00%) were unpaired; of these:

    5672261 (19.21%) aligned 0 times

    18769679 (63.57%) aligned exactly 1 time

    5085775 (17.22%) aligned >1 times

80.79% overall alignment rate

Female_abdominal_glands.fastq:

27786784 reads; of these:

  27786784 (100.00%) were unpaired; of these:

    3946194 (14.20%) aligned 0 times

    20227761 (72.80%) aligned exactly 1 time

    3612829 (13.00%) aligned >1 times

85.80% overall alignment rate

Female_prothoracic_glands.fastq:

29350110 reads; of these:

  29350110 (100.00%) were unpaired; of these:

    4770869 (16.26%) aligned 0 times

    20285250 (69.11%) aligned exactly 1 time

    4293991 (14.63%) aligned >1 times

83.74% overall alignment rate

Male_abdominal_glands.fastq:
27929437 reads; of these:
  27929437 (100.00%) were unpaired; of these:
    5793024 (20.74%) aligned 0 times
    18627458 (66.69%) aligned exactly 1 time
    3508955 (12.56%) aligned >1 times
79.26% overall alignment rate

Male_prothoracic_glands.fastq:
28544764 reads; of these:
  28544764 (100.00%) were unpaired; of these:
    4713998 (16.51%) aligned 0 times
    19476745 (68.23%) aligned exactly 1 time
    4354021 (15.25%) aligned >1 times
83.49% overall alignment rate

Prothoracic_glands_tar_mut.fastq:
29690989 reads; of these:
  29690989 (100.00%) were unpaired; of these:
    4840284 (16.30%) aligned 0 times
    20603484 (69.39%) aligned exactly 1 time
    4247221 (14.30%) aligned >1 times
83.70% overall alignment rate

3.3 Partition-regulated sulfonation-based detoxification used for self-protecting production of toxic substances in defensive stink glands of the red flour beetle

Summary

In this study, we analyzed a subset of genes that play a pivotal role in the production of benzoquinone in the stink gland of the red flour beetle. Odoriferous glands in *Tribolium* beetles are highly specialized for synthesis and secretion of various chemical for beetle defence. Benzoquinones are the major groups of chemical compounds present in stink glands of beetles. Benzoquinones are volatile, highly unstable, reactive, toxic and have irritant effects. As benzoquinone is very toxic and reactive, it requires careful handling and detoxication systems. It is used by *Tribolium* beetles in chemical defence. It has been noted that cuticular linings of producing organelle and storing reservoir protect adult beetles from their own toxic secretions. Hence, if the development of adequate self-protective barrier is disturbed then the beetle will harm themselves. There is not much data available which genes are involved in the process of self-protected synthesis of defensive compounds in the stink glands. In the process of the genome-wide identification of genes necessary for defensive stink gland function of the red flour beetle *Tribolium* casteneum. By RNA-based transcriptomics and a phenotypic screen based on RNA intereference, we identified a complete set of sulfur metabolism genes especially those involved in sulfonation, which is a way of detoxification in insects.. We selected *SUMF1, SLC26A11* and *CHST5* from the 1st and the 2nd phase of the genome-wide iBeetle screening while *ARSB* selected from the transcriptomic data of Li *et.al.* 2013. In this study, we analyzed these genes function in the self-protected synthesis of toxic substances in the defensive stink glands

Bibi Atika[1*], Kirstin Feußner[2*], Musa Dan'azumi Isah[1], Ivo Feußner[2], Ernst A. Wimmer[1†]

Authors contribution to the practical work

Bibi Atika: All experiments besides the ones performed by Kirstin. Writing of first draft of manuscript and composition of figures.

Kirstin Feußner: performed LC-MS analysis and provided the respective figures.

Musa Dan'azumi Isah: performed microinjection and cloning of some genes.

Status: Work in progress

Partition-regulated sulfonation-based detoxification used for self-protecting production of toxic substances in defensive stink glands of the red flour beetle

Bibi Atika[1*], Kirstin Feußner[2*], Musa Dan'azumi Isah[1], Ivo Feußner[2], Ernst A. Wimmer[1†]

bibi.atika@biologie.uni-goettingen.de

kirstin.feussner@biologie.uni-goettingen.de

musa-danazumi.isah@biologie.uni-goettingen.de

ifeussn@gwdg.de

ewimmer@gwdg.de

[1] Georg-August-University Goettingen, Johann-Friedrich-Blumenbach-Institute for Zoology and Anthropology, Dept. of Developmental Biology, GZMB, Ernst-Caspari-Haus, Justus-von-Liebig-Weg 11, 37077 Goettingen, Germany

[2] Albrecht-von-Haller Institute for Plant Sciences, Dept. of Plant Biochemistry, GZMB, Ernst-Caspari-Haus, Justus-von-Liebig-Weg 11, 37077 Goettingen, 37077 Goettingen, Germany

[*] equal contribution

[†] corresponding author: ewimmer@gwdg.de, Tel.: +49 551 39 28666; Fax: +49 551 39 25416

Abstract

Odoriferous glands in *Tribolium* beetles are highly specialized for synthesis and secretion of various chemical for beetle defence. The stink glands secretion of the adult red flour beetle is rich in benzoquinone. Benzoquinones are volatile, highly unstable, reactive, toxic and have irritant effects. As benzoquinone is very toxic and reactive, it requires careful handling and detoxication systems. It is used by *Tribolium* beetles in chemical defence. It has been noted that cuticular linings of producing organelle and storing reservoir protect adult beetles from their own toxic secretions. Hence, if the development of adequate self-protective barrier is disturbed then the beetle will harm themselves. There is not much data available which genes are involved in the process of self-protected synthesis of defensive compounds in the stink glands. However, safe production of self-protected benzoquinone production is not completely understood. Genome-wide analysis based on transcriptome and

phenotypic screen isolated a large number of genes necessary for the benzoquinone synthesis. In these genes, we recognized a complete set of genes involved in sulfate metabolism. Knowing the role of sulfonation in detoxification therefore we analyze this set of genes whether these genes could be involved in the self-protected production of benyoquinone in the defensive stink glands of the *Tribolium*. The identified genes set consist of arylsulfatase B (*ARSB*), Sulfatase modifying factor 1 (*SUMF1*), sodium independent sulfate transporter (*SLC26A11*) and Carbohydrate sulfotransferase 5 (*CHST5*). We selected *SUMF1, SLC26A11* and *CHST5* from the 1st, 2nd and 3rd phase of the genome-wide iBeetle screening while *ARSB* selected from the transcriptomic data of Li et.al. 2013. The RNAi-mediated disruption of *ARSB*, *SUMF1* and *SLC26A11* resulted in strongly altered phenotype of both abdominal and prothoracic stink gland contents while in *CHST5*. RNAi-mediated gene silencing show a slightly altered gland phenotype. In GC-MS data, volatiles secretion of stink gland in the RNAi-mediated gene silencing of these genes (*ARSB*, *SUMF1* and *SLC26A11*) showed a strongly altered content chemical composition, while *CHST5* RNAi showed slightly reduced alteration in composition of gland contents. The expression profiles of *CHST5, ARSB*, *SUMF1* and *SLC26A11* mRNAs were checked and compared in the adult wt beetle gut, fat body and gland tissues by real time qPCR. *CHST5* mRNAs was significantly highly expressed in gut and fat body as compared to gland. The high expression of *CHST5* shows involvement for sulfate conjugation in the gut and fat body. Sulfate conjugation is used by many insects for self-protected production of toxic compounds. *CHST5* was not present in glands so further analyses was done on three genes. Our *in situ* hybridization data demonstrated that these three genes are expressed around the cells type-2 vesicle in stink gland of the red flour beetle. In the LC-MS analysis of knockdown situation for the three gland expressed genes *ARSB*, *SUMF1* and *SLC26A11*, 2-methyl-4-hydoxyphenyl glycosylsulfate 2-ethyl-4-hydoxyphenyl glycosylsulfate precursors were noted for the first time suggesting a major role as precursors in the gland secretion biosynthesis. These studies on deciphering the mechanisms of protected biosynthesis of beetle defensive compounds will enhance our knowledge of the molecular biological mechanism of the self-protected biosynthesis of toxic chemical substances in defensive stink glands.

Introduction

The red flour beetle (*Tribolium castaneum*) is a member of insects order Coleoptera that contain all living

and extinct beetle species (Chapman, 2009; Crowson, 1960; Grove and Stork, 2000). It attacks different types of products in storage, including nuts, legumes, dried fruits, many other grains and wheat. Particularly, it prefers flours and other processed agriculture products (Johnson, 2013). The red flour beetle is the global pest. Recently, it has emerged as one of the key insect models for understanding metamorphosis, comparative evolutionary developmental biology, insect/beetle diversity, basic physiology and insect pest management research (Brown et al., 2009).

There are two pairs of stink or odoriferous glands in *Tribolium* beetles including the red flour beetle. These glands are highly specialized for synthesis and secretion of various chemical for beetle defence. One pair of these odoriferous glands is located in abdomen and a second pair in prothoracic region (Roth, 1943; Sokoloff, Ackermann and Overton, 1967; Sokoloff, 1972). Each gland consists of two main portions, a manufacturing portion and a storing portion. In the manufacturing portion, the defensive secretions are produced in the glandular cells. The storing portion is consisting of a chitinous reservoir. There are two distinct types of defensive secretions manufacturing glandular cells in *Tribolium* abdominal stink glands (Roth, 1943; Eisner et al., 1964). The type 1 cells are single cells that cover the reservoir surface. Each cell type 1 contains a large vesicle, inside which there is a cuticle-lined organelle. This organelle (consisting of a cylindrical body and head) open to an efferent tubule, which connects the vesicular organelle lumen with the reservoir (Eisner et al., 1964; Happ, 1968). The type 2 cells of stink gland of red flour beetles form lobules. Each individual cell-2 is formed by the two cells fusion of 2a and 2b. Both 2a and 2b cells contain a nucleus and a large vesicle in the middle with a cuticle lined organelle (Happ, 1968).

Quinones and hydrocarbons are the two major groups of chemical compounds present in stink glands of beetles. The main quinone derivatives noted in stink glands are 2-ethyl-*p*-benzoquionone (EBQ), 2-methyl-*p*-benzoquinone (MBQ) and hydrocarbons (Alexander and Barton, 1943; Ladisch et al., 1967; Pappas and Morrison, 1995). The major hydrocarbons present in the stink gland are 1-pentadecene and 1,6-pentadecadiene (Tschinkel, 1975; Baker et al., 1978; Howard, 1987; Luciana Villaverde, Juárez and Mijailovsky, 2007). Moreover, Li and co-researchers (2013) through GC-MS analysis of the red flour beetle stink glands reported the occurrence of *para*-benzoquinones MBQ and EBQ, 1,8-heptadecadiene, hydrocarbons 1-pentadecene, and 1-heptadecene.

Benzoquinones are volatile, highly unstable, reactive, toxic and have irritant effects (Eisner et al., 1964; Tschinkel, 1975; Blum, 1981). As benzoquinone is very toxic and reactive, it requires careful handling and detoxication systems. It is used by *Tribolium* beetles in chemical defence. It has been noted that cuticular linings of producing organelle and storing reservoir protect adults beetles from their own toxic secretions (Roth, 1943; Happ, 1968). Roth and Howland (1941) reported that exposure of juvenile beetle to high concentrations of adult beetle stink gland benzoquinones caused a premature death. Of important note, the young *Tribolium* adults do not possess the defensive secretions, indicating that defensive secretions are produced only after formation of a self-protective cuticle lining barrier (Unruhet al., 1998). Hence, if the development of adequate self-protective barrier is disturbed then the pests will harm themselves. This can lead to a better control and management of the beetle pest. There is not much data available which genes are involved in the process of self-protected synthesis of defensive compounds in the stink glands.

The sulfate conjugation system is a very important detoxification mechanism in many organisms. In several insect species, sulfate conjugation is a common mechanism for phenolic compound detoxification (Kerkut, 1985). Sulfate conjugation is considered as a primitive type of detoxification mechanism because *Peripatus*, a primitive arthropod, has been reported to detoxify phenols by phosphate and sulfate conjugation with absence of glycoside conjugation (Jordan, et al., 1970). The insect and mammalian SULTs have been documented to show similar properties especially with regard to subcellular localization, cofactor requirements, and pH optima (Capinera, 2008). The SULT presence has been noted in gut, fat body and malpighian tubules in different insects species. The insect SULT system proper function depends on Mg^{2+}, ATP, and inorganic sulfate for the sulfonation. In insects, sulfate conjugation occurs in a 3-step reaction as shown below (Abou-Donia, 2015). However, APS (adenosine-S-phosphosulfate) and (PAPS 3'-Phosphoadenosine-5'-phosphosulfate) utilization in the mechanism of insect sulfate conjugation has not been certainly found. SULTs catalyze sulfate transfer to the amino group or hydroxyl from PAPS of a number of different acceptors molecules, such as carbohydrates, peptides, lipids, xenobiotics, hormone precursors, etc. In this reaction, a sulfate ester bond is formed by SULTs by catalyzing transfer of a sulfate ($-SO_3$) from the PAPS donor to a nitrogen or oxygen of the acceptor molecule (Falany, 1997).

In vivo sulfate conjugates formed with various phenolic compounds in many insect species after treatment (Smith, 1955; Binning et al., 1967; Yang and Wilkinson, 1972a). In southern worm, researchers for the first time reported sulphoconjugation in insects at the enzymatic level. Sulphotransferase system exist in the gut tissues of southern-armyworm larvae and is active in the sulphation of α-ecdysone, *p*-nitrophenol, dehydroepiandrosterone, cholesterol, β-sitosterol, oestrone and many steroids of plant origin, insect and mammalian (Yang and Wilkinson, 1972).

Many of these steroid sulfates play pivotal role in various physiological process including the detoxication and formed as a consequence of biochemical transformations reactions. Sulfate esters of campesterol, cholesterol and β-sitosterol have been separated and recognized from the tobacco-hornworm meconium (*Manducasexta*) pupae (Hutchins and Kaplanis, 1969). These steroids are precursors of a-ecdysone. In house-flies (*Musca domestica*) convert 22,25-bisdeoxy-ecdysone into glucoside conjugates and sulfate (Thompson et al., 1972). Sulfation of both synthetic and natural chemicals biomolecules take place in all organisms from bacteria to humans. The cytosolic SULT enzyme family members regulate the xenobiotic and endogenous small molecules like hormones and neurotransmitters sulfate conjugates formation (Chapman et al., 2004; Gibbs et al., 2006; Niehrs et al., 1990; Strott, 2002). Insects have both arylsulphatases and sulphotransferases, these possible act in metabolic mechanism for the regulation of insect steroids (Yang and Wilkinson, 1972).

CHST5 (*iB_13656, Tc-011350*) gene is selected from 3rd phase of iBeetle screen. This gene caused a slightly altered morphological glands (less secretion) phenotype upon RNAi mediated knockdown in both abdominal and thoracic stink glands. Many subfamilies of SULTs have been unveiled that demonstrate a large sequence conservation and showed related catalytic activities. SULTs perform N-acetylglucosamine 6-O-sulfotransferase activity and is engaged in many biological processes including metabolic process of sulfur compound and N-acetylglucosamine (Elfasakhany et al., 2003, Uchimura et al., 1998, Fukuda et al., 2001). In summary, even though the insect's detoxification systems have not been given great attention, however, insects detoxification system is basically similar to well reported mammalian detoxification system.

ARSB (*iB_05763, Tc-015151*) caused morphologically altered glands phenotype upon RNAi mediated knockdown, where it results in colourless phenotype in both abdominal and thoracic

stink glands. A sulphatase was identified in transcriptomics data Li et al. (2013) but was not analyzed in any part of the iBeetle screen. In Transcriptomic comparisons of the red flour beetle, Li and colleagues (2013) find out that 511 genes showed differential expression between male and female, prothoracic vs abdominal, and wildtype (wt) vs *Tar* mutant beetles. One of these differential expressed genes is *ARSB*, a member of sulfatase family of enzymes that cause hydrolysis of sulfate esters. The sulfatase domain of *ARSB* protein is causing hydrolysis of sulfates in glycosaminoglycans (GAGs), the large unbranched polysaccharide in body (Yang et al., 1973). Within cells, *ARSB* is present in lysosomes, which are cell organelles that are responsible for digestion and recycling of various types of molecules. Till date, more than 130 single nucleotide mutations have been reported for *ARSB*. Each of these mutations results in *ARSB* deficiency in the body. In mammals including human, the *ARSB* deficiency lead to mucopolysaccharidosis-VI (MPS-VI). In MPS-VI, tissues and organs are progressively enlarged, scarred and inflamed (Litjens and Hopwood, 2001).

SUMF1 (*iB-09043, Tc-016314*) was identified in the second phase of the iBeetle screen. RNAi-mediated knockdown of this caused morphologically altered glands phenotype i.e., melanized glands contents phenotype in both abdominal and thoracic stink glands. *SUMF1* causes activation of sulfatases by cysteine residue oxidization to oxoalanine residue in the inactive sulfatase (Schmidt et al., 1995; Diez-Roux and Ballabio, 2005). *SUMF1* mutations result in a lysosomal disorder in which multiple sulfatase deficiency (MSD) occurs. In MSD, an impairment of sulfatases causes the accumulation of sulfolipids or GAGs, leading to early infant death. Overexpression of *SUMF1* along with sulfatases induces a great increase in the sulfatase cellular activities (Fraldi et al., 2007; Cosma et al., 2003). Sulfatases and *SUMF1* are involved in different processes such as biosynthesis of hormones, macromolecules degradation and cellular signalling modulation during development. However, it is not known whether *SUMF1* and *ARSB* play pivotal role in protected biosynthesis of benzoquinone. Sulfatases are used by some insects such as the diamondback moth, *Plutella xylostella*, to neutralize host cruciferous plant defensive system, which consists of glucosinolate-myrosinase activity, that prevent feeding of insect. The genome of this insect contains 12 sulfatases and two *SUMF1* genes (Ma et al., 2018). The analysis of moth sulfatases and *SUMF1* transcript levels via RNA-seq and qPCR showed that sulfatases 2, 3 and two glucosinolate sulfatases were mainly expressed in 3rd- and 4th-instar larvae midgut. Both *SUMF1* and moth sulfatase encoding genes are documented to be pivotal factors for the *P.*

xylostella success against cruciferous plants defensive system (Ma et al., 2018). The major reported *SUMF1* substrates are, *ARSA*, *ARSB*, *ARSE* and steroid sulfatase (STS). *SUMF1* belongs to an evolutionary highly conserved gene family that has maintained a high sequence homology in prokaryotes and eukaryotes (Sardiello et al., 2005).

From the second phase of iBeetle screen a sulfate transporter *SLC26A11* (*iB-09413, Tc-005389*) was identified. *SLC26A11* showed altered glands phenotype in RNAi-mediated knockdown. The stink glands were melanized in glands contents phenotype in both abdominal and thoracic stink glands. Different systems of sulfate transport depend on the transported sulfate metabolism. After deliver to the cell, sulfate acts as a substrate for the sulfur containing protein (Takahashi et al., 2011). Before metabolic conversion steps, cytoplasmic sulfate is sequestered to vacuoles (Buchner, 2004; Takahashi, 2010). Moreover, the sulfate uptake across the plasma membrane is also affected by sulfate transport to extracellular space. This transport occurs through some veiled passive transport systems because the membrane potentials at vacuolar lumen and extra-cellular sides are positive (Buchner, 2004; Takahashi, 2010).

The sulfate transport across and within cells is regulate by various sulfate transporter of the SLC26 transporters family (Alper and Sharma, 2013). The SLC26 gene family encodes polypeptides that have been described as anion channels and anion exchangers. There are 11 members (*SLC26A1-A11*) in this SLC26 gene family. All of this gene family members play role in different cell functions such as homeostasis and electrolyte balance inside cells (Aravind and Koonin, 2000). The SLC26 family sulfate transport mechanism is the sulfate/anion exchange system. These proteins carry out the sulfate transport in exchange for other anions, such as chloride (Cl^-), bicarbonate ($HCO3^-$) and iodide (I^-) (Mount and Romero, 2004). Once sulfate inside the cell, sulfate acts as a substrate for the sulfur containing proteins in cells. *SLC26A11* gene encodes a sodium independent sulfate transporter protein. In human, *SLC26A11* expression has been also reported in several lysosomal membrane proteome catalogs (Stewart et al., 2011), it may facilitate transport of lysosomal SO_4^{2-}(Alper and Sharma, 2013). In insect, 9 SLC26 homologues have been documented in *Drosophila melanogaster* genomic DNA (Josephs et al., 2003). Of note, it has been noted that eight paralogues structure is closely related to *SLC26A11* while structure of just one orthologue (dPrestin) show similarity to *SLC26A1* to A9, particularly to *SLC26A5* and A6. However, the mechanism of regulation of *SLC26A11* conductance and exchange activities in various subcellular

portions, different types of cells or physiological situations is still less understood.

In 1968, Happ carried out a detail histochemical analysis of *Tribolium castaneum* quinone-producing glands. The *p*-quinone is synthesized in a multi-steps process in a two-chambered secretory unit that consists of cuticular organelles, secretory cells and their associated vesicles, and afferent tubules. The benzoquinone biosynthesis occurs in cell type 2 secretory cells of stink gland. The phenolic β-glucoside, the precursors of quinone, located in the cytoplasm of cell type 2a secretory cells, is secreted into the lumen of cell type 2a vesicle. Inside vesicle, the phenolic β-glucoside is hydrolysed to quinol and glucose by a β-glucosidase and resulting glucose may enter back to cytoplasm. Subsequently, the free and nontoxic quinol is transferred to the vesicular organelles where under action of polyphenol oxidase a portion of quinol is oxidized to 1,4 quinones. The quinol and 1,4 quinone mixture are transported through the efferent duct where haemoprotein peroxidase induces oxidization of remaining quinol. This resulted in formation of highly reactive toxic *p*-quinones in the cuticle-lined reaction chamber. The *p*-quinones are produced in the head of vesicular organelle which is separated from the cytoplasm of the secretory cells (Eisner et al., 1964; Happ, 1968).

The main aim of this study is to uncover genes that participate in stink gland benzoquinone biosynthesis, sulfate conjugation and to decipher the molecular genetics mechanism of toxic benzoquinone self-protected synthesis in stink glands. Specifically, we worked on unveiling the role of genes encoding *T. castaneum CHST5*, *ARSB*, *SUMF1* and *SLC26A11* to identify these the functions if gene involvement in the protected benzoquinone biosynthesis mechanisms.

Material & Method

Candidate genes double-stranded RNA

For RNA interference (RNAi) experiments, Double-stranded RNAs (dsRNAs) were purchased (Eupheria, Dresden, Germany). The dsRNAs was diluted in injection buffer (0.3 mM KH_2PO_4, 0.7 mM Na_2HPO_4 $2H_2O$, 40 mM KCl, 10x stock: 14 mM NaCl) and kept at -20°C.

Selected genes were injected with original iBeetle template (iB) and rescreened with non-overlapping fragments (NOF). NOF is gene template independent from the iB template and was employed for the dsRNA injection to confirm that iBeetle annotated changed glandular phenotypes were not because

of injected dsRNA off-target effects. List of NOF sequence is provided (Additional file 7. Table S7).

Transcriptome Data of Stink Gland

The transcript levels of the *SUMF1*, *SLC26A11* and *ARSB* were checked in previously reported *T. castaneum* gland transcriptome data of Li et al. (2013).

Phylogenetic analysis

Phylogenetic analysis of gene families was performed using Geneious prime software (version 2019). Sequences of protein corresponding to the respective genes were obtained Blast analysis from http://bioinf.uni greifswald.de/blast/tribolium/blast.php (*Tribolium*) and NCBI (other species).and aligned in Geneious using the MUSCLE alignment (Edgar, 2004). The phylogenetic trees were constructed in PHYML (Guindon et al., 2010) and Fast-tree based (Price et al., 2009) using maximum likelihood method, with each applying the JTT substitution model (Jones et al., 1992). Bootstrap tests with 500 repeats were used for PhyML trees (Felsenstein, 1985) and 40 'rate categories per site' were used for Fast-tree (Price et al., 2009).

DNA sequences analysis

Geneious 9 was used to plan blunt end cloning and Multalin (http://multalin.toulouse.inra.fr/multalin/, Corpet, 1988) were used for sequence alignments of the selected genes. Chromas Lite 2.1.1 (Technelysium Pty Ltd) was employed for DNA sequencing analysis results and to display the chromatograms.

Primers design

Primers for all selected genes were designed through Primer 3 programme and checked in Geneious®. These primers were bought from Eurofins Genomics (Ebersberg, Germany) or IDT (Integrated DNA technologies, Germany). These primers sequence along with their *Tribolium* gene are given in the table (Additional file 8. Table S8).

Extraction of RNA from beetle tissues

Stink glands of 10 days old beetle after RNAi injection along with wt control were used for extraction of

RNA using Insect RNA Microprep kit (Zymo Research Tissue & Insect RNA Microprep™ Cat#R2030, USA) according to the manufacturer's protocol. Isolated RNA was treated with TURBO™ DNase to remove any traces of the genomic DNA contamination. The RNA concentration was determined using the NanoDrop 1000 Spectrophotometer (Thermo ScientificTM, USA) of each sample.

cDNA synthesis

1µg RNA of each sample was used for the cDNA synthesis from glands tissues of 10 days adult beetles using the SMART PCR cDNA kit (ClonTech Saint-Germain-en-Laye, France). The synthesized cDNA was diluted with deionized water to a 15 ng/µL of concentration and freeze at −20 °C until used for qPCR analysis.

Cloning

Cloning was done according to standard protocols (Green and Sambrook, 2012). PCR reaction was done in the PCR cycler Mastercycler (Eppendorf AG, Hamburg, Germany) to amplify DNA sequence. Purification of amplified DNA sequence from agarose gel was done via PCR Clean-up and NucleoSpin® Gel Kit (Macherey-Nagel, Germany), subsequently T4 DNA ligase enzyme was used (New England-Biolabs, Frankfurt, Germany) for ligation. pJET1.2/blunt vector (Thermo Fisher Scientific) was used to ligate the DNA template for synthesis of RNA probe. Transformation was carried out with DH5α *E. coli* and positive colony was verified via colony PCR. Plasmid NucleoSpin® Kit (Macherey-Nagel, Düren, Germany) was used for the isolation of plasmid DNA. Samples were sequenced from Microsynth Seqlab (Goettingen, Germany) for DNA sequencing. Geneious 9 software (http://www.geneious.com, Kearse et al., 2012) was used for all cloning procedures.

Preparation of RNA probes

Sense and antisense probes were produced from cloned cDNA templates. To prepare sense and anti-sense RNA probes for *ARSB*, *SUMF1* and *SLC26A11 in vitro* transcription reactions were prepared from Digoxegenin-UTP (DIG), Fluorescein RNA *Labelling Mix* (Roche, Germany), Biotin RNA Labelling Mix (sigma Aldrich), RNase inhibitor, T3- and T7-RNA polymerase (Roche Applied Science, Mannheim, Germany) as per instructions given in supplier protocol. A mixture of 0.1% Tween20, 50% formamide, 20 µg/ml heparin, and 5x SSC pH 4.5 was used for dissolving the RNA probes.

The dissolved probes were stored for long time at -80°C or for short-time at -20°C.

Fluorescent *in situ* hybridization

Fluorescent *in situ* hiberidization (FISH) was done according to the protocol described with a few modification mentioned below (Friedrich and Benzer, 2000; Schinko et al., 2009). For FISH on whole mount glands, around twenty abdominal and prothoracic stink glands from adult beetles were isolated on ice along with a small part of the exoskeleton and attached to 12 well-plate sylgard bottom (World Precision Instruments, Berlin, Germany) with a pin. Subsequently, phosphate-buffered saline (1x PBS) was added to gland containing wells. For fixation, the glands were put at 8°C for 2-2.5 h or at 4°C overnight in 4% of paraformaldehyde (PFA, Sigma-Aldrich® Chemie GmbH, Munich, Germany) in PBS. Glands were rinsed and washed two times in 50% methanol/PBT (0.03% TritonX-100 in 1x PBS).

The glands were incubated with proteinase K solution (0,5 µl in 500 µl PBT) for 5 min. After rinsing and washing glands in PBT for 10 min, the gland tissues were post-fixed at room temperature (RT) in 4% PFA for 30 min. Glands were again rinsed and washed for 5 min four times with PBT. Afterward, 50% pre-warmed Hyb-buffer (0.03% TritonX-100, 5x SSC pH 5.5, 50% Formamide, heparin 100 µg/ml, 100 µg/ml Yeast RNA, 100 µg/ml salmon sperm DNA) in PBT was used to wash the glands for 5 min at 60°C. In the next step, the gland tissues were incubated in Hyb-buffer at 60°C for 3 hours. To prepare working solution, RNA probes were diluted to 100 ng/ml in Hyb-buffer. Probes solution was put at 95°C for 2 min then instantly kept for 10 min on ice. Subsequently, glands were places in 1 ml probe solution (per well) and put at 60°C overnight.

On the following day, 2x SSC pre-warmed (20x stock: sodium citrate 300mM, 3M NaCl, pH 5.5 made through citric acid) was used to rinse and two times washed at 60°C for 10 min. Washing buffer (2x SSC, 0.03% TritonX-100, 50% Formamide) was put to the gland tissues and put for 45 min at 60°C. Afterwards, washing buffer-TBST 50% (0.03% TritonX-100 in TBS) was added and placed at 60°C for 10 min, then in TBST for 10 min at 65°C and at RT in TBST for 10 min. Blocking solution (1:10 in TBST, Roche Applied Science, Mannheim, Germany) was put to the gland tissues at 8°C for 3 h. In the next step, the gland tissues were incubated overnight at 8°C in streptavidin (1:200 in blocking solution) and Hoechst 33342 (1 mg/ml stock 1:1000, Sigma-Aldrich® Munich, Germany). On the morning of third day, after 4 times washing in TBST,

staining solution was added to the glands. (200 amplification diluent + 4µl tyramides; TSA® fluorescein detection kit, Cat#: NEL701A001KT, PerkinElmer, USA). Gland tissues were incubated for 90 min in the dark at RT. After incubation, the tissues were rinsed in TBST and four times washed for 10 min in TBST. Glands were put on a microscopic glass slide and applied Mowiol® 4-88 (Sigma-Aldrich GmbH, Munich, Germany) and covered with a coverslip. The slides were kept at 8°C overnight before microscopic analysis.

Immunohistochemical staining of *Tribolium* gland references

Immunohistochemical staining was carried according to the method previously reported by Baumer and colleagues with few modifications as described below (Bäumer et al., 2011). For whole mount immunohistochemical staining of glands, around twenty abdominal and prothoracic stink glands from adult beetles were taken out after dissection along with a small part of the exoskeleton and attached to 12 well-plate sylgard bottom (World Precision Instruments, Berlin, Germany) with a pin. For fixation, the glands were placed for 150 min at 8°C or 4°C for overnight in 4% PFA (Sigma-Aldrich® Chemie GmbH, Munich, Germany) in PBS. Glands were rinsed and washed three times in PBT (0.03% TritonX-100 in 1x PBS) for 20min. Gland tissues were put in 5% normal goat serum (Sigma-Aldrich® Chemie GmbH, Munich, Germany) to block unspecific binding and 1% of Fraktion V Albumin (Carl Roth GmbH, Karlsruhe, Germany) dissolved in PBST at RT for 1h. After blocking, the primary antibody (polyclonal rabbit *SUMF1*) in 1:4000 dilution in blocking buffer were added to tissues and put for incubation at 8°C overnight.

After four times washing in PBS, secondary antibody (goat Anti-rabbit) 1:1000 diluted in blocking buffer was added to the gland tissues and put for incubation at RT for 2 h. Gland tissues were washed in PBST for two times (10 min each). In the next step incubated in detection buffer (0.05 M $MgCl_2$, 0.1 M NaCl, 100 mM Tris-HCl pH 9.5) for 5 min. Gland tissue were incubated with 1:1000 Hoechst (Sigma-Aldrich® GmbH, Munich, Germany) diluted in staining solution (3.5 µl BCIP® and 4.5 µl NBT added to each ml of detection buffer) for 90min at RT in the dark. To stop staining reaction, glands were rinsed twice with PBS and PBT and again washed for 20 min in PBS. Glands were placed on Microscopic glass slide and embedded in Mowiol (Sigma-Aldrich ® GmbH, Munich, Germany) and coverved with cover slip. The slides were kept at 8°C atleast overnight before microscopic examination.

Semi-quantitative RT-qPCR Analysis

To perform real-time qPCR, a StepOnePlus™ Real-Time quantitative PCR machine (Applied Biosystems, Carlsbad, USA) was used. Each PCR reaction was done in volumes of 20 µL, consisting cDNA of 2 µL, 10 µL SybrGreen qPCR MasterMix (Applied Biosystems, Carlsbad, USA), 4 µL nuclease free water, 4 µL forward plus reverse primers. The primer sequences are provided in (Additional file 8. Table S8). Each reaction was carried in triplicate. Additionally, three technical replicates, three biological replicates, no template control and with no reverse transcriptase enzyme control were prepared and run in parallel with samples. The melting curve and primer efficiency analysis were done for all primers of internal control RPS3 gene. The normalization of gene expression was done with RPS3 housekeeping gene. The double delta Ct method (Livak and Schmittgen, 2001) was used for calculation of relative gene expression between RNAi knockdown and wt gland tissue as well as gland tissue in comparison to gut and fat body. The statistically significant difference in gene expression between two groups (wt vs knockdown or gland tissue vs gut/fat body) was determined with Student's t-test.

Gas chromatography-mass spectrometry analysis

Analysis of glands volatiles was carried out independently for prothoracic and abdominal glands of control and RNAi-mediated gene knockdown beetles through GC-MS analysis. For GC-MS analysis, three glands from adult ten days beetles were isolated and mashed in 100 µl methanol (Merck, Darmstadt, Germany). After preparation, the samples were kept in -20°C freezer until analyzed by GC-MS. The GC-MS analysis was done within 48 h. This analysis is described in detail in material and method of Chapter 1 (Lehmann et al. in preparation).

Liquid chromatography–mass spectrometry (LC-MS)

Liquid chromatography (LC) and high resolution mass spectrometry (HRMS) can be combined to separate analytes within a sample. LC separates the sample based on its physicochemical properties. Subsequently, MS is used to detect analytes based on mass to charge ratio (*m/z*). Analysis of glands metabolites was carried out independently for prothoracic and abdominal glands of both control and RNAi-mediated gene knockdown beetles through LC-MS analysis. For LC-MS analysis, ten abdominal and thoracic glands of beetles were dissected separately into 4 replicates, frozen

homogenized in liquid nitrogen. Samples were dissolved in 100 µl methanol (Thermo Fisher Scientific). Glands were crushed with a pistall and centrifuged (5 min at 14,000 rpm, 4°C). Taking the supernatant to a glass vial for analysis. Supernatants of 1 µl of the solution in positive as well as negative ionization mode were then analyzed by UPLC-DAD-ESI-TOF-MS analysis. After preparation, the samples were kept in -80°C freezer until analyzed by LC-HRMS.

Analysis of metabolite was done with a UHPLC1290 Infinity of Agilent Technologies which is paired to a HRMS device (Accurate-Mass Q-TOF 6540 UHD (quadrupole time-of-flight), Agilent Technologies) through Technology of an Agilent Dual Jet Stream that serves as source of electrospray ionization (Agilent Technologies). As a second detector, the photo diode array (PDA) detector of the UHPLC1290 Infinity (Agilent Technologies) was used for analysis. An ACQUITY HSS T3 column (Waters Corporation, particle size 2.1 × 100 mm, 1.8 µm) was employed at 40°C for chromatographic separation. A 500 µl/min flow rate was utilized. Two solvent systems, A, water, 0.1% (*v/v*) in formic acid and B, acetonitrile, 0.1% (*v/v*) in formic acid were employed to make a solvent gradient: 1% to 20% B: 0 to 3 min; 20% to 97%: B 3 to 8 min; 100% B: 8 to 12 min; % B: 12 to 15 min1. Experimental data were obtained to *m/z* 1700 from *m/z* 50 with a 4 GHz frequency of detection, a 3000 V capillary voltage, and 200 V and 100 V nozzle and fragmentor voltage. The gas set to 250°C while sheath gas to 300 °C. The setting of both drying and sheath gas was 8 l/min. Acquisition of data was carried out with the Mass Hunter Acquisition (Agilent Technologies) B.03.01 software in both negative and positive ESI mode. Information about the chemical structure of the compounds of interest were obtained by tandem-MS (LC-HRMS/MS) analysis. For the measurements 4 biological replicates of 1 independent experiments were analyzed.

Image processing

Fluorescent *in situ* hybridization and immunohistochemistry staining of glands were checked and pictures taken with a Zeiss LSM780 confocal laser microscope. For capturing photos of prothoracic and abdominal stink glands of RNAi knockdown and wt beetles, a stereomicroscope (Leica MZ16 FA) linked to a Qimaging camera was used. Adobe photoshop (CS5), Adobe Illustrator (CS5) and ImageJ software (http://rsbweb.nih.gov/ij/disclaimer.html) were used to adjust brightness/contrast of captured pictures and to draw sketches of abdominal and thoracic gland cells.

Results

Phylogenetic trees

Carbohydrate sulfotransferase 5 (*CHST5*) like Predicted protein

CHST5 best fly ortholog is dm_CG31637-(CG31637). Based on conserved domains analysis showed that its is a member of the sulfotransferase family of enzymes (Figure 1A). This fly ortholog enzyme is responsible for N-acetylglucosamine 6-O-sulfotransferase activity (Bistrup and Rosen, 2002). SULTs catalyze a reaction in which a sulfuryl group (SO3) is transferred from a donor molecule, 3'-phosphoadenosine 5'-phosphosulfate, to a number of acceptors such as hydroxy and amine substrates, producing the sulfated derivative and 3'-phosphoadenosine 5'-phosphate (Chapman et al., 2004).

Arylsulphatase B (*ARSB*)

ARSB best fly ortholog is CG7402 - (CG7402). On the Basis of conserved domains, this gene is a member of the alkaline phosphatases and sulfatases like Superfamily and predicted to have sulfuric ester hydrolase activity (Arevalo and Uribe Ardila, 2011). it belongs from AslA Superfamily (Figure 1B). *ARSB* molecular function is sulfuric ester hydrolase activity.

Sulfatase modifying factor 1 (*SUMF1*)

SUMF1 best fly ortholog is CG7049-(CG7049). Based on conserved domains, it belongs to *SUMF*-sulfatase superfamily (Figure 1C). *SUMF1* is an enzyme. Its molecular function is formylglycine-generating oxidase activity (Zito et al., 2007) and responsible for the activation of all sulphatases. BLAST analysis showed *Drosophila* homolog (CG7049) for this gene. This homolog has been characterized and reported to have formylglycine-generating oxidase activity and localize to the endoplasmic reticulum. Human ortholog(s) of this gene is *SUMF1* is implicated in mucosulfatidosis and sphingolipidosis.

Sodium independent sulfate transporter (*SLC26A11*)

SLC26A11 best fly ortholog is Esp - Epidermal stripes and patches (CG7005). Based on conserved domains it belongs to Sulfate_transp Superfamily (Figure 1D). *SLC26A11* is a transporter and its

molecular function is sulfate transmembrane transporter activity (Vincourt et al., 2003). Prestin (*SCL26a5*), another member of SLC26 family is well characterized, expressed in the malpighian tubules and gut of insects (Hirata et al., 2012).

Gland morphology and gland volatiles affected by gene knockdown

For confirmation of the stink gland phenotypes of four selected genes noted before in the genome-wide gene identified screens, dsRNA of iB and NOF of candidate genes were injected for rescreening into the San Bernardino strain. These genes phenotypes were confirmed in the rescreen, pictures of alteration in glands morpholohgy knockdown of these genes documented (Figure 2).

CHST5 RNAi-mediated knockdown experiment, this gene caused a slight morphological altered stink gland phenotype with less secretion in both abdominal and prothoracic stink glands and confirmed with NOF injecton. *ARSB* caused morphologically altered glands phenotype in RNAi mediated knockdown, where it results in colourless phenotype in both abdominal and thoracic stink glands. RNAi-mediated *SUMF1* gene disruption resulted in darker/melanized gland secretion in abdominal and thoracic stink glands in comparison to yellowish gland fluid in wt beetles glands. *SLC26A11* RNAi-mediated knockdown caused altered melanized phenotype in both abdominal and thoracic stink glands. In the rescreen of RNAi mediated knockdown of *CHST5, ARSB, SUMF1* and *SLC26A11* phenotype were same like previous screen (Figure 2A).

Confirmation analysis

GC-MS analysis was carried out on RNAi mediated knockdown gland content with iBeetle fragment and nonoverlapping fragments on ten days old beetles. This analysis was done on three prothoracic and three abdominal glands, separately. The control samples were the gland content of wt beetle injected with buffer. In order to see whether the GC-MS analysis is gender specific for these genes, GC-MS was also performed on gland contents of male and female RNAi mediated knockdown and wild type beetles (Table 1). Levels of each chemical in gland contents was determined as percentage with respect to wt levels . For calculation, wt level of each chemical was considered as 100% percent increase and decrease of respective chemical was determined in knockdown situations in comparison to wild type. The four most abundantly expressed volatile

substances in GC-MS analysis of wild type beetles abdominal glands are EBQ, MBQ, 1-heptadecene and 1-pentadecene (Additional file 1. Figure S1).

In GC-MS analysis of gland content volatiles of *CHST5* RNAi-mediated knockdown slightly reduces level of MBQ, EBQ and alkenes was observed. In case of *ARSB* disrupted beetles gland content volatiles showed that the two quinonoids, MBQ and EBQ are not present in GC-MS analysis. Additionally, GC-MS data of gland volatiles contents showed that *SUMF1* silencing resulted in great reduction of MBQ and EBQ in gland secretions. While in case of *SLC26A11* knockdown resulted in highly reduction of the two benzoquinone compounds, EBQ and MBQ in gland content volatiles secretions in GC-MS analysis (Additional file 1. Figure S1). RNAi knockdown of *SUMF1* and *SLC26A11* benzoquinone levels were less than 10% as compared to wild type (Table 1). RNAi knockdown of all these genes in both male and female showed almost same results, it is showing that this gender independent (data not shown).

Expression analysis of the four sulfate metabolism gene

A: Stink gland Transcriptome data

To uncover the genes that are important for gland activity, four genes were picked were for RNAi-mediated silencing experiments on the basis of their documented molecular function. The respective dataset and read counts are given in the (Figure 3 (A), Table 2 (B).

To uncover candidates that are important for gland activity, four genes were picked for RT-qPCR experiments on the basis of their transcriptomic data and molecular function.

B: RT-qPCR

The expression profiles of *CHST5*, *ARSB*, *SUMF1* and *SLC26A11*mRNAs were checked and compared in the adult wt beetle gut, fat body and gland tissues by real time qPCR (Figure 4). *CHST5* highly expressed in gut and fat body and significantly higher than in gland tissue (Figure 4A). As compared to gut and fat tissue, *ARSB* mRNA abundance was significantly higher in gland tissue. (Figure 4B). *SUMF1* transcript abundance was also statistically significantly higher in gland tissue than in gut and fat body (Figure 4C). There was a statistically noteworthy increase in gland tissue *SLC26A11* mRNA expression levels in comparison to fat body and gut transcript abundance.

Moreover, the transcript abundance of *SLC26A11* was also significantly higher in fat body as compared to gut tissue (Figure 4D). In contrast altogether it was statistically higher expressed in gland tissue verses gut and fat body, while in *ARSB* extremely highly expressed in glands.

As *CHST5* mRNA level is not present in glands so we have not done further analysis for this gene. Three genes *ARSB*, *SUMF1* and *SLC26A11* which are highly expressed in glands were selected for further analysis. These genes were chosen for further detail analysis.

In situ hybridization of stink glands

To check the exact expression pattern of two gland specially expressed genes (*SUMF1* and *SLC26A11*), FISH staining was carried out on stink gland tissues of the red flour beetles. The TSA fluorescence kit was used in FISH. The FISH staining of these genes *SUMF1*, and *SLC26A11* with clear expression pattern in glands is shown in Figure 5. Moreover, FISH method was carried out in parallel on stink gland of candidate genes RNAi-mediated knockdown beetles. In FISH staining, these selected genes showed signals in both abdominal and thoracic stink glands of beetles. The *SUMF1* and *SLC26A11* signals were observed on the surrounding of the cell type 2b vesicle of both abdomen and prothoracic glands (Figure 5A1, A2, C1, C2). The *SUMF1* signals were also noted on surrounding of vesicle of cell type 2b. In *SLC26A11* and *SUMF1* RNAi knockdown, no signals were detected in cell type 2b in both abdominal and prothoracic glands (Figure 5B1,B2, B3, B4). While in case of *ARSB* it is already mentioned in Li et al. 2013 that *ARSB* FISH staining showed signal pattern in the cell type 2. Its signal was observed in the surrounding of vesicle of cell type 2a and 2b.

Immunohistochemical detection of *SUMF1*/*FGE* protein

Immunohistochemical staining was carried out on the dissected glands of 10 days old adult *Tribolium* beetle for detection of *SUMF1* in both abdominal and prothoracic glands Immunohistochemistry was done for determination of protein expression site in subcellular structure of gland cells. Rabbit anti-human *SUMF1* polyclonal antibody was kindly given by Professor Thomas Dierks group, Bielefeld University, Germany. Besides human, this antibody also cross-react with mouse (not checked in other species) *SUMF1* (Schlotawa et al., 2011). As

SUMF1 is highly conserved from human to bacteria, and it is tested to see cross relatives. This anti-serum also cross-reacts with purified bacterial *SUMF1* (which share less than 50% homology).

As the *SUMF1* antibody is polyclonal and raised against the whole protein, therefore this antibody was used to stain beetle *SUMF1*. Strong *SUMF1* signals above background were observed in cell-type 2b of both abdominal and prothoracic glands of adult wild type beetles. Its expression was on surrounding of vesicle and vesicular membranes of 2b cell type also confirmed *in situ* expression pattern. No signals of *SUMF1* was observed in abdominal and prothoracic glands of knockdown beetles. Of note, no signals of *SUMF1* was observed in cell type 1 of abdominal stink glands, indicating that *SUMF1* expression and activity are occurring only in cell type 2 (Additional file 2. Figure S2).

Liquid chromatography–mass spectrometry (LC-MS) of stink gland

So far no sulphonated compounds had been detected in the glands, which could have been for two reasons, a) these compounds are precursors that are only in small amounts in the glands as they are metabolized rapidly, b)so far mostly GC-MS was used for analysing gland content, which only allows for detecting volatiles and sulphonated substances are unlikely to be volatiles. Thus to examine wether sulphonated precursurs could be involved in quinone synthesis, we used liquid chromatography mass-spectrometry on the knockdown of the three glands specificially expressed genes to see whether missing of these genes could lead to the detection of such substances.

RT-qPCR in knockdown situation

Before perfoming LC-MS first we compared the relative levels of *ARSB, SUMF1* and *SLC26A11* mRNA profiles in wild type (wt) and RNAi mediated knockdown beetle glandular tissue (Figure 6) in RT-qPCR. In *ARSB* highly significantly decreased or almost no expression of this gene mRNA relative to RSP3 was observed in RNAi mediated knockdown beetle gland tissues as compared to wt control beetles. While relative levels of *SUMF1 and SLC26A11* in wt and RNAi mediated knockdown beetle glandular tissue demonstrated a significant decreased in expression of its relative mRNA in RNAi mediated knockdown beetle gland tissues as compared to wt control beetles. A significantly decreased expression of all three genes mRNA relative to RSP3 was observed in RNAi mediated knockdown beetle gland tissues as compared to wild type control beetles.

Liquid chromatography (LC) was coupled to two detectors, a photo diode array (PDA) and high resolution mass spectrometer (HRMS). For the analysis prothoracic and abdominal glands of ten day old beetles were isolated and the gland content extracted with methanol. Subsequently, the samples were analyzed by LC- PDA HRMS analysis. As an appropriate control sample, the gland content of wt beetle that were injected with dsRNA of red fluorescent protein (*DsRed*) of *Discosoma sp* was used to ensure that the changes were independent of dsRNA injection. Data obtained by the UV/VIS analysis in the range of 190 – 600 nm were used to search for changes in the abundance of dominant gland compounds in wt and mutant lines and to obtain first insights into the chemical structure by checking the UV/VIS spectra. The in-line HRMS analysis via accurate mass measurement and tandem HRMS (HRMSMS) allowed structure elucidation for a part of the signals. The total wavelength chromatograms (TWC) of the wt abdominal gland is shown in (Figure 6). In case of wt situation, five major signals (1 - 5) were observed. Compound 3 and 4 were later on identified as 2-methyl benzoquinone (MBQ) as well as 2-ethyl benzoquinone (EBQ), respectively. The identities of the compounds 1, 2 and 5 have not been solved so far (Additional file 4. Figure S4). In addition, we calculated the compound area of the seven signals from the total wavelength chromatograms to obtain data for relative abundance. Compound area can only be used to compare the relative abundance of one compound (or two compounds with the same UV/Vis maxima) between the lines (Figure 6).

In the *ARSB* knockdown compound 1, 2 and 5 as well as MBQ and EBQ were not detectable in the TWC. However, two novel compound 6 and 7 were showed up which subsequently identified as 2-methyl-4-hydroxyphenyl glycosylsulfate (MHP-$GlcSO_4$)and 2-ethyl-4-hydroxyphenyl glycosylsulfate (EHP-$GlcSO_4$), respectively (Additional file 6. Figure S6). Abdominal glands of the *SUMF1* which is necessary for *ARSB* activation, showed in RNAi mediated knockdown reduced signals for compound 1 and 2 and no signal for MBQ, EBQ and compound 5, but showed also the two new signals for (MHP-$GlcSO_4$) and 2-ethyl-4-hydroxyphenyl glycosylsulfate (EHP-$GlcSO_4$). In the abdominal glands of the mutant beetle *SCL26A11* also only small signals remained for compounds 1 and 2, while signals for MBQ, EBQ and compound 5 were barely detectable. However, for the two new compounds (MHP-$GlcSO_4$)and 2-ethyl-4-hydroxyphenyl glycosylsulfate (EHP-$GlcSO_4$) no peaks could be detectable. Mainly the same pattern was obtained in the TWC of wt prothoracic glands and glands RNAi of mediated knockdown beetles for *ARSB*, *SUMF1* and *SLC26A11* (Figure 6, Additional file 4. Figure S4).

Since *ARSB* encodes a sulphatase and *SUMF1* sulfatsase activating enzyme, the expectation was that the substrate of this sulfatase, which should at the same time present the precursors of the quinones, accumulates in the glands, which could explain the two intense signals in the knockdown situation of these two genes (Figure 6). The UV spectra for compound 1-7 are shown in (Additional file 5. Figure S5). Compound 1, 2, 6 and 7 show comparable spectra with three maxima and similar intensity. Compound 1, 2 have absorption maxima at about 200 nm, 220 nm and 282-290 nm, while compound 6 and 7 show maxima at about 194nm, 214nm, 283 and 195 nm, 216 nm, 283nm respectively. MQB and EQB have a massive maximum at 250 nm and a much smaller one 325 nm. Only compound 5 shows a unique UV spectrum with three maxima at 220 nm, 280 nm and 315 nm.

Structure elucidation for the so far not described compounds 6 und 7 was done via LC-HRMS, analysing a extract of abdominal glands of RNAi mediated *ARSB* knockdown beetles (Additional file. 6. Figure SA). Total ion chromatogram in the negative ionisation mode with two dominant signals showed for compound 6 and 7 at 2.38 min und 3.15 min retention time, respectively. In addition, the respective mass spectra for both compounds are shown. Compound 6 is represented by the ion $[M-H]^-$ 365.064 and compound 7 by $[M-H]^-$ 379.0799, respectively (Additional file 6. Figure S6 B, C). Sum formula for compound 6 ($C_{13}H_{18}O_{10}S$) and compound 7 ($C_{14}H_{20}O_{10}S$) could be deduced from the accurate mass information and the isotopologue pattern. To obtain more detailed information about the structure of both compounds fragmentation analysis by high resolution tandem MS (HRMSMS) was done. For both compounds a strong fragment of m/z 96.959 was found, which represents a sulfate moiety (HSO_4^-). A second joint fragment is detectable at m/z 241.0017. It fits to a hexosyl sulfate moiety. Finally very tiny signal of m/z 285.097 and m/z 299.1136 hint to a 2-methyl-4-hydroxyphenyl glycosyl fragment and a 2-ethyl-4-hydroxyphenyl glycosyl fragment, respectively (Additional file 6. Figure S6 D, E, F, G). The interpretation of all fragments obtained proviide strong evidence, that compound 6 is 2-methyl-4-hydroxyphenyl glycosylsulfate and compound 7 is 2-ethyl-4-hydroxyphenyl glycosylsulfate, respectively. The compounds 6 and 7 with the accurate mass of 365.0640 Da (2.8 min) and 379.0799 Da (3.149 min) seems therefore to be the sulfated glucosylated phenolic precursors of ethyl- and methyl benzoquinone (Additional file 6. Figure S6 D, E).

Discussion

The stink glands secretion of adult beetle is rich in benzoquinones. Benzoquinones are volatile, highly unstable reactive and toxic compounds (Eisner et al., 1964; Tschinkel, 1975; Blum, 1981; Howard, 1987). In order to protect from the auto intoxicative effects of benzoquinone and other defence compounds, *Tribolium* beetles have evolved a number of mechanisms for self protection. This is achieved by the partition of the defensive secretion from other adjacent cell body. The defensive secretions are produced in organelles which are lined by cuticle and are stored in reservoirs which arise from cuticle invaginations (Roth, 1943; Happ, 1968). However, the molecular mechanisms of benzoquinone biosynthesis and self-protection synthesis are still poorly understood.

As it is well-known that BQs in the stink gland of red flour beetles are formed from phenolic glucosides precursors (Happ, 1968). Based on expression pattern *CHST5* might be involved in sulfonation of these sulfated glucosilated phenolic precursors in the gut and fat body. These observation supports the idea that the sulfotransferase catalyzes the sulfate conjugation in the gut and fat body to produce the precursors for the benzoquinone production in the stink glands of the red flour beetle.

ARSB is a member of arylsulfatase group of enzymes that are mainly located in the in lysosomes of the various tissues and secreted. In *in situ* hybridization studies, *ARSB* signals detected by Li et al. 2013 in the surrounding of vesicle cells type 2a and 2b of the adult stink gland tissue (Li et al., 2013). *ARSB* responds major sulfatase required for benzoquinones synthesis for activating detoxified precursors expressed in cell type 2a and 2b and serected to the organelle. In LC-MS analysis showed the presence of high signal peaks of sulfated precursors that are 2-methyl-4-hydroxyphenyl glycosylsulfate and 2-ethyl-4-hydroxyphenyl glycosylsulfate were observed in *ARSB* RNAi mediated knockdown situation which was absent in wild type beetle gland (Figure 6). Taken together, these data identified *ARSB* essential role in biosynthesis of benzoquinone in the red flour beetle stink glands. It is possibly involved in catalysing the reaction in which the sulfated glycosylated phenolic precursors are converted to sulfate and glycosylated phenol prior to the lost oxidation reaction in which *p*-diphenolic precursors are processed to *p*-benzoquinones according to Happ proposed model (1968).

Sulfate modifying factor 1 (*SUMF1*) *Tc_016314*

Keeping in view the role of *Drosophila* and human formylglycine-generating enzyme (*SUMF1*), one can hypothesize that *Tribolium SUMF1* is essential for sulfatase activity (Zito et al., 2007). In *in-situ* hybridization, strong signal of *SUMF1* expression was noted in adult stink gland tissue of beetle. Importantly, signals of *SUMF1* were detected in cells type 2b of both prothoracic and abdominal glands (Happ, 1968). Staining of gland tissue via immunohistochemistry demonstrated the presence of active *SUMF1* protein in cuticular organelle of cells 2b which links the cell and the gland reservoir through a tubule (as shown in Figure 5). Sulfatase activated only in oraganelle part 2b. In LC-MS analysis showed the presence of sulfated precursors ie., 2-methyl-4-hydroxyphenyl glycosylsulfate and 2-ethyl-4-hydroxyphenyl glycosylsulfate in *SUMF1* RNAi knockdown situation. Put together, the activities of *SUMF1* and *ARSB* are pivotal in biosynthesis of benzoquinone prior to the final diphenolic precursors oxidation step in which these change to *p*-benzoquinones in the secretory cells type 2 cuticular organelle, as has been described by Happ (1968).

Sodium independent sulfate transporter (*SLC26A11*) *Tc-005389*

SLC26A11 is a sulfate anion transporter and works independent of sodium (Alper and Sharma, 2013). *SLC2611* is a solute carrier family 26 (SLC26) member, which consists of anion channel and multifunctional anion exchangers (Mount and Romero, 2004). The *SLC26A11* and other members of *SLC26* family are involved in the transport of sulfate ion/anion exchange across the plasma membrane (Mount and Romero, 2004; Ohana et al., 2011; Alper and Sharma, 2013).

In *in situ* hybridization, *SLC26A11* expression was noted in stink gland tissue of adult beetle (Figure 5). Transcripts of *SLC26A11* were observed in both prothoracic and abdominal glands in cells-2b which is reported to be responsible for production of the benzoquinone (Happ, 1968). The sulfate transporter seemd to be essential to keep the biosynthesis of benzoquinones going. By the metabolism of the sulphnated precursors sulfate is produce, that needs to be removed to keep the reaction going and not to cause a product inhibition. Therefore it seems necrsary to transport the sulfate away from the cuticle line organelle. In LC-MS analysis of gland contents of RNAi mediated knockdown of *SLC26A11* only the presence of the two sulfated precursors that is 2-methyl-4-hydroxyphenyl glycosylsulfate and 2-ethyl-4-hydroxyphenyl glycosylsulfate was not observed. Only less amount was present because of incomplete knockdown, the reason for that would be that knockdown was not complete or that the reaction could still go on to some degree

as the sulfatase can work in principle (Figure 6). These data identified *SLC26A11* as the sulfate transporter which transports sulfate outside of the gland to keep the balance. Therefore, it may act as a transporter of sulfate group outside the cell in the benzoquinone biosynthesis pathway in the red flour beetle stink glands (1968).

Revised model for benzoquinone biosynthesis in *Tribolium* odoriferous glands

In 1968, Happ proposed a model for production of benzoquinone in *Tribolium castaneum* stink gland on the basis of various enzymatic and chemical tests on gland tissue and defensive secretion. This is the most widely acceptable model and is valid till today. According to this model, production of benzoquinone occurs inside a vesicular organelle in type 2a and 2b cells. The vesicular organelle is cuticle-lined, hence, serves as a safe, protected and sealed off organelle for production of toxic and highly reactive benzoquinones.

A number of different enzymes, such as glucosidase, phenoloxidase and transporters are proposed to participate in benzoquinone synthesis pathway. These enzymes include a phenoloxidase that catalyses the phenolic precursor oxidation to benzoquinone. In our group, a previous study carried out by Sabrina Lehman uncovered that the phenoloxidase catalysing the *p*-diphenols oxidation to *p*-benzoquinones in odoriferous glands of *Tribolium* is encoded by *Lac2*.

Our study show an important role of *CHST5*, *ARSB, SUMF1* and *SLC26A11* in the benzoquinone synthesis. *CHST5* caused sulfonation of potentially toxic compounds, *SUMF1* is essential for sulfatase activation and *ARSB* processed the sulfated glycosylated phenolic precursors.

There we shown that in the *Tribolium* odoriferous gland secretion, benzoquinones are synthesized from sulfated glycosylated phenolic precursors (Figure 7). First of all, *CHST5* is responsible for conversion of toxic compounds (phenol) into sulfate conjugated compounds (sulfated glycosylated phenolic precursors) in the gut and the fat body. Then sulfated glycosylated phenolic precursors enter into gland tissue type 2a cells. After that three genes *ARSB, SUMF1* and *SLC26A11* might be participating in the desulfonation of these sulfated glycosylated phenolic precursors for the benzoquinones in the cell type 2 of gland tissue.

SUMF1 is responsible for the activation of all sulfates. *SUMF1* activates *ARSB* and after this activation *ARSB* acts on the sulfated glycosylated phenolic precursors of ethyl and methyl benzoquinone in the

presence of water and convert these to glycosylated phenol and sulfate, which actively needs to be transported away from the reaction chamber by the action of *SLC26A11*.

The tentative model demonstrating the pathway of *CHST5, SUMF1*, *ARSB* and *SCLC26A11* role in biosynthesis of BQ is given in Figure 7 and will be solved in thos cuticle linned organ. Expression of *SUMF1 and SLC26A11* is noted in the surrounding of vesicle cell type 2b in the FISH analysis. There is an N-terminal signal peptide in the protein structure of *SUMF1.* Inside the ER this signal peptide targets *SUMF1* for co-translational translocation. Then *SUMF1* protein is packed in vesicles. From the ER, the protein is transported to the *cis*-Golgi, then passes through a number of sections of the Golgi-apparatus. Finally, *SUMF1* arrives at the *trans*-Golgi. Subsequently, these enters to secretory vesicle from Golgi apparatus. *ARSB* passed via the membrane of the vesicle of cell type 2a and 2b cell. The *ARSB* protein enters the cuticle-lined vesicular organelle is activated by *SUMF1* and acts on sulfated precursors by removing the sulfate group. This sulfate group is then transported from the cell type 2-vesicle to the outside through *SLC26A11*. Glucosidase will act on glycosylated phenolic precursors of ethyl- and methyl benzoquinone and remove the glucose group. Then diphenol is converted into benzoquinone through the phenoloxidase (*Lac2*) catalysing the *p*-diphenols oxidation to *p*- benzoquinones in odoriferous glands of *Tribolium* (Figure 7). The synthesized benzoquinone passes to the gland reservoir through a canal.

Conclusions

Sulfate conjugation is used by many insects for detoxification of phenolic compound. However, sulfate role in stink gland was not studied previously. We identified the role of candidate genes via RNAi-mediated gene knockdowns, qPCR, GC-MS, LC-MS and *in situ* hybridization. Presence of sulfate precursors of benzoquinone through LC-MS analysis was noted *CHST5* is involved in the sulfonation of toxic compounds while *ARSB*, *SUMF1* and *SLC26A11* play a role specifically in benzoquinone biosynthesis in red flour beetle stink glands.

References

Abou-Donia, M. (2015) *Mammalian Toxicology*. John Wiley & Sons.

Alexander, P. and Barton, D. H. R. (1943) 'The excretion of ethylquinone by the flour beetle', *Biochemical Journal*, 37(4), pp. 463–465.

Alper, S. L. and Sharma, A. K. (2013) 'The SLC26 gene family of anion transporters and channels', *Molecular Aspects of Medicine*, 34(2), pp. 494–515. doi: 10.1016/j.mam.2012.07.009.

Aravind, L. and Koonin, E. V. (2000) 'The STAS domain — a link between anion transporters and antisigma-factor antagonists', *Current Biology*, 10(2), pp. R53–R55. doi: 10.1016/S0960-9822(00)00335-3.

Arevalo, I. and Uribe Ardila, A. (2011) 'Metachromatic Leukodystrophy detection in a Colombian population of high risk assesment by leukocyte Arylsulfatase A.', in.

Baker, J. E. *et al.* (1978) 'Cuticular hydrocarbons of Tribolium castaneum: Effects of the food additive tricalcium phosphate', *Insect Biochemistry*, 8(3), pp. 159–167. doi: 10.1016/0020-1790(78)90068-9.

Bäumer, D. *et al.* (2011) 'JAK-STAT signalling is required throughout telotrophic oogenesis and short-germ embryogenesis of the beetle Tribolium', *Developmental Biology*, 350(1), pp. 169–182. doi: 10.1016/j.ydbio.2010.10.020.

Binning, A. *et al.* (1967) 'The conjugation of phenols with phosphate in grass grubs and flies', *Biochemical Journal*, 103(1), pp. 42–48.

Bistrup, A. and Rosen, S. (2002) 'High Endothelial Cell N-Acetylglucosamine 6-O-Sulfotransferase', in, pp. 439–444. doi: 10.1007/978-4-431-67877-9_63.

Blum, M. S. (1981) 'Chemical defenses of arthropods.', *Chemical defenses of arthropods.* Available at: https://www.cabdirect.org/cabdirect/abstract/19820594729 (Accessed: 19 January 2020).

Brown, S. J. *et al.* (2009) 'The Red Flour Beetle, Tribolium castaneum (Coleoptera): A Model for Studies of Development and Pest Biology', *Cold Spring Harbor Protocols*, 2009(8), p. pdb.emo126. doi: 10.1101/pdb.emo126.

Buchner, P. (2004) 'Plant sulphate transporters: co-ordination of uptake, intracellular and long-distance transport', *Journal of Experimental Botany*, 55(404), pp. 1765–1773. doi: 10.1093/jxb/erh206.

Capinera, J. L. (2008) *Encyclopedia of Entomology*. Springer Science & Business Media.

Chapman, A. (2009) *Numbers of Living Species in Australia and the World 2nd edn.*

Chapman, E. *et al.* (2004) 'Sulfotransferases: Structure, Mechanism, Biological Activity, Inhibition, and Synthetic Utility', *Angewandte Chemie International Edition*, 43(27), pp. 3526–3548. doi: 10.1002/anie.200300631.

Cosma, M. P. *et al.* (2003) 'The multiple sulfatase deficiency gene encodes an essential and limiting factor for the activity of sulfatases', *Cell*, 113(4), pp. 445–456. doi: 10.1016/s0092-8674(03)00348-9.

Crowson, R. A. (1960) 'The Phylogeny of Coleoptera', *Annual Review of Entomology*, 5(1), pp. 111–134. doi: 10.1146/annurev.en.05.010160.000551.

Diez-Roux, G. and Ballabio, A. (2005) 'Sulfatases and human disease', *Annual Review of Genomics and Human Genetics*, 6, pp. 355–379. doi: 10.1146/annurev.genom.6.080604.162334.

Edgar, R. C. (2004) 'MUSCLE: multiple sequence alignment with high accuracy and high throughput', *Nucleic Acids Research*, 32(5), pp. 1792–1797. doi: 10.1093/nar/gkh340.

Eisner, T., McHenry, F. and Salpeter, M. M. (1964) 'Defense mechanisms of arthropods. XV. Morphology of the quinone-producing glands of a tenebrionid beetle (ELEODES longicollis lec.)', *Journal of Morphology*, 115(3), pp. 355–399. doi: 10.1002/jmor.1051150304.

Elfasakhany, F. *et al.* (2003) 'N-Acetylglucosamine-6-O-sulfotransferase-1: Production in the Baculovirus system and its applications to the synthesis of a sulfated oligosaccharide and to the modification of oligosaccharides in fibrinogen', *Journal of biochemistry*, 133, pp. 287–93. doi: 10.1093/jb/mvg039.

Falany, C. N. (1997) 'Enzymology of human cytosolic sulfotransferases', *FASEB journal: official publication of the Federation of American Societies for Experimental Biology*, 11(4), pp. 206–216. doi: 10.1096/fasebj.11.4.9068609.

Felsenstein, J. (1985) 'Confidence Limits on Phylogenies: An Approach Using the Bootstrap', *Evolution*, 39(4), pp. 783–791. doi: 10.2307/2408678.

Fraldi, A. *et al.* (2007) 'SUMF1 enhances sulfatase activities in vivo in five sulfatase deficiencies', *Biochemical Journal*, 403(Pt 2), pp. 305–312. doi: 10.1042/BJ20061783.

Friedrich, M. and Benzer, S. (2000) 'Divergent decapentaplegic expression patterns in compound eye development and the evolution of insect metamorphosis', *The Journal of Experimental Zoology*, 288(1), pp. 39–55. doi: 10.1002/(sici)1097-010x(20000415)288:1<39::aid-jez5>3.0.co;2-t.

Fukuda, M. *et al.* (2001) 'Carbohydrate-modifying sulfotransferases: structure, function, and pathophysiology', *The Journal of Biological Chemistry*, 276(51), pp. 47747–47750. doi: 10.1074/jbc.R100049200.

Gibbs, T. T., Russek, S. J. and Farb, D. H. (2006) 'Sulfated steroids as endogenous neuromodulators', *Pharmacology Biochemistry and Behavior*, 84(4), pp. 555–567. doi: 10.1016/j.pbb.2006.07.031.

Grove, S. J. and Stork, N. E. (2000) 'An inordinate fondness for beetles', *Invertebrate Systematics*, 14(6), pp. 733–739. doi: 10.1071/it00023.

Green, M. R. and Sambrook, J. (2012) *Molecular Cloning: A Laboratory Manual*. Cold Spring Harbor Laboratory Press.

Guindon, S. *et al.* (2010) 'New Algorithms and Methods to Estimate Maximum-Likelihood Phylogenies: Assessing the Performance of PhyML 3.0', *Systematic Biology*, 59(3), pp. 307–321. doi: 10.1093/sysbio/syq010.

Happ, G. M. (1968) 'Quinone and hydrocarbon production in the defensive glands of Eleodes longicollis and Tribolium castaneum (Coleoptera, Tenebrionidae)', *Journal of Insect Physiology*, 14(12), pp. 1821–1837. doi: 10.1016/0022-1910(68)90214-X.

Hirata, T. *et al.* (2012) 'Ion and solute transport by Prestin in Drosophila and Anopheles', *Journal of Insect Physiology*, 58(4), pp. 563–569. doi: 10.1016/j.jinsphys.2012.01.009.

Howard, R. W. (1987) 'Chemosystematic Studies of the Triboliini (Coleoptera: Tenebrionidae): Phylogenetic Inferences from the Defensive Chemicals of Eight Tribolium spp., Palorus ratzeburgi (Wissmann), and Latheticus oryzae Waterhouse', *Annals of the Entomological Society of America*, 80(3), pp. 398–405. doi: 10.1093/aesa/80.3.398.

Hutchins, R. F. N. and Kaplanis, J. N. (1969) 'STEROL SULFATES I~ A~ //~SECT', *ST ER O ID S*, p. 10.

Johnson, J. (2013) '4 - Pest control in postharvest nuts', in Harris, L. J. (ed.) *Improving the Safety and Quality of Nuts*. Woodhead Publishing (Woodhead Publishing Series in Food Science, Technology and Nutrition), pp. 56–87. doi: 10.1533/9780857097484.1.56.

Jones, D. T., Taylor, W. R. and Thornton, J. M. (1992) 'The rapid generation of mutation data matrices from protein sequences', *Bioinformatics*, 8(3), pp. 275–282. doi: 10.1093/bioinformatics/8.3.275.

Jordan, T. W., McNaught, R. W. and Smith, J. N. (1970) 'Detoxications in peripatus. Sulphate, phosphate and histidine conjugations', *Biochemical Journal*, 118(1), pp. 1–8.

Josephs, R. A. *et al.* (2003) 'Status, testosterone, and human intellectual performance: stereotype threat as status concern', *Psychological Science*, 14(2), pp. 158–163. doi: 10.1111/1467-9280.t01-1-01435.

Kearse, M. *et al.* (2012) 'Geneious Basic: An Integrated and Extendable Desktop Software Platform for the Organization and Analysis of Sequence Data', *Bioinformatics (Oxford, England)*, 28, pp. 1647–9. doi: 10.1093/bioinformatics/bts199.

Kerkut, G. A. (1985) *Insect Control: Volume 12*. Elsevier.

Ladisch, R. K., Ladisch, S. K. and Howe, P. M. (1967) 'Quinoid Secretions in Grain and Flour Beetles', *Nature*, 215(5104), pp. 939–940. doi: 10.1038/215939a0.

Li, J. *et al.* (2013) 'Odoriferous Defensive Stink Gland Transcriptome to Identify Novel Genes Necessary for Quinone Synthesis in the Red Flour Beetle, Tribolium castaneum', *PLoS Genetics*, 9(7). doi: 10.1371/journal.pgen.1003596.

Litjens, T. and Hopwood, J. J. (2001) 'Mucopolysaccharidosis type VI: Structural and clinical implications of mutations in N-acetylgalactosamine-4-sulfatase', *Human Mutation*, 18(4), pp. 282–295. doi: 10.1002/humu.1190.

Livak, K. J. and Schmittgen, T. D. (2001) 'Analysis of Relative Gene Expression Data Using Real-Time Quantitative PCR and the 2−ΔΔCT Method', *Methods*, 25(4), pp. 402–408. doi: 10.1006/meth.2001.1262.

Luciana Villaverde, M., Juárez, M. P. and Mijailovsky, S. (2007) 'Detection of Tribolium castaneum (Herbst) volatile defensive secretions by solid phase microextraction–capillary gas chromatography (SPME-CGC)', *Journal of Stored Products Research - J STORED PROD RES*, 43, pp. 540–545. doi: 10.1016/j.jspr.2007.03.003.

Ma, X.-L. *et al.* (2018) 'Structure and expression of sulfatase and sulfatase modifying factor genes in the diamondback moth, Plutella xylostella', *Insect Science*, 25(6), pp. 946–958. doi: 10.1111/1744-7917.12487.

Mount, D. B. and Romero, M. F. (2004) 'The SLC26 gene family of multifunctional anion exchangers', *Pflugers Archiv: European Journal of Physiology*, 447(5), pp. 710–721. doi: 10.1007/s00424-003-1090-3.

Niehrs, C. *et al.* (1990) 'Conversion of recombinant hirudin to the natural form by in vitro tyrosine sulfation. Differential substrate specificities of leech and bovine tyrosylprotein sulfotransferases.', *Journal of Biological Chemistry*, 265(16), pp. 9314–9318.

Ohana, E. *et al.* (2011) 'Determinants of coupled transport and uncoupled current by the electrogenic SLC26 transporters', *The Journal of General Physiology*, 137(2), pp. 239–251. doi: 10.1085/jgp.201010531.

Pappas, P. W. and Morrison, S. E. (1995) 'Benzoquinones of the beetles, Tribolium castaneum and Tribolium confusum', *Preparative Biochemistry*, 25(3), pp. 155–168. doi: 10.1080/10826069508010117.

Price, M. N., Dehal, P. S. and Arkin, A. P. (2009) 'FastTree: Computing Large Minimum Evolution Trees with Profiles instead of a Distance Matrix', *Molecular Biology and Evolution*, 26(7), pp. 1641–1650. doi: 10.1093/molbev/msp077.

Roth, L. M. and Howland, R. B. (1941) 'Studies on the Gaseous Secretion of Tribolium Confusum Duval I. Abnormalities Produced in Tribolium Confusum Duval by Exposure to a Secretion given off by the Adults', *Annals of the Entomological Society of America*, 34(1), pp. 151–175. doi: 10.1093/aesa/34.1.151.

Roth, L. M. (1943) 'Studies on the Gaseous Secretion of Tribolium Confusum Duval II. the Odoriferous Glands of Tribolium Confusum', *Annals of the Entomological Society of America*, 36(3), pp. 397–424. doi: 10.1093/aesa/36.3.397.

Sardiello, M. *et al.* (2005) 'Sulfatases and sulfatase modifying factors: an exclusive and promiscuous relationship', *Human Molecular Genetics*, 14(21), pp. 3203–3217. doi: 10.1093/hmg/ddi351.

Schinko, J. *et al.* (2009) 'Single and Double Whole-Mount In Situ Hybridization in Red Flour Beetle (Tribolium) Embryos', *Cold Spring Harbor Protocols*, 2009(8), p. pdb.prot5258. doi: 10.1101/pdb.prot5258.

Schlotawa, L. *et al.* (2011) 'SUMF1 mutations affecting stability and activity of formylglycine generating enzyme predict clinical outcome in multiple sulfatase deficiency', *European journal of human genetics: EJHG*, 19(3), pp. 253–261. doi: 10.1038/ejhg.2010.219.

Schmidt, B. *et al.* (1995) 'A novel amino acid modification in sulfatases that is defective in multiple sulfatase deficiency', *Cell*, 82(2), pp. 271–278. doi: 10.1016/0092-8674(95)90314-3.

Schmitt-Engel, C. *et al.* (2015) 'The iBeetle large-scale RNAi screen reveals gene functions for insect development and physiology', *Nature Communications*, 6(1), pp. 1–10. doi: 10.1038/ncomms8822.

Sokoloff, A. (1972) *The biology of Tribolium: with special emphasis on genetic aspects*. Oxford: Clarendon Press.

Sokoloff, A., Ackermann, M. and Overton, L. F. (1967) 'Linkage Studies in Tribolium Confusum Duval. Ii. the Map Position of Three Homeotic Mutants.', *Canadian Journal of Genetics and Cytology*, 9(3), pp. 490–502. doi: 10.1139/g67-053.

Stewart, A. K. *et al.* (2011) 'SLC26 anion exchangers of guinea pig pancreatic duct: molecular cloning and functional characterization', *American Journal of Physiology-Cell Physiology*, 301(2), pp. C289–C303. doi: 10.1152/ajpcell.00089.2011.

Strott, C. A. (2002) 'Sulfonation and molecular action', *Endocrine Reviews*, 23(5), pp. 703–732. doi: 10.1210/er.2001-0040.

Takahashi, H. (2010) 'Regulation of sulfate transport and assimilation in plants', *International Review of Cell and Molecular Biology*, 281, pp. 129–159. doi: 10.1016/S1937-6448(10)81004-4.

Takahashi, H. *et al.* (2011) 'Sulfur Assimilation in Photosynthetic Organisms: Molecular Functions and Regulations of Transporters and Assimilatory Enzymes', *Annual Review of Plant Biology*, 62(1), pp. 157–184. doi: 10.1146/annurev-arplant-042110-103921.

Thompson, M. J. *et al.* (1972) 'Metabolic pathways of steroids in insects', *Proceedings of the Royal Society of London. Series B. Biological Sciences*, 180(1059), pp. 203–221. doi: 10.1098/rspb.1972.0015.

Tschinkel, W. R. (1975) 'A comparative study of the chemical defensive system of tenebrionid beetles: Chemistry of the secretions', *Journal of Insect Physiology*, 21(4), pp. 753–783. doi: 10.1016/0022-1910(75)90008-6.

Uchimura, K. *et al.* (1998) 'Human N-acetylglucosamine-6-O-sulfotransferase involved in the biosynthesis of 6-sulfo sialyl Lewis X: molecular cloning, chromosomal mapping, and expression in various organs and tumor cells', *Journal of Biochemistry*, 124(3), pp. 670–678. doi: 10.1093/oxfordjournals.jbchem.a022164.

Unruh, L. M., Xu, R. and Kramer, K. J. (1998) 'Benzoquinone levels as a function of age and gender of the red flour beetle, Tribolium castaneum'. Available at: https://pubag.nal.usda.gov/catalog/13250 (Accessed: 19 January 2020).

Vincourt, J.-B. *et al.* (2003) 'Molecular and functional characterization of SLC26A11, a sodium-independent sulfate transporter from high endothelial venules', *FASEB journal: official publication of the Federation of American Societies for Experimental Biology*, 17(8), pp. 890–892. doi: 10.1096/fj.02-0787fje.

Yang, R. S. H., Pelliccia, J. G. and Wilkinson, C. F. (1973) 'Age-dependent arylsulphatase and sulphotransferase activities in the southern armyworm: a possible insect endocrine regulatory mechanism? (Short Communication)', *Biochemical Journal*, 136(3), pp. 817–820.

Yang, R. S. H. and Wilkinson, C. F. (1972) 'Enzymic sulphation of p-nitrophenol and steroids by larval gut tissues of the southern armyworm (Prodenia eridania Cramer)', *Biochemical Journal*, 130(2), pp. 487–493. doi: 10.1042/bj1300487.

Zito, E. *et al.* (2007) 'Sulfatase modifying factor 1 trafficking through the cells: from endoplasmic reticulum to the endoplasmic reticulum', *The EMBO Journal*, 26(10), pp. 2443–2453. doi: 10.1038/sj.emboj.7601695.

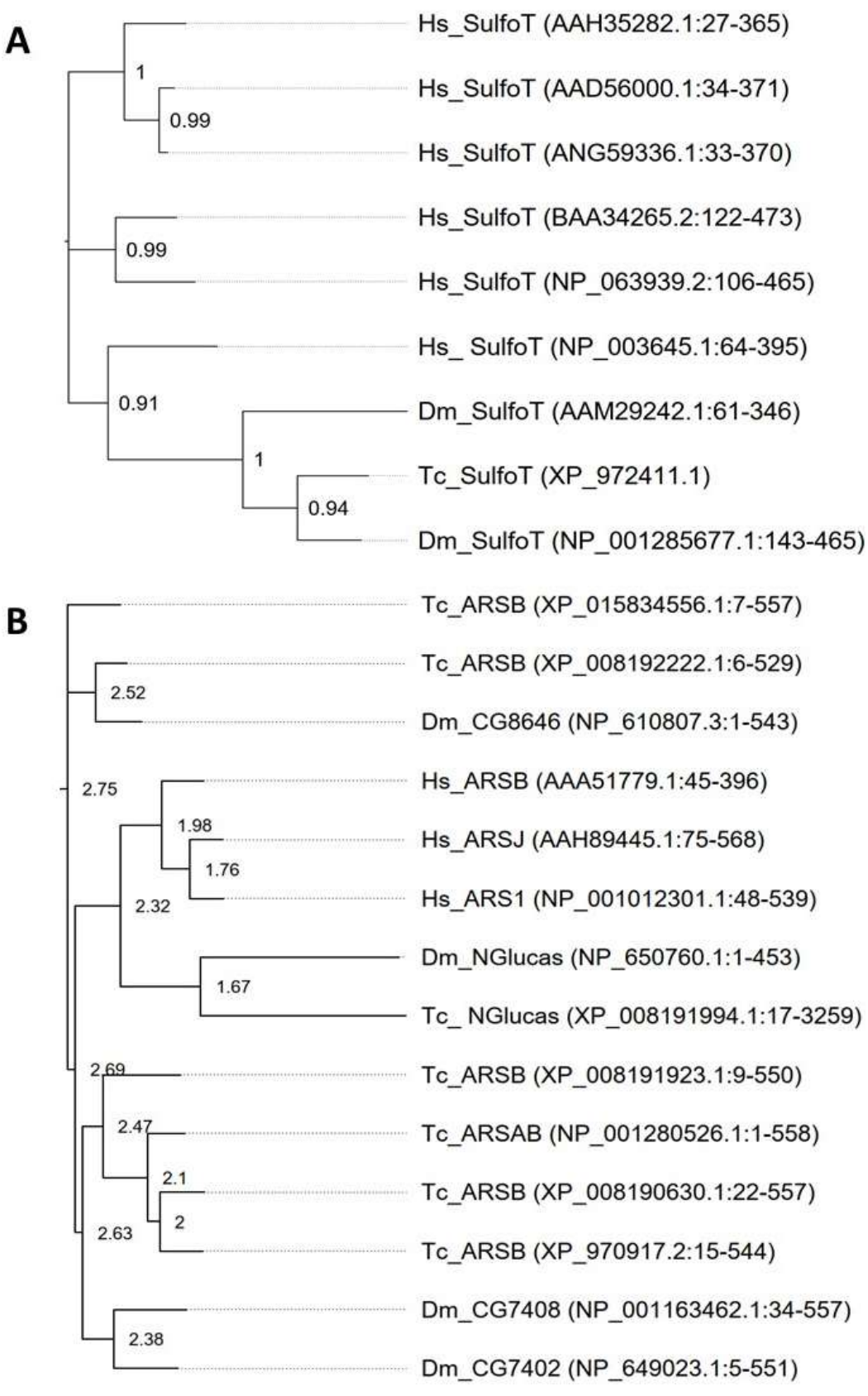
A
Hs_SulfoT (AAH35282.1:27-365)
Hs_SulfoT (AAD56000.1:34-371)
Hs_SulfoT (ANG59336.1:33-370)
Hs_SulfoT (BAA34265.2:122-473)
Hs_SulfoT (NP_063939.2:106-465)
Hs_ SulfoT (NP_003645.1:64-395)
Dm_SulfoT (AAM29242.1:61-346)
Tc_SulfoT (XP_972411.1)
Dm_SulfoT (NP_001285677.1:143-465)
1
0.99
0.99
0.91
1
0.94
B
Tc_ARSB (XP_015834556.1:7-557)
Tc_ARSB (XP_008192222.1:6-529)
Dm_CG8646 (NP_610807.3:1-543)
Hs_ARSB (AAA51779.1:45-396)
Hs_ARSJ (AAH89445.1:75-568)
Hs_ARS1 (NP_001012301.1:48-539)
Dm_NGlucas (NP_650760.1:1-453)
Tc_ NGlucas (XP_008191994.1:17-3259)
Tc_ARSB (XP_008191923.1:9-550)
Tc_ARSAB (NP_001280526.1:1-558)
Tc_ARSB (XP_008190630.1:22-557)
Tc_ARSB (XP_970917.2:15-544)
Dm_CG7408 (NP_001163462.1:34-557)
Dm_CG7402 (NP_649023.1:5-551)
2.52
2.75
1.98
1.76
2.32
1.67
2.69
2.47
2.1
2
2.63
2.38

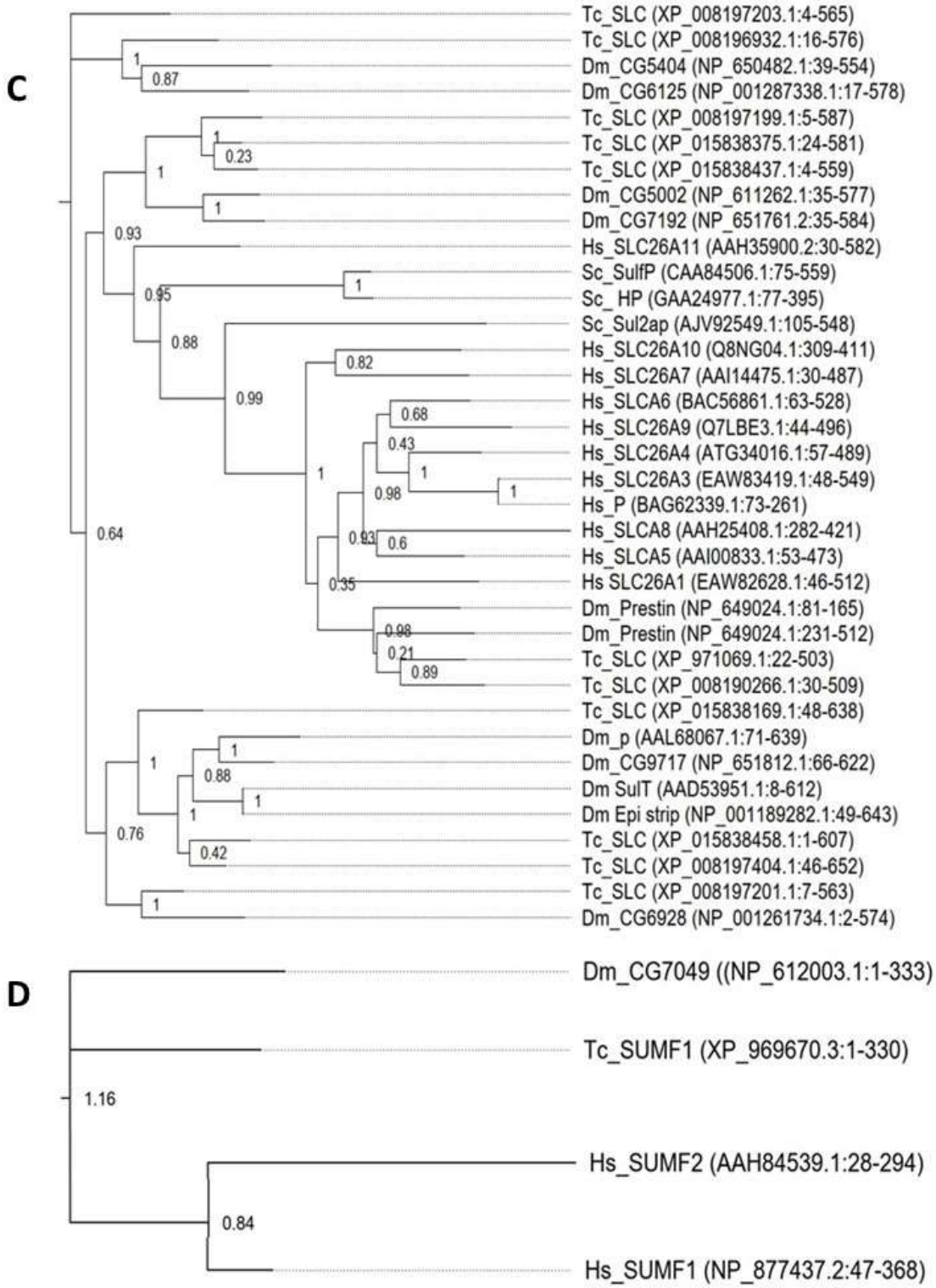
C
Tc_SLC (XP_008197203.1:4-565)
Tc_SLC (XP_008196932.1:16-576)
Dm_CG5404 (NP_650482.1:39-554)
Dm_CG6125 (NP_001287338.1:17-578)
Tc_SLC (XP_008197199.1:5-587)
Tc_SLC (XP_015838375.1:24-581)
Tc_SLC (XP_015838437.1:4-559)
Dm_CG5002 (NP_611262.1:35-577)
Dm_CG7192 (NP_651761.2:35-584)
Hs_SLC26A11 (AAH35900.2:30-582)
Sc_SulfP (CAA84506.1:75-559)
Sc_ HP (GAA24977.1:77-395)
Sc_Sul2ap (AJV92549.1:105-548)
Hs_SLC26A10 (Q8NG04.1:309-411)
Hs_SLC26A7 (AAI14475.1:30-487)
Hs_SLCA6 (BAC56861.1:63-528)
Hs_SLC26A9 (Q7LBE3.1:44-496)
Hs_SLC26A4 (ATG34016.1:57-489)
Hs_SLC26A3 (EAW83419.1:48-549)
Hs_P (BAG62339.1:73-261)
Hs_SLCA8 (AAH25408.1:282-421)
Hs_SLCA5 (AAI00833.1:53-473)
Hs SLC26A1 (EAW82628.1:46-512)
Dm_Prestin (NP_649024.1:81-165)
Dm_Prestin (NP_649024.1:231-512)
Tc_SLC (XP_971069.1:22-503)
Tc_SLC (XP_008190266.1:30-509)
Tc_SLC (XP_015838169.1:48-638)
Dm_p (AAL68067.1:71-639)
Dm_CG9717 (NP_651812.1:66-622)
Dm SulT (AAD53951.1:8-612)
Dm Epi strip (NP_001189282.1:49-643)
Tc_SLC (XP_015838458.1:1-607)
Tc_SLC (XP_008197404.1:46-652)
Tc_SLC (XP_008197201.1:7-563)
Dm_CG6928 (NP_001261734.1:2-574)
D
Dm_CG7049 ((NP_612003.1:1-333)
Tc_SUMF1 (XP_969670.3:1-330)
Hs_SUMF2 (AAH84539.1:28-294)
Hs_SUMF1 (NP_877437.2:47-368)

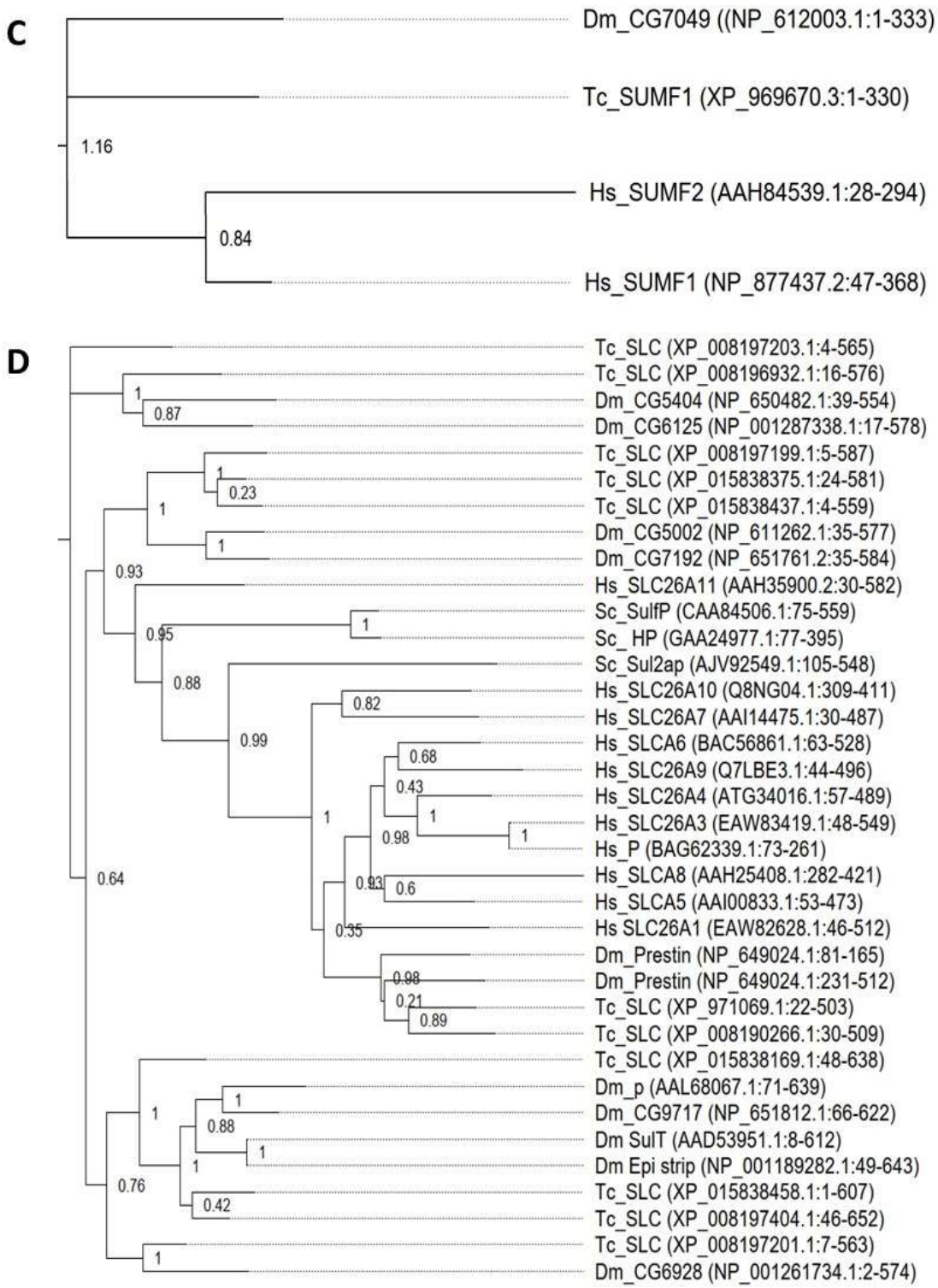

Figure 1. Phylogenetic tree of *CHST5* (A), *ARSB* (B), *SUMF1* (C) and *SLC26A11* (D) in *T. castaneum*: Tc, *D. melanogaster:* Dm and *H. sapiens:* Hs.

A: Figure 2. Stink gland phenotype of candidate genes.

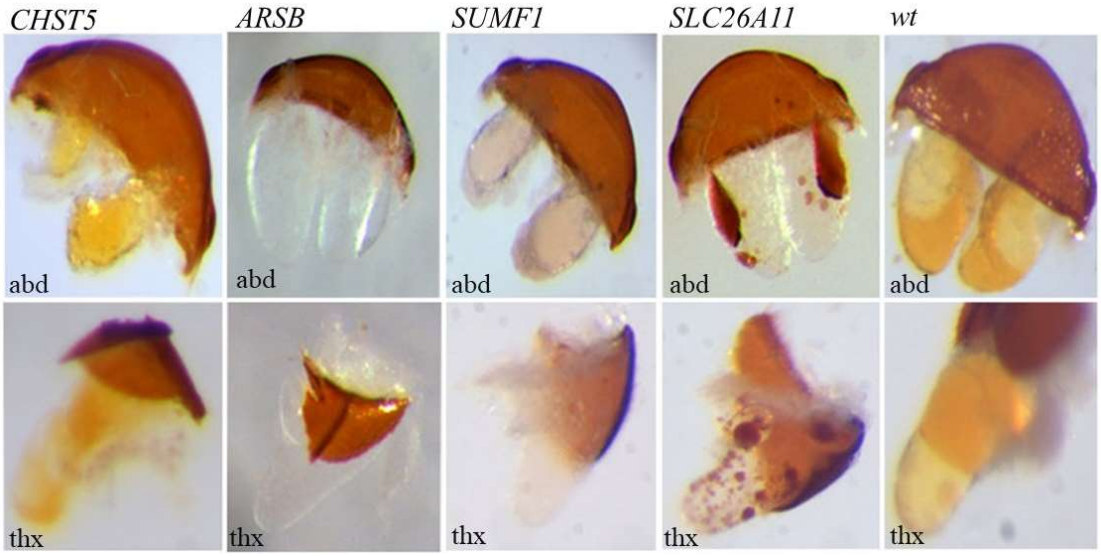

B: Table 1. Selected candidate genes analysis via GC-MS analysis. Prothoracic and abdominal glands of RNAi-mediated knockdowns of *CHST5, ARSB*, *SUMF1* and *SLC26A11*were separately processed and each sample contained the three beetle glands content. Levels of each chemical in gland contents was determined as percentage with respect to wt levels. EBQ: 2ethyl-1,4-benzoquinone, MBQ: 2-methyl-1,4-benzoquinone, 1-C17: 1-heptadecene, 1-C15: 1-pentadecene.

Gene	abdominal gland				thoracic gland			
	MBQ%	EBQ%	1-C15%	1-C17%	MBQ%	EBQ%	1-C15%	1-C17%
CHST5	50	52	93	107	29	30	50	42
ARSB	0	0	61	59	0	0	13	14
SUMF1	0	6	28	24	0	0	50	49
SLC26A11	7	9	20	12	0	0	5	0

0%	substance not present
1-50%	strongly reduced
51-75%	reduced
>76%	not reduced, wt=100%

A. Figure 3. Expression levels of candidate genes. Alterations in expression levels of the selected four candidate genes *CHST5, ARSB*, *SUMF1* and *SLC26A11* are determined in stink glands of *Tribolium* beetle. The respective dataset of log2 Fold change (FC) of gland sample/body control is given. A

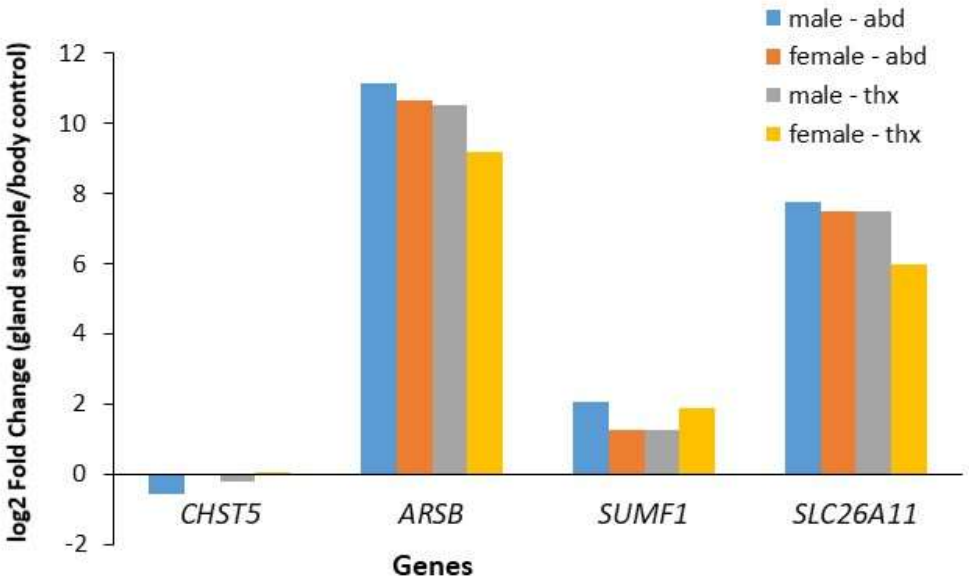

B. Table 2. Transcriptomic read counts of candidate genes in gland tissues. Read counts of four genes are given in the Table. m-thx: male prothoracic gland, fm-thx: female prothoracic gland, m-abd: male abdominal gland, fm-abd: female abdominal gland.

Genes	Reads			
	m – thx	**fm - thx**	**m - abd**	**fm – abd**
CHST5	356	416	276	405
ARSB	114281	124457	176434	45114
SUMF1	665	623	1315	1283
SLC26A11	4693	4731	5706	1632

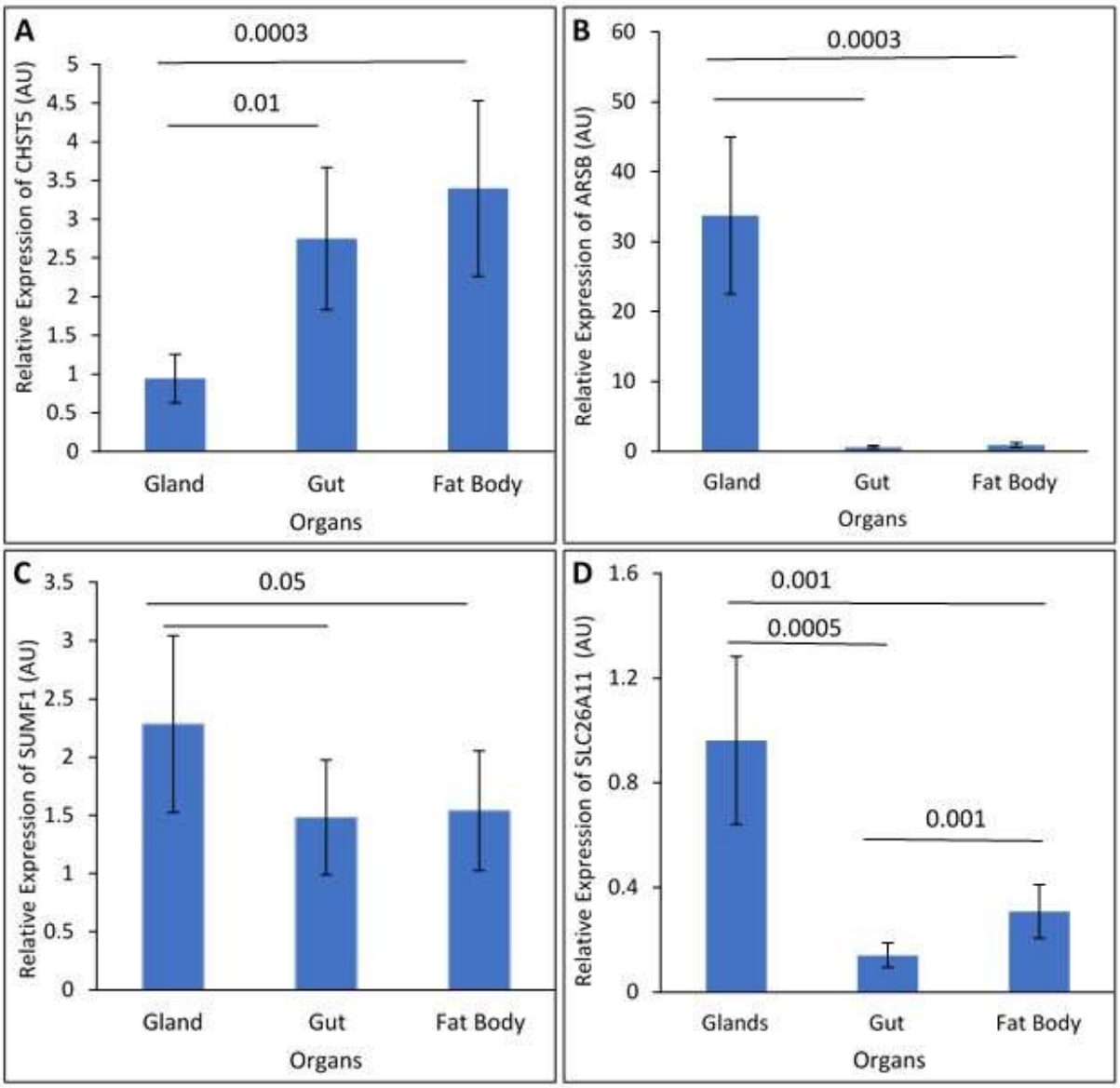

Figure 4. Quantification of Transcript Levels by RT-qPCR: (A) Relative expression of *CHST5* mRNA was significant lowered in glandular tissue and higher in gut and fat body as compared to *ARSB*, *SUMF1, SLC26A11* (B, C, D).

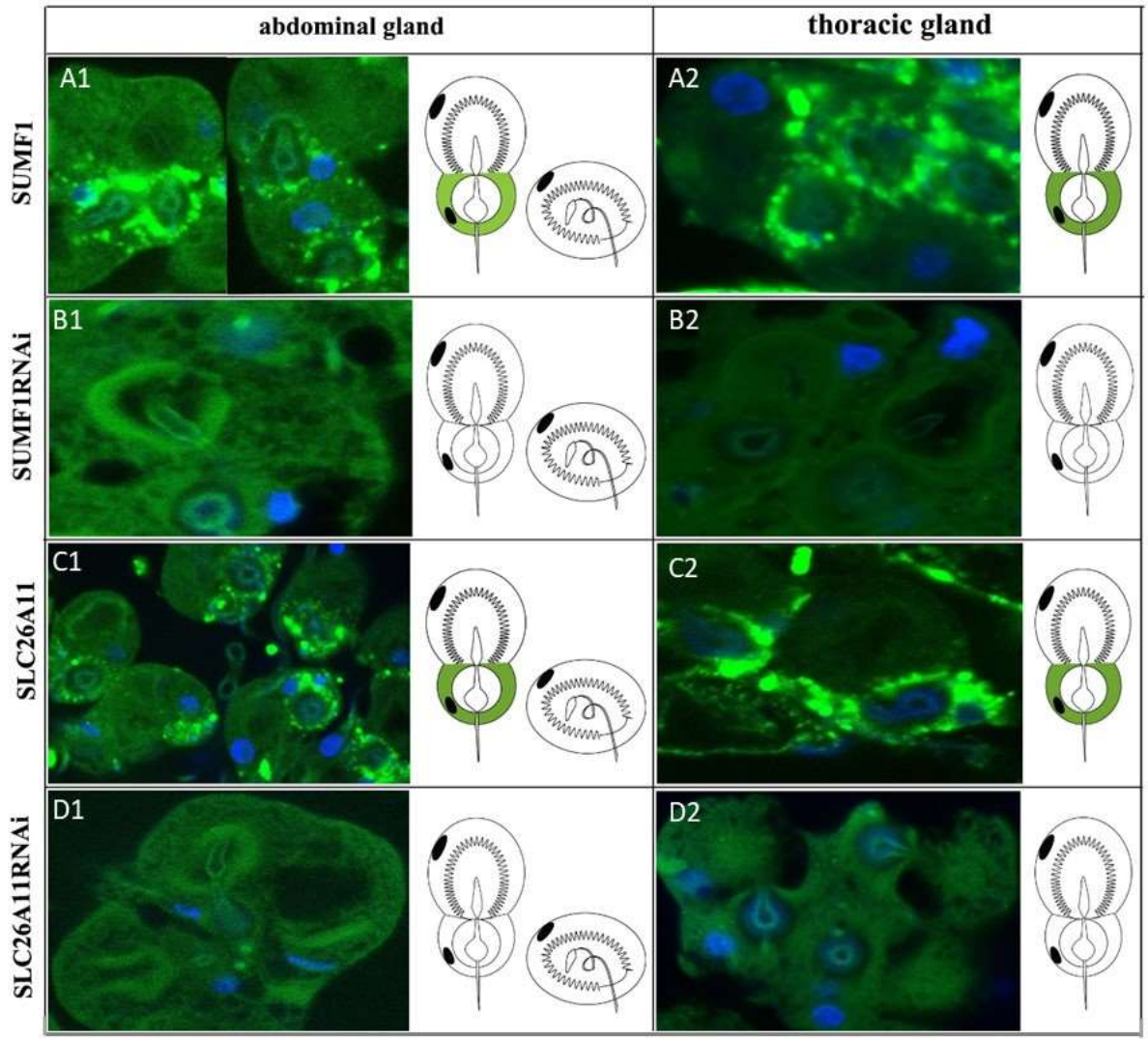

Figure 5. *In situ* hybridization for candidate genes in beetle stink glands. FISH analysis was carried out on prothoracic and abdominal glands of knockdown and wt of ten days old adult beetle. Abdominal gland expression is demonstrated in right side while prothoracic glands in left side. A summary of expression pattern is given in schemes to the right. Staining with probes against *SUMF1* (A1), *SLC26A11* (C1) respectively. Staining of these candidate genes in the RNAi is shown in Figure (B1, D1).

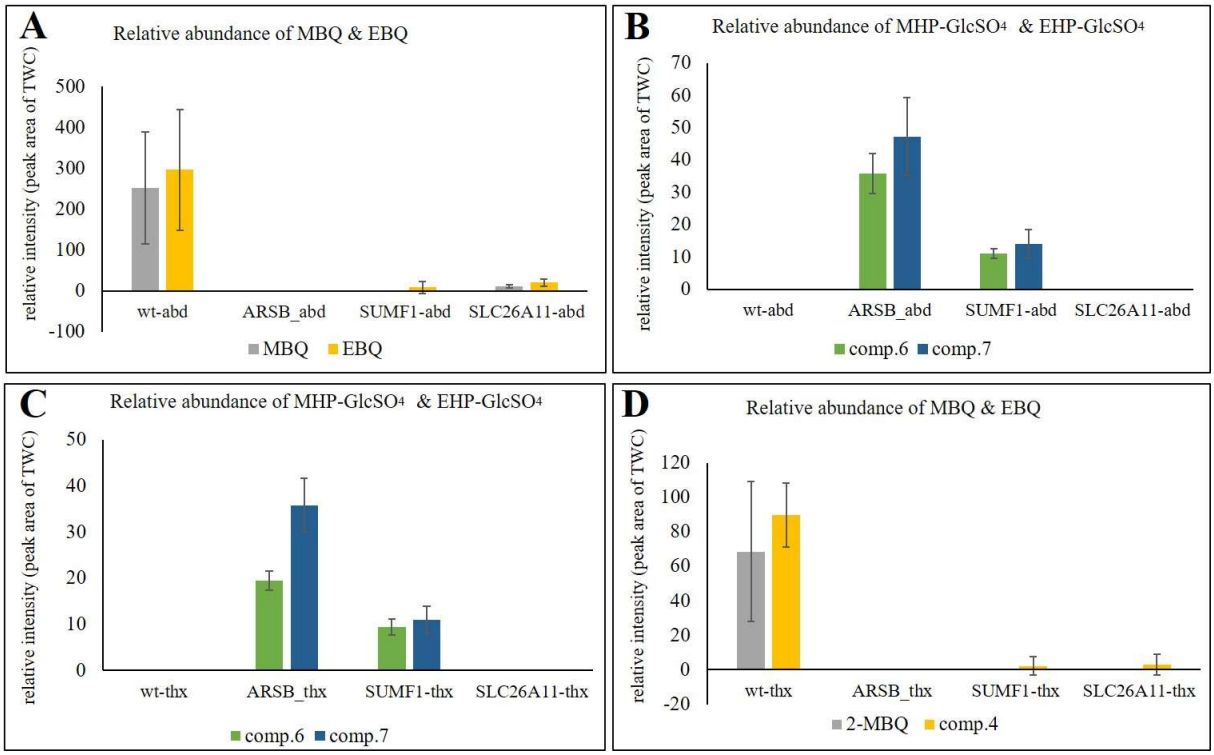

Figure 6. Relative abundance of four compounds (compound 3: 2-methyl benzoquinone, compound 4: 2-ethyl benzoquinone, compound 6: 2-methyl-4-hydroxyphenyl glycosylsulfate and compound 7: 2-ethyl-4-hydroxyphenyl glycosylsulfate). in wt and RNAi mediated knockdown of *ARSB*, *SUMF1* and *SLC26A11* in abdominal gland contents of iBeetle are shown in (A, B) and thoracic gland (C, D) respectively.

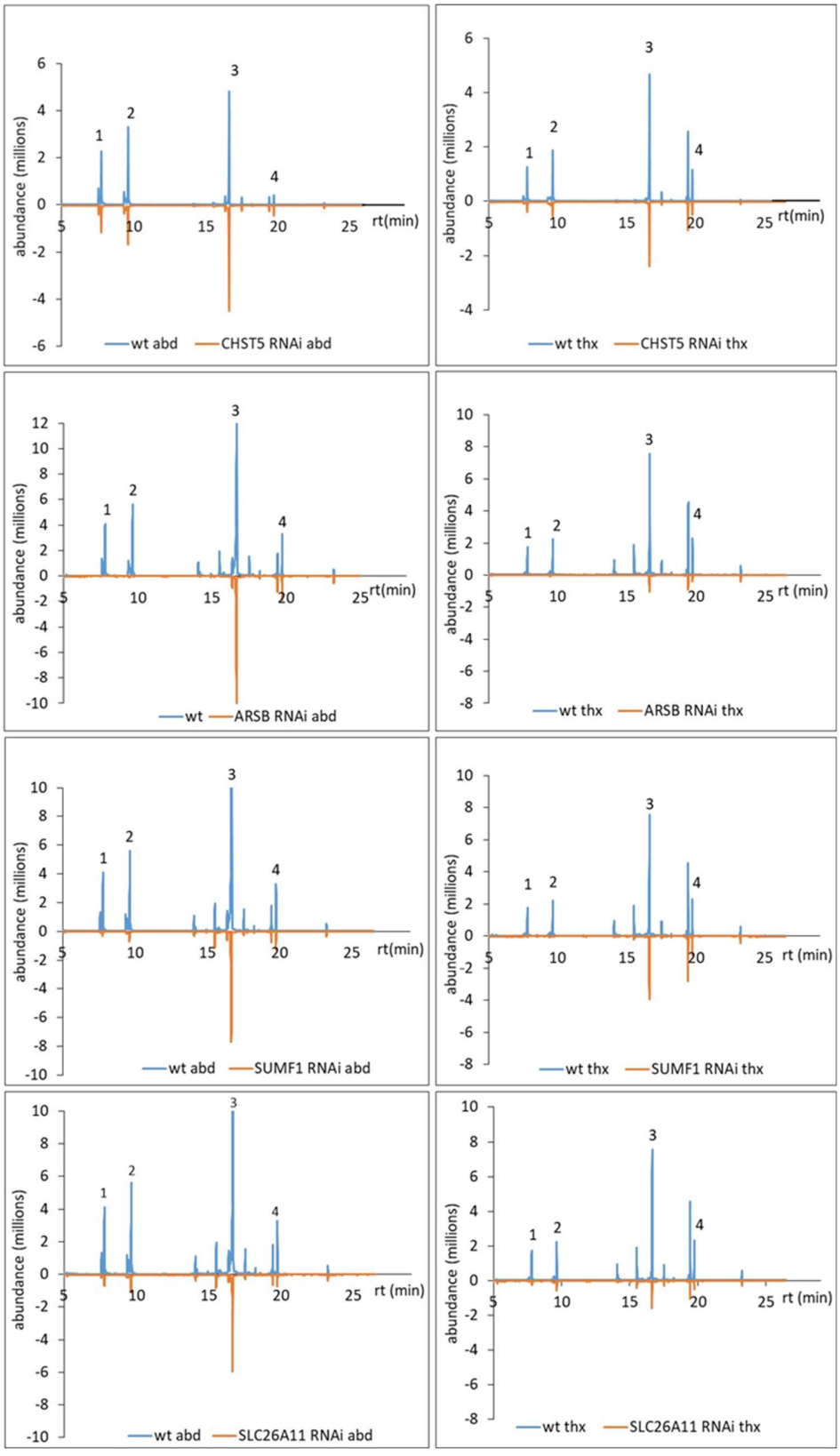
abundance (millions)
rt(min)
wt abd
CHST5 RNAi abd
wt thx
CHST5 RNAi thx
wt
ARSB RNAi abd
ARSB RNAi thx
SUMF1 RNAi abd
SUMF1 RNAi thx
SLC26A11 RNAi abd
SLC26A11 RNAi thx

Additional file 1. Figure S1. Gas chromatograms showing contents of odoriferous gland. The most abundantly expressed four volatile secretion substances in GC-MS analysis of wild type beetles abdominal and prothoracic glands as compared to knockdown beetle are: 1) 2-methyl-1,4-benzoquinone, 2) 2ethyl-1,4-benzoquinone, 3) 1-pentadecene and 4) 1-heptadecene. The benzoquinones peaks (1 and 2) are missing in gland contents of RNAi-mediated knockdowns of *ARSB* while in *CHST5*, *SUMF1* and *SLC26A11* RNAi less peaks of benzoquinones were observed as compare to wild type (red lines show negative values) in beetles. rt: retention time.

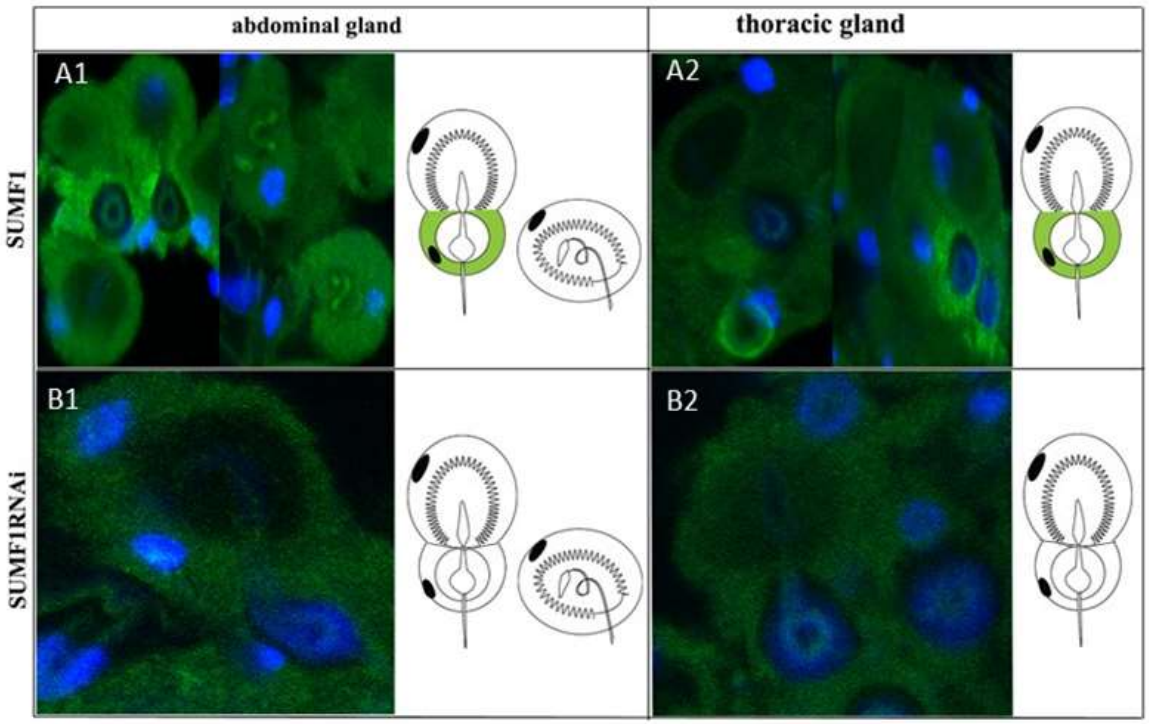

Additional file 2. Figure S2. *SUMF1* protein immunohistochemical staining in *Tribolium* glands. Photomicrograph showing *SUMF1* staining of abdominal (right panel) and prothoracic (left panel) stink glands of ten days-old wt (A1, A2) and *SUMF1* RNAi knockdown (B1, B2) beetles. Important findings of *SUMF1* signals are shown in schemes to the right side in figure.

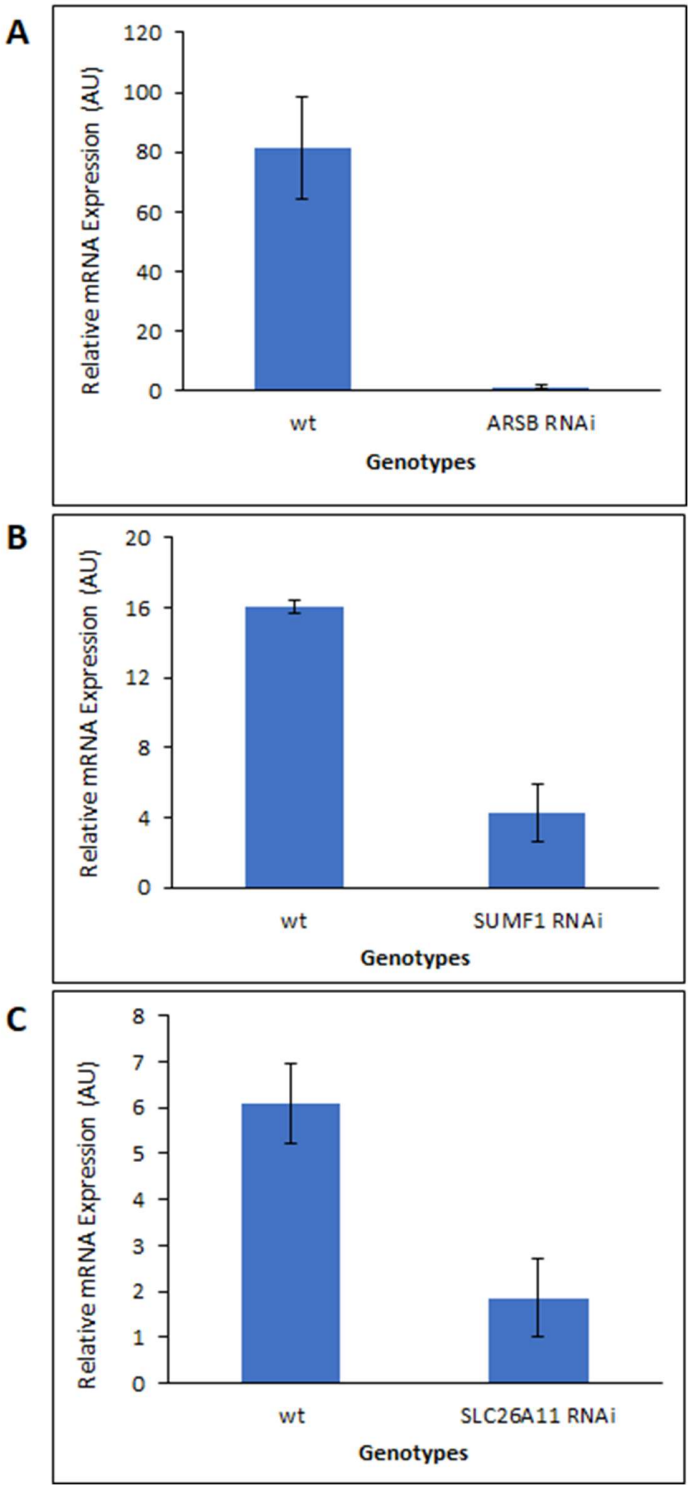

Additional file 3. Figure S3. Quantification of Transcript Levels by RT-qPCR in wt and knockdown Beetle: Relative transcript abundance of *ARSB, SUMF1*and *SLC26A11* was greatly reduced in RNAi knockdown beetle glandular tissue as compared to wt beetle gland.

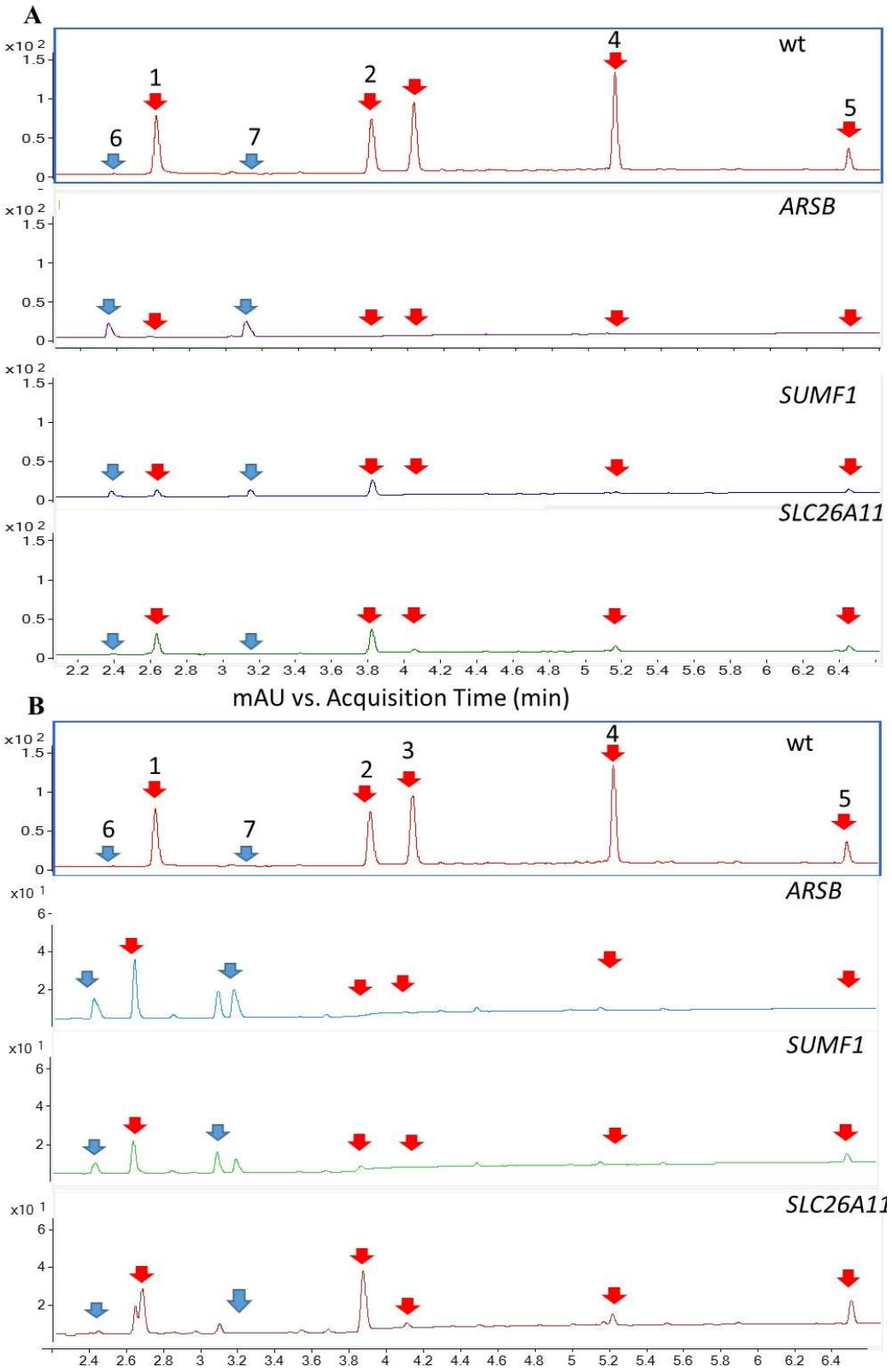
A
wt
ARSB
SUMF1
SLC26A11
1
2
3
4
5
6
7
mAU vs. Acquisition Time (min)
B
wt
ARSB
SUMF1
SLC26A11
1
2
3
4
5
6
7
mAU vs. Acquisition Time (min)

Additional file 4. Figure S4. (A)UV/VIS analysis of extracts from abdominal glands of wt and RNAi mediated knockdown beetles for *ARSB*, *SUMF1* and *SLC26A11*. Isolated glands of 10 days old beetles were crushed and subsequently extracted with methanol. The supernatant were analyzed by liquid chromatography (LC) coupled to a photo diode array (PDA). Data acquisition was done in the range from 190 to 600 nm. Shown are total wavelength chromatograms for the indicated lines/genotypes with dominant signals (1-7). **(B)**.UV/VIS analysis of extracts from prothoracic glands of wt and RNAi mediated knockdown beetles for *ARSB*, *SUMF1* and *SLC26A11*. Data acquisition was done in the range from 190 to 600 nm. Total wavelength chromatograms for the indicated lines/genotypes with dominant signals (1-7) are shown in B. The identity of the following compounds were confirmed by UV/VIS spectra and high resolution tandem mass spectrometry: compound 3, 2-methyl benzoquinone; compound 4, 2-ethyl benzoquinone; compound 6, 2-methyl-4-hydroxyphenyl glycosylsulfate and compound 7, 2-ethyl-4-hydroxyphenyl glycosylsulfate**.**

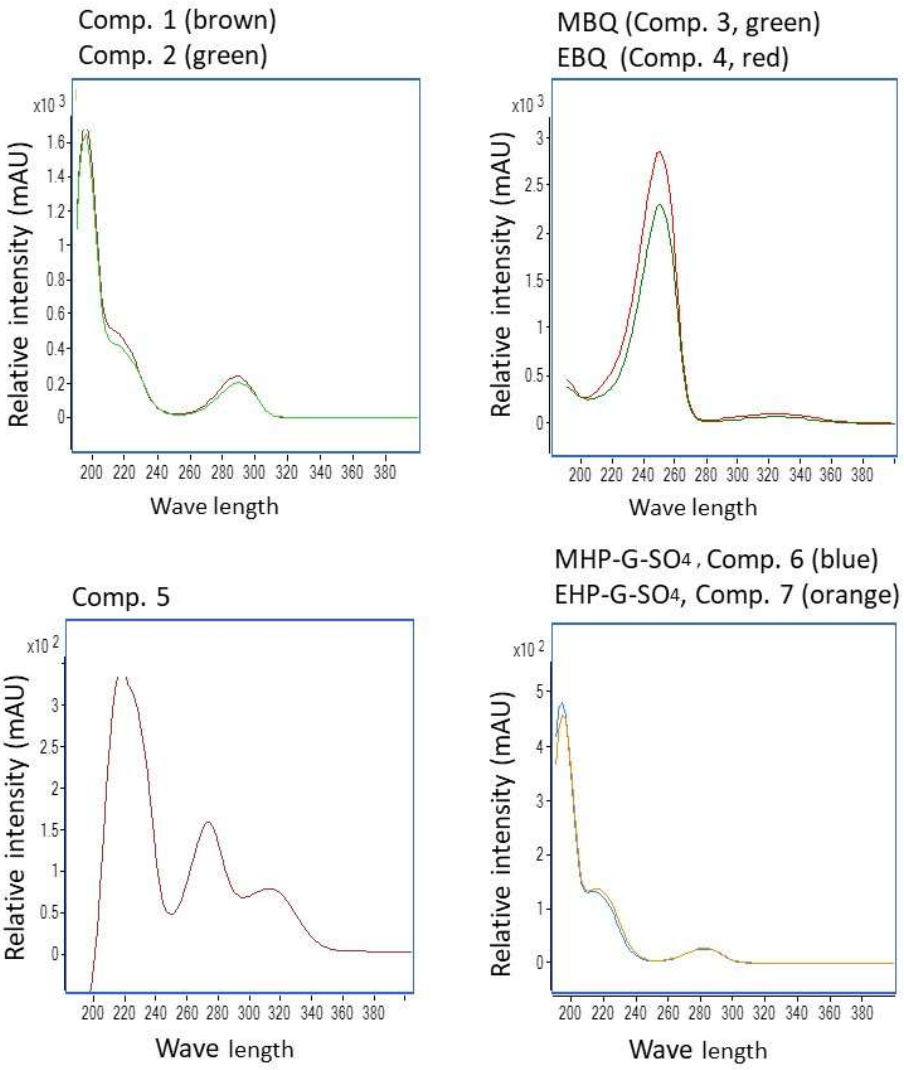

Additional file 5. Figure S5. UV/Vis spectra of the main compounds from abdominal glands. Isolated glands of 10 days old beetles were crushed and subsequently extracted with methanol. The supernatant were analyzed by liquid chromatography (LC) coupled to a photo diode array (PDA) in the range from 190 to 600 nm. The identity of the following compounds were confirmed by UV/VIS spectra and high resolution tandem mass spectrometry: compound 3, 2-methyl benzoquinone; compound 4, 2-ethyl benzoquinone; compound 6, 2-methyl-4-hydroxyphenyl glycosylsulfate and compound 7, 2-ethyl-4-hydroxyphenyl glycosylsulfate.

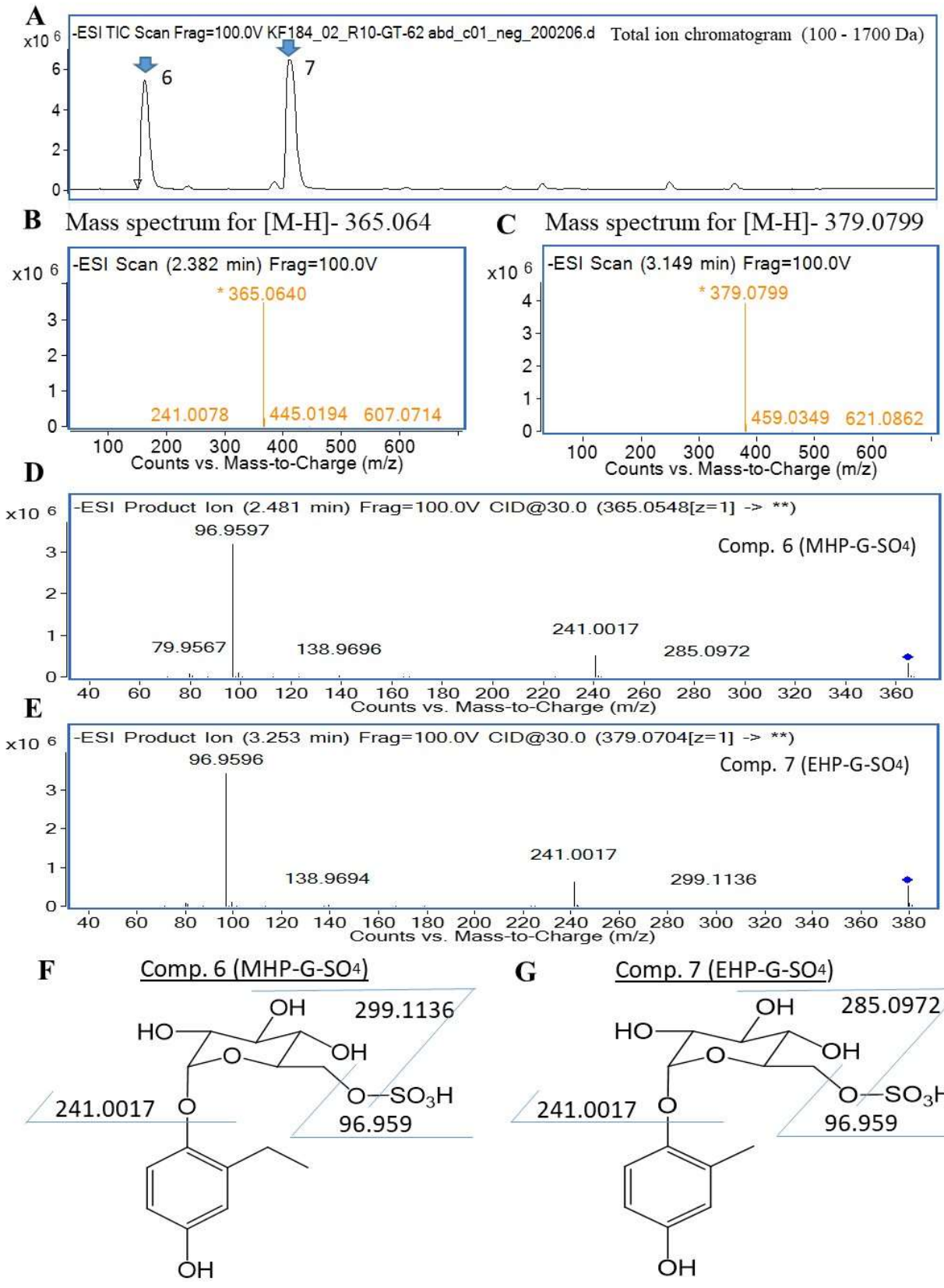
A
-ESI TIC Scan Frag=100.0V KF184_02_R10-GT-62 abd_c01_neg_200206.d Total ion chromatogram (100 - 1700 Da)
6
7
B Mass spectrum for [M-H]- 365.064
-ESI Scan (2.382 min) Frag=100.0V
* 365.0640
241.0078
445.0194
607.0714
Counts vs. Mass-to-Charge (m/z)
C Mass spectrum for [M-H]- 379.0799
-ESI Scan (3.149 min) Frag=100.0V
* 379.0799
459.0349
621.0862
Counts vs. Mass-to-Charge (m/z)
D
-ESI Product Ion (2.481 min) Frag=100.0V CID@30.0 (365.0548[z=1] -> **)
96.9597
Comp. 6 (MHP-G-SO4)
79.9567
138.9696
241.0017
285.0972
Counts vs. Mass-to-Charge (m/z)
E
-ESI Product Ion (3.253 min) Frag=100.0V CID@30.0 (379.0704[z=1] -> **)
96.9596
Comp. 7 (EHP-G-SO4)
138.9694
241.0017
299.1136
Counts vs. Mass-to-Charge (m/z)
F
Comp. 6 (MHP-G-SO4)
299.1136
241.0017
96.959
G
Comp. 7 (EHP-G-SO4)
285.0972
241.0017
96.959

Additional file 6. Figure S6. Liquid chromatography high resolution mass spectrometry (LC-HRMS) analysis of extract from abdominal glands of RNAi mediated *ARSB* knockdown beetles. The total ion chromatogram (A) and the respective mass spectra of compound 6 (B) and 7 (C) are shown. Extracts from abdominal glands of RNAi mediated *ARSB* knockdown beetles were analyzed in the negative ionization mode for the fragmentation analysis of compound 6 and 7. The mass spectra of compound 6 and 7 obtained by tandem HRMS are shown in D and E. High resolution tandem (Interpretation of the fragments) mass spectrometry hints to proposed structure of the compound 6 and compound 7 are methyl sulfated glycosylated phenolic (MHP-$GlcSO_4$) and ethyl sulfated glycosylated phenolic (EHP-$GlcSO_4$) precursurs shown in E and F.

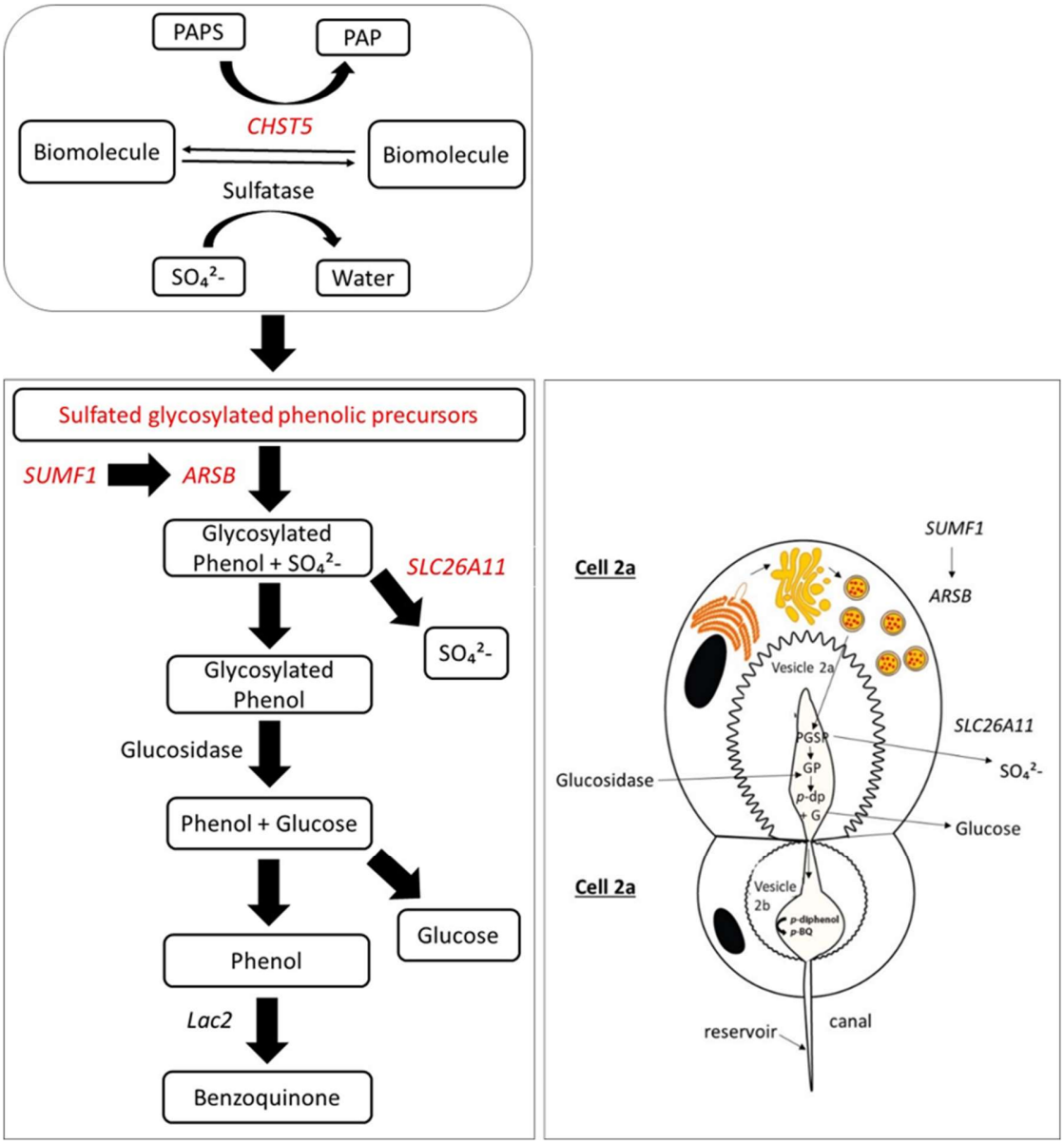

Sulfated glycosylated phenolic precursors (SGPP)

Glycosylated Phenol (GP) + SO_4^{2-}

p-diphenol (*p*-dp) + Glucose (G)

p-benzoquinone (BQ)

Endoplasmic reticulum, Nucleus, Golgi apparatus, vacuole

Figure 7. Model of *p*-benzoquinone synthesis in the odoriferous stink glands of *Tribolium*.

Additional file 7. Table S7. Non overlapping sequence

Gene	iB_#	OGS_# (ass. 3.0)	dsRNA sequence (5' --> 3')
CHST5	iB_13656	TC011350	
ARSB	iB_05763	Tc015151	TTAGTCGCCTCACCGTCTTTAAGCACAGTTAACATGAAAATA CTTCTCCTTATTTTCCTAACTTCCTTAATACAAAACTCGAGTC AAGTATGCCGCGTACGCCGACCCCGACCCCACATTATCGTGA TAATGGGCGACGATATGGGACATAACGATATTGGTCTTCGGA CGAACCAAATCCCGACCCCTAACATCGACGCTTTGTCCTCAC CGGAAACTACCCCATCCGGTCT
SUMF1	iB_09043	TC016314	GTCTGGGAATGGACTCAGGATAATTGGTTGAATGACCCTGAC GCCAAAGTGAAGAAAGGGGGCTCCTACCTCTGTCATGAGTCT TACTGTTGGAGGTATCGCTGCGCTGCAAGATCTTTCAATACC AAAGACAGTTCGGCCGGAAATTTAGGCTTTCGATGTGCCGGT GATGTCAAATAATTTGGCAGTGAATAACAAACAAACCCAAGT ACTTAAATCATCCTGCCATCAAGTCTTCC
SLC26A11	iB_09413	TC005389	TGCTTGATTTTTCCCTCAGCTGATTATGTCCGAAATTTGGTGA TTAAGCAATCGATGAGGCAAAAAATTCCGGTTGTTATCGACT GTTCACACATTTATGGTGCTGATTATACGGCAGCTACAGTCAT TGAGAGTTTAACCAAAGATTTCAAAACGCGACAACAACCGCT GTTTTTTTACAATCTCAAGTCAAGTGTGAGCTCGGTTTTTGTC GGCCTAAACCTGGACTATTTTCTAGTCTATTACAACGAAGAT GAGTTGGATGATATGCTCAAGAAGTGGACCGAAA

Additional file 8. Table S8. Oligonucleotides

Primer labeling	**Sequence 5' – 3'**
9413NE_forword_p	TCGACATGGTCACCAACCTA
9413NE_reverse_p	CAGGCGTCACAAGCAAATAA
Ib_04702b_f	AAGTGTGCGAGGGTATGTGG
Ib_04702b_r	GTCTCAAACGTCGGCCTTTT
9043n_forword	GTGGCTGTCACCTCAACAGA
9043n_reverse	TCCTGAGTCCATTCCCAGAC
9413n_forward	AGGGATTGCGTGTTTGGTAG
9413n_reverse	CAGGCGTCACAAGCAAATAA
Ib_08760b_f	CGATCAGGATTTGCTGCCAA
Ib_08760b_r	TGTGACCCGCTTGAAAGTTG
Ib_07361_f	ATGAAACAAATTTATTGTTTAATAACCGTC
IB_07361_r	TTAGTCTAACGGAAACCATGGTA
5389NE_forword_p	CTCGGGAGTTGTAAGGACGT
5389NE_reverse_p	CCAAGATGGCGTTACGTGAG
IB_04702_f	ATGGGGAATTGCCTCAGC
IB_04702_r	TCAGTAAGCCGACGCTTC
IB_08760_f	ATGTCCAAAAACAAGTTTGATG
IB_08760_r	CTACAGGTGTAGAATACCATCTTC
IB_07902_f	ATGGTGGTGCAGAAAATTGAC
IB_07902_r	TTACAGATCTTGTGTACTTCTAAAAGC
IB_09043_f	ATGTACTTAATTCTTTTATACTTAACTACTG
IB_09043_R	TTATTTGACATCACCGGC

IB_09413a_f	ATGGAGGTAAAAACCGAGTCTC
IB_09413a_r	CTAGATTTTATCACAGATTTCGGTC
IB_09413b_f	GGATTCCCCGCAATACAACC
IB_09413b_r	TCGGTCCACTTCTTGAGCAT
IB_09043b_f	CCTCAACAGAAACTCTCAGTGC
IB_09043b_r	CTAAATTTCCGGCCGAACTGTC
TC_14870_F2	AATGCAGAACATGCGTTCG
TC_14870_R2	CCAATAGAACCCATCAGCGT
IB_08398_f	ATGCTCCAAGAGGCAGAA
IB_08398_r	CTAACGAATATTCTTACCAGTTG
Ib_04702_f_wt_T	GAATTGTAATACGACTCACTATAGGAAGTGTGGGAGGGTATGTGG
Ib_04702_r_wt_T	GAATTGTAATACGACTCACTATAGGGTCTCAAACGTCGGCCTTTT
IB_08760B_f_wt_T	GAATTGTAATACGACTCACTATAGGCGATCAGGATTTGCCAA
IB_08760B_r_wt_T	GAATTGTAATACGACTCACTATAGGTGTGACCCGCTTGAAAGTTG
Ib_04702F_wt_T7	TAATACGACTCACTATAGGAAGTCTGGGAGGGTATGTGG
Ib_04702R_wt_T7	TAATACGACTCACTATAGGGTCTCAAACGTCGGCCTTTT
IB_08760F_wt_T7	TAATACGACTCACTATAGGCGATCAGGATTTGCTGCCAA
IB_08760R_wt_T7	TAATACGACTCACTATAGGTGTGACCCGCTTGAAAGAAGTTG
1_GT-62_Fw.pr	CGATTGAAGGGTTTGATTTAC
1_GT-62_Rv.pr	GGTCTGGTGGTATTATGC
2_GT-62_Fw.pr	CCGAAAGGGCATTAGATATTATAG
2_GT-62_Rv.pr	GGTCCAACTCTGCTACAA
3_GT-62_Fw.pr	TTCGGAGATCCTCGTCAA
3_GT-62_Rv.pr	ATCGTATGTGCCACCTCC
BA_SulfoT_q1_fw	CTCCTCAACTGTGATTACT
BA_SulfoT_q1_rv	AATTCCATAACCTCCGATT
BA_SulfoT_q2_fw	AGGCAAGTCTTTAAGTGAT
BA_SulfoT_q2_rv	GGCTCATAATGGTAGTAGTT
BA_SulfoT_q3_fd	ACAGGCAAGTCTTTAAGTG
BA_SulfoT_q3_rv	GGCTCATAATGGTAGTAGTTC
BA-RSP3.3.q1-Fw	AGGGTGTGCTGGGAATTAAAG
BA-RSP3.3.q1-Rv	GGGTAGGCAGGCAAAATCTC
BA-RSP18.3.q2-Fw	AACCCTCGCCAATACAAAATC
BA-RSP18.3.q2-Rv	CTTCATGCGTTCCAAATCCTC
9413.1-F-q	TTATGGTGCTGATTATAC
9413.1-R-q	TCATCTTCGTTGTAATAG
9413.2-F-q	ATTCAAGGTGATTGGTTA
9413.2-R-q	TGTGTTGTTGTAAGTGTA
9043.1-F-q	AAGGCTCCACAATTAACG
9043.1-R-q	TTACCAACAAACTCGCAATA
9043.2-F-q	AACGAAGAACCTCACAAC
9043.2-R-q	CCTCATGGTCACTCTCAA

4. General Discussion

Understanding molecular mechanisms of stink gland development and unveiling the metabolic pathway, its regulation, and the enzymes participating in the synthesis of defensive chemicals are essential for a better understanding of the self-protected synthesis of toxic compounds. Identification and characterization of novel genes roles in quinone synthesis in odoriferous stink glands of the red flour beetle is done by the following two genomic-wide approaches: 1) comparative analysis of tissue-specifically expressed genes by RNAseq-based transcriptomics, 2) RNAi-interference based phenotypic screen (iBeetle). Out of the identified genes four pivotal candidates genes *CHST5, ARSB*, *SUMF1* and *SLC26A11* were selected for detailed functional analysis.

4.1 iBeetle screen

The iBeetle screen resulted in a large online database for the genome-wide analyzed genes related to different phenotypes including stink glands in red flour beetle (Dönitz et al., 2015; Schmitt-Engel et al., 2015). In this online database, findings of a large scale RNAi-mediated knockdown screen of the red flour beetle genome are summarized. In the first phase of the iBeetle screen, about 5300 genes and in the second phase approximately 3200 genes had been knocked-down via dsRNA injection. While in the 3rd phase of a large scale RNAi mediated beetle genome screen, around 4748 genes had been knocked down from the *T. castaneum* genome, checked for morphological and developmental defects. Thus altogether 13248 genes were analyzed.

Since in the 1st and 2nd phase unexperienced researchers scored for the gland phenotype without dissection. The ibeetle-base annotations needed to be treated as a first pass screen and thus needed to be checked by a re-screen. In the rescreen of 130 genes, the stink gland phenotype of RNAi mediated gene disruption with injection of non-overlapping fragments could not be reproduced for 61 genes, even with injections of larva and higher concentrations of dsRNA. It has been reported by Kitzmann and colleagues that different beetle strains may show variation in RNAi sensitivity (Kitzmann et al., 2013). Nevertheless, higher concentrations (3 µg/µl) of dsRNA injection during rescreen also did not reproduce the phenotypes, showing that variation in effect of dsRNA doses between strains is not responsible for lack of effect on phenotype. While in 3rd phase 178 genes were found to cause alteration in stink gland morphology and volatile compound composition in

the adult beetle. 3rd phase of iBeetle was more efficient as compare to 1st and 2nd phase. In the 3rd phase, we identified a large number of candidate genes, because it was a direct screening of all the genes and I did the dissection of all the beetles. However all of phase 3 genes are not yet tested by NOF.-Genes were targeted after a reannotation of the *Triboilum* genome in the 3rd phase of the iBeetle screen, which was substantially improved by transcriptomics data, which allows for the annotation of species specific genes. We identified novel genes in this tissue specific screen also possible novel tissue which are taxon specific genes not as well covered in first genome annotation.

4.1.1 Stink gland phenotype

The altered stink gland phenotypes of 247 genes induced by RNAi mediated knockdown from 1st 2nd and 3rd phase were categorized into different types of altered stink gland phenotypes. Gland secretion in majority of altered gland phenotypes showed less secretion, decrease in glands size, darker secretion color, secretion color lighter, irregular reservoir size, melanized gland content, irregular separation, empty glands and colorless secretion. These alterations in stink gland phenotypes suggest a key role of these genes in development and physiology of the stink glands.

4.1.2 GC-MS analysis of 247 genes

In this GC-MS analysis, a subset of genes which are important for the composition of volatile chemical secretion was unveiled. Around 198 genes from all the three phases showed changes in volatile compound composition in the stink gland of adult beetle. In GC-MS analysis from all genes of the three phases of the iBeetle screen in respective knockdown beetles, 198 confirmed gland genes were unveiled, which effect the composition of volatile chemical secretion of beetle stink glands as compare to wildtype after RNAi mediated knockdown. 37 genes showed strongly reduced levels of benzoquinones (MBQ and EBQ) and alkenes (C-15 and C-17) in both abdominal and thoracic glands. In 71 genes, strongly reduced level of benzoquinone (MBQ and EBQ) was observed in both abdominal and thoracic glands. A number of so far uncharacterized genes were identified with altered gland phenotype and strongly reduced benzoquinones after RNAi-mediated knockdown, suggesting that the protein products of these genes are essential for the benzoquinone biosynthesis.

From all the three phases, we found that only 35 of the 247 gland genes with a strong secretion phenotype possess an expression fold change of two or higher in stink gland tissue. Thus, the other

212 genes that showed a morphological phenotype as well as alterations in the secretion volatiles would have been easily missed in a transcriptomics-based approach, as they are not differentially and highly expressed in the glands.

4.1.3 Bioinformatics analysis of confirmed genes

On the basis of their possible molecular function, the bioinformatics analysis of the 247 genes having a confirmed phenotype showed the following categories: enzymes, transcription factors, regulator/receptor binding, channels, other molecular function, transporters, receptor and unknown function. In total, the iBeetle screen uncovers many different types of genes that have various molecular functions and all are necessary for proper functioning of the stink glands. The 'Unknown function' gene group are 33% and these includes genes in which no conserved domains and nor any orthologs could be identified. Therefore, no molecular function was predicted for these genes.

4.2 Transcriptomis analysis

We re-analyzed a gland-specific transcriptomic dataset to get a more comprehensive insight into stink-gland function, which was generated 2013 by Li et al. The very recently assembled gene set reference of *Tribolium* (OGS3) allowed us to increase the mapping rates by about 30% compared to the initial analysis. After mapping the 2013 dataset to the current version of the *T. castaneum* transcriptome, we found 75 transcripts, which are specifically expressed in the odiferous stink glands of *T. castaneum* (FC >= 16) and applied the same filter to the dataset of 2013 (Li et al., 2013) and found 61 gland-specific transcripts. 39 of these overlapped, whereas 33 of the remaining 36 transcripts from the new analysis, could not have been detected previously. The remaining 3 "new transcripts" were also analyzed in the old analysis, but showed a slightly lower gland specific expression. 22 transcripts were not found in the new analysis. 5 out of the 61 transcripts that were found in the analysis of 2013 as "gland specific" were lower expressed according the new analysis and therefore did not pass the filtering threshold of Log2FC >= 4. The remaining 17 out of 22 transcripts are not annotated in the new version of the transcriptome and could therefore not be found (they are "former" TC numbers). We found 33 newly annotated genes that were expressed at least 16 times higher compared to the control sample, which could not have been found in the initial analysis. Since they are very highly expressed in the *Tribolium* gland tissue compared to the control sample, it is definitely worth to analyze these genes in more detail on a functional level.

4.3 Comparative phenotypic screen and transcriptomics

Based on transcriptomic stink gland data, Li et al. (2013) identified 77 genes which are specifically and highly expressed in the stink glands (FC ≥ 64). 71 of them were analyzed in gene knockdowns for morphological and secretion volatile stink gland phenotypes. 36 of them were also analyzed in iBeetle. 29 of the 71 genes showed morphological and secretion volatile phenotypes in the stink glands. 13 of which were also covered by iBeetle, from these just one gene (Tc-005389) was confirmed. The iBeetle screen missed eight gland genes that have been identified (among 21 others) in the transcriptomics-based approach by Li et al. (2013).

We re-analyzed a gland-specific transcriptomic dataset to get a more comprehensive insight into stink-gland function, which was generated 2013 by Li et al. We found 33 newly annotated genes that were expressed at least 16 times higher compared to the control sample, which could not have been found in the initial analysis and were also missed in the iBeetle screen. Only one gene (Tc_008780) has been identified as Gland specific 2013 and in the completely new 2020 transcriptomics analysis. Tc_033013 is found in the Gland specific set from the new analysis 2020. Only these two genes were also covered in iBeetle screen of 3rd phase. Altogether only three gene identified both in transcriptomics and iBeetle screen. This confirmed previous finding that the different approaches of functional genomics phenotypic screen and transcriptomics approaches, complement each other in identifying genes functionally important for the physiology of a certain tissue.

4.4.Outlook

In genome wide approaches, we identified a large list of 247 candidate genes with various known and 33% with unknown functions. 70 genes out of 247 genes were with novel functions. Thus characterizing this genes with unknown or novel functions might be redeeming in identifiying novel molecular pathways.

On the basis of stink gland transcriptome and iBeetle screen data, we studied the function of some genes, e.g. *CHST5, ARSB*, *SUMF1* and *SLC26A11* in sulfate metabolism in the stink gland of beetle. Particularly, we unveiled the role of these genes in regulation of sulphur metabolism and the self-protective biosynthesis of benzoquinone in the stink glands of *T. castaneum*. Our study showed that based on the involvement of some gene (s) in a certain metabolic process, we can predict process involved in self-protectioning production of defensive secretion containing toxic benzoquinones. Therefore, searching the list of candidate genes, might allow the identification of further pathways.

In reanalysis of an existing transcriptomic dataset, we identified 56 genes of which 33 transcripts were from the new analysis, which were not identified previously, that are potentially involved in *Tribolium* stink gland biology. These were newly annotated in the current version of the *T. castaneum* transcriptome and they are very highly expressed in the *Tribolium* gland tissue compared to the control sample. Thus it is definitely worth to analyze these genes in more detail on a functional level.

This might be particularly important for the identification of gene functions involved in some metabolic or other regulatory pathway in a tissue so far not studied on a molecular biology level in other model organisms. To look for gene set important in stink gland, we utilized both phenotypic screen and transcriptomic data. Some genes, e.g., *CHST5* is not expressed in glands but identified by phenotypic screen and present in transcriptomic data. *Lacase2*, *ATP7* and *SUMF1* are not gland specific but present everywhere and were identified in the 2nd phase.

5. References

Abou-Donia, M. (2015) *Mammalian Toxicology*. John Wiley & Sons.

Alexander, P. and Barton, D. H. R. (1943) 'The excretion of ethylquinone by the flour beetle', *Biochemical Journal*, 37(4), pp. 463–465.

Beeman, R. W. *et al.* (1996) 'Chromosome extraction and revision of linkage group 2 in Tribolium castaneum', *The Journal of Heredity*, 87(3), pp. 224–232. doi: 10.1093/oxfordjournals.jhered.a022989.

Blum, M. S. (1981) 'Chemical defenses of arthropods.', *Chemical defenses of arthropods.* Available at: https://www.cabdirect.org/cabdirect/abstract/19820594729 (Accessed: 19 January 2020).

Brown, S. J. *et al.* (2009) 'The Red Flour Beetle, Tribolium castaneum (Coleoptera): A Model for Studies of Development and Pest Biology', *Cold Spring Harbor Protocols*, 2009(8), p. pdb.emo126. doi: 10.1101/pdb.emo126.

Brown, W. V. *et al.* (1992) 'Chemical Composition and Taxonomic Significance of Defensive Secretions of Some Australian Tenebrionidae (coleoptera)', *Australian Journal of Entomology*, 31(1), pp. 79–89. doi: 10.1111/j.1440-6055.1992.tb00461.x.

Bucher, G., Scholten, J. and Klingler, M. (2002) 'Parental RNAi in Tribolium (Coleoptera)', *Current Biology*, 12(3), pp. R85–R86. doi: 10.1016/S0960-9822(02)00666-8.

Capinera, J. L. (2008) *Encyclopedia of Entomology*. Springer Science & Business Media.

Chapman, E. *et al.* (2004) 'Sulfotransferases: Structure, Mechanism, Biological Activity, Inhibition, and Synthetic Utility', *Angewandte Chemie International Edition*, 43(27), pp. 3526–3548. doi: 10.1002/anie.200300631.

Crowson, R. A. (1960) 'The Phylogeny of Coleoptera', *Annual Review of Entomology*, 5(1), pp. 111–134. doi: 10.1146/annurev.en.05.010160.000551.

Crowson, R. A. (1981) 'Chapter 1 - Introduction: The Study of Beetles', in Crowson, R. A. (ed.) *The Biology of the Coleoptera*. Academic Press, pp. 1–14. doi: 10.1016/B978-0-12-196050-6.50006-3.

Dönitz, J. *et al.* (2015) 'iBeetle-Base: a database for RNAi phenotypes in the red flour beetle Tribolium castaneum', *Nucleic Acids Research*, 43(Database issue), pp. D720–D725. doi: 10.1093/nar/gku1054.

Duehl, A. J., Arbogast, R. T. and Teal, P. E. A. (2011) 'Density-related volatile emissions and responses in the red flour beetle, Tribolium castaneum', *Journal of Chemical Ecology*, 37(5), pp. 525–532. doi: 10.1007/s10886-011-9942-3.

Eisner, T., McHenry, F. and Salpeter, M. M. (1964) 'Defense mechanisms of arthropods. XV. Morphology of the quinone-producing glands of a tenebrionid beetle (ELEODES longicollis lec.)', *Journal of Morphology*, 115(3), pp. 355–399. doi: 10.1002/jmor.1051150304.

Endt, D. W. von and Wheeler, J. W. (1971) '1-Pentadecene Production in Tribolium confusum', *Science*, 172(3978), pp. 60–61. doi: 10.1126/science.172.3978.60.

Falany, C. N. (1997) 'Enzymology of human cytosolic sulfotransferases', *FASEB journal: official publication of the Federation of American Societies for Experimental Biology*, 11(4), pp. 206–216. doi: 10.1096/fasebj.11.4.9068609.

Gibbs, T. T., Russek, S. J. and Farb, D. H. (2006) 'Sulfated steroids as endogenous neuromodulators', *Pharmacology Biochemistry and Behavior*, 84(4), pp. 555–567. doi: 10.1016/j.pbb.2006.07.031.

Görgen, G. *et al.* (1990) 'Biosynthesis of 1-alkenes in the defensive secretions ofTribolium confusum (Tenebrionidae); stereochemical implications', *Experientia*, 46(7), pp. 700–704. doi: 10.1007/BF01939939.

Grove, S. J. and Stork, N. E. (2000) 'An inordinate fondness for beetles', *Invertebrate Systematics*, 14(6), pp. 733–739. doi: 10.1071/it00023.

Grün, F. *et al.* (1996) 'Purification, cloning, and bacterial expression of retinol dehydratase from Spodoptera frugiperda', *The Journal of Biological Chemistry*, 271(27), pp. 16135–16138. doi: 10.1074/jbc.271.27.16135.

Happ, G. M. (1968) 'Quinone and hydrocarbon production in the defensive glands of Eleodes longicollis and Tribolium castaneum (Coleoptera, Tenebrionidae)', *Journal of Insect Physiology*, 14(12), pp. 1821–1837. doi: 10.1016/0022-1910(68)90214-X.

Hattori, K. *et al.* (2006) 'A novel sulfotransferase abundantly expressed in the dauer larvae of Caenorhabditis elegans', *Journal of Biochemistry*, 139(3), pp. 355–362. doi: 10.1093/jb/mvj041.

Hattori, K. *et al.* (2007) 'Cloning and expression of a novel sulfotransferase with unique substrate specificity from Bombyx mori', *Bioscience, Biotechnology, and Biochemistry*, 71(4), pp. 1044–1051. doi: 10.1271/bbb.60703.

Hattori, K. *et al.* (2008) 'Cloning, expression, and characterization of cytosolic sulfotransferase isozymes from Drosophila melanogaster', *Bioscience, Biotechnology, and Biochemistry*, 72(2), pp. 540–547. doi: 10.1271/bbb.70647.

Herndon, N. *et al.* (2020) 'Enhanced genome assembly and a new official gene set for Tribolium castaneum', *BMC Genomics*, 21(1), p. 47. doi: 10.1186/s12864-019-6394-6.

Howard, R. W. (1987) 'Chemosystematic Studies of the Triboliini (Coleoptera: Tenebrionidae): Phylogenetic Inferences from the Defensive Chemicals of Eight Tribolium spp., Palorus ratzeburgi (Wissmann), and Latheticus oryzae Waterhouse', *Annals of the Entomological Society of America*, 80(3), pp. 398–405. doi: 10.1093/aesa/80.3.398.

Hunt, T. *et al.* (2007) 'A Comprehensive Phylogeny of Beetles Reveals the Evolutionary Origins of a Superradiation', *Science*, 318(5858), pp. 1913–1916. doi: 10.1126/science.1146954.

Joop, G. *et al.* (2014) 'Experimental evolution of external immune defences in the red flour beetle', *Journal of Evolutionary Biology*, 27(8), pp. 1562–1571. doi: 10.1111/jeb.12406.

Jordan, T. W., McNaught, R. W. and Smith, J. N. (1970) 'Detoxications in peripatus. Sulphate, phosphate and histidine conjugations', *Biochemical Journal*, 118(1), pp. 1–8.

Kerkut, G. A. (1985) *Insect Control: Volume 12*. Elsevier.

Keville, R. and Kannowski, P. B. (1975) 'Sexual excitation by pheromones of the confused flour beetle', *Journal of Insect Physiology*, 21(1), pp. 81–84. doi: 10.1016/0022-1910(75)90070-0.

Kim, H. S. *et al.* (2010) 'BeetleBase in 2010: revisions to provide comprehensive genomic information for Tribolium castaneum', *Nucleic Acids Research*, 38(Database issue), pp. D437-442. doi: 10.1093/nar/gkp807.

Kitzmann, P. *et al.* (2013) 'RNAi phenotypes are influenced by the genetic background of the injected strain', *BMC genomics*, 14, p. 5. doi: 10.1186/1471-2164-14-5.

Ladisch, R. K., Ladisch, S. K. and Howe, P. M. (1967) 'Quinoid Secretions in Grain and Flour Beetles', *Nature*, 215(5104), pp. 939–940. doi: 10.1038/215939a0.

Li, J. *et al.* (2013) 'Odoriferous Defensive Stink Gland Transcriptome to Identify Novel Genes Necessary for Quinone Synthesis in the Red Flour Beetle, Tribolium castaneum', *PLoS Genetics*, 9(7). doi: 10.1371/journal.pgen.1003596.

Lis, Ł. *et al.* (2011) 'The carcinogenic effects of benzoquinones produced by the flour beetle', *Polish Journal of Veterinary Sciences*, 14(1). doi: 10.2478/v10181-011-0025-8.

Liu, T.-A., Liu, M.-C. and Yang, Y.-S. (2008) 'Immunohistochemical analysis of a novel dehydroepiandrosterone sulfotransferase-like protein in Drosophila neural circuits', *Biochemical and Biophysical Research Communications*, 367(1), pp. 14–20. doi: 10.1016/j.bbrc.2007.12.082.

Loconti, J. D. and Roth, L. M. (1953) 'Composition of the Odorous Secretion of Tribolium Castaneum', *Annals of the Entomological Society of America*, 46(2), pp. 281–289. doi: 10.1093/aesa/46.2.281.

Lorenzen, M. *et al.* (2005) 'Genetic Linkage Maps of the Red Flour Beetle, Tribolium castaneum, Based on Bacterial Artificial Chromosomes and Expressed Sequence Tags', *Genetics*, 170, pp. 741–7. doi: 10.1534/genetics.104.032227.

Lorenzen, M. D. *et al.* (2003) 'piggyBac-mediated germline transformation in the beetle Tribolium castaneum', *Insect Molecular Biology*, 12(5), pp. 433–440. doi: 10.1046/j.1365-2583.2003.00427.x.

Luciana Villaverde, M., Juárez, M. P. and Mijailovsky, S. (2007) 'Detection of Tribolium castaneum (Herbst) volatile defensive secretions by solid phase microextraction–capillary gas chromatography (SPME-CGC)', *Journal of Stored Products Research - J STORED PROD RES*, 43, pp. 540–545. doi: 10.1016/j.jspr.2007.03.003.

Markarian, H., Florentine, G. J. and Pratt, J. J. (1978) 'Quinone production of some species of Tribolium', *Journal of Insect Physiology*, 24(12), pp. 785–790. doi: 10.1016/0022-1910(78)90096-3.

Niehrs, C. *et al.* (1990) 'Conversion of recombinant hirudin to the natural form by in vitro tyrosine sulfation. Differential substrate specificities of leech and bovine tyrosylprotein sulfotransferases.', *Journal of Biological Chemistry*, 265(16), pp. 9314–9318.

Noh, M. Y. *et al.* (2016) 'Cuticle formation and pigmentation in beetles', *Current Opinion in Insect Science*, 17, pp. 1–9. doi: 10.1016/j.cois.2016.05.004.

Pappas, P. W. and Morrison, S. E. (1995) 'Benzoquinones of the beetles, Tribolium castaneum and Tribolium confusum', *Preparative Biochemistry*, 25(3), pp. 155–168. doi: 10.1080/10826069508010117.

Pappas, P. W. and Wardrop, S. M. (1996) 'Quantification of benzoquinones in the flour beetles. Tribolium castaneum and Tribolium confusum', *Preparative Biochemistry & Biotechnology*, 26(1), pp. 53–66. doi: 10.1080/10826069608000050.

Payne, N. M. (1925) 'Some Effects of Triboliumon on Flour', *Journal of Economic Entomology*, 18(5), pp. 737–744. doi: 10.1093/jee/18.5.737.

Pedrini, N. *et al.* (2015) 'Tenebrionid secretions and a fungal benzoquinone oxidoreductase form competing components of an arms race between a host and pathogen', *Proceedings of the National Academy of Sciences of the United States of America*, 112(28), pp. E3651–E3660. doi: 10.1073/pnas.1504552112.

Peschke, K. and Eisner, T. (1987) 'Defensive secretion of the tenebrionid beetle,Blaps mucronata: Physical and chemical determinants of effectiveness', *Journal of Comparative Physiology A*, 161(3), pp. 377–388. doi: 10.1007/BF00603963.

Posnien, N. *et al.* (2010) 'Genetics, development and composition of the insect head - A beetle's view', *Arthropod structure & development*, 39, pp. 399–410. doi: 10.1016/j.asd.2010.08.002.

Prendeville, H. R. and Stevens, L. (2002) 'Microbe Inhibition by Tribolium Flour Beetles Varies with Beetle Species, Strain, Sex, and Microbe Group', *Journal of Chemical Ecology*, 28(6), pp. 1183–1190. doi: 10.1023/A:1016281600915.

Rafaluk-Mohr, C., Wagner, S. and Joop, G. (2018) 'Cryptic changes in immune response and fitness in Tribolium castaneum as a consequence of coevolution with Beauveria bassiana', *Journal of Invertebrate Pathology*, 152, pp. 1–7. doi: 10.1016/j.jip.2017.12.003.

Roth, L. M. (1943) ‘Studies on the Gaseous Secretion of Tribolium Confusum Duval II. the Odoriferous Glands of Tribolium Confusum’, *Annals of the Entomological Society of America*, 36(3), pp. 397–424. doi: 10.1093/aesa/36.3.397.

Roth, L. M. and Howland, R. B. (1941) ‘Studies on the Gaseous Secretion of Tribolium Confusum Duval I. Abnormalities Produced in Tribolium Confusum Duval by Exposure to a Secretion given off by the Adults’, *Annals of the Entomological Society of America*, 34(1), pp. 151–175. doi: 10.1093/aesa/34.1.151.

Schierling, A. and Dettner, K. (2013) ‘The Pygidial Defense Gland System of the Steninae (Coleoptera, Staphylinidae): Morphology, Ultrastructure and Evolution.’, *Arthropod structure & development*, 42, pp. 197–208. doi: 10.1016/j.asd.2013.03.001.

Schildknecht, H. *et al.* (1964) ‘Defensive Substances of the Arthropods, Their Isolation and Identification’, *Angewandte Chemie International Edition in English*, 3(2), pp. 73–82. doi: 10.1002/anie.196400731.

Schinko, J. B. *et al.* (2010) ‘Functionality of the GAL4/UAS system in Tribolium requires the use of endogenous core promoters’, *BMC Developmental Biology*, 10(1), p. 53. doi: 10.1186/1471-213X-10-53.

Schinko, J., Thoene (née Hillebrand), K. and Bucher, G. (2012) ‘Heat shock-Mediated misexpression of genes in the beetle Tribolium castaneum’, *Development genes and evolution*, 222, pp. 287–98. doi: 10.1007/s00427-012-0412-x.

Schmitt-Engel, C. *et al.* (2015) ‘The iBeetle large-scale RNAi screen reveals gene functions for insect development and physiology’, *Nature Communications*, 6(1), pp. 1–10. doi: 10.1038/ncomms8822.

Schultheis, D. *et al.* (2019) ‘A Large Scale Systemic RNAi Screen in the Red Flour Beetle Tribolium castaneum Identifies Novel Genes Involved in Insect Muscle Development’, *G3: Genes|Genomes|Genetics*, 9(4), pp. 1009–1026. doi: 10.1534/g3.118.200995.

Schultheis, D., Schwirz, J. and Frasch, M. (2018) ‘RNAi screen in Tribolium reveals involvement of F-BAR proteins in myoblast fusion and visceral muscle morphogenesis in arthropods’, *bioRxiv*, p. 397232. doi: 10.1101/397232.

Siemanowski, J. *et al.* (2015) ‘Notch signaling induces cell proliferation in the labrum in a regulatory network different from the thoracic legs’, *Developmental Biology*, 408(1), pp. 164–177. doi: 10.1016/j.ydbio.2015.09.018.

Smith, L. W. *et al.* (1971) ‘Baking and taste properties of bread made from hard wheat flour infested with species of Tribolium, Tenebrio, Trogoderma and Oryzaephilus’, *Journal of Stored Products Research*, 6(4), pp. 307–316. doi: 10.1016/0022-474X(71)90043-9.

Sokoloff, A. (1972) *The biology of Tribolium: with special emphasis on genetic aspects*. Oxford: Clarendon Press.

Sokoloff, A., Ackermann, M. and Overton, L. F. (1967) 'Linkage Studies in Tribolium Confusum Duval. Ii. the Map Position of Three Homeotic Mutants.', *Canadian Journal of Genetics and Cytology*, 9(3), pp. 490–502. doi: 10.1139/g67-053.

Stork, N. E. (2009) 'Chapter 21 - Biodiversity', in Resh, V. H. and Cardé, R. T. (eds) *Encyclopedia of Insects (Second Edition)*. San Diego: Academic Press, pp. 75–80. doi: 10.1016/B978-0-12-374144-8.00021-7.

Strott, C. A. (2002) 'Sulfonation and molecular action', *Endocrine Reviews*, 23(5), pp. 703–732. doi: 10.1210/er.2001-0040.

Suzuki, Takahisa *et al.* (1975) 'Hydrocarbon Repellents Isolated from Tribolium castaneum and T. confusum (Coleoptera: Tenebrionidae)', *Agricultural and Biological Chemistry*, 39(11), pp. 2207–2211. doi: 10.1080/00021369.1975.10861925.

Trauner, J. *et al.* (2009) 'Large-scale insertional mutagenesis of a coleopteran stored grain pest, the red flour beetle Tribolium castaneum, identifies embryonic lethal mutations and enhancer traps', *BMC Biology*, 7, p. 73. doi: 10.1186/1741-7007-7-73.

Tschinkel, W. R. (1975) 'A comparative study of the chemical defensive system of tenebrionid beetles: Chemistry of the secretions', *Journal of Insect Physiology*, 21(4), pp. 753–783. doi: 10.1016/0022-1910(75)90008-6.

Unruh, L. M., Xu, R. and Kramer, K. J. (1998) 'Benzoquinone levels as a function of age and gender of the red flour beetle, Tribolium castaneum'. Available at: https://pubag.nal.usda.gov/catalog/13250 (Accessed: 19 January 2020).

Wang, L. *et al.* (2007) 'BeetleBase: the model organism database for Tribolium castaneum', *Nucleic Acids Research*, 35(Database issue), pp. D476–D479. doi: 10.1093/nar/gkl776.

Wirtz, R. A., Taylor, S. L. and Semey, H. G. (1978) 'Concentrations of substituted p-benzoquinones and 1-pentadecene in the flour beetles Tribolium madens (charp.) and Tribolium brevicornis (lec.) (coleoptera, tenebrionidae)', *Comparative Biochemistry and Physiology Part C: Comparative Pharmacology*, 61(2), pp. 287–290. doi: 10.1016/0306-4492(78)90056-4.

Yezerski, A. *et al.* (2007) 'The effects of a naturally produced benzoquinone on microbes common to flour', *Journal of Chemical Ecology*, 33(6), pp. 1217–1225. doi: 10.1007/s10886-007-9293-2.

Curriculum Vitae

Personal Data

Name: Bibi Atika

Date of birth: August 14th, 1987

Place of birth: Mansehra, Pakistan

Family status: Married

Nationality: Pakistani

Address: Supply street 3, Abbottabad, Pakistan.

Email: batika@gwdg.de

Education

Degree	**Year**	**Subjects**	**University**	**% Marks / grade**
PhD	2020	Developmental Biology	Georg August University, Germany	-
Mphil.	2012	Biological Sciences (Animal Sciences)	Quaid-i-Azam University, Pakistan	83% / first
M.Sc.	2010	Biological Sciences (Animal Sciences)	Quaid-i-Azam University, Pakistan	70% / first
B.Sc.	2007	Biology	Hazara University, Pakistan	83.6 % / first
Intermediate (12^{th})	2005	Biology, Chemistry, Physics	BISE Abbottabad, Pakistan	75 % / first

Research Experience:

PhD project (2014- 2020).

1st. Phenotypic screen and transcriptomics approach complement each other in functional genomics of defensive stink gland physiology of the red flour beetle (*Tribolium castaneum*) stink glands**.**

2nd. Genome-wide identification of genes involved in defensive stink gland function of the red flour beetle, *Tribolium casteneum*.

3rd. Partition-regulated sulfonation-based detoxification used for self-protecting production of toxic substances in defensive stink glands of the red flour beetle

Supervisor: Prof. Ernst Wimmer, Department of Developmental Biology
Genetics, Georg-August-Universität Göttingen, Germany.

Mphil. Thesis (2010-2012)

Role of Dietary Selenium against Cypermethrin induced Oxidative Stress in Juvenile Mahaseer Tor puitora.

Supervisor: Prof. Amina Zuberi, Quaid-i-Azam University, Pakistan.

Publications

Manuscript under process

1. Phenotypic screen and transcriptomics approach complement each other in functional genomics of defensive stink gland physiology of the red flour beetle (*Tribolium castaneum*) stink glands. In submission process.

Sabrina Lehmann[1*], **Bibi Atika[1*]**, Jianwei Li[1‡], Bernhard Weißbecker[2], Gregor Bucher[3], Ernst A. Wimmer[1†]

2. Genome-wide identification of genes involved in defensive stink gland function of the red flour beetle, *Tribolium casteneum*.

Bibi Atika[1], Elisa Buchberger[1], Musa Dan'azumi Isah[1], Bernhard Weißbecker[2], Gregor Bucher[3], Ernst A. Wimmer[1*]

3. Partition-regulated sulfonation-based detoxification used for self-protecting production of toxic substances in defensive stink glands of the red flour beetle

Bibi Atika[1*], Kirstin Feußner[2*], Musa Dan'azumi Isah[1], Ivo Feußner[2], Ernst A. Wimmer[1†]

4. Identification and characterization of potential cellularization Gene (s) for the Development of Transgenic Embryonic and Sex specific lethality systems in *Tribolium casteneum*.

Musa Dan'azumi Isah[1*], **Bibi Atika**[1], Ernst A. Wimmer[1†]

5. Transgenic marking in *Tribolium casteneum* to enhance monitoring of coleopteran insect pest.

Musa Dan'azumi Isah[1*], **Bibi Atika**[1], Stefan Dippel[1], Ernst A. Wimmer[1†]

Seminars, Conferences and Workshops attended

110th meeting of the German Zoological Society, September 2017 Bielefeld University, Germany.
World Academy of Science, Engineering and Technology October 2017 Paris, France.
SPIRIT-Summer School "Molecular genetics for Zoologists" September 2018 Göttingen, Germany.
SPIRIT-Summer School "Molecular genetics for Zoologists" September 2019 Göttingen, Germany.
32nd International Congress of Zoology 2012 Lahore Pakistan
National Symposium on Current Trends in Cellular, Medical and Environmental Physiology, May 2010 Quaid-i-Azam University, Islamabad, Pakistan.
Third National Symposium Recent Trends in Endocrinology and Reproductive Sciences May 2010 Lahore, Pakistan.

Language skills

Native- Urdu Full proficiency- English A2.1- German